Reliability assessment of the EN 1992 restrained shrinkage crack model as applied to liquid retaining structures in South Africa

by

Esther Mwamba

Submitted in fulfilment of the academic requirements of

Master of Science

In Civil engineering

College of Agriculture, Engineering and Science

University of KwaZulu-Natal

Durban

South Africa

2nd December 2016

Supervisor: Mrs C.H. McLeod

Declaration

The research contained in this dissertation was completed by the candidate while based in the discipline of civil engineering, of the College of Agriculture, Engineering and Science, University of KwaZulu-Natal, Howard College, South Africa. The contents of this work have not been submitted in any form to another university and, except where the work of others is acknowledged in the text, the results reported are due to investigations by the candidate.

_____

Signed: (Candidate: Esther Mwamba. Student Number: 211505003)

_____

Signed: (Supervisor)

Date:

Abstract

The South African design of liquid retaining structures (LRS) has traditionally involved the use of the British codes of practice, namely BS 8007:1987 and BS 8110-2:1985, due to South Africa not yet having developed its own equivalent code. BS 8007:1987 and BS 8110-2:1985 have since been replaced by EN 1992-3:2006 and EN 1992-1-1:2004 respectively. South African engineers are presented with the option of adopting the Eurocode 2 (EN 1992) design code for the design of LRS in place of the superseded corresponding British design codes; however, in the case of adoption, the issue of the code's suitability for use under local conditions and thus its reliability requires investigation. Hence, an investigation into the reliability performance of the EN 1992 crack model as applied in the South African context will be undertaken. Cracking, a serviceability limit state, takes precedence over the effects of the ultimate limit state where the infringement of crack limits in liquid retaining structures may result in the loss of structural integrity.

The First Order Reliability Method (FORM) of analysis was the probabilistic method of choice in this investigation. This research focussed on cracking due to restrained deformation with edge and end restraint conditions both being considered. The influence of significant parameters of the crack model was assessed in probabilistic terms. Model uncertainty and the restraint factor were both found to have borne the most influence on the reliability performance of the crack model. This research aimed to improve the reliability of the EN 1992 crack model for use in the South African context. This was achieved through attaining an understanding of the influence held by respective design variables on the crack model, thus bringing to light where within the crack models sensitivities lay. This then indicated the potentially most effective ways in which reliability compliance could be brought about in the case of code calibration. Future research must be conducted on the stochastic nature of the restraint factor and other basic variables. Research must also be conducted into the model uncertainty for crack formation.

Acknowledgement

This dissertation could not have been completed without the help and continued support of my supervisor Mrs C. H. McLeod, your tireless work and knowledge have been greatly appreciated. A huge thank you is also extended towards my colleagues who were always there to lend an ear and help out where they could. Lastly, I'd like to extend my sincerest thanks to my family and friends- you all have played a part in making this experience all the more enjoyable and rewarding.

Table of Contents

List of Figures

List of Tables

List of Symbols

Symbol	Explanation
A_c	Concrete area
$A_{c,eff}$	Effective tension area of concrete
A_s	Steel reinforcement
α_e	Modular ratio
$\alpha_{T,c}$	Coefficient of thermal expansion of mature concrete
c	Concrete cover
ε_{ca}	Autogenous shrinkage
ε_{cd}	Drying shrinkage
ε_{ctu}	Tensile strain capacity of concrete
ε, ε_r	Restrained strain
E_s	modulus of elasticity of the steel reinforcement
f_b	average bond strength between concrete and steel
f_{ctm} (t), $f_{ct,eff}$	Concrete tensile strength at time 't'
h	Section thickness
$h_{c,eff}$	Effective depth of tension area
k_1	coefficients that accounts for the bonding properties of reinforcement in the concrete
k_2	coefficient that accounts for the distribution of strain
kc	coefficient for stress distribution
k	coefficient that accounts for the effect of self-equilibrating stresses
φ	Bar diameter
R	Restraint degree
$S_{r,\,m}$	mean crack spacing
$S_{r,max}$	Maximum crack spacing
T_1	Fall in temperature from the hydration peak and ambient
T_2	Fall in temperature because of season variations
w_{lim}	Crack width limit

Reliability

α_c	Sensitivity factor/direction cosine of concrete cover
α_h	Sensitivity factor/direction cosine of section thickness
$\alpha_{fct,eff}$	Sensitivity factor/direction cosine of concrete tensile strength
α_θ	Sensitivity factor/direction cosine of model uncertainty
μx, σx	mean and standard deviation of random variables

β	Reliability index
β_t	Target reliability index
γ_c	Theoretical partial safety factor of concrete cover
γ_h	Theoretical partial safety factor of section thickness
$\gamma_{fct,eff}$	Theoretical partial safety factor of concrete tensile strength
γ_θ	Theoretical partial safety factor of model uncertainty

Chapter 1: Introduction

1.1 Introduction

Cracking is an expected phenomenon in concrete structures and has been described in Eurocode 1992-1-1: 2004 as being a normal part of reinforced concrete structures subjected to various loading conditions experienced within its lifetime. Cracking is regarded as a serviceability limit state problem (where generally its effects on the structural integrity are secondary to those of ultimate limit state conditions). However, this otherwise secondary problem of cracking becomes more pressing when dealing with structures where the formation of cracks is detrimental to the structure's function. Structures of this nature include liquid retaining structures where permeability of the structure is an important design criterion. Thus cracking, a serviceability limit state, becomes the dominant limit state in liquid retaining structure design.

Historically, South African codes of practice for the design of engineering structures have been based on the British standards for design. In dealing with water retaining structures, where no equivalent code of practice had been developed in South Africa, the British code BS 8007:1987 and those relevant parts of BS 8110-2:1985 were adopted as they stood. These codes have since been withdrawn and superseded by Eurocode EN 1992-3: 2006 and EN 1992-1-1:2004. If South Africa were to go on to adopt those parts of EN 1992-1-1:2004 pertaining to cracking and EN 1992-3:2006 for the design of liquid retaining structures, the question of its performance against South African reliability requirements comes into effect. It is this concern that warrants the reliability assessment of the EN 1992 restrained strain crack model (through which the reliability performance of the crack model may be gauged) for the design of liquid retaining structures under South African conditions.

The reliability of a structure may be described as the extent to which the structure performs as designed by the engineer for its intended design life (Green & Bourne, 1972). Not only is it important to determine the failure probabilities of structures for safety reasons, knowing the reliability of a structure can prevent dire financial loss. There exists some level of uncertainty in any engineering undertaking as complete structural reliability cannot be guaranteed. These uncertainties may be measured and assessed through probability methods of analysis (Holicky, 2009). The First Order Reliability Method (FORM) – said to be the most dependable computational method for structural reliability analysis (Zhao and Ono, 1999) – was the reliability assessment methodology employed in this investigation.

1.2 Aim

The aim of this research was to undertake a reliability assessment of the presently adopted European crack model as outlined in codes of practice EN 1992-1-1: 2004 and EN 1992-3:2006 for cracks due to the restrained deformation of concrete applied to the design of liquid retaining structures in South Africa. The findings made in this investigation would work towards improving the reliability of the EN 1992 design code where it is used for the design of liquid retaining structures in South Africa.

1.3 Objectives

The principal objective is to assess the performance of the reliability of the Eurocode 2 crack model against the reliability targets and reliability performance requirements stipulated in the South African design codes for the irreversible serviceability limit state of cracking. This may be achieved through:

i) Establishing the influence of key identified design parameters on the reliability performance of the Eurocode 2 crack model as applied to the South African context. A deterministic (excluding inherent variability of input variables) and a reliability-based (accounting for inherent variability and uncertainty existing in input variables) parametric study will be employed for this purpose.

ii) A sensitivity analysis in which greater insight into the relative influence held by the key identified design parameters on the reliability of the crack model may be determined.

In this way, the reliability of the Eurocode 2 crack model may be improved for use in the South African environment.

Regarding the restrained shrinkage cracking models, some design parameters of interest include concrete cover and the reinforcing bar diameter to effective reinforcement ratio. For example, in BS 8007:1987, the cover was not included in the equation for crack spacing. However, in the now implemented EN 1992-1-1: 2004, the concrete cover was considered to have a significant influence on the determination of the crack spacing and ultimately on the estimation of the surface crack width. Moreover, where the now superseded BS 8007:1987 outlined the same design approach for both edge and end restraint, EN 1992-3:2006 had completely done away with this approach- leaving only the methodology for edge restraint as it stood under BS 8007:1987. Also, EN 1992-3:2006 stipulates more stringent crack width limits than BS 8007:1987. An exploration

into the implication of these and other such significant differences in calculation methodologies between the above-mentioned design codes on the design of LRS in South Africa was performed in this research.

1.4 Outline of Thesis

Chapter 1 includes within it the introduction, aims and objectives of this research.

Chapter 2 marks the first half of the literature review in which relevant concepts relating to the design of LRS in South Africa are explored. The ideology of autogenous healing and issues around crack width estimation, a background into restrained cracking and a review of the Eurocode and British design codes for the design of liquid retaining structures were covered. The historical design of liquid retaining structures in South Africa was also considered.

Chapter 3 deals with the second half of the literature review. It gives a collection of relevant literature and research pertaining to basic reliability theory. In this chapter FORM, the reliability method of choice for this thesis was explained and the target reliability index for use in the reliability analysis selected.

Chapter 4 outlines the methodology for the deterministic parametric study of both the Eurocode 2 and superseded British crack model. Comparisons between the two codes were made. The design implications of adopting the EN 1992 design code are evaluated. Those input variables found to bear the most influence on the Eurocode 2 crack model were identified for further investigation in the reliability analysis. Also, a realistic set of parameters for a representative liquid retaining structure were thus established for use in the reliability analysis.

Chapter 5 presents the reliability analysis of the EN 1992 crack model as applied to a representative liquid retaining structure subject to South African conditions. Here the influences of selected design parameters are investigated through a reliability-based parametric study.

Chapter 6: Those results obtained through the reliability analysis presented in Chapter 5 are expanded upon through a sensitivity analysis of the random variables of the crack model.

Chapter 7 marks the end of the thesis in which concluding remarks and recommendations for future research are made.

The **Appendices** contains relevant data not already included in the main chapters of this dissertation.

Chapter 2: Review of Restrained Cracking in Liquid Retaining Structure Design

2.1 Liquid Retaining Structures in South Africa

2.1.1 Introduction

The design of liquid retaining structures (LRS) is one that involves special attention to the serviceability limit state (which takes precedence over the demands of the ultimate limit states). Cracking is a serviceability limit state problem, which generally is a secondary concern in the design of concrete structures. As is commonly understood by all civil engineers, serviceability limit states deal particularly with the appearance of the structure and its functionality under working conditions. This is contrary to the ultimate limit states of design which concerns itself with the collapse of structures and the safety of its occupants and thus has a higher required level of reliability. However, where cracking forms an integral part of a structure's design, the problem of cracking becomes a more pressing issue. Liquid retaining structures are a good example of structures where cracking is an important part of the structure's function. At present, South African engineers tasked with the design of a liquid retaining structure would do so under the guidance and stipulations of the British codes of practice (Wium, 2008). This is due to the fact that South Africa had not yet come to develop an equivalent code of its own. The British code of practice used to design LRS, namely BS 8110-2:1985 and BS 8007: 1987 have since been superseded by the Eurocodes EN 1992-1-1: 2004 and EN 1992-3:2006 respectively.

At the Structural Eurocode Summit in 2008, held in Pretoria over the issue of the move towards Eurocode use in South Africa, in a lecture held by Wium (2008) the options of perhaps updating existing codes for concrete design in South Africa, adopting Eurocode, adapting a foreign code and using said code as reference; or just developing a new code were put forth. The option to update was abandoned by a previous working group tasked with this alternative learned of a new generation of codes being underway (Wium, 2008). Wium (2008) suggested that adopting or either adapting EN 1992 would require less work and be ideal due to the internationally widespread use of Eurocode. The development of a new code would be taxing both monetarily and time wise (Wium, 2008). Thus, regarding liquid retaining structures, it was best to just adopt Eurocode and incorporate South African nationally determined parameters in a code annex. An equivalent code for liquid retaining structures, SANS 10100-3, is being developed and has been said to closely follow the format of EN 1992-3 (Wium, Retief & Barnardo- Viljoen, 2014). SANS 10100-3 will incorporate additional sections, clauses, informative annexes and provisions (some of which being derived from BS 8007) where necessary (Wium, Retief & Barnardo-Viljoen,

2014). Hence, a reliability assessment of the EN 1992 restrained shrinkage crack model should contribute to the development of the proposed SANS 10100-3.

2.1.2 Design of Liquid Retaining Structures in South Africa

As previously mentioned, South African engineers generally design LRS in accordance to BS 8007 and BS 8110, with a full transition into the use of Eurocode 2 not yet being realised. This, along with a few other findings, was made after a survey, which focused particularly on the design and construction practices of water reservoirs in South Africa (McLeod, 2013). Other noteworthy findings made from this survey are listed below:

- Whether designed to be rectangular or circular in plan, the specified storage capacity of the LRS will determine its ultimate size.
- A 40 mm concrete cover to reinforcement is often used for durability. A 50 mm concrete cover may be used instead where the reservoir is meant to stand against soil.
- Generally, the water reservoirs are constructed with a 35 MPa 28 day concrete strength with a minimum of 375 kg/m^3 good quality binder content. The upper limit for binder content is set at 500 kg/m^3 to control thermal shrinkage. Thermal shrinkage may be further limited through the avoidance of slagment in cement and through the use of rapid hardening cement.
- It is also common practice to use concrete with a 0.5 water/cement ratio.
- The permeability restrictions mean that the serviceability requirements of the LRS dominate the design. This generally translates into more steel reinforcement being required to meet the crack widths than those required for the fulfilment of ultimate limit states.
- In South Africa, high-yield steel reinforcement is used with a 450 MPa characteristic strength.
- LRS may be designed either to be fully or partially buried. Buried reservoirs are normally built onto excavated land or on a fill embankment. The choice of arrangement depends ultimately on the design conditions and the client's own preferences.
- The design of water reservoirs may be broken into three main structural elements: the wall, floor slabs and foundation as well as roof. Walls are either built as continuous or joined vertically. In rectangular reservoir walls are usually designed as cantilever walls. In the case of pre-stressed circular reservoirs in South Africa, the walls are generally equipped with a sliding joint at the base of the wall stem. For a circular water reservoir with a capacity of less than 10 Ml, a ratio of diameter to wall height of 4 is usually employed in South Africa. The floors slabs are normally cast discontinuously with the walls in the case of larger reservoirs, or may otherwise be cast to be continuous with the

walls. The floors of rectangular reservoirs are constructed with reinforced concrete slabs that are cast in square panels. A radial pattern is used when casting the floors in circular reservoirs. The most common roof type used for water reservoirs in South Africa is the flat slab.

It is obvious that in order for water reservoirs (along with other LRS) to meet their required function, they must be constructed with a combination of both good design and proper construction practices.

2.2 Restrained Cracking

Cracking in concrete is a natural phenomenon that occurs may occur due to loading, expansive chemical reactions in the concrete, plastic settlement just after casting or otherwise due to restrained deformation (Beeby and Narayanan, 2005). The focus of this thesis is on cracks that occur from restrained deformation, where the deformation comes after shrinkage and thermal movement of concrete during hydration. During the hydration reaction the concrete generates heat at a faster rate than what is lost to the environment, this then increases the temperature in the concrete. As heat is released from the hydration reaction in concrete, the concrete will expand and hence be under compression with the steel reinforcement being under tension. The concrete will then begin to cool to ambient temperature and contract, putting the concrete under tension and the steel reinforcement in compression (Greensmith, 2005). If the concrete is not restrained in any way and insulated, the movement induced by the temperature changes will be allowed to take place (Mosley, Bungey and Hulse, 2012). This allowed movement will result in there being no changes in concrete stresses. If a restraint is applied onto a concrete member, either from an external attachment or from temperature differentials within thick concrete members, the free movement of the concrete will be restricted. This restriction in movement would subsequently bring about stress changes within the concrete. The introduction of steel reinforcement within the concrete member would restrain the concrete's movement during the hydration process Mosley *et al.* (2012). Where the concrete reaches a tensile stress that is greater than the tensile capacity of the concrete, a crack will form.

The Figure 2.1 illustrates the above-mentioned relationship between stress and strain development in the concrete member as the temperature changes during hydration. It is evident in Figure 2.1 that creep significantly reduces the amount of early age thermal strain and consequently the stress in the concrete.

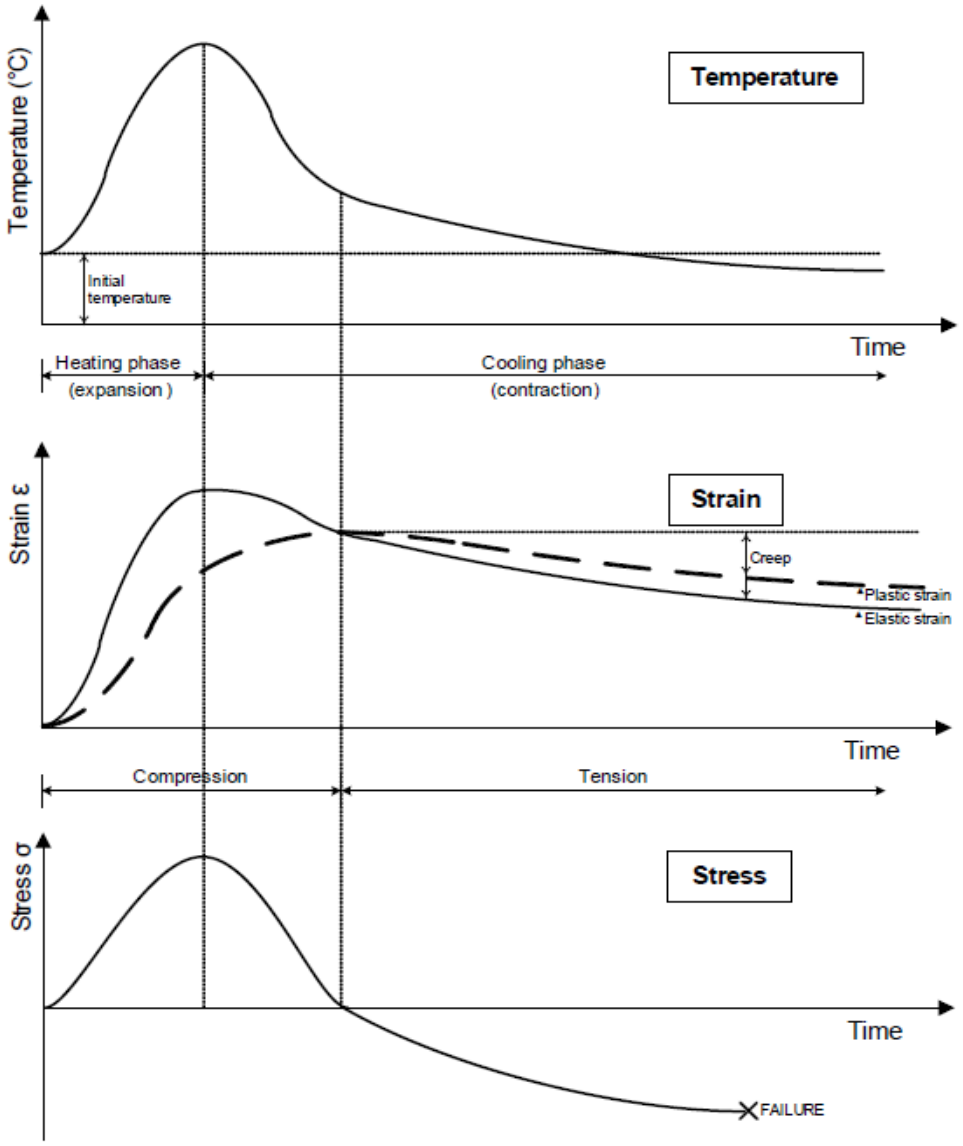

Figure 2.1: Relationship between Stress and Strain from Change in Temperature due to Concrete Hydration (Greensmith, 2005)

2.2.2 Restraint Conditions

The restraint to deformation (or otherwise volume change) of the concrete may occur either internally, externally or a combination of both (ACI, 2002). Internal restraint takes place where one part of the concrete section undergoes a change in volume that is different to those parts adjacent to it. More specifically, one part of the concrete will expand or contract relative to another part of the concrete section. Thus the relative movement of one part of a concrete section would be restricted by another. Design guide, CIRIA C660 (Bamforth, 2007) gives an example of such an occurrence: where in thick sections the concrete core generates heat faster than the concrete's surface creating a differential temperature gradient within the concrete section. In this instance, the core of the concrete section would expand and be in compression whilst the cooler surface of

the concrete section undergoes contraction and experiences tension. Cracks may then form at the concrete's surface. As the concrete begins to cool, the core cools faster than the concrete's surface– this time contracting whilst the concrete's surface expands. The crack widths of the cracks formed on the concrete's surface subsequently decrease in magnitude.

External restraint may be imposed onto a concrete member through its support conditions. The support conditions acting on the concrete member prevent the member from fully expanding during the heating phase. Cases dealt with in both BS 8007 and EN 1992-3 are end restraint and edge restraint (as illustrated in Figure 2.2).

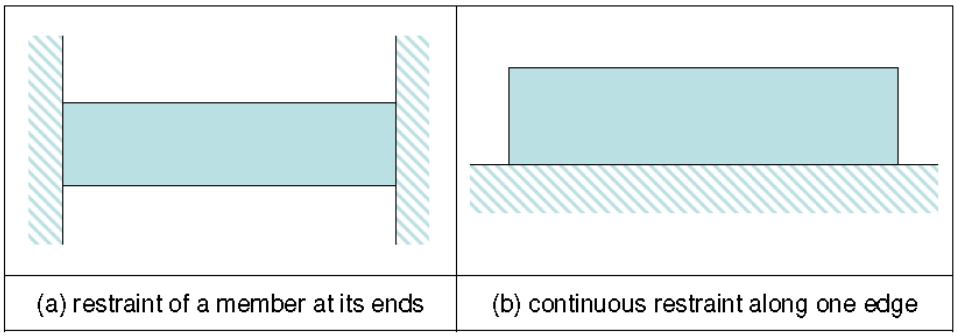

Figure 2.2: Difference between End and Edge Restraint (Bamforth, 2010).

End restraint comes about where a member is fixed in place along its ends whereas edge restraint comes after the concrete member being held in place all along its edge. EN 1992-1-1 suggests that the load is transferred entirely to the reinforcement during end restraint. Bamforth (2010) suggests that end restraint results in the crack width being limited and the number of cracks that occur being increased.

Edge restraint is assumed to be directly proportional to the strain developed in the concrete. The crack width then will be increased with an increase in strain since the crack width itself is directly proportional to the strain and crack spacing. BS 8007 and EN 1992-3 both assume that the cracking due to edge restraint not only increases the crack width, but also that it has no influence on the number of cracks formed– the cracks are considered to act independently of each other (Bamforth, 2010). An illustration of the crack pattern formed from edge restraint is presented in Figure 2.3. The restraint of the concrete member along the edge provides a resisting horizontal force that brings about cracking in the mid-span of the concrete member. The vertical tensile force generated in the concrete to resist the warping in the wall from the horizontal resisting force produces cracks that spread off diagonally towards the ends of the concrete member (Highways England, 1987).

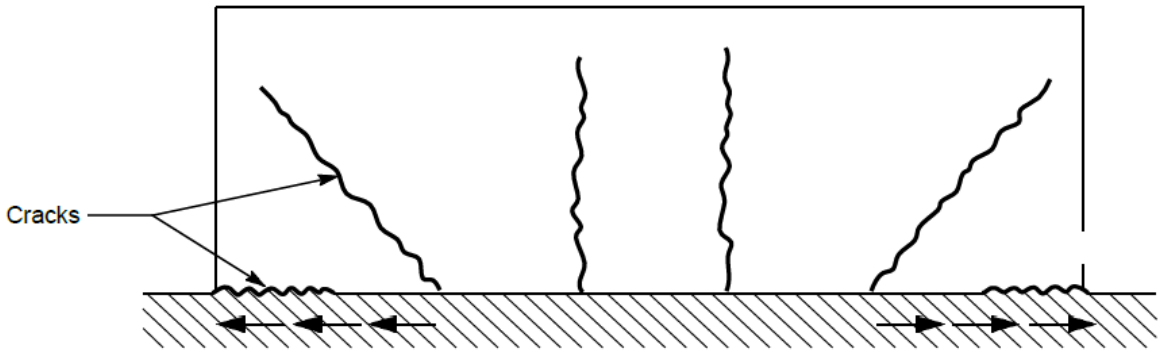

Figure 2.3: Crack Pattern of Concrete Member Subjected to Edge Restraint (Highways England, 1987)

Pure end restraint comes about where the restraining member is short. The distribution of cracks due to end restraint is illustrated in Figure 2.4:

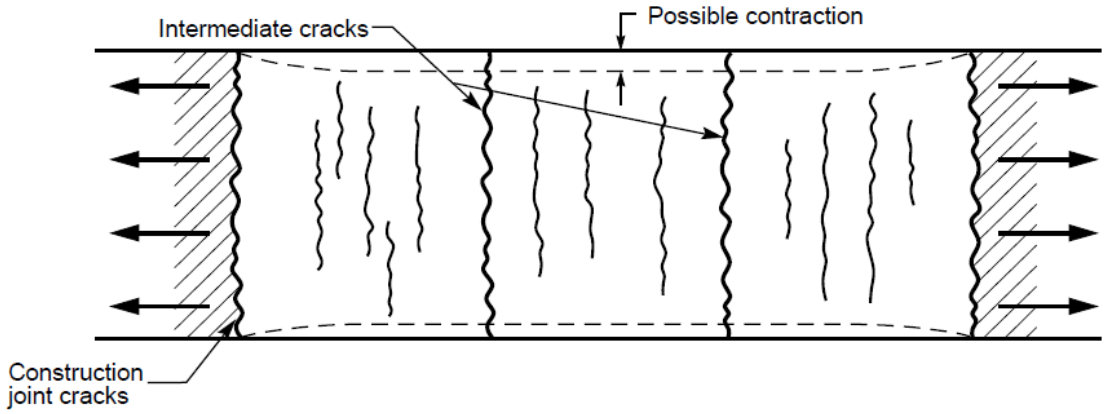

Figure 2.4: Crack Pattern of Concrete Member Subjected to End Restraint (Highways England, 1987)

Figure 2.5 illustrates the difference in the cracking between end and edge restraint (as found in EN 1992-3:2006 annex M). The Y axis represents the crack width, whilst the X axis represents the imposed deformation. The key to Figure 2.5 are as follows:

- 1- The end restraint equation graph.
- 2- Cracking due to end restraint,
- 3- Cracking due to edge restraint.

Clearly, end restraint may be found to produce crack widths that a larger than those resulting from concrete members subjected to edge restraint.

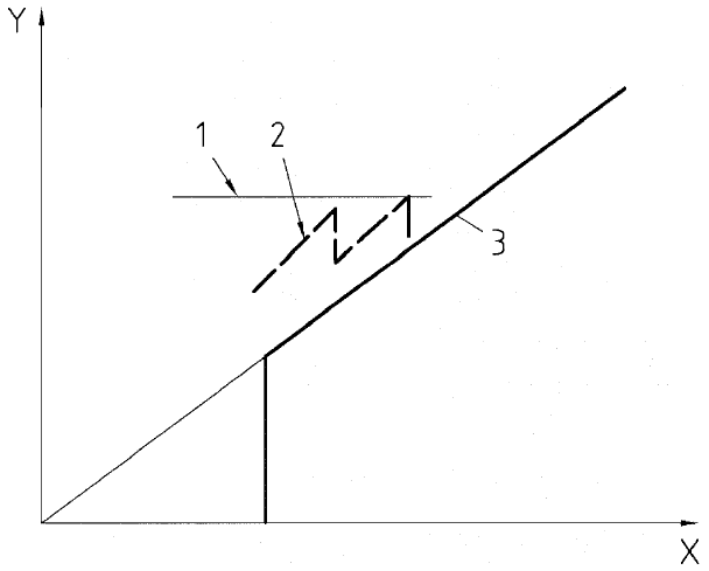

Figure 2.5: Difference in Cracking between End and Edge Restraint (Figure M.2 of EN 1992-3:2006)

A combination of both edge and end restraint may occur where a thin section is constructed in an alternative construction sequence. An advice note of the Design Manual for Roads and Bridges (Highways England, 1987), puts forth that where the restraining member is up to 5 m, the restrained member is also under edge restraint and no longer only enduring the effects of end restraint. A member subjected to both edge and end restraint would result in the above mentioned typical crack patterns for either restraint conditions (Figures 2.3 and 2.4 respectively) developing into the pattern presented in Figure 2.6.

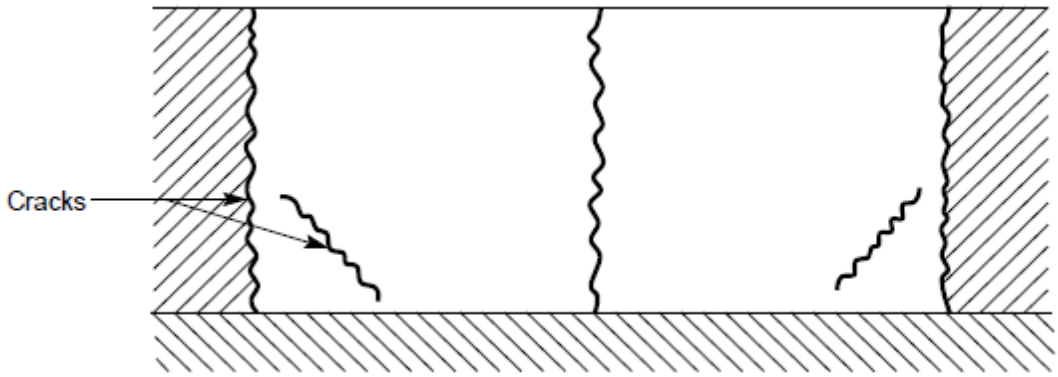

Figure 2.6: Crack Pattern of Concrete Member Subjected to Edge and End Restraint (Highways England, 1987)

External and internal restraint may also act together in the concrete member. An example where this may occur is the case where alternative panels are constructed for a thick concrete wall. The

design guide for early-age thermal crack control, CIRIA C660 (Bamforth, 2007), explains this occurrence well. Surface cracks may occur where the concrete's core generates more heat than at the surface of the concrete. The cracks on the concrete's surface are reduced due to the presence of the external restraint which restricts the expansion of the concrete's core, subsequently restricting the potential amount of tension to be developed in the surface zone. Hence the effect of external restraint cancels that of the internal restraint during concrete heating. However, the opposite is true when concrete cooling occurs. The concrete's core will cool faster than the surface and will thus have its contraction restricted by the surface zone– generating cracks within the core. This is further aggravated by the effect of the external restraint which also restricts the contraction of the concrete's core. Thus, during concrete cooling, the external and internal restraint work together to restrict movement in the restrained concrete member.

2.2.3 Restraint Degree

The restraint, or otherwise expressed as the degree of freedom of movement, is essentially a ratio of the actual imposed strain to the imposed strain resulting from full restraint (Antona and Johansson, 2011):

$$\text{Restrain Factor} = \frac{\text{actual imposed strain}}{\text{imposed strain in case of full restraint}} \tag{2.1}$$

At full restraint the restraint factor will stand at 1 and in instances in which some freedom of movement is allowed, the restraint factor will be less than 1.

Both EN 1992-3 and BS 8007 prescribe a restraint factor for instances of external restraint in which the concrete member in question is restrained continuously along its edge. Figure 2.7 illustrates the way in which restraint varies in the case with respect to the geometry of the restrained member. Those parts of the restrained member farther away from the restraining member are freer to move and so bear lower degrees of restraint, whilst a greater restriction to movement may be observed for those parts of the restrained member close to the restrained base.

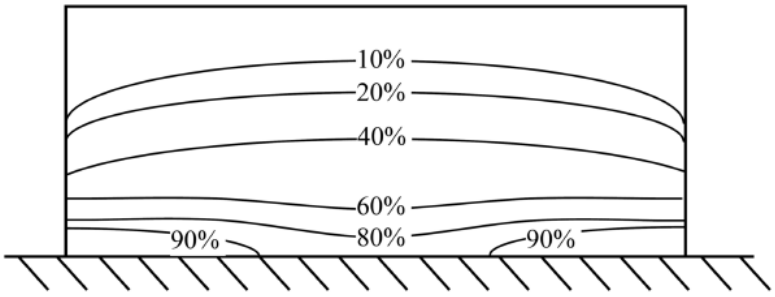

Figure 2.7: Change in Degree Of Freedom (Kamali, Svedholm and Johansson, 2013)

A methodology for the estimation of the restraint factor was developed by the American Institute of Concrete (ACI, 2002) for both edge (continuous external restraint) and end restraint conditions (or otherwise described as being a discontinuous external restraint). For edge restraint, ACI-207.2R-95 (2002) describes a multiplier to be used in conjunction with the restraint values based on test data (ACI, 2002). These restraint values obtained (reproduced in Figure 2.8) were related to the configuration of the concrete member in question, namely the length to height ratio of the restrained concrete member.

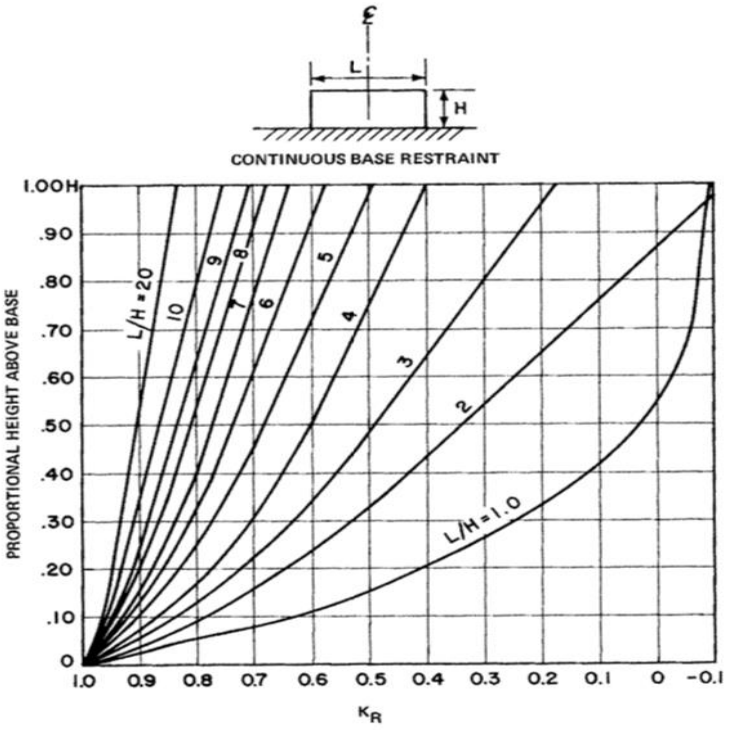

Figure 2.8: Restraint Level at Centre of Section (ACI, 2002)

The ACI-207.2R-95 (2002) given multiplier is described as follows:

$$X = \frac{1}{1+\frac{A_g E_c}{A_F E_F}} \tag{2.2}$$

where,

- A_g denotes the gross concrete cross-sectional area of the restrained concrete member (or otherwise the new concrete pour)
- E_c is the modulus of elasticity of the newly poured concrete
- A_F marks the cross-sectional area of the restraining concrete base
- E_F represents the modulus of elasticity of the old (restraining) concrete element

The restraint factor calculated from ACI-207.2R-95 (2002) would then be a product of the above-described multiplier and the applying restraint value read from Figure 2.8. ACI-207.2R-95 suggests that for mass concrete on rock, the maximum effective area of the restraining element (A_F) can be assumed to be 2.5 times greater than the gross cross-sectional area of the restrained member (A_g). Moreover, it was recommended in design guide CIRIA C660 (Bamforth, 2007) that an E_c/E_F value of 0.7 to 0.8 may be assumed where the ACI approach for restraint estimation is used. In instances in which cooling in the concrete is found to be most rapid, the lower value of the E_c/E_F ratio should be used (Bamforth, 2007). CIRIA C660 (2007) includes this ACI method for restraint estimation, adding a factor K_1 to account for the effects of creep. Bamforth (2007) suggests a typical value of $K_1 = 0.65$ for where 35% reduction in the stresses in the concrete is anticipated to have resulted from the effects of creep.

The true restraints observed from experimental data are listed in BS 8110-2:1985 and HA BD 28/87 (Highways England, 1987) - a supplementary code to BS 5400-4:1984 for bridge design. The effects of creep are not included in these values. BS 8007 and EN 1992-3 account for the effect of creep (with a modification factor of 0.5) on the restrained concrete member (Bamforth, 2007). The various restraint levels for a range restraint conditions, after CIRIA C660, are reproduced in Table 2.1:

Table 2.1: External Restraint Degrees for Various Restraint Conditions (Bamforth, 2007)

Restraint Condition	**BS 8110-2**	**HA BD 28/87**	**BS 8007**	**EN 1992-3**
Base of wall onto a massive base	0.6-0.8	0.6	0.5	0.5
Top of a wall cast on to a massive base	0.1-0.2		0-0.5	0-0.5
Edge restraint in box type deck cast in stages		0.5		
Edge element cast onto slab		0.8		
Massive pour cast onto blinding	0.1-0.2	0.2		
Base of massive pour cast onto existing mass concrete	0.3-0.4			
Suspended slabs	0.2-0.4			
Infill bays (e.g. rigid restraint)	0.8-1	1	0.5	0.5

However, when regarding end restraint, EN 1992-3 does not apply a restraint factor to the estimation of the restrained strain as BS 8007 did. ACI-207.2R-95 gives a restraint factor to be used for end restraint (or otherwise, discontinuous external restraint) conditions. The restraint factor is given by the formula:

$$R = \frac{1}{1+\frac{A_B h^3}{4LI_c}} \tag{2.3}$$

in which,

- A_B represents the area of the deforming member (the member being restrained)
- h denotes the height of the supporting ends restraining the deforming member
- L is the length of the deforming member (the member being restrained)
- I_c refers to the average moment of inertia of the supporting ends restraining the deformed member

Much like the definition given for the restraint factor (degree) given by Antona and Johansson (2011) in Equation 2.1, researcher Gilbert (2016) outlined a rational method to estimate the restraint degree of the boundary between the wall and concrete base for an edge restrained concrete element. The restraint degree was said to be estimated using the formula:

$$R = \varepsilon_r/\Delta\varepsilon_{free}, \tag{2.4}$$

where ε_r denotes the restrained strain at the bottom of the wall which is equal to the ratio between the tensile stress (σ_{cs}) at the bottom of the wall (caused by the restraining force acting at some distance $\bar{y}$ below the interface of the wall and base) and the age-adjusted effective concrete modulus ($\bar{E}_c$) of the wall.

Moreover, $\Delta\varepsilon_{free}$ represents the change in the free contraction at the interface of the wall and base which is the sum of the strain induced by the changes in the temperature of the concrete, the autogenous shrinkage as well as the drying shrinkage.

2.3 Review of Design Codes

A review of the parts of design codes used in South Africa for the design of the cracking serviceability limit state are considered in the subsequent text. The estimation of cracks induced from the restrained shrinkage was the focus of the review. A look through the South African code of practice for the structural use of concrete (SANS 10100-1:2000) reveals few references to the control of crack widths. Formulae to predict the characteristic crack width are given in Annex A

(under section A.3), which covers the methods for the checking of compliance to serviceability limit state criteria. Annex B gives some general information on the use of movement joints in controlling cracking. A maximum crack width limit of 0.3 mm is given in clause 4.11.8.2.1.1 for the design of concrete elements where the serviceability limit state is not dominant (e.g. buildings).

Although BS 8007 and BS 8110-2 have both evidently been dependable for use in South Africa, they have been superseded. The adoption of EN 1992 could, therefore, prove to be beneficial. In a lecture on the relevance of the Eurocodes in South Africa, Zingoni (2008) listed a few of the benefits to be had with the Eurocode adoption. These benefits include the added competitiveness of South African engineers as they will be more equipped to bid for international projects in a wide variety of countries in which Eurocode adoption had already been established. South African engineers also stand to gain from international software and design manuals, making for a smoother transition into complete adoption. Additionally, through the Eurocode's general framework and flexibility, the opportunity is available for South African engineers to include local partial factors and unique geographical and climatic parameters. However, the implications of this change over into Eurocode use must be quantified. In this way, a full assessment of the pros and cons of Eurocode adoption in South Africa may be done.

There are several ways in which the British and Eurocode differ in their approach on the estimation of crack widths formed from restrained shrinkage. The crack spacing equation of Eurocode 2 include the effects of the concrete cover, whereas the British code of practice does not. This has come after studies proved that concrete cover plays a significant role in the crack spacing (Beeby and Narayanan, 2005). Moreover, the ratio of concrete tensile strength for immature concrete with respect to the bond strength of the steel reinforcement (f_{ct}/f_b) in BS 8007 has been replaced by the factor k_1 in EN 1992-1-1 to account for the bond properties of the reinforcement used. The estimation of the restrained strain under either edge or end restraint are dealt with differently between the two codes.

Restrained strain from edge restraint in EN 1992 is dealt with in a similar way to the British codes. However, historically autogenous shrinkage has been assumed to occur only in concretes with very low water/cement ratios. For normal strength concretes– where the water/ cement ratio is greater than 0.4– drying shrinkage is assumed to make up the total measured shrinkage since very little autogenous shrinkage is said to occur (Addis and Owens, 2001). Eurocode 2, on the other hand, assumes that autogenous shrinkage comes into effect for all concretes with characteristic cylinder strength greater than 10 MPa. The greatest difference between both codes lies in their estimation of restrained strain after end restraint conditions, where completely different

approaches are adopted. It appears that not one parameter is shared between the codes with regards to this estimation. Even with the differences in approach for most crack models, it is the general consensus of researchers that the most influential parameters of the crack model – in order of importance- include the reinforcing steel stress, concrete cover, reinforcement spacing and area of concrete surrounding each reinforcing bar (Zahalan, 2010). The following section looks closer into the approaches adopted by both the British and Eurocode cracking models.

2.3.2 BS cracking model

The old British design code of practice for the design and construction of liquid retaining structures was BS 8007, which covered particularly tanks, reservoirs and other vessels that either contained or excluded an aqueous liquid (except for the case of aggressive liquids). Liquid retaining structures designed to BS 8007 were done so together with relevant parts of BS 8110-1 and BS 8110-2.

2.3.2.1 Permissible Crack Widths

A limit has been imposed on the maximum design crack width (based on the allowable permeability for the concrete) for liquid retaining structures depending on the exposure conditions that are to be endured by the structure. Under the BS 8007 code, it has been recommended that the maximum design surface crack width be limited to 0.2 mm for severe or very severe exposure conditions. However, where aesthetic appearance is a matter of concern, a limiting crack width of 0.1 mm was recommended.

2.3.2.2 Minimum Area of Steel

BS 8007 states that after the first crack has formed, the formation of cracks thereafter will be influenced by the provision of reinforcing in the concrete. The steel reinforcement controls the distribution of cracks by increasing the number of cracks that form whilst limiting their width to within the limiting crack width. This occurs where the reinforcement across the initial crack does not yield.

Where the tensile force experienced by the concrete is beyond the maximum tensile force capacity of the concrete ($A_c f_{ct}$), cracking will occur. The steel reinforcement provided must be sufficient enough that the resistant tension force of the steel ($A_s f_y$) is at least equal to the maximum tensile force capacity of the concrete ($A_s f_y \geq A_c f_{ct}$). For the steel reinforcements to effectively reduce the crack widths to within the limiting value, the minimum amount of steel reinforcement in the concrete needs to be as set out by BS 8007:

$$A_s = A_c \times \rho_{crit}, \quad (2.5)$$

where,

- $\rho_{crit} = \frac{fct}{fy}$ (the ratio between the direct tensile strength of the concrete taken at 3 days and the characteristic strength of the steel reinforcement).
- A_s is the minimum area of steel
- A_c is the area of concrete effective surface zones which follow the recommendations listed in figures A.1 and A.2 of Appendix A of BS 8007:1987.

In figure A.1, BS 8007 suggests that the effective tension zone (effective surface zones) for walls and suspended slabs with thickness 'h' less than or equal to 500 mm take up half the section depth. Where the wall and suspended slab thickness is greater than 500 mm, it is assumed that each reinforcement face will control 250 mm of the concrete's depth. figure A.2, on the other hand, proposes that the effective tension zone of ground floor slabs with thickness 'h' under 300 mm will be h/2 on one reinforcement face with no reinforcement required for the bottom face of the section. Values for the ground slab thicknesses between 300 mm and 500 mm will produce an effective tension zone that is half the section thickness for the top reinforcement face and 100 mm was recommended for the bottom reinforcement face. Finally, where the ground slab thickness is found to exceed 500 mm, the surface zone was assumed to be 250 mm for the top reinforcement face with the bottom reinforcement face set at 100 mm.

2.3.2.3 Crack Spacing

A comprehensive discussion of the BS 8007 crack spacing formula is given by Bhatt, Thomas, McGinley and Choo (2006), a summary of which is presented below:

Slipping between the reinforcement and the concrete begins after the first crack forms. More cracks will then start occurring where the bond stress (f_b) between steel and concrete is greater than the concrete tensile strength (f_{ct}) as such,

$$f_b s \Sigma u \geq f_{ct} A_c.$$

In this inequality's' refers to the development length of bond stress and Σu is the total perimeter of bars at the section. Considering the ratio of the sum of the perimeter of reinforcement bars to area of reinforcement,

$$\sum u/A_s = \pi\varphi/(\pi\varphi^2/4),$$

it is understood that generally the same bar diameter is used at a cross section. The ratio of the sum of the steel reinforcement perimeter to steel area then becomes:

$$\sum u/A_s = 4/\varphi$$

Ultimately the inequality may be rewritten in the form:

$$s \geq \frac{fct}{fb} \times \frac{\Phi}{4\rho}$$

This describes the minimum crack spacing, with the maximum crack spacing being twice the minimum (Bhatt *et al.*,2006). Therefore, the maximum spacing to BS 8007 of the cracks formed in the concrete is to be determined by the following equation:

$$S_{max} = \frac{fct}{fb} x \frac{\varphi}{2\rho} \ , \qquad (2.6)$$

where:

- The ratio $\frac{fct}{fb}$ is the relationship between the tensile strength of the concrete and the average bond strength of the steel reinforcement with respect to the concrete.
- φ is the bar diameter of the steel reinforcement
- And ρ is the ratio of steel based on the effective concrete tension areas defined in figures A.1 and A.2 of appendix A of BS 8007: 1987 (reproduced here as Figure 2.9)

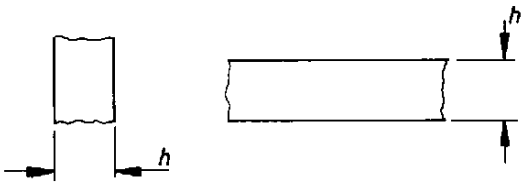

NOTE. For $h \leq 500$ mm, assume each reinforcement face controls $h/2$ depth of concrete.
For $h > 500$ mm, assume each reinforcement face controls 250 mm depth of concrete, ignoring any central core beyond this surface depth.

Figure A.1 Surface zones: walls and suspended slabs

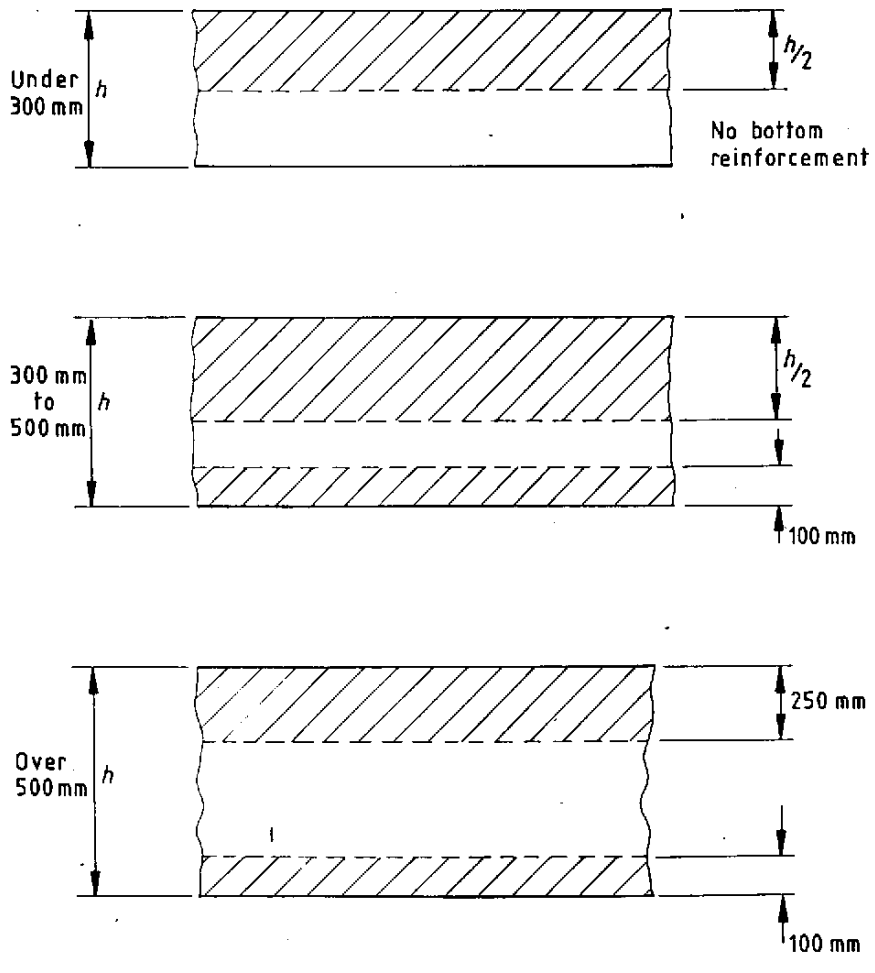

Figure A.2 Surface zones: ground slabs

Figure 2.9 Effective Concrete Area (BS 8007:1987)

2.3.2.4 Crack Width Calculation

As per BS 8007 the estimated maximum crack width that can develop in the concrete due to thermal changes is equated to the product of the maximum crack spacing and the restrained strain:

$$w_{max} = S_{max} \times \varepsilon \quad (2.7)$$

where,

- S_{max} is the maximum spacing of cracks as defined in equation 2.6 of section 2.3.2.3
- ε is the restrained strain

Here, ε, the restrained strain of the concrete is assumed to follow the relationship:

$$\varepsilon = R\ \alpha_{T,c}\ (T_1 + T_2),\ \text{(or otherwise } \varepsilon = 0.5\alpha_{T,c}\ (T_1 + T_2)\ ) \quad (2.8)$$

where,

- $\alpha_{T,c}$ is the coefficient of thermal expansion of the mature concrete
- R is the restraint factor that ranges from 0 to 0.5 (where creep is accounted for)
- T_1 is the drop in temperature from the hydration peak to the ambient temperature
- T_2 is the fall in temperature because of season variations

2.3.2.5 Restraint Conditions

The restraint that causes cracking may be either internal or external. Internal restraint is dominant where the concrete member is thick. Various external restraint conditions are given in figure A.3 of annex A in BS 8007, where the corresponding restraint factor R is given. As is evident in Figure 2.10, the restraint factor varies with its location within the member, the member's proportions, as well as the type of restraint it is subjected to (be it edge or end restraint). This may be illustrated in Figure 2.10 taken from BS 8007:

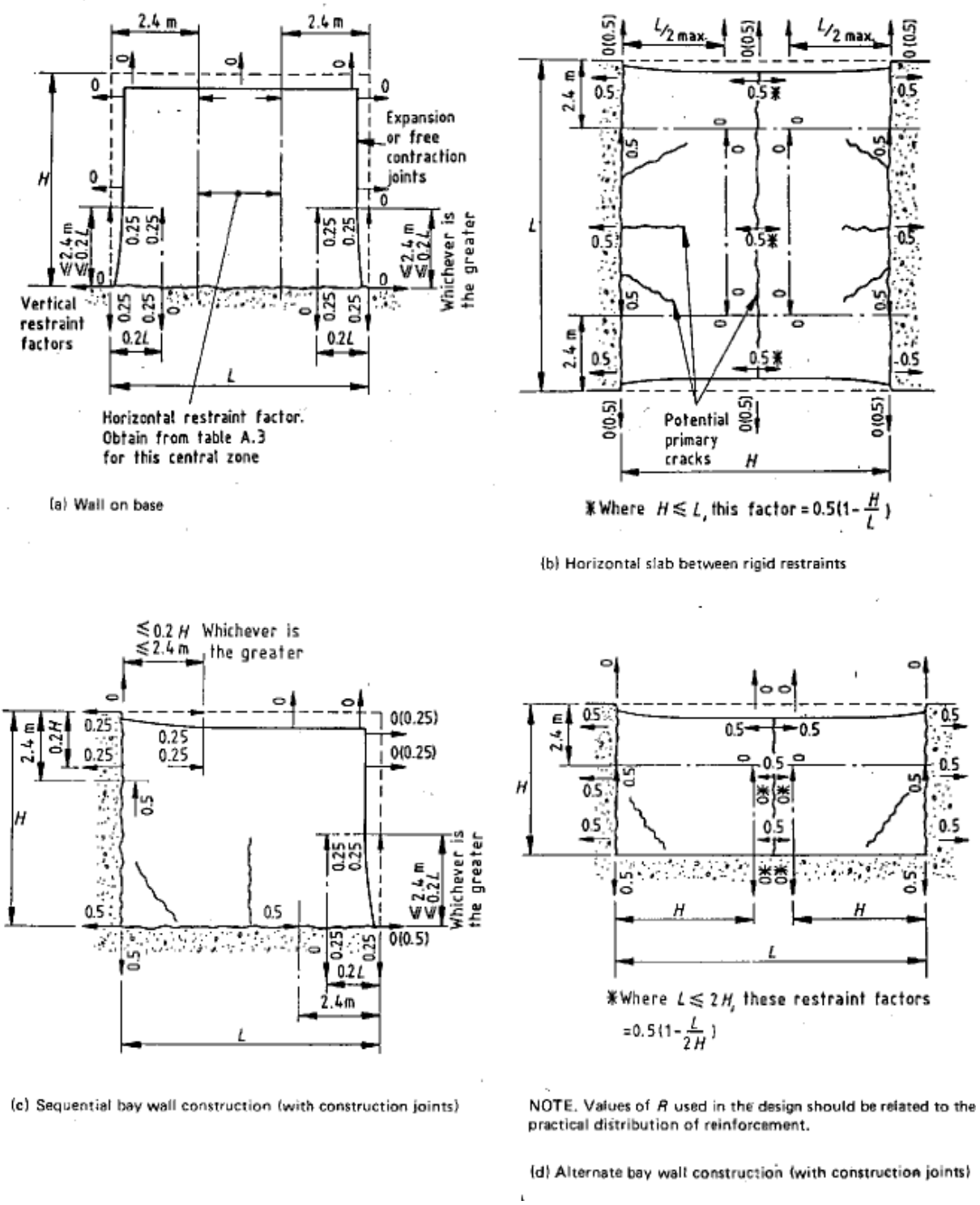

Figure 2.10: Restraint Factors (Figure A.3 of BS 8007:1987)

Table 2.2 (initially table A.3 of BS 8007:1987) presents the differences in the restraint factors from the fixed edge (e.g. the base for a wall slab) of a restrained member to the opposite free edge (e.g. the top section of a wall slab) of that same restrained member.

Table 2.2: Restraint Factors at Centreline of Slab (Table A.3 of BS 8007:1987)

Ratio L/H	Design Centreline Horizontal Restraint Factors	
	Base of Panel	Top of Panel
1	0.5	0
2	0.5	0
3	0.5	0.05
4	0.5	0.3
>8	0.5	0.5
• H is the height or width to the free edge • L is the distance between full contraction joints • All values of the restraint factor, except where the restraint is zero at the top panel, may be less where L < 4.8 m		

R = 0.5 is the restraint factor for a ground slab at mid-length cast onto smooth blinding concrete. This restraint applies for the seasonal change in temperature T_2, where the slab length is 30m or more. In accordance with BS 8007, the restraint factor R = 0.5 is assumed to vary uniformly from 0.5 to 0 at the ends of the slab.

Some restraint factors based on typical values of restraints that have been recorded for various pour configurations found in industry have been included in table 3.3 of BS 8110-2:1985, reproduced here as Table 2.3:

Table 2.3: Restraint Factors (Table 3.3 of BS 8110-2:1985)

Pour Configuration	**Restraint Factor**
Thin wall cast on to massive concrete base	0.6 to 0.8 at base
	0.1 to 0.2 at top
Massive pour cast into blinding	0.1 to 0.2
Massive pour cast on to existing mass concrete	0.3 to 0.4 at base
	0.1 to 0.2 at top
Suspended slabs	0.2 to 0.4
Infill bays, i.e. rigid restraint	0.8 to 1

2.3.3 Eurocode cracking model

2.3.3.1 Permissible Crack Widths

As with the BS 8007, the permissible crack widths for liquid retaining structures have been determined for structures depending on their function. The different categories concerning the degree to which permeability is permitted, as defined by EN1992-3, are as follows:

- Tightness Class 0 are all those structures where some degree of leakage will not be detrimental to the structures function. Here the permissible crack width will follow the requirements outlined in clause 7.3.1 of EN 1992-1-1. Under clause 7.3.1 of EN 1992-1-1 the permissible crack widths are listed in table 7.1 with the limits being:

Table 2.4: Exposure conditions to EN 1992-1-1:2004: Table 7.1

Exposure Class	**Reinforced Members and Pre-stressed members with Unbonded Tendons**
	Quasi-permanent Load Combination
X0, XC1	0.4 mm
XC2, XC3, XC4	0.3 mm
XD1, XD2, XD3, XS1, XS2, XS3	0.3 mm

Exposure conditions X0 and XC1 are for where the crack width has no real effect on the structures durability. Here the crack width limit is set for aesthetic reasons and would not apply to LRS.

- Tightness Class 1 deals with liquid retaining structures that are allowed to leak to some extent. There is some surface dampness and surface staining that is allowed to take place. Where cracks are expected to pass the section thickness, the crack width needs to be limited to w_{k1}. The crack limit w_{k1} is based on the ratio of hydrostatic pressure h_D to wall thickness h. If the ratio $h_D/h \leq 5$ then w_{k1} = 0.2mm, and where the ratio $h_D/h \geq 35$ then w_{k1} = 0.05mm.Values of crack width lying somewhere between these ratio may be interpolated. Where the crack is not expected to pass completely through the section thickness then the crack width may be limited to those outlined in clause 7.3.1 of EN 1992-1-1.
- Tightness Class 2 covers structures where leakage is to be kept to a minimum and where surface dampness and surface staining is not permitted. Under this tightness class, cracks that are expected to pass through the section are to be avoided altogether.
- Tightness Class 3 pertains to structures where no amount of leakage is permissible.

Where these crack limits are met, EN 1992-3 expects that the cracks should be able to heal themselves under normal changes in temperature and loading in service. This is assumed to

occur where strain under service conditions is expected to range below $150x10^{-6}$. It is important that these crack limits are met so that the self-healing of the cracks is made possible. Where the self-healing of the reinforced concrete doesn't take place, it is expected that any crack that forms will result in leakage.

2.3.3.2 Minimum Area of Steel

Under the same school of thought employed for the minimum required reinforcement for crack control in BS 8007, for the control of crack formation in the concrete the tensile force in the steel ($F_{steel} = A_s f_y$) should be at least the tensile force capacity of the concrete (where $F_{concrete} = A_c f_{ct}$– is the minimum force necessary to cause cracks to form in the concrete) or otherwise greater. Where this is satisfied, the steel reinforcement will not yield at the crack-inducing force. In this way, the steel reinforcement remains within the elastic range, which is an essential requirement for the validity of the crack width estimation under EN 1992 (Beeby and Narayanan, 2005). The derivation of the formula for minimum steel reinforcement given in EN 1992 does not account for where the steel reinforcement yields (Beeby and Narayanan, 2005). The minimum area of reinforcement required to control crack formation is given in EN 1992-1-1:2004 as follows:

$$A_{s,\,min} = \frac{k_c f_{ct,eff} A_{ct}}{f_{ky}} \tag{2.9}$$

where,

- $A_{s,\,min}$ describes the minimum area of reinforcement where the concrete section will be under tension.
- k_c is a coefficient that considers the stress distribution in the concrete section just before cracking occurs. The coefficient k_c is 1 for pure tension
- k is a coefficient that accounts for non-uniform self-equilibrating stresses that reduce the restraint forces. The coefficient will be 1 where the member's web, h, is up to 300 mm thick or when the member's flange is less than 300 mm wide. The coefficient k will be 0.65 where the member's web is at least 800 mm or has a flange with a width greater than 800 mm. Any values lying in between these limits may be interpolated.
- $f_{ct,eff}$ is the mean value of the concrete tensile strength for the time where the concrete is expected to first appear. For early age cracking this time is usually taken to be 3 days and for long term cracking the mean tensile strength is generally taken at 28 days.
- A_{ct} refers to the area of concrete that is under tension just before the formation of a crack.
- f_{ky} is the characteristic yield strength of the reinforcement.

2.3.3.3 Crack Spacing

The spacing of cracks in concrete members lies within S_o and $2S_0$, where S_0 is the minimum crack spacing and $2S_0$ is the maximum. Any distance beyond $2S_0$ will result in the formation of another crack. The crack spacing depends on the rate of transfer of tensile stress from the crack to the concrete; this is influenced by bond strength between the concrete and the reinforcement (Beeby and Narayanan, 2005).

The ensuing description of the crack spacing derivation follows from the works of Beeby and Narayana (2005) as well as from the design guide for crack control in reinforced concrete beams produced by the Centre for Construction Technology Research (2000). After the first crack occurs, slippage between the concrete and reinforcing bars will follow. Bond stress will then develop between the concrete and the reinforcing steel over a transfer length on either side of the crack. The minimum crack spacing may be equated to this transfer length,

$$S_{r,min}=l_{tr.}$$

The maximum crack spacing is twice the minimum crack spacing:

$$S_{r,max}=2l_{tr}$$

The transfer length may be described by the formula:

$$l_{tr} = \varphi f_{ct}/4f_b\rho,$$

in which φ is the bar diameter, f_{ct} is the tensile strength of the concrete, f_b is the average bond stress over the transfer length and ρ denotes the ratio of the gross cross-sectional area of concrete to the area of steel reinforcing .

This would then make the maximum crack spacing equal to:

$$S_{r,max} = \varphi f_{ct}/2f_b\rho.$$

The average crack spacing between cracks is assumed to be given by multiplying the transfer length by 1.5, giving the relationship:

$$S_{rm}= k_1\varphi/4\rho.$$

Where $k_1 = 1.5(f_{ct}/f_b)$, is a coefficient accounting for the bond characteristics of the concrete. Thus, including the effects of cover (a parameter found empirically to have a direct effect on the crack width), the average crack spacing may then be described using the equation:

$$S_{rm}= 2c + k_1k_2\varphi/4\rho_{p,eff}.$$

The inclusion of k_2 was to have the crack spacing formula also cater to cracking due to flexure since the crack spacing formula had been derived for concrete members under pure tension. The introduction of an effective tension area ($\rho_{p,eff}$) rather than the gross-cross sectional area (ρ) of the concrete also accounts for instances in which the concrete member is not just under pure tension in which the full cross section is under tension

EN 1992 puts forth that the maximum crack spacing that will result in the characteristic crack width having only a 5% probability of exceedance is 1.7 times bigger than the average crack spacing. This assumption was based on experimental data (Beeby & Narayanan, 2005). Thus the maximum crack spacing that appears in the EN 1992 is:

$$S_{r,\,max} = 1.7S_{r,m} = 3.4c + 0.425k_1k_2\varphi/\rho_{p,eff} \quad (2.10)$$

where,

- $S_{r,max}$ is the maximum crack spacing
- c is the value of the cover to the reinforcement
- k_1 is a coefficient that considers the bonding properties of reinforcement in the concrete. This coefficient is 0.8 where high bond steel reinforcement is used and is 1.6 in instances where reinforcement bars with a plain surface are used.
- k_2 is a coefficient that accounts for the distribution of strain. This coefficient is 0.5 for bending and 1 when dealing with pure tension (as for restrained shrinkage). Any values that lie between these above-mentioned values, the k_1 value may be determined using the formula $k_1 = (\varepsilon_1 + \varepsilon_2)/(2\varepsilon_1)$. In this formula, ε_1 represents the greater tensile strain at the boundary and ε_2 describes the lesser tensile strain.
- φ is the bar diameter of the steel reinforcement.

As per the requirements specified in EN 1992-3, in a situation where the steel reinforcement spacing exceeds $5(c+ \varphi/2)$ or where there is no bonded reinforcement in the tension zone, the maximum crack spacing becomes $S_{r.max} = 1.3(h-x)$.

The crack spacing formula includes the use of a reinforcement to effective concrete ratio ($\rho_{p,eff} = A_s/A_{c,eff}$) rather than the steel reinforcement to gross concrete ratio ($\rho = A_s/A_c$) used to determine the minimum required steel reinforcement for crack control. The effective concrete area is generally defined as being 2.5 times the distance from the tension face to the centroid of the steel reinforcement ($2.5(h-d)$), or limited to a third of the difference between the section thickness (h) and the neutral axis (x) for slabs ($(h – x)/3$) (Mosley, Bungey & Hulse, 2012). These limits are represented graphically in Figure 2.11.

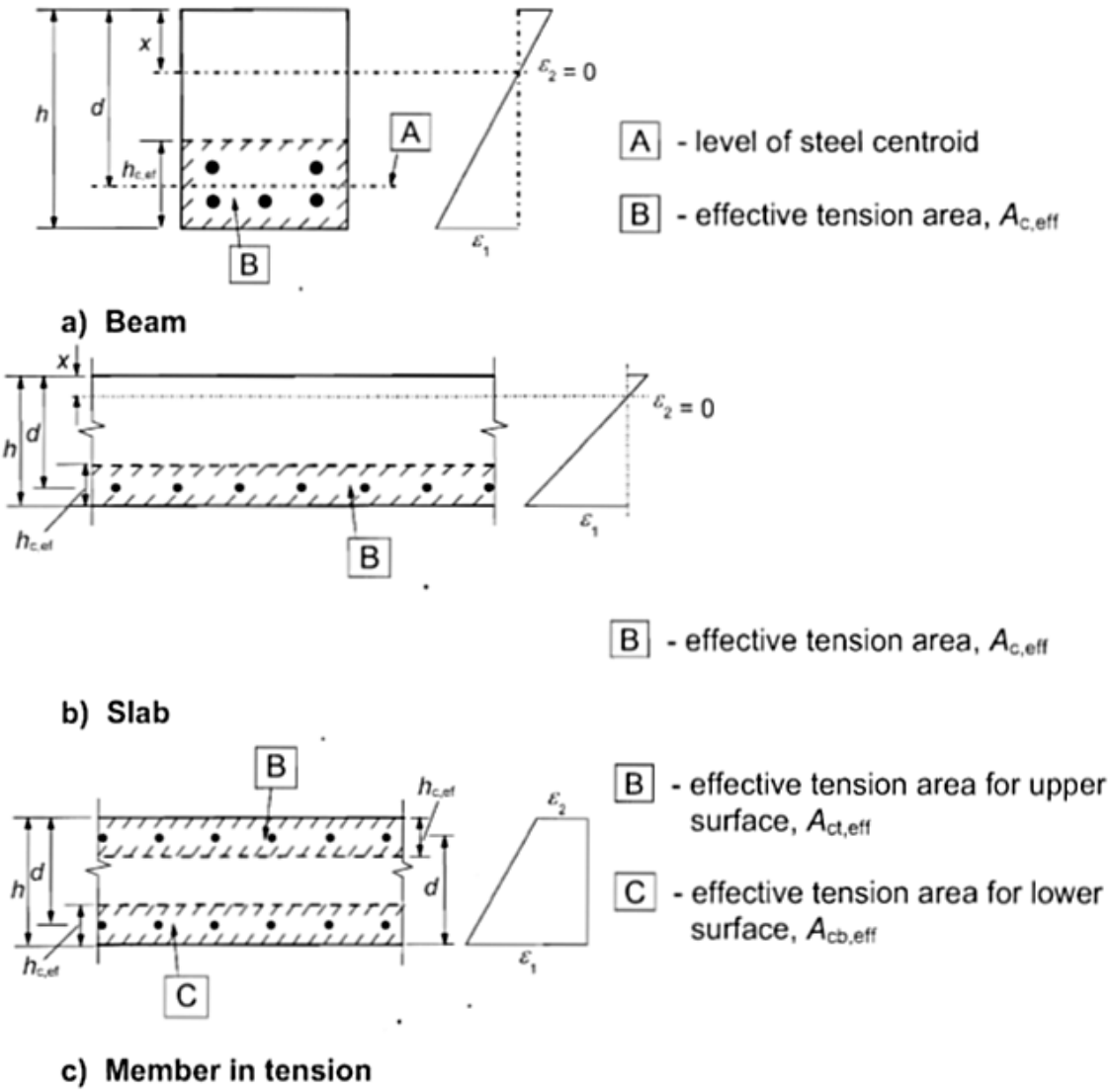

Figure 2.11: Typical Cases of Effective Concrete Area Following (Figure 7.1 of EN 1992-1-1:2004)

2.3.3.4 Crack Width Calculation

The calculation for the maximum crack width may be obtained from the compatibility equation given as (similar to BS 8007):

$$w_k = S_{r,\max}\,\varepsilon_r,$$

in which the crack width is equal to the product of the maximum crack spacing and the average strain. The strain induced by either an end or edge restraint is dealt with separately in EN 1992-3, unlike in the superseded BS 8007 standard which dealt with both end and edge restraint using the same equation. Where a member is restrained along its ends the restrained strain follows the equation:

$$\varepsilon_r = (\varepsilon_{sm} - \varepsilon_{cm}) = \frac{0.5\alpha_e k_c k f_{ct,eff}(1+1/\alpha_e\rho)}{E_s} \qquad (2.11)$$

where,

- ε_{sm} is the average strain in the reinforcement
- ε_{cm} represents the average tensile strain in the concrete between cracks
- α_e is the ratio of the steel modulus of elasticity of steel to the modulus of elasticity of concrete for the appropriate age of concrete
- k_c is the coefficient for stress distribution
- k is the coefficient that accounts for the effect of self-equilibrating stresses.
- $f_{ct,eff}$ is the mean tensile strength of the concrete at the time of cracking
- ρ is the ratio of steel area to the gross concrete area
- E_s is the modulus of elasticity of the steel reinforcement

Members that are restrained along one edge are estimated in EN 1992-3 by the following formula:

$$(\varepsilon_{sm} - \varepsilon_{cm}) = R_{ax}\,\varepsilon_{free}$$

where,

- R_{ax} is the restraint factor
- ε_{free} is the strain that would occur if the member were completely unrestrained

ε_{free} = The free strain may be approximated by:

$$\varepsilon_{free} = \varepsilon_{cd}+\varepsilon_{ca}+\alpha_{T,c}(\,T_1+T_2), \qquad (2.12)$$

where ε_{cd} is the drying shrinkage strain, ε_{ca} is the autogenous shrinkage strain; $\alpha_{T,c}$ is the coefficient of thermal expansion of concrete, T_1 denotes the fall in temperature from hydration peak to mean ambient temperature in the concrete. T_2 is the seasonal fall in temperature.

2.3.3.5 Restraint Conditions

The restraint factors that may be obtained for calculations under EN 1992-3 may be obtained in the same way as BS 8007. As in BS 8007, the factors for common situations and construction sequences are given in the code (figure A.3 of BS 8007 was reproduced as figure L.1 of EN 1992-3. Also, table A.3 of BS 8007 is as table L.1 of EN 1992-3).

2.3.4 Issues Surrounding Crack Width Estimation

There has been much deliberation around the way in which crack formation may be estimated with many variations of the crack width model currently available, according to Caldentey *et al*. (2013). The crack spacing has been modelled in as much as 23 different ways (Caldentey *et al.,* 2013). Many national codes differ in their formulation of the crack spacing (Beeby & Narayanan, 2005). One particular point of contention regarding the Eurocode 2 crack model involves the inclusion of the $\varphi/\rho_{p,eff}$, whose influence on the crack spacing has been questioned by Beeby (2004) article entitled *The Influence Of Parameter Φ/P Eff on Crack Widths* for the journal

Structural Concrete (as cited in Caldentey *et al*., 2013). Beeby (2004) stated further that the real influence the $\varphi/\rho_{p,eff}$ ratio may have on the crack spacing is due to the implicit consideration of the concrete cover parameter in the ratio of reinforcing steel to effective concrete area, $\rho_{p,eff}$ (Caldentey *et al.*, 2005).

Caldentey *et al.* (2013) conducted an experiment on the influence of concrete cover and the $\varphi/\rho_{p,eff}$ ratio on the crack spacing for cracks induced under flexure, where 12 beam specimens were loaded at a constant moment span of 3.42 m. All the rectangular cross-sections used were 0.35 m by 0.45 m and were made of class C25/33 concrete. Different reinforcement configurations were looked at, one with no stirrups, and another with stirrups (8 mm diameter) spaced at 100 mm and 300 mm centre to centre respectively. Caldentey *et al*. (2013) showed clearly in this research that crack spacing, and thus the crack width, increased with an increase in concrete cover to reinforcement. This result confirmed that cover was, in fact, an important part of the estimation of crack spacing for the load induced crack case. The inclusion of cover in the EN 1992 crack spacing formula comes after previous experimental findings revealed the concrete cover to be an important contributor to crack spacing (Caldentey *et al.*, 2013). The influence of $\varphi/\rho_{p,eff}$ may be derived, using bond theory, from the equilibrium of the reinforcement bar and the parts of the concrete cross section found between the crack and the section of zero slip. The concept of transfer length is applied in this instance (Caldentey *et al.*, 2013).

The bond theory to which the $\varphi/\rho_{p,eff}$ ratio is based still stands for both the load-induced case, which may mean that its influence in the restrained shrinkage case could be comparable to that of the load-induced cracking case. The same crack spacing equation used to predict the crack widths of load induced cracks in EN 1992 is also used for the restrained shrinkage case. The EN 1992 crack spacing model was conceptually derived for concrete members under pure tension. Accounts are taken for instances of flexure through the introduction of coefficient k_2 and the effective steel ratio ($\rho_{p,eff}$) where only parts of the concrete section will be experiencing tension. Thus, the modifications (particularly of the second term) of the EN 1992 crack spacing equation allows for a crossover in application. The contribution made by concrete cover towards the crack spacing, as theorized by Caldentey *et al.* (2013), is through the need for the transfer of stresses from the reinforcing steel to the centre of the effective concrete area located on either side of the bar. It must be reiterated that the findings made by Caldentey *et al.* (2013) on the influence of either variable are based on cracks due to bending. Data on the influence of concrete cover on crack spacing for the restrained shrinkage case were not found. However, it could be assumed that this parameter would be influential in this case. The same may be said about the $\varphi/\rho_{p,eff}$ variable.

Caldentey (2005) had also compiled an earlier report in which Beeby's 2004 claim had been challenged. In this report, Caldentey (2005), put together several tests done by others on this matter and compared their findings. The data in these tests were obtained with the cover being kept mainly constant, whilst the $\varphi/\rho_{p,eff}$ ratio was varied. The works of Hartl (1977), Eligehausen (1976) and Rüsch & Rehm (1963) were reviewed. The experiments reviewed were for concrete tested in tension.

Hartl's (1977) test had square concrete elements being subjected to pure tension, reinforced with just one reinforcing steel rod where it was revealed that, even though the $\varphi/\rho_{p,eff}$ ratio and concrete cover were both found to influence the crack spacing, the influence of the $\varphi/\rho_{p,eff}$ ratio could not be distinguished from that of the cover in this experiment. Here changing the $\varphi/\rho_{p,eff}$ ratio required changing the bar diameter value, which implied a change in the concrete cover value. Eligehausen (1976) found that the $\varphi/\rho_{p,eff}$ ratio had a small influence on crack spacing, while Rüsch & Rehm (1963) determined that crack spacing became smaller with an increase in the $\varphi/\rho_{p,\,eff}$ ratio. Rüsch & Rehm's (1963) results were found to have been effected by the reinforcing configuration, the difference in the types of ribs used in the reinforcement and reinforcing cross section between specimens having similar concrete cover values. The paper eventually concluded that Andrew Beeby's theory was, in fact, sound and that the $\varphi/\rho_{p,\,eff}$ ratio had no real effect on crack spacing. It was further stated that the use of this ratio in the current formula for crack spacing in EN 1992-1-1 is due to there being a lack of critical examination into a more suitable formula.

Essentially, as may have been deduced from the earlier studies, the crack spacing may be separated into two terms (Kaethner, 2011). That is, crack spacing is the sum of the cover zone cracking (k_3c, contributing 50- 80% of the crack spacing value) and the cracking near the bar ($k_1k_2k_4\varphi/\rho_{p,eff}$, contributing 20-50% of the value). In an investigation carried out by Kaethner (2011) comparing the two terms found in the crack spacing formula to those values of the crack width at the concrete surface and at the bar surface found in practice. It was found in this comparison that the calculated cover term contributed less to the crack spacing than found in practice. However, the bar slip term predicted a stronger value than what may be observed in practice. Kaethner's (2011) findings once again prove the relevance of both the concrete cover and bar slip term in the EN 1992 crack spacing formulation- both of which having a clear contribution to the ultimate value of the crack width (particularly the cover term). Although, the experimental data collected were done so on cracks resulting from flexural loading. The observation made is represented graphically in Figure 2.12:

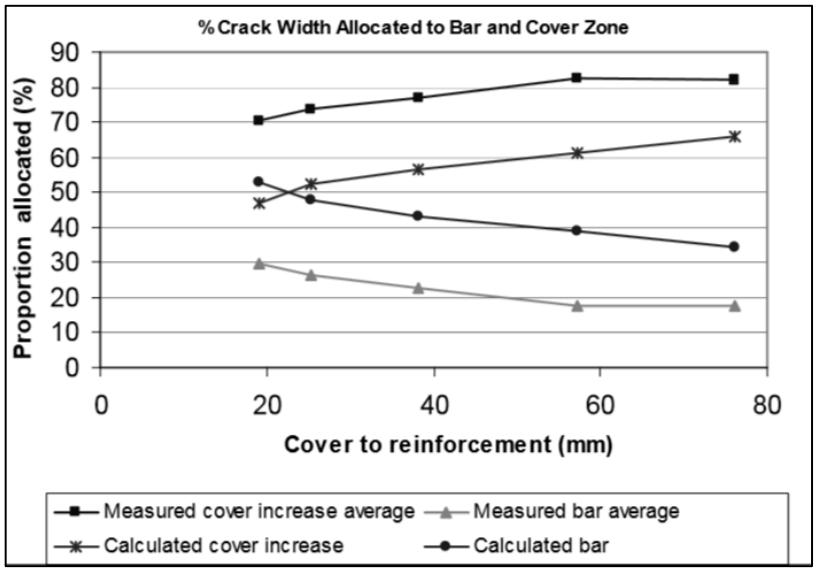

Figure 2.12: Comparison of the Cover and Bar Slip Terms of the EN 1992 Crack Spacing Formula with Experimental Data (Kaethner, 2011)

Most findings relating to the crack spacing formulation, and in particular the debates of the inclusion of either the cover term or the bond slip term in EN 1992, have included experiments and observation based on the load induced cracking case. It is recommended for future research that the same exercise is extended towards cracks resulting from restrained shrinkage.

A study was conducted by Bamforth, Denton and Shave (2010) on the development of a unified approach to estimating crack width from both end and edge restraint. In this study it was concluded that the methods used in determining the edge restraint in Eurocode 2 were based on flawed assumptions. For instance, different parameters are used to calculate edge restraint and end restraint, resulting in the formulae being considerably different. Bamforth *et al. (2010)* also noted in this study that, for the edge restraint case of both BS 8007 and EN 1992, the transfer of the load from the restrained concrete member onto the reinforcing steel when cracking occurs was neglected. This stands contradictory to the concept behind the required minimum amount of reinforcing steel for crack control which is based on the idea that the steel reinforcing carries the load from the concrete section after cracking (Bamforth *et al., 2010)*.

It was found in this investigation into the EN 1992-3 edge restraint crack model that the geometry of the restrained member had not been considered in the crack spacing equation. Bamforth *et al*. (2010) observed that the tensile strength of the concrete was also not accounted for in the edge restraint model. In addition to this, the positive effect that the restraining member has on the crack formation was neglected. Here, Bamforth *et al*. (2010) suggests that the restraining base member actually works to prevent the crack widths that are generated from reaching their full potential.

Moreover, the minimum reinforcement area as determined using EN 1992-1-1 was found to be conservative when applied to the edge restraint crack model (Bamforth *et al*., 2010). Instead, Bamforth *et al*. (2010) suggest that further research is required to develop a crack model that better models the formation of cracks in structures.

Bamforth's unified method assumes the formation of the maximum crack width follows the model for end restraint in EN 1992-3. However, where edge restraint is being considered, Bamforth (2010) suggests development of the same maximum crack would be reduced due the following factors:

- Some of the load is transferred to the restraining member and so decreases the amount of load that would normally get transferred to the reinforcement.
- The edge restraint prevents the crack width from expanding to its full potential width.
- The existence (or non-existence) of cracks in the concrete may determine the degree of stress relaxation between cracks, potentially affecting any new cracks that forms.

In this new model developed it is suggested that cracks actually develop in 2 stages:

- Stage 1 cracking is based on the EN 1992-3 model for end restraint, the only modification made in this stage is the inclusion of the effect of the edge restraint. The edge restraint inhibits the extent to which the cracks may open and attracts some of the load onto the restraining member. In stage 1, a crack of width w_{k1} opens instantaneously and part of the load is transferred onto the reinforcement. The relative lengths of the cracked (assumed length of debonding) and uncracked lengths are accounted for in this stage.
- The second stage of the crack model considers the continued contraction of the cracked concrete relative to the steel reinforcing (the crack width opens up further by a value w_{k2}). As with stage 1, it is assumed that increased restraint reduces the extent to which cracks may open.

The full crack width would then amount to the sum of the cracks obtained at each stage of cracking ($w_k = w_{k1} + w_{k2}$). Bamforth (2010) found, after comparison to observed cracks, that the proposed unified approach better reflected the formation of crack widths for edge restraint then EN 1992-3 currently does.

2.4 **Autogenous healing**

Autogenous healing (self-healing) of concrete, according to EN 1992-1-1:2004 is said to occur to some degree in all concrete structures. In a technical report, Edvardsen (1999) identified the participation of calcium carbonate crystals as being the main culprit of self-healing in concrete (Edvardsen, 1999). Other contributors to concrete's autogenous healing observed by Edvardsen (1999) include: the flow of the concrete being blocked by impurities from the water or loose particles from the cracking and swelling of the cement paste during hydration. Essentially, all of the mentioned contributors to the concrete's self-healing serve to reduce the amount of water flowing through the member with time. Other more secondary causes include the crack width, water hardness of the retained water, aggregate type as well as the type of cement used for the structure and the water pressure (Edvardsen, 1999) . Self-healing of the concrete was also said to generally occur during the first 3 to 5 days of the concrete structure. In EN 1992-1-1: 2004, it is suggested that a crack width of 0.05 mm with a water pressure gradient (water depth to wall thickness) limited to 35 would heal itself. This is also true for crack widths of 0.2 mm with a water pressure gradient of up to 5. Crack widths with water pressure gradients between these two values may also heal autogenously.

At current, the South African equivalent of the EN 1992-3 (2006) design code, namely SANS 10100-3, is in the draft phase. However, some of what may be expected by designers were outlined in a research paper by Wium, Retief and Barnardo-Viljoen (2014) and reiterated in a doctoral thesis by Retief (2015). Wium *et al.* (2014) noted that the jump in the crack width limitations set out by BS 8007 to the stricter crack limits of the EN 1992-3 design code would incur considerable increases in cost to meet those more rigorous limitations in crack width. The EN 1992 crack width limit required increases in reinforcement of factor 1.4 and 2 where the crack width limit was reduced from the BS 8007 specified 0.2 mm to crack widths of 0.1 and 0.05 mm respectively- which are crack limits included within the EN 1992 specified range of permissible crack widths (McLeod, Retief & Wium 2013). The SANS 10100-3 draft was reported to have done away with the rigorous crack limits of EN 1992-3 and employ those crack limits of BS 8007 instead (Wium, Retief and Barnardo-Vijoen, 2014). Although, it must be noted that the implications of the more onerous crack width limits stipulated by the EN 1992 as compared to those of BS 8007 were considered for the load induced cracking case and not for cracks resulting from restrained deformation. Extending this investigation to include the restrained strain crack model would present a complete gauge of the ramifications of the change in crack width limits from BS 8007 to EN 1992-3. It was suggested by Retief (2015) that a rational basis for the use of the more onerous EN 1992 crack limits may be established through a probability-based economic optimisation.

An experimental research aimed at studying the phenomenon of autogenous healing was carried out and the results reported in a technical paper for the American Concrete Institute Materials Journal (Edvardsen, 1999). The experiments were conducted on concrete specimens with a single tension crack set in each specimen. The crack widths tested in this experiment were 0.1, 0.2 and 0.3 mm respectively. The crack lengths varied at 200, 300, and 400 mm with the water head varied from 2.5 to 20 m of water. The hydraulic gradient (water pressure head /thickness of structure) for this research varied from 6.25 to 50. It was determined in this investigation that for 50 % of the specimens with a 0.2 mm crack width and hydraulic gradient of 6.25 (water pressure head of 2.5 m) healed completely in 7 weeks. For 25 % of the specimens with a 0.2 mm crack width and hydraulic gradient of 25 (water pressure head of 10 m), the concrete specimen also healed within 7 weeks. The experiments showed that the influence of the hydraulic gradient on the water flow was smaller than that of the crack width. The permissible crack widths, expected to obtain almost total self- healing, recommended for use after the experimentation were (Table 2.5):

Table 2.5: Permissible Crack Widths for Autogenous Healing (Edvardsen, 1999)

Hydraulic gradient (m/m)	*w_k (mm)	$^{+}w_k$ (mm)
40	0.1 to 0.15	≤ 0.1
25	0.15 to 0.20	0.10 to 0.15
15	0.2 to 0.25	0.15 to 0.20
Notes: *$\Delta w \leq 10\%$ $^{+}10\% \leq \Delta w \leq 90\%$		

In a similar study on the influences of both hydraulic pressure and crack width on the water permeability of crack- induced concrete specimens, Yi, Hyun and Kim (2011) found that as the crack width and hydraulic pressure increased, so did the transport of water through the concrete. Three particular crack widths were examined in this study, namely 0.03, 0.05 and 0.1 mm. The permeability of the water through the crack-induced concrete specimens was measured for hydraulic pressures of 0.01, 0.025, 0.05 and 0.2 MPa. Yi *et al*. (2011) determined in this study that crack widths smaller than 0.05 mm had little effect on the permeability of the concrete due to autogenous healing. Where the crack widths were found to be between 0.05 mm to 0.1 mm, with a hydraulic pressure greater than 0.025 MPa, the permeability of concrete increased considerably. Ultimately, Yi *et al*. (2011) suggested that in the case where a structure experiences a hydraulic pressure of less than 0.01 MPa, the allowable crack width may be set at 0.1 mm. For

a hydraulic pressure of 0.025 MPa or greater, the allowable crack widths should be 0.05 mm (or otherwise be between 0.05 and 0.1 mm).

Yet another test on the phenomenon of autogenous healing carried out at the University of Kwa-Zulu Natal (Mans, 2012) revealed that concrete samples with a crack width of ±0.2 mm through cracks showed considerable healing within 72 hours of testing. The test was conducted for 250 hours under a hydraulic gradient of 12.

Conclusively, it may be deduced from the various experiments studied herein that the autogenous healing does, in fact, occur between the crack widths of 0.05 mm and 0.2 mm as suggested by EN 1992 with a similar range of hydraulic gradients proposed by EN 1992. Moreover, the size of crack widths was found to have more of an influence on the concrete's permeability than the hydraulic gradient. Although, still increasing the size of both the crack width and the hydraulic gradient would result in an increase in the permeability in of the concrete.

2.5 Conclusion

Liquid retaining structures in South Africa are designed using design code BS 8007 and those relevant parts of BS 8110-2. The replacement of BS 8007 and BS 8110-2 with EN 1992-3 and EN 1992-1-1 respectively for the design of liquid retaining structures presents South African engineers with the opportunity to also changeover into the use of the Eurocodes for LRS design. Much stands to be gained from Eurocode adoption, namely reaping from the technical expertise of the Eurocodes with supporting design guides and software easing the transition into adoption. Additionally, there would be an increase opportunity for local engineers to participate in some international projects. Moreover, the choice to either adapt or adopt is a less demanding alternative than the more labour intensive, expensive and time-consuming task of developing a completely new code. However, the question of the possible implications of this changeover of codes as applied in the South African context is raised. These implications have already been quantified for the load induced cracking case by past researchers, making an investigation into these implications for the restrained shrinkage cracking case relevant.

Points of interest raised by past researchers and to be further investigated in this research include the implications of the more stringent crack limits of the EN 1992 crack model, the influence of the concrete cover and $\phi/\rho_{p,eff}$ values on the crack spacing, and issues surrounding the ways in which the edge and end restrained strain are modelled. Ultimately, a better understanding of the EN 1992 crack model would aid towards improving its reliability for the South African

environment. The increased demand of the EN 1992 cracking serviceability limit state as compared to the ultimate limit state gives a reliability analysis into the EN 1992 crack model significance (evidently, since the failed compliance of the crack limits may lead to the loss of structural integrity).

Chapter 3: Structural Reliability

3.1 Introduction

The reliability of a structure is described as its ability to successfully perform its function under working conditions throughout its required working life (Green, 1972). No structure or system can perform at 100% reliability. One can expect some probability of failure in the structure's lifetime as the engineer cannot escape from uncertainties that exist in design. Some examples of where uncertainties in design may arise include, amongst others: the randomness of geometric data, statistical uncertainties, simplification of actual conditions in determining theoretical models and errors in design (Holický, 2009). The effect of these uncertainties on the design may be quantified and evaluated through probabilistic concepts and reliability theory. The idea of using reliability concepts in engineering design is not a new one, dating as far back as World War One. During World War One there was increased interest in knowing the failure rate of flights, consequently a reliability criterion was developed to ensure maintenance of a reasonable failure rate (Green, 1972). Determining the failure probability of a system is important in that it will not only help in evaluating whether or not the system performs satisfactorily in its lifespan, but it may also help to avoid dire financial loss from system failure. The principles involved in reliability theory are outlined hereunder.

3.2 Limit State

The satisfactory performance of a structure is ensured by the implementation of limit states. The performance limit states of structures may be thought of as a kind of boundary, beyond which the structure will be considered inadequate. Limit states may be divided into two major categories, namely the ultimate limit state and the serviceability limit state. The ultimate limit state deals with the collapse of the structure as well as the safety of its occupants. Whereas the serviceability limit state pertains to the normal working conditions of the structure with its most important areas of concern being: deflection, cracking and durability (Mosley *et al*., 2012). The serviceability limit state can be further broken up into irreversible and reversible limit states. The irreversible serviceability limit state, as can be deducted from the name, is where the damage caused remains permanent even after the cause of the damage itself has been removed. Contrary to this state is the reversible serviceability state where the damage incurred does not remain permanent even after the cause of the damage is removed (Holický, 2009). Generally, the ultimate limit state has taken on greater relative importance to the serviceability limit state. However, for liquid retaining structures, the serviceability limit state takes on more importance in the structure’s performance.

A crack width that is wider than what is allowed for under the serviceability limit state will result in the structure becoming permeable and thus losing its structural integrity.

3.3 Basic Reliability Theory

A model is a representation of an existing object or phenomenon in which some aspects of this representation vary somewhat from the original object or phenomenon. This is because some simplifications and assumptions have to be made in the development of the representative model. Subsequently, uncertainties may arise from the simplifications and assumptions made in forming the model (Croce, Diamantidis and Vrouwenvelder, 2012). Other sources of uncertainty are the characteristic randomness of a physical phenomenon, as well as the predictions of states of nature made with inadequate information (Ang and Tang, 1984). With increased data and information, models representing physical phenomenon may be improved and made more accurate with inadvertent biases reduced. However, the inherent randomness of physical phenomena cannot be avoided. It cannot be guaranteed with absolute certainty that a variable will take on a particular value; instead, a range of possible outcomes may be attributed to this same variable. The likelihood of occurrence for a specific value may be determined by its probability distribution function (Holický, 2009).

As described by Ang *et al*. (1984), most engineering problems may be described as supply and demand problems where the safe state of the structure is where the supply exceeds the maximum amount of demand experienced over a lifetime. The supply and demand may be expressed as either random variables (X_i) or functions of random variables with their own distribution functions. In other words, the resistance of a structure (R) needs to be greater than the action effect (E) of the structure in order for the structure to remain reliable (E<R). The performance function separating the safe state of the structure or engineering process may be expressed as:

$$g(X_i) = R-E = 0 \tag{3.1}$$

A negative value of the performance function is indicative of a failure in performance, whilst a positive answer shows that the resistance of the structure exceeds the load effect and thus the structure is safe. The limit state may be defined as the distinct separation between the safe state of the structure where it performs reliably and the unsafe state where it no longer functions. So primarily, the performance function, $g(X_i)$, is itself a limit state.

The equivalent normal distributions of the demand and supply variables are used to approximate the failure probability. Where the reduced variate (equivalent normal variate) of the resistance (supply) may be described by the equation 3.2:

$$R' = \frac{R - \mu_R}{\sigma_R}, \tag{3.2}$$

where μ_R and σ_R respectively denote the mean and standard deviation of the resistance variable. And the reduced variate of the action effect E (demand) may be determined using the formula:

$$E' = \frac{R - \mu_E}{\sigma_E}, \tag{3.3}$$

where μ_E and σ_E are the respective symbols for the mean and standard deviation of the action effect, E. Then the performance function may be rewritten as:

$$g(X_i) = R' - E' = 0. \tag{3.4}$$

This then equates to,

$$g(X_i) = \sigma_R R' - \sigma_E E' + \mu_R - \mu_E = 0$$

Then the linear failure distance from the origin to the failure line $g(X_i) = 0$ can be expressed as:

$$\beta = \frac{\mu_R - \mu_Y}{\sqrt{\sigma_R^2 - \sigma_E^2}} = \frac{\mu_G}{\sigma_G}, \tag{3.5}$$

This distance β is the safety index, and describes the shortest distance from the reduced variate origin to the limit state (Wu, Lo and Wang, 2011). In other words, this distance describes the distance to the most likely point of failure along the limit state (this is illustrated in Figure 3.1). In general, a structure is said to be in a desirable state where the limit state function is greater than zero and at values less than zero the structure will be in an undesirable state. At zero, the structure just meets the limit state as shown in Figure 3.1.

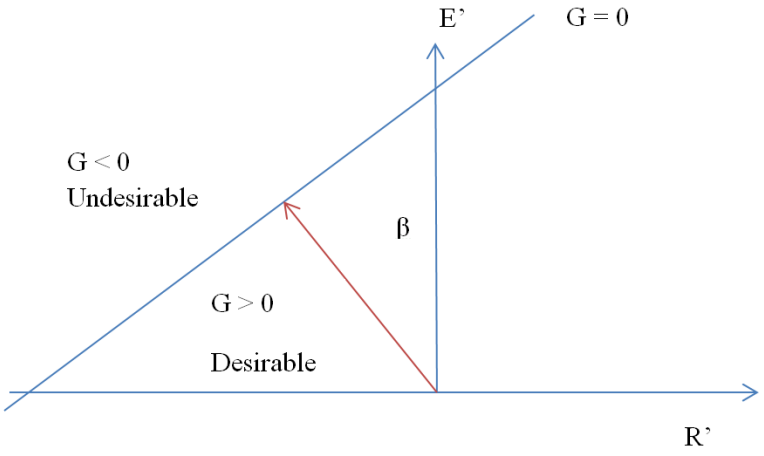

Figure 3.1: Space of Reduced Variates E' and R' (as adapted from Ang and Tang. (1984))

For the serviceability limit state, the performance function described above is structured such that an exceedance of a limiting design criterion (like a set deflection value, or in this case an allowable crack width) would take the form:

$$g(X_i) = C - S = 0, \tag{3.6}$$

where C represents the serviceability criterion in question and S denotes the action effects (as described in SANS 2394:2004). Clearly, regarding cracking in liquid retaining structures, where the action effect exceeds the serviceability criterion the limit state would be exceeded and the undesirable (unsafe) state entered into. The EN 1992 cracking serviceability limit state may be similarly formulated:

$$g(Xi) = w_{lim} - \theta w, \tag{3.7}$$

where w_{lim} describes the permissible crack limit and w represents the mean crack width based on the EN 1992 maximum characteristic crack width. In developing the crack width formula for EN 1992-1-1 it was determined through experimental data that a factor of 1.7 be applied to the average crack spacing in order to calculate the maximum crack width (Beeby and Narayanan, 2005). However, the reliability analysis undertaken herein (described in chapter 5) requires the use of the mean crack width and so a reduction in value of 1.7 to the EN 1992 maximum characteristic crack width formula should return a function for the mean crack width.

The value, θ accounts for the model uncertainty in the EN 1992 crack model and is regarded as a random variable in the reliability analysis. An elaboration of the formation of the limit state function to be used in this investigation is given in chapter 5.

The probability of safety may then be determined by:

$$p_s = \Phi(\beta), \tag{3.8}$$

where Φ is the standardized normal distribution function and β is the reliability index as defined in equation 3.5. The failure probability may then be determined using the relationship $p_f = 1 - p_s$, so that $p_f = 1 - \Phi(\beta) = \Phi(-\beta)$.

A simple illustration of the relationship between the reliability index and the failure probability may be outlined in Table 3.1:

Table 3.1: Relationship between Failure Probability and Reliability Index JCSS Part 1 (Joint Committee of Structural Saftey, 2001).

P_f	10^{-1}	10^{-2}	10^{-3}	10^{-4}	10^{-5}	10^{-6}	10^{-7}
β	1.3	2.3	3.1	3.7	4.2	4.7	5.2

3.4 Reliability Index and Target Reliability

The reliability index, β, is indicative of a structure or engineering phenomena's failure probability over the lifetime of the structure, thus the designer may design a structure to meet a certain reliability index. This particular reliability index may be referred to as the target reliability index, β_t. In other words, in designing towards a specific target reliability index, the designer is ensuring that the structure does not fail beyond an accepted failure probability (Holický and Marková, 2012). The reliability index may be determined using reliability methods, the obtained β value may subsequently be compared to the target reliability (β_t) for its class of structure and design working life (the design working life of the structure may be defined as the period of time in which the structure is intended to be in use without there being any major repair required. Although, it is expected that the structure will have to encounter some minor maintenance attempts throughout its service life (Holický, 2009)). An acceptable structure is one where the target reliability is either just met or the reliability index calculated is approximately equal to the target reliability index (Holický and Marková, 2012). The JCSS (Joint Committee on Structural Safety) have recommended a set of reliability indices for use under both the ultimate limit state as well as the serviceability limit state. Their recommended values for the ultimate limit states are as follows:

Table 3.2: Ultimate Limit State Target Reliability Indices and Related Failure Probabilities for a 1 Year Reference Period (Joint Committee of Structural Saftey, 2001).

1	**2**	**3**	**4**
Relative cost of safety measure	**Minor consequences of failure**	**Moderate consequences of failure**	**Large consequences of failure**
Large (A)	$\beta = 3.1$ ($p_f \approx 10^{-3}$)	$\beta = 3.3$ ($p_f \approx 5\ 10^{-4}$)	$\beta = 3.7$ ($p_f \approx 10^{-4}$)
Normal (B)	$\beta = 3.7$ ($p_f \approx 10^{-4}$)	$\beta = 4.2$ ($p_f \approx 10^{-5}$)	$\beta = 4.4$ ($p_f \approx 5\ 10^{-6}$)
Small (C)	$\beta = 4.2$ ($p_f \approx 10^{-5}$)	$\beta = 4.4$ ($p_f \approx 5\ 10^{-6}$)	$\beta = 4.7$ ($p_f \approx 10^{-6}$)

The above-mentioned values are also based on a cost-benefit analysis for a representative set of engineering structures. As can be deducted from the table, the indices are categorized according

to relative cost of safety measure and level of failure consequence. The failure consequences are determined from looking at the ratio between the total costs (which includes the sum of the construction cost and failure costs) and construction cost. Where this ratio is less than 2, the structure may be categorized as having a minor consequence failure (minor risk to life, with negligible economic loss in instance of failure). If the total cost to failure cost ratio were to be somewhere between 2 and 5, then the structure may be seen as having a moderate consequence of failure (there is a moderate level of risk to life in the event of failure and economic loss, in this case, would be significant). The last class of failure consequence, the large consequence of failure class, is for structures where the ratio lays between 5 and 10. In this class, the risk to life and economic loss in the case of failure is sizeable.

The target reliability indices as recommended in part of 1 of the Probabilistic Model Code (JCSS, 2001) for the irreversible serviceability limit state are listed in the following table:

Table 3.3: Irreversible Serviceability Limit State Target Reliability Indices and Related Failure Probabilities for a 1 Year Reference Period (Joint Committee of Structural Saftey, 2001).

Relative Cost of Safety Measure	**Target Index (Irreversible SLS)**
High	$\beta = 1.3$ ($p_f \approx 0.1$)
Normal	$\beta = 1.7$ ($p_f \approx 0.05$)
Low	$\beta = 2.3$ ($p_f \approx 0.01$)

Values for the reversible serviceability limit state have been given no real general rule in this JCSS document. In EN 1990 (Eurocode 0), the target reliability index of an ultimate limit state for a reference period of 1 year is given by $\beta_{t,1} = 4.7$. The reliability indices then for time periods other than a year may be calculated from the approximate formula (Holický, 2009):

$$\Phi(\beta_{t,n}) = [\Phi(\beta_{t,1})]^n,$$

where n denotes the number of years.

Holický (2009) puts forth that where a structure is to be designed for a particular reliability level and design working life, the target reliability index for the 1 year reference period may be changed accordingly. For instance, for a structure designed for a target reliability index of 3.8 and a design working life of 50 years, the target reliability index for the reference period of 1 year should be $\beta_{t,1} = 4.7$. It must be noted that the above-mentioned reliability indices represent the same level of reliability, namely an accepted lethal accident rate of 10^{-6} per year applied to different reference

periods. Additionally, for the same 3.8 target reliability index and a 25-year design life, the 1 year reference period's reliability index should be set at 4.5 (Holický, 2009).

The target reliability indices with corresponding reliability classes and limit states as presented in EN 1990 are reproduced in the following table:

Table 3.4: Suggested Reliability Classes and Recommended Minimum Values for Reliability Index β from EN 1990 for Ultimate Limit State, Fatigue and Serviceability Limit State (Holický, 2009).

		Minimum Values for β					
		Ultimate Limit States		**Fatigue**		**Serviceability (Irreversible)**	
Reliability Class	**Building Example**	1-Year Reference Period	50-Year Reference Period	1-Year Reference Period	50-Year Reference Period	1-Year Reference Period	50-Year Reference Period
RC-3 High	Bridges, public buildings	5.2	4.3				
RC-2 Normal	Residential and office buildings	4.7	3.8		1.5 to 3.8	2.9	1.5
RC-1 Low	Agricultural buildings, greenhouses	4.2	3.3				

The class divisions – high, normal (moderate) and low – set out in the above-mentioned EN 1990 table of reliability indices follow much of the same descriptions as those mentioned in the JCSS part 1 (2001). Another code of practice that recommends values for the target reliability index for the design of structures is ISO 2394:1998 (SANS 2394:2004), which summaries the indices as follows:

Table 3.5: ISO 2394 Lifetime Target Reliability Indices (Holický, 2009).

Relative cost of Safety Measures	**Consequences of Failure**			
	Small	**Some**	**Moderate**	**Great**
High	0 (reversible serviceability limit state)	1.5 (irreversible serviceability limit states)	2.3 (fatigue limit states)	3.1 (ultimate limit states)
Moderate	1.3	2.3	3.1 (fatigue limit states)	3.8 (ultimate limit states)
Low	2.3	3.1	3.8	4.3 (ultimate limit states)

The shaded values from this table are those values of the reliability index that are also shared in EN 1990. SANS 10160-1:2011 also sets target reliability indices for structures categorised according to their consequence of failure. The target reliability index values presented in Table 3.5 have been obtained assuming lognormal distribution or the Weibull distribution for resistance. A normal distribution was assumed for permanent loads and a Gumbel distribution was assumed for variable loads (Holický, 2009).

South Africa also categorises different structure types according to what their expected design working life should be. The table for the design working life and their respective working life categories from SANS 10160-1:2011 is reproduced here as Table 3.6:

Table 3.6: Design Working Life as Described in SANS 10160-1:2011

Design Working Life Category	Indicative Design Working Life In Years	Description of Structure
1	10	*Temporary structures (not pertaining to structures that are intended for re-use after being dismantled).
2	25	Replaceable structural parts, agricultural structures and other such structures with a low consequences of failure
3	50	Building structures and other common structures**
4	100	Essential building structures such as hospitals, communication centres or rescue centres with high consequences of failure+
*Refer to SANS 10160-8 for assessment of temporary structures during execution ** The design working life category applies to the reference reliability class referred to in clause 4.5.2.3. + Consequences of structural failure could be determined in accordance with annex A		

Knowing the design working life intended for the liquid retaining structure allows for the appropriate target reliability index to be used in comparison to the reliability index determined through the reliability assessment of the crack model. In accordance with SANS 10160-1:2011, an appropriate design working life of 50 years will be used for liquid retaining structures in South Africa.

The recommended target reliability index for a 50-year design working life would be $\beta_t = 1.5$, for the irreversible serviceability state of cracking (ISO 2394:1998/SANS 2394:2004). This target reliability index is the same as the one found in EN 1990, also for a structure with a 50-year design life under an irreversible serviceability limit state. However, considering that for liquid retaining structures the serviceability limit state has an increased level of importance and demand when compared to the ultimate limits state, it may be plausible that a higher target reliability index be applied to this specialized structure. This, along with the idea that a reliability class (RC) of 3 classification (as described in SANS 10160-1) be used for liquid retaining structures, was put forth by researchers Barnardo-Viljoen, Mensah *et al*. (2014). Typical values of $\beta_t = 0.5$ for the reversible limit state and 1.5-2 were said to be appropriate for cracking in buildings (Barnardo-Viljoen, Mensah *et al*. (2014)). After an assessment of the influence that a change in target reliability index would have on the load induced crack model of EN 1992 it was determined that,

where a default target reliability index of 0.5 was selected, an increase in β_t from 1.5 to 2 resulted in a 10 and 15% respective increase in the amount of reinforcement required to meet reliability targets (Retief, 2015). An assessment of the implications of a change in choice of target reliability index for the restrained shrinkage cracking case should give a complete understanding of how an increase in the target reliability index value, β_t, of the cracking serviceability limit state would affect the design of liquid retaining structures.

3.5 The First Order Reliability Method

There are various probability methods available that may be used to determine the reliability index and thus the failure probability of a structure. As outlined in SANS 2394:2004, these methods for the determination of a structures failure probability include: exact analytical methods or a numerical integration approach, as well as other methodologies such as the Monte Carlo simulation, and lastly approximate methods such as the First Order Reliability Method (FORM). Exact analytical methods are generally used for exceptional cases, whilst numerical methods are used more often in reliability assessment with approximate methods being the most frequently used method (Holický and Marková, 2012). The First Order Reliability Method also acts as a fundamental procedure for a lot of commercially available software used in reliability assessment (Holický and Marková, 2012). Simulation methods, such as the Monte Carlo method, are most appropriate for more complex problems where a closed-form solution may be determined (if many simplifying assumptions are made) or where closed-form solutions are difficult to get (Nowak and Collins, 2000). This was not necessary for the reliability assessment undertaken herein. This thesis adopted the First Order Reliability Method. According to Zhao and Ono (1999), it is one of the most efficient structural reliability assessment methods and is also one of the methods used in the development of the Eurocode (Eurocode 2's restrained shrinkage crack model was investigated in this research and hence FORM seemed the more appropriate probability method to use in this study). FORM is an approximate method that was developed to circumvent the difficult computation of the failure probability integral,

$$p_f = \int_{g(x)<0} f_x(x)dx. \tag{3.9}$$

The SORM method is a refinement of the FORM method where the failure surface ($g(X_i) = 0$) is approximated by a quadratic surface at the design point (SANS 2934:2004).

The following basic outline describes the FORM methodology. The steps presented are adapted after Holický (2009) and Ang & Tang (1984):

1. The performance function, $g(X_i) = 0$, is defined and the initial values for the limit state basic variables X_i lying on the failure surface are assumed. The initial assumption is generally taken to be the mean of the basic variable.
2. The mean and standard deviation of non- normal random variables are transformed into their normal equivalents. In other words, the non-normal μ becomes μ^N_{xi} and the non-normal σ is converted to σ^N_{xi}. Non-normal random variables are then transformed to the standardised normal equivalent:

$$x_i' = x_i - \mu^N_{xi} / \sigma^N_{xi}$$

3. The partial derivatives of the performance function with respect to the standardised random variables are determined

$$\frac{\partial g}{\partial X'_i}.$$

The derivatives are used to find the direction cosines, α^*_i, at the failure point.

$$\alpha^*_i = \frac{\frac{\partial g}{\partial X'_i}}{\sqrt{\sum_i \left(\frac{\partial g}{\partial X'_i}\right)^2}}$$

4. The direction cosine found in the previous step is then used to determine the new failure point in terms of the reliability index, 'β',

$$x_i^* = \mu^N_{xi} - \alpha^*_i \sigma^N_{xi} \beta.$$

This new failure point is then substituted into the performance function $g(X_i) = 0$ and solved for β.

5. The β value is then used to find the numerical value for the design point at the limit state. This failure point may then be used as the new starting failure point in the next iteration.
6. Steps 2 to 5 are repeated until convergence of β and the subsequent design failure point is reached.
7. The failure probability can then be calculated using the formula $p_f = \Phi(-\beta)$.

The sensitivity factors/direction cosines generated from the FORM analysis describes the relative influence each random variable has with respect to the others utilised in the analysis. This normalised value is represented in either decimal or percentage form, where the closer the value is to 1 (or 100%), the stronger the relative influence of the random variable in question is with respect to the others being analysed in a particular FORM analysis. The square of the sum of the direction cosines should add up to 1 (or 100%). Needless to say, the variable found to be most influential contributes the most to the reliability index obtained at the end of the FORM analysis (Saassouh and Lounis, 2012). The sensitivity factor (direction cosine) can either be found to be

positive or negative. A negative direction cosine represents an unfavourable action (Holický, 2009).

3.6 Statistical Parameters of the EN 1992 Restrained Cracking Serviceability Limit State

3.6.1 Introduction

The probability distribution functions (pdf's), as well as the mean (μ) and standard deviations (σ) of the random variables, are required for the FORM analysis (as outlined in section 3.5). The choice of theoretical model assumed for the basic variables significantly affects the reliability indices obtained in a reliability analysis (Holický, 2009). An investigation on the variability of the basic variables used in the EN 1992 crack model was therefore conducted. Conventional models for the time-invariant basic variables used in crack width estimation are summarised in Table 3.7. These statistical parameters have been derived primarily from the works of Holický (2009). In addition to this, literature on the stochastic nature of the respective variables as well as information from the Joint Committee on Structural Safety's (JCSS, 2001) probabilistic model code documents were gathered and included in Table 3.7.

In a background on typical probabilistic distributions used to describe random variables, Holický (2009), gives examples of generally accepted assignments of these distributions for load, geometric and material variables. Geometric basic variables may be described by a normal probabilistic distribution, log-normal distribution and beta distribution. Material properties may usually be described by normal distribution and log-normal (considering material strengths). Additionally, load effects may be categorised by a normal distribution and Gumbel distribution (Holický, 2009). Model uncertainty has generally been known to follow a log-normal distribution function (Holický, 2009).

For this particular investigation the variables:

- Model uncertainty, concrete cover, concrete tensile strength and section thickness were treated as random variables (where their inherent variabilities accounted for in the analysis).
- The restraint factor and the remainder of the basic variables of the EN 1992 restrained shrinkage crack model were regarded as being deterministic.

The investigations into literature regarding the statistical parameters of the variables and the ultimate choice of said parameters for use in this investigation are addressed in the subsequent text.

Table 3.7: Theoretical Models of Basic Variables in EN 1992 Crack Model (Holický, 2009).

	Name	**Sym.**	**Units**	**Distribution**	**Mean μ_x**	**St. Dev. σ_x**
Geometry	Cross section thickness	h	m	Normal	h_k	0.005-0.01
	Cross section depth	b	m	Normal	b_k	0.005-0.01
	Concrete cover	c	m	Both- Sided Limited Beta/Gamma	c_k	0.005-0.015
	Reinforcement diameter	φ	mm	Deterministic		0
Material	Concrete Compressive strength (cube)	f_c	MPa	Lognormal	$f_{yk} + 2\sigma$	0.1-0.18μ_k
	Concrete Tensile Strength	f_{ctm}	MPa	Lognormal	$f_{yk} + 2\sigma$	0.1-0.18μ_k
	Steel Yield Point	f_y	MPa	Lognormal	$f_{yk} + 2\sigma$	0.07-0.1μ_k
	Concrete Modulus	$E_{c,eff}$	GPa	Deterministic		0
	Steel Modulus	E_s	GPa	Deterministic		0
Coefficients	Coefficient-Reinforcement	k_1	-	Deterministic		0
	Coefficient-Tension	k_2	-	Deterministic		0
	Limiting Crack Width	w_{lim}	mm	Deterministic		0
	Cracking Model Uncertainty	θ	-	Lognormal	1	0.3

3.6.2 Model uncertainty (θ)

The model uncertainty may be determined by comparing experimental data to those values obtained through the existing prediction model (JCSS, 2000). There are instances in which not

much data is available on the model uncertainty and experience and professional judgement is depended upon (Holický, 2009). Considering a sensitivity analysis conducted of the EN 1992 load induced crack model with respect to variations in model uncertainty conducted by McLeod (2013), model uncertainty had been found to bear the most influence on the tension load case and was found to be the second most influential random variable of the flexural loading case. The above-mentioned tension load case may be indicative of how influential model uncertainty might be on the restrained shrinkage crack model of EN 1992. ISO 2394:1998 (reproduced as SANS 2394:2004) includes model uncertainty as a random variable, θ, to be used in reliability assessments of performance functions accounting for a) inherent variability within the analysed model, b) inadequate knowledge and c) statistical uncertainty. Moreover, d) mathematical simplifications and assumptions made in developing the prediction model generates a certain degree of uncertainty (McLeod, Viljoen & Retief, 2016).

Looking more carefully into these above-mentioned sources of uncertainty with respect to the restrained shrinkage crack model it may be gathered that:

a) Cracking is a naturally random phenomenon with inherent variability.
b) The knowledge base regarding the stochastic nature of the restrained thermal and shrinkage cracking case is limited, meaning that there must be a heavy reliance on experience and professional judgement in this regard. Increased research in this area would result in a more accurate depiction of restrained cracking's statistical parameters and thus increased accuracy in the reliability assessment of its model. Most knowledge in the area of reliability-based assessments of the cracking serviceability limit state veered towards those cracks resulting from load (be it a concrete member under flexure or tension).

   The Eurocode 2 crack model along with other crack models have been tested against experimental data several times in previous research. One such comparison of the experimental crack widths to those predicted by EN 1992-3 was found in the investigations of Kamali *et al.* (2013) on the crack width control of a concrete slab bridge under restrained cracking (particularly for tensile forces in the transversal direction). It was determined in the course of this study that for 90% of all the observed crack widths, the EN 1992-3 crack model overestimated the crack widths (more crack widths were found to fall below where the measured crack widths equalled those estimated by EN 1992-3, as denoted by the broken red line of Figure 3.2). This experiment was done for crack widths greater than 0.2 mm. This fact is made clear in Figure 3.2 where the majority of the estimated crack widths are either comparable to the measured crack widths (at lower crack widths) or greater than the measured crack widths where the crack widths are

larger than ±0.4 mm. This finding reinforces the notion that the EN 1992-3 is conservative in its estimation of the crack width due to restrained strains.

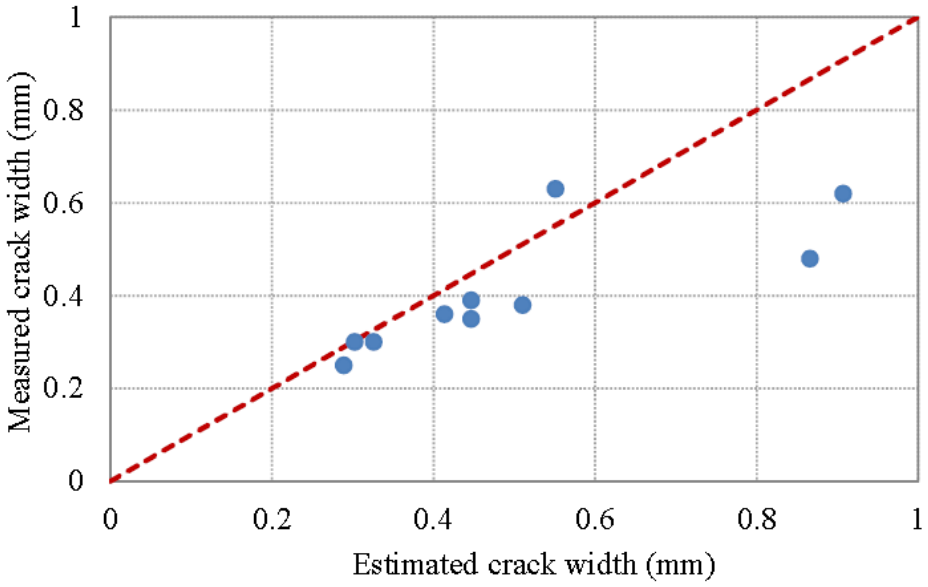

Figure 3.2: Comparison of Measure Crack Widths against the EN 1992-3 Predicted Crack Widths for a Concrete Member Restrained Along its Base (Kamali, Svedholm and Johansson, 2013).

In another comparison of the EN 1992-3 and BS 8007 crack prediction models to observe cracks, both models were found to under-predict the observed crack widths – this is presented in Figure 3.3 (Bamforth, Shave & Denton, 2011). In some instances, this underestimation of observed cracks would be by as much as 50%. This is contrary to what was found in the previous case by Kamali *et al.* (2013), alluding to the considerable amount of scatter in model uncertainty of the EN 1992-3 crack model for restrained shrinkage. Both Kamali *et al.* (2013) and Bamforth *et al.*'s (2011) comparisons were done so against data obtained for research on the control of cracking resulting from restrained contraction.

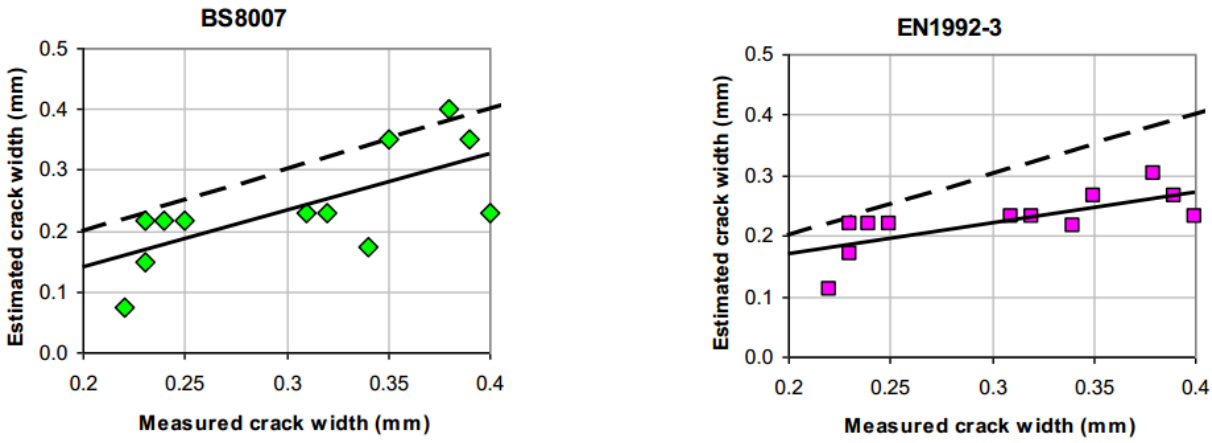

Figure 3.3: Comparison of Measured Crack Widths to Predicted Crack Widths of BS 8007:1987 and EN 1992-3:2006 (Bamforth, Shave & Denton, 2011)

Although the determination of model uncertainty depends on the formulation of the prediction model used (McLeod, 2016), the findings of model uncertainty related to the load induced cracking model were included in the subsequent text. Given the scarcity of probability based investigations done on the restrained thermal and shrinkage strain cracking, the load induced crack case should give indications as to how the EN 1992 may be described in terms of its statistical parameters. Quan and Gengwei (2002) found the model uncertainty for the crack widths of reinforced concrete beams to have a coefficient of variance of 0.298 (or otherwise 0.3) and an estimated mean of 1.05. These results came after a statistical study of 116 beams with varying configurations, strengths and applied loads (Quan and Gengwei, 2002). The model uncertainty was found to follow a lognormal probability distribution model. Thus subsequently, a mean of 1 and a maximum coefficient of variance of 0.3 will be adopted for the reliability analysis in this thesis.

c) Statistical uncertainty results from there being some uncertainty in the ways in which statistical parameters are estimated. Increases in the data base and sample size of the cracking from restrained shrinkage through testing and recording of observations should increase the accuracy of reliability assessments.

d) Examples of mathematical simplifications or assumptions made in modelling cracking include, for instance, the crack spacing formula of EN 1992 which contains some empirical fixed-value coefficients (McLeod, Viljoen, Retief, 2016). Such as the coefficient k_1, accounting for bond properties in EN 1992. A value of 0.8 is stipulated in EN 1992 for instances of good bond. This coefficient is the equivalent of BS 8007's f_{ct}/f_b

(taking on a value of 0.67 for type 2 deformed bars for class C35A concrete. Previous research has also indicated that 0.67 could be safely applied to all strength classes of concrete (Bamforth, 2007)). Even though the concrete tensile strength to reinforcing bond strength ratio (f_{ct}/f_b) was found in past research to decrease with an increase in concrete strength class, EN 1992 gives a constant value (0.8 for good bond) that is to be applied across all strength classes. This would then mean that at higher concrete strength classes, the k_1 coefficient provides an added margin of safety (or otherwise an added degree of conservatism).

Additionally, creep is accounted for particularly in the restraint factor since it has the effect of reducing restraint over time. However, where creep test methods are not given in the South African and British standards, most creep test methods involve loading concrete cylinders hydraulically and then measuring the deformation that results over time (Owens, 2013). This would mean that the creep value obtained would be based on compression rather than tension in the concrete (particularly tension arising from restrained contraction in the concrete). Thus in applying this same creep factor to tension cases (such as where there is restrained shrinkage) there could be a margin of error that arises since the creep prediction model does not necessarily represent the tension case. Furthermore, it had been found in past research that the tensile creep of concrete is lower under restrained shrinkage as opposed to where the concrete is under constant stress (Sajedi *et al.*, 2011).

Bearing all of these sources of uncertainty in mind, the EN 1992-3 restrained shrinkage crack model's coefficient of variance value will be varied in the reliability assessment to gauge what influence it has on the reliability performance of the crack model. This would be a particularly relevant assessment given model uncertainty's observed dominance in previous research (Retief, 2015).

3.6.3 Concrete cover (c)

The concrete cover is found to generally have a both-sided beta, or otherwise, gamma distribution (Holický, 2009). British construction practices are categorised into either high quality (near-laboratory precision), good, moderate or poor quality. The coefficients of variation associated with each quality level are 10%, 15%, 20% and 30% respectively (McLeod, 2013). Assuming that liquid retaining structures in South Africa are constructed under good quality management practices, the coefficient of variation for concrete cover selected for use in this investigation will be 15%. Concrete cover has also been found to follow a lognormal distribution (Holický 2007)

and will be the distribution of choice in the reliability analysis of the EN 1992-3 crack model performed herein (presented in chapter 5).

3.6.4 Limiting crack width (w_{lim})

An example of an observation of a typical crack pattern for a concrete member restrained at its edge is shown in Figure 3.4 (Kamali *et al.*, 2013). This was taken from the experimental data of researcher Kheder (1997) who investigated the control of cracks induced by restrained deformation. Kheder (1997) found that the largest cracks occurred in the middle of the concrete member with inclined cracks appearing along the sides. The crack widths established in the example below from experimental data suggests that there is considerable variability in the crack widths found in a restrained member.

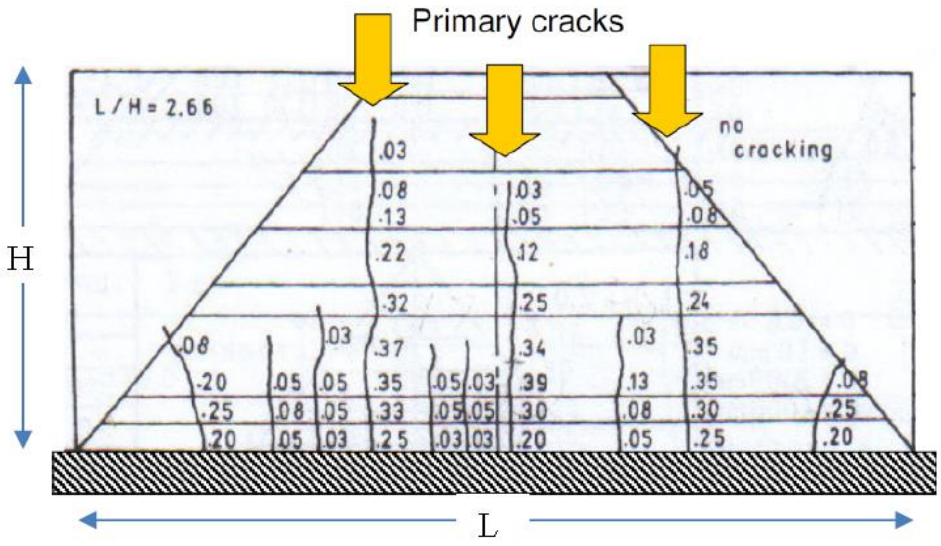

Figure 3.4: Example of Observed Crack Pattern and their Correlating Restraint Factor (Kamali *et al*., 2013).

The limiting crack widths set forth in design standards have been established for both load induced cracking and thermal cracking. However, past researchers considering the variability of various crack width models have done so typically on cracking due to loading. The limiting (or allowable) crack width used in these analyses were either regarded as having a stochastic nature or being deterministic. Holický (2010) conducted a fuzzy probabilistic analysis (where a broad transition region exists between the satisfactory and unsatisfactory state of a structure, rather than there being an abrupt change in state) of the EN 1992 load induced crack model. The crack width limit was said in this analysis to follow a beta distribution (the lower limit of the transition region was 0.05 mm and the upper limit was set at 0.2 mm). In assessing the reliability of cracking, the maximum allowable crack width value for load induced cracks in the Chinese design code was

regarded as being deterministic when used to calculate the reliability index of reinforced concrete beams under service conditions (Quan and Gengwei, 2002). The First Order Reliability Method of analysis was used in that particular study. Holický *et al*. (2009) regarded the limiting crack width in the EN 1992 load induced crack model (looking particularly at cracking in a cylindrical water retaining structure under pure tension) as being deterministic in a probabilistic analysis. Thus, considering the above findings on the probabilistic nature of the permissible crack width, the limiting crack width used for the reliability analysis in this thesis will also be regarded as being deterministic.

3.6.5 Concrete tensile strength ($f_{ct,eff}$)

The concrete tensile strength may be found to follow a lognormal distribution- much like most resistance variables (Holický, 2009). The characteristic value for the concrete tensile strength was found in EN 1992 to be $f_{ctk,\,0.05}$ = 2 MPa and mean value of 2.9 MPa for class C30/37 concrete (as derived from table 3.1 of EN 1992-1-1:2004). As part of the revision of early age cracking design guide, from CIRIA 91 to CIRIA C660, a probabilistic analysis of the design effective concrete tensile strength ($f_{ct,eff}$) was conducted to determine its exceedance probability. The findings are presented in Figure 3.5:

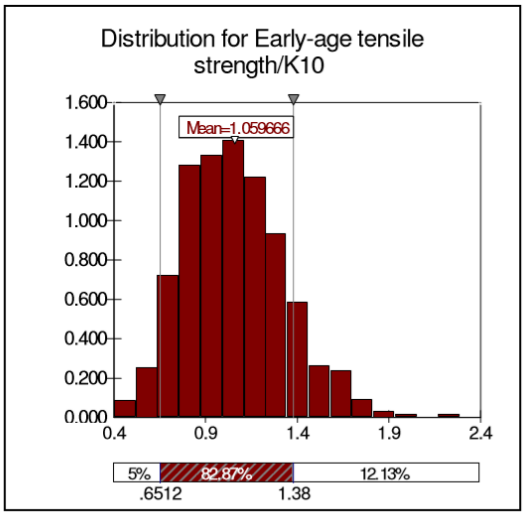

Figure 3.5: Probability Distribution of the Early Age In-Situ Tensile Strength of C30/37 Concrete (Bamforth, 2010).

Input data for concrete tensile strength into the probabilistic analysis assumed a normal distribution and coefficient of variance of 18% (standard deviation 0.53). A mean of 1.06 was obtained from the analysed data. The 5% fractile for the concrete tensile strength was found to be 0.65, whilst the 95% fractile was 1.54. Holický (2009) suggests the concrete strength follows a

log-normal distribution and generally has coefficient of variances that range from 0.1 to 0.18. Researchers investigating the reliability performance of the EN 1992 load induced cracking serviceability limit state have also regarded the concrete tensile strength has having a log-normal distribution, with a concrete grade of C30/37 (as with this investigation) having a mean of 2.9MPa and coefficient of variance of 0.19 (Holický, Reteif & Wium, 2009 and McLeod, 2013). Also undergoing the reliability analysis of the load induced cracking case, Zahalan (2010) regarded the concrete strength as following a log-normal distribution. This particular investigation will also be assuming a log-normal distribution for the concrete tensile strength, with a mean of 2.9 MPa and coefficient of variance of 0.19.

3.6.6 Restraint degree/factor (R)

The restraint degree also has an inherent variability. The restraint degree's variations depends on the elastic modulus of the new concrete pour which varies with time. Figure 3.6 illustrates how the change in concrete elastic modulus effects the restraint factor at the joint, calculated using the ACI method (the ratio of the cross-sectional area of the restraining element to the cross-sectional area of the restrained member, A_0/A_n, was assumed to be 1). Restraint also varies with the length to height ratio of the restrained member, with the degree of restraint decreasing with increased distance away from the restraining element. A review of literature on the variability of the restraint degree returned no real findings on the statistical parameters of this variable. One way to obtain these statistical parameters would be to compile experimental data on the restraint degree and use the data to obtain a theoretical probability model (Holický, 2009), a process that should be undertaken in future. Therefore based on the above mentioned short coming, the restraint degree will be treated as a deterministic variable. It is suggested that further research is done on the probability distribution and statistical parameters for the restraint degree.

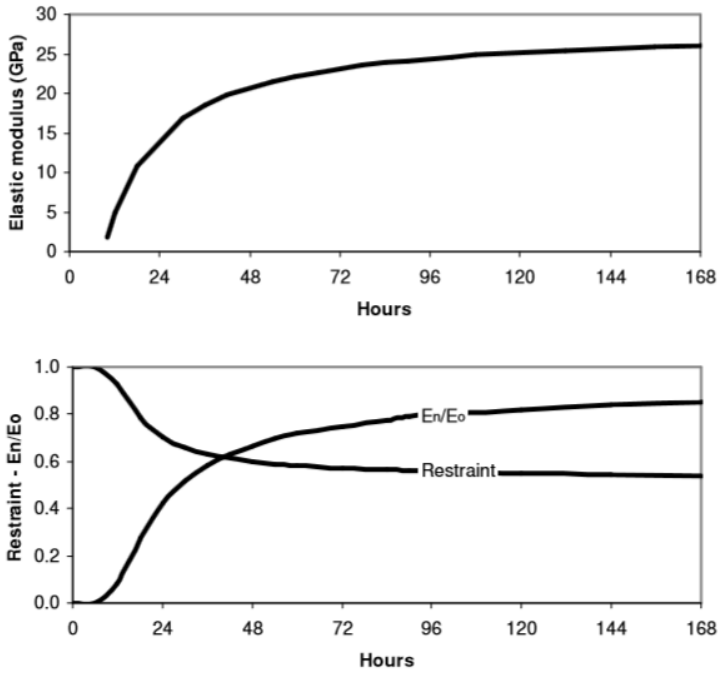

Figure 3.6: Variation of ACI Calculated Restraint Degree with Change in Concrete Elastic Modulus at Early Age (A_0/A_n = 1), (Bamforth *et al.*, 2010).

The remainder of the parameters to be used in the reliability analysis of the EN 1992 crack model will be treated as deterministic variables. These include parameters such as coefficients and a few other material properties.

3.7 Partial Safety Factors

For a design to be considered safe, it needs to be ensured that the action effect acting on the structure or structural element is either equal to or does not exceed the capacity (resistance) of the structure or structural element. To do this, a factor of safety may be applied onto both the demand and supply values that increases the nominal demand value and decreases the nominal supply value. The increased demand and decreased supply values are then used in the design of the engineering facility. This is a notion that is adopted in EN 1990 to EN 1999 (as well as in SANS 10160-1: 2011), in which the design value of a material property becomes:

$$X_d = \frac{X_k}{\gamma_M}.$$

In this case, the characteristic value for the material property is divided by a factor before being used for design purposes (Holický, 2009). Here the characteristic value, with a recommended probability of exceedance, for the material property may also be replaced by the nominal (X_{nom})

value for the material property. The same may be done for the design load F_d, where the design point may be found using the formula:

$$F_d = \gamma_F F_k.$$

Both γ_M and γ_F symbolise the partial safety factor for the material property and force respectively (Holický, 2009).

Partial factors account for there being some level of uncertainty in the design model and for any limitation in available data for a given level of reliability. For instance, in the Eurocodes the partial factor for material properties (γ_M) is made up of the product of the material property factor ($\gamma_m = \frac{X_k}{X_d}$) and resistance model uncertainty, γ_{Rd} (Holický, 2009). Similarly, the partial factor for loads, γ_F, comes as the product of both the load intensity uncertainty ($\gamma_f = \frac{X_d}{X_k}$) and the load model uncertainty (γ_{Ed}). The required factors for use in design must satisfy the inequality:

$$\phi R \geq \sum_{i=1}^{n} \gamma_i E_i ,$$

where ϕ is the supply factor and γ_i is the demand partial factor (Ang and Tang, 1984). In other words, for the performance function/limit state function to meet a target reliability index, partial safety factors are applied to the basic variables of the performance function. Thus, essentially, the limit state criteria ($g(X_i) > 0$) must still be met where the characteristic basic variables have been adjusted by the partial factors to meet the design value for the basic variables in question (symbolically the limit state criteria for safe design then becomes ($g(X_{id}) > 0$). If, say, the basic variables were represented by X_i, then the limit state equation:

$$g(\overline{\gamma}_1 \mu_{x1}, \overline{\gamma}_2 \mu_{x2}, \ldots, \overline{\gamma}_n \mu_{xn}) = 0.$$

Each $\overline{\gamma}_1 \ \mu_{X1}$ value is representative of the failure points on the performance function failure surface, x^* (the design value), where the target reliability index will most probably be met. Thus the formula for the failure point,

$$x^* = \overline{\gamma}_1 \mu_{x1}$$

may be rewritten as:

$$\overline{\gamma} = \frac{x^*_i}{\mu_x}$$

It may be found that the design failure points using FORM may be calculated using the subsequent formula:

$$x^* = \mu_x (1 - \alpha_i^* \beta w_{Xi}).$$

And so consequently, the theoretical partial factor becomes:

$$\overline{\gamma} = \frac{x^*_i}{\mu_x} = 1 - \alpha_i^* \beta w_{Xi},$$

where α_i^* is the direction cosine (sensitivity factor) for a failure point obtained at the end of the iterative FORM algorithm and w_{Xi} is the coefficient of variation of the basic variable in question (Ang and Tang, 1984).

The theoretical partial safety factor may be obtained using the following algorithm which is essentially the reverse of the FORM method, where the reliability index is known beforehand (as outlined by Ang and Tang (1984)):

1. The failure points are assumed (generally taken as the mean of the basic variables in question)
2. Non-normal means and standard deviations of random variables are converted to their normal equivalents.
3. The partial derivatives $\left(\frac{\partial g}{\partial X_i}\right)$ of the performance function is determined and the directional cosines found ($\alpha_i = \frac{\frac{\partial g}{\partial X_i'}}{\sqrt{\Sigma_i\left(\frac{\partial g}{\partial X_i'}\right)^2}}$)
4. Then the new failure point is determined via the equation:
$$x^* = \mu^N_x - \alpha\sigma^N_x\beta,$$
and substituted into the limit state equation and solved for an unknown basic variable
5. Steps 2 through to 4 are repeated until convergence of the basic variables in question is reached.

On a very basic level, the calibration of partial factors for a design code would involve selecting a set of partial factors such that the structural element under design has a reliability level that lies as close as possible to the stipulated target reliability index whilst meeting the limit state criteria. The reliability standard code, SANS 2394:2004, puts forth that an array of design conditions should be considered so as to ultimately determine a combination of partial safety factors that covers a large scope of expected performance applications. As indicated in SANS 2394:2004, the set of partial factors that are found to generate a reliability index that has the least amount of deviation from the target reliability would then be the best set of partial factors to be used in the design of the structural element under consideration. The calibration process is one that involves optimization, which is beyond the scope of this investigation.

3.8 Previous Research on the Reliability of the Cracking Serviceability Limit State

Overall, investigations into the reliability assessment of the serviceability limit state returned research geared more towards the load induced cracking case rather than that of the restrained shrinkage (as evidenced by this section). This justifies the relevance of assessing the reliability of the restrained cracking serviceability limit state. Fortunately, some inferences may be made from the load induced cracking cases- where clues towards the reliability performance of the restrained shrinkage cracking serviceability limit state may be found. The nature of reliability assessment is such that the ultimate reliability index or failure probability arrived at after analysis depends significantly on the probabilistic distribution (or otherwise, theoretical models) to which the basic variables are assumed to follow (SANS 2394:2004). For example, direct comparisons may be unfeasible even where the same limit state function was being considered among comparative research works, but the shared basic variables utilised have been said to follow different probability distributions - a likely occurrence due to some deficiencies in the knowledge of the stochastic nature of some basic variables. The formulation of the limit state function also affects the reliability indices obtained, thus making it difficult to directly compare research findings to past works where a different limit state function was considered. For instance, the use of a different physical model describing the same phenomenon (e.g. the various models in existence modelling cracking) disallows the option of direct comparison. However, that being said, inferences may be made relevant to restrained cracking. A summary of past investigations on the reliability assessment of the cracking serviceability limit state has been compiled:

Holický, Retief and Wium (2009) assessed the reliability performance of the EN 1992 load induced crack model. Here the crack widths of water retaining structures were investigated probabilistically (using FORM) and compared to a deterministic analysis of the same representative water retaining structure. The probabilistic method was determined to be more economical than employing a deterministic design methodology. It was found in this research that reinforcing required for the serviceability limit state for crack control exceeded that which was required satisfy the ultimate limit state. The degree of exceedance increased with a decrease in the permissible crack width limit. Research by Holický *et al*. (2009) also indicated that 2 to 5 times more reinforcement than the basic reinforcement required for the ultimate limit state was necessary for crack limit compliance. This was true for the EN 1992 load induced cracking case, with the enhancement factors applying to crack limits 0.2 mm and 0.05 mm respectively. Clearly, from Holický *et al*.'s (2009) findings it may be observed that regarding LRS the serviceability limit state is the more critical limit state with regards to liquid retaining structures. With restrained cracking falling under the same serviceability design criterion as that of load induced cracking,

one may presume that it too would require larger amounts of reinforcing as compared to that which is required for the ultimate limit state design criteria in LRS design.

Holický (2010) conducted a probabilistic optimization of the EN 1992 load induced crack model to ascertain what optimal value of the ratio of a generic reinforcement to the reinforcement required for ultimate limit state compliance ($\omega = A/A_0$). This ratio may also be described as a measure of what enhancement in magnitude was required of the reinforcement determined for ultimate limit state agreement to meet the crack limit. It was determined that the reinforcement calculated for ultimate limit state agreement needed to be significantly increased for crack limit compliance. Moreover, in this analysis, Holický (2010) determined that a range of optimal reliability indices of 0 to 3.5 was calculated for the EN 1992 load induced crack model depending on the ratio of cost of failure to the cost per unit of $\omega = A/A_{0,} (C_f/C_1)$. For a high cost of failure, the reliability indices calculated were as large as those generally required for ultimate limit states (Holický, 2010). This discovery is one that may also be applied to the restrained shrinkage case since it is a significant design criterion in LRS design and the cost of failure may most likely be found to be high. Evidently, increased knowledge of the potential cost of serviceability failure for liquid retaining structures will give an indication of what reliability index is most appropriate for liquid retaining structures where the load induced and restrained shrinkage cracking cases are both accounted for.

Using a target reliability index similar in magnitude to those used for ultimate limit states, Zahalan (2010) conducted a reliability-based analysis on the reliability index, again, on load induced cracking. The target reliability used in this exercise was 3.5 for beams. The limit state function in this particular research was derived from Frosch's (1999, as cited in Zahalan, 2010, p.55) equation and principles of reinforced concrete analysis (specifically the force and moment equilibrium in concrete sections). The Monte Carlo method was adopted for the analysis of the failure probability of the crack model. In this particular investigation, concrete cover and reinforcement spacing were found to have the most influence on the overall reliability of the crack model. Beam width, effective depth, concrete strength and steel strength were found to have a lesser influence on the reliability indices achieved by the crack model. The reinforcement area was found to have a limited influence on the reliability of the crack model since only a certain amount of reinforcement may feasibly be included in the concrete beam.

McLeod, Wium and Retief (2012) also performed a reliability analysis of the EN 1992 crack model as part of research undertaken for the development of the proposed design code for liquid retaining structures in South Africa. It was determined in this analysis that the crack width limit and model uncertainty had a significant effect on the reliability of the EN 1992 crack model. The

limiting equation of the effective depth was also found to bear some influence on the reliability of the crack model for the tension load case. It is important to extend this analysis to include the restrained shrinkage case to fully gauge these variables' overall influence on the EN 1992 cracking serviceability limit state.

3.9 Concluding Remarks

Since the serviceability limit state was found in past research to be the more dominant limit state, the question of what the appropriate reliability index for this limit state becomes an important one. Clearly, being the more critical limit state, its target reliability index should be greater than those set for conventional serviceability limit states. Hence it is important that reliability performance of this serviceability limit state be assessed. An assessment of the influence of various design parameters on the load induced cracking model have already been conducted in past research for a variety of design codes. Thus, it is necessary that a similar investigation is conducted for the restrained shrinkage case. An investigation on the influence of concrete cover, the $\varphi/\rho_{p,\,eff}$ ratio, the effective tension area, section thickness, the reinforcement area as well as the restraint factor on the reliability of the crack model will be assessed in the subsequent chapter 4. Moreover, model uncertainty has been found in past research to contribute considerably to the reliability of the EN 1992 load induced crack model - pointing towards its potential on the restrained shrinkage crack model. Thus an investigation into the influence of model uncertainty on the EN 1992 restrained shrinkage crack model should be conducted. An understanding of the reliability performance of the EN 1992 shrinkage cracking model in the South African context provides an opportunity for improving this code for South African use.

Chapter 4: Parametric Study of the EN 1992-1-1 & 3 and Corresponding Codes BS 8007 & BS 8110-2 Restrained Shrinkage Crack Models

4.1 Introduction

The objective of this study was to closely examine relationships of interest within both the restrained shrinkage crack model of BS 8007 and EN 1992. As far as possible, typical South African conditions, materials and configurations where used in this study. The values for the typical South African liquid retaining structures were those taken from a survey done on South Africa's practices in the construction of water reservoirs (Holicky, 2009). In addition to understanding the relationship of parameters within the respective crack models, the parametric study will serve to indicate which parameters bear the most influence on the EN 1992 crack model. The parameters to which the crack model is most sensitive are indicative of where sensitivities might lie within the reliability model. Consequently, the influence of these identified parameters on the reliability of the EN 1992 crack model may then be more closely examined in the reliability analysis.

Questions raised from a review of relevant literature included the debate around the equation for maximum spacing in which EN 1992-1-1 includes concrete cover as an influencing parameter in its estimation of crack spacing. In the superseded BS 8007 code, concrete cover was not included in the crack spacing model. The influence held by concrete cover and the $\varphi/\rho_{p,eff}$ (or φ/ρ in the BS 8007 case) parameter was examined. This, as before mentioned, should give an indication of what bearing these parameters have on the reliability model and also be able to quantify the effects that the inclusion of the cover value in the EN 1992 crack model has. Moreover, in observing both codes of practice, it can be noted that the way in which the restrained strain in the end restraint case is dealt with in EN 1992-1-1 differs markedly from BS 8007, with no two parameters shared between codes. This is contrary to edge restraint, which both codes have dealt with in a similar way. The implication of this changeover in methodology in the design of water retaining structures in South Africa will be examined herein.

4.2 Design Parameters:

The parametric study was deterministic in nature, meaning that the inherent variability and uncertainty in each input variable were disregarded. Instead, each input variable was regarded as

having a fixed value. A list of both the material and physical parameters used in this study are given below:

4.2.1 Material parameters

Concrete compressive strength (characteristic value)

A survey of South African water retaining structures revealed that typical concrete grade used included either C25/30 OPC concrete or otherwise grade C30/37(Holicky, Retief & Wium, 2009). The latter of the two was chosen as the concrete grade of choice. A concrete grade of C30/37 was selected.

Concrete tensile strength (mean value)

For C30/37 concrete at 3 days f_{ctm} (3) = 1.73 MPa ($f_{ctm} = f_{ct,eff}$). The tensile strength taken at 28 days is f_{ctm} (28) = 2.9 MPa for C30/37.Values are for concrete tensile strength are taken from CIRIA C660, table 3.2 (Bamforth, 2007).

Reinforcement yield strength (characteristic value)

The reinforcement yield strength common in South Africa is 450 MPa.

Modulus of elasticity of steel

The modulus of elasticity of steel is 200 GPa.

Modular ratio

The modular ratio is $\alpha_e = E_s/E_c$, where E_s denotes the modulus of elasticity of the steel and E_c relates to the modulus of elasticity of concrete at the appropriate age. This value can be estimated by from EN 1992-1-1:2004 equation (under clause 3.1.3):

$$E_{cm}(t) = (f_{ctm}(t)/f_{cm})^{0.3} E_{cm},$$

where,

- $E_{cm}(t)$ is the modulus of elasticity at 't' days
- $f_{cm}(t)$ is the mean concrete compressive strength at 't' days (EN 1992-1-1 (2004), clause 3.1.2, equation 3.1)
- E_{cm} is the modulus of elasticity at 28 days
- f_{cm} is the mean concrete compressive strength at 28 days (taken from table 3.1 of EN 1992-1-1:2004)

$E_{cm}(3) = (22.8/38)^{0.3}x33 = 28$ GPa, This makes the modular ratio for C30/37 concrete $\alpha_e = 200/28 = 7.14$ for concrete at 3 days. At 28 days $E_{cm} = (38/38)^{0.3}x33 = 33$ GPa, making $\alpha_e = 200/33 = 6.06$ for C30/37 concrete.

Coefficient of thermal expansion, $\alpha_{c,T}$

The most used aggregate in South African concrete is quartzite and sandstone (Addis and Owens, 2001) and thus reading from table 4.4 in CIRIA C660 (Bamforth, 2007), the coefficient of thermal expansion for quartzite containing concrete was (was $\alpha_{T,c} = 14\mu\varepsilon/^{\circ}C$, which acted as the reference thermal expansion coefficient for calculations). This was a proposed conservative design value on the high-end of the observed range of concrete thermal expansion coefficients (after Browne 1972 as cited by Bamforth, 2007 in CIRIA C660).

Autogenous shrinkage, ε_{ca}

The values for autogenous shrinkage strain obtained from table 4.5 of CIRIA C660 were $\varepsilon_{ca} = 15\mu\varepsilon$ (at 3 days) for C30/37 concrete and $\varepsilon_{ca} = 33\mu\varepsilon$ (28 days) – used in calculations, taking into consideration long term effects. Or otherwise the autogenous shrinkage may be obtained via the formulae for autogenous shrinkage in EN 1992-1-1:2004, under clause 3.1.4:

$$\varepsilon_{ca}(t) = \beta_{as}(t)\varepsilon_{ca}(\infty) \text{ where,}$$

$$\varepsilon_{ca}(\infty) = 2.5(f_{ck} - 10)x10^{-6} \text{ and}$$

$$\beta_{as}(t) = 1\text{-}\exp(-0.2t^{0.5}).$$

The time, t, input is given in days. Using these formulae it may be found that:

- For t = 3 days, $\varepsilon_{ca}(3)=(1\text{-}\exp(-0.2(3)^{0.5})x2.5(30\text{-}10)10^{-6} = 14.64\mu\varepsilon$ ($\approx 15\mu\varepsilon$)
- For t = 28 days, $\varepsilon_{ca}(28)=(1\text{-}\exp(-0.2(28)^{0.5})x2.5(30\text{-}10)10^{-6} = 32.65\mu\varepsilon$ ($\approx 33\mu\varepsilon$)

T_1

The most common formwork used in South Africa is steel formwork (Addis and Owens, 2001). Table 4.2 of CIRIA C660 gives 340kg/m^3 binder content for C30/37 CEM I (ordinary Portland cement) concrete. Figure 4.5 from CIRIA C660 (this value is based on a mean ambient temperature of 15°C and placing temperature of 20°C) gives, T_1 value of 15°C.

T_2

Considering the concrete placement in summer, the T_2 fall in temperature selected for the analysis was 23°C (estimating from data obtained by SouthAfrica.info, 2015 and the Climate Change Knowledge Portal, 2009).

Drying shrinkage strain, ε_{cd}

For relative humidity was said to be 80% for coastal areas (Addis and Owens, 2001) where the section thickness h = 250 mm and the width of the section considered is b = 1000 mm. The effective section thickness h_0 may then be obtained by dividing twice the concrete cross-sectional area by the perimeter of the parts of the cross-section that would be exposed to the drying ($2A_c/u$). Applying this formula in this context gave the following result:

$2A_c/u=2(250 \times 1000)/ (2x1000) = 250$ mm (considering a section of wall, top and bottom of cross section not exposed)

Reading from figure 8.20 from Fulton's Concrete Technology (Addis and Owens, 2001), the drying shrinkage strain is interpolate between values for h_0 = 150 and 300 in this instance where h_0 = 250 mm, yielding ε_{cd} = 220με (30 year shrinkage) - this was the value to be adopted in the subsequent parametric calculations. For inland areas, the relative humidity in South Africa is 60%. For h_0 of 250 mm lying between 150 mm and 300 mm, as before, the drying shrinkage read for 60% relative humidity was ε_{cd} = 340με (30-year shrinkage).

Tensile strain capacity, ε_{ctu}

The tensile strain capacity represents the maximum amount of strain that the concrete can sustain before the formation of a crack (Bamforth, 2007). This value may be obtained by dividing the mean tensile strength of the concrete by the mean modulus of elasticity of the concrete. The values of the tensile strain capacity were taken from table 4.11 of CIRIA C660 (Bamforth, 2007) where the effects of creep and sustained loading were accounted for.

- ε_{ctu} = 76 με for C30/37 concrete at 3 days.
- ε_{ctu} = 108 με for C30/37 concrete at 28 days.

4.2.2 Physical parameters

Section thickness, h

The typical section thickness in South Africa for water retaining structures was found to be 250mm (Holicky, Retief & Wium, 2009).

Cover, c

The concrete cover was taken to be 40mm (this value takes into consideration the minimum concrete covers for the durability of water retaining structures in accordance with BS 8007. It was also found to be the typical choice for engineers in South Africa (Holicky, Retief & Wium, 2009)).

Diameter of reinforcement, φ

This value may vary depending on the parameter being studied, a reinforcing steel diameter of 16 mm was selected as the reference case.

Area of tension reinforcement, A_s

Varies as required in the comparisons considered. The maximum amount of area of steel reinforcement (A_s) allowed in South Africa as stipulated by SANS10100-1 (clause 4.11.5.3) is 4% of the gross cross-sectional area of concrete (A_c). A feasible minimum limit of 75 mm spacing for single bars of reinforcement was used.

Restraint degree, R

A maximum restraint degree, with creep accounted for, will be used. Otherwise, the reference value for the restraint factor is taken to be 0.5 (for a concrete member under full restraint with the effects of creep accounted for).

4.3 Methodology for Crack Width Estimation

Calculations pertaining to both end and edge restraint were done so using both the Eurocode (EN 1992-1-1:2004 and EN 1992-3:2006) and British (BS 8110-2:1985 and BS 8007:1987) codes of practice.

4.3.1 Crack Estimation Following EN 1992

The Eurocode crack calculation procedure for restrained cracking went as follows:

- The crack width is the product of both the restrained strain and the crack spacing ($S_{r,\,max} \times \varepsilon_r$). Thus, initially, both the crack spacing and restrained strain need be determined.
- Determine the retrained strain by substituting the appropriate, above mentioned, input parameters into the strain equation for either end (α_e, k, k_c, $f_{ct,\,eff}$, E_s, A_s and A_c) or edge (α_c, T_1, T_2, ε_{cd}, R and $\boldsymbol{\varepsilon_{ca}}$) restraint. The applicable restrained strain formula for end restraint is

$$\varepsilon_r = (\varepsilon_{sm} - \varepsilon_{cm}) = \frac{0.5\alpha_e k_c k f_{ct.eff}\left(1 + 1/\alpha_e \rho\right))}{E_s},$$

whilst that for edge restraint is

$$\varepsilon_r = (\varepsilon_{sm} - \varepsilon_{cm}) = R_{ax}\,\varepsilon_{free}.$$

- Determine the effective depth of the tension area, $h_{c,eff}$, which is the lesser of either h/2 or 2.5(c+ φ/2).
- Crack spacing is then calculated the same way for both end and edge restraint conditions using the equation

$$S_{r,\,max} = 3.4c + 0.425k_1k_2\Phi/\rho_{p,\,eff.}$$

It must be noted that the ratio of steel reinforcement to gross concrete is represented by $\rho = A_s/A_c$, which is not to be confused with the ratio of steel reinforcement to effective concrete area ratio symbolised by $\rho_{p,\,eff} = A_s/A_{c,eff.}$ The effective tension area can, of course, be obtained by multiplying the depth of the effective tension area by the section width ($h_{c,eff} \times b$). The depth of the effective tension area is determined as the lesser of h/2 and 2.5(c + φ/2).

4.3.2 Crack Estimation Following BS 8007 and BS 8110-2

The crack calculation procedure for restrained cracking as per BS 8110-2:1985 and BS 8007:1987 respectively went as follows:

- As in the case for EN 1992-1-1:2004 and EN 1992-3:2006, the crack width is the product of the restrained strain and crack spacing.
- Once again, the restrained strain (ε_r) resulting from end or edge restraint must be calculated. The strain calculation is the same for both end and edge restraint under the British codes,

$$\varepsilon_r = R\alpha\,(T_1 + T_2).$$

- The crack spacing may then be calculating using

$$S_{max} = \frac{f_{ct,eff}}{f_b} \times \frac{\varphi}{2\rho}.$$

4.4 Influence of cover versus $\varphi/\rho_{p,\,eff}$

The modelling of crack spacing model is an aspect of crack estimation that differs most across design codes (Beeby & Narayanan, 2005). Such a vast set of possible ways in which crack spacing may be determined is cause for an investigation. This is particularly of interest here where the crack spacing equations adopted by BS 8007 and EN 1992-1-1 have some noticeable differences. An investigation into the influence of cover and the $\varphi/\rho_{p,eff}$ ratio on crack spacing had been undertaken.

4.4.1 Influence of Cover on Crack Spacing

The first part of this exploration involved assessing the influence of cover on the crack spacing in the EN 1992-1-1: 2004 equation. To examine the influence of cover on crack spacing, the cover was varied and its effect compared against a comparable set of $\varphi/\rho_{p,\,eff}$ ratios. The section thickness was kept constant at 250 mm and the reinforcing bar diameter remained 16 mm throughout the analysis. The reinforcing bars were assumed to be spaced at 250 mm centre to centre. A section width (b) of 1000 mm was selected for this analysis. The $\varphi/\rho_{p,\,eff}$ ratio is limited by the effective tension area and only those ratios that were close in value were included in the study. Given the concrete covers chosen and the choice of bar diameter (parameters onto which the effective tension area depends) it was determined that the $\varphi/\rho_{p,\,eff}$ ratio became constant after the cover value of 50 mm since the limiting effective depth from a 50 mm cover onwards was limited to 2.5(c + φ/2). Hence, the ratio developed from concrete cover values greater than 50 mm was compared against a constant $\varphi/\rho_{p,\,eff}$ ratio and the subsequent findings (as presented in Table 4.1) were made:

Table 4.1: Influence of Cover on EN 1992 Crack Spacing Model

			$h_{e,eff}$ (mm)						
cover (mm)	**bar dia. (mm)**	**A_s/face (mm^2)**	**h/2**	**2.5(c + φ/2)**	**$\rho_{p,eff}$**	**$\varphi/\rho_{p,eff}$ (mm)**	**$S_{r,max}$ (mm)**	**Term 'X' %**	**Term 'Y' %**
40	16	804	125	120	0.0067	2387	948	14	86
50	16	804	125	145	0.0064	2487	1016	17	83
60	16	804	125	170	0.0064	2487	1050	19	81
70	16	804	125	195	0.0064	2487	1084	22	78
80	16	804	125	220	0.0064	2487	1118	24	76
100	16	804	125	270	0.0064	2487	1186	29	71

Notes:

- Cover varied as presented whilst only the shaded values considered in study
- Reinforcement spacing was set at 250 mm centre to centre
- $h_{e,\,eff}$ is limited to the lesser of h/2 or 2.5(c + φ/2). The value for $h_{e,\,eff}$ stabilised after cover = 50 mm and so values $\varphi/\rho_{p,\,eff}$ became constant thereafter.
- Term 'X' = 3.4c
- Term 'Y' = $0.425k_1k_2\varphi/\rho_{p,\,eff}$

If one were to consider the two terms (the cover and effective reinforcement ratio term) in the EN 1992-1-1: 2004 crack spacing model separately, an estimation of either one's influence may be more clearly assessed. Considering that the crack equation is $Sr_{, max} = 3.4c + 0.425k_1k_2\varphi/\rho_{p, eff}$, it may be separated such that the cover term is represented by term 'X' = 3.4c and the second half of the crack spacing which deals with the effective reinforcement ratio is represented by term 'Y' = $0.425k_1k_2\varphi/\rho_{p, eff}$, then the influence held by each term on the overall crack spacing may be assessed. It is evident from the results that an increase in the concrete cover term 'X' value brings about an increase in crack spacing calculated, although this increase in crack spacing is marginal. For cover values 50 and greater used in the assessment presented in Table 4.1, the limiting effective depth was h/2 meaning that the concrete cover had no influence on term 'Y' since it did not feature. It is evident from results that concrete cover makes a relatively small contribution on the crack spacing in the EN 1992 crack spacing model. The second term of the crack spacing formula, term 'Y', carries a greater influence on the crack spacing model.

A graphical representation of this data is displayed in Figure 4.1. Here, the estimation of crack spacing as done under both EN 1992 and BS 8007 was included. Since BS 8007 does not include the cover variable, it was independent of this variable and thus remained constant as the concrete cover value varied. It can be seen, in the EN 1992 case that increasing the cover resulted in an increase in crack spacing. However, this increase in crack spacing was gradual. It may also be deduced from Figure 4.1 that the EN 1992 crack spacing model predicts larger crack spacing as compared to those calculated from BS 8007. The difference between the predicted crack spacing as calculated from EN 1992 and BS 8007, of course, would increase with an increase in cover value.

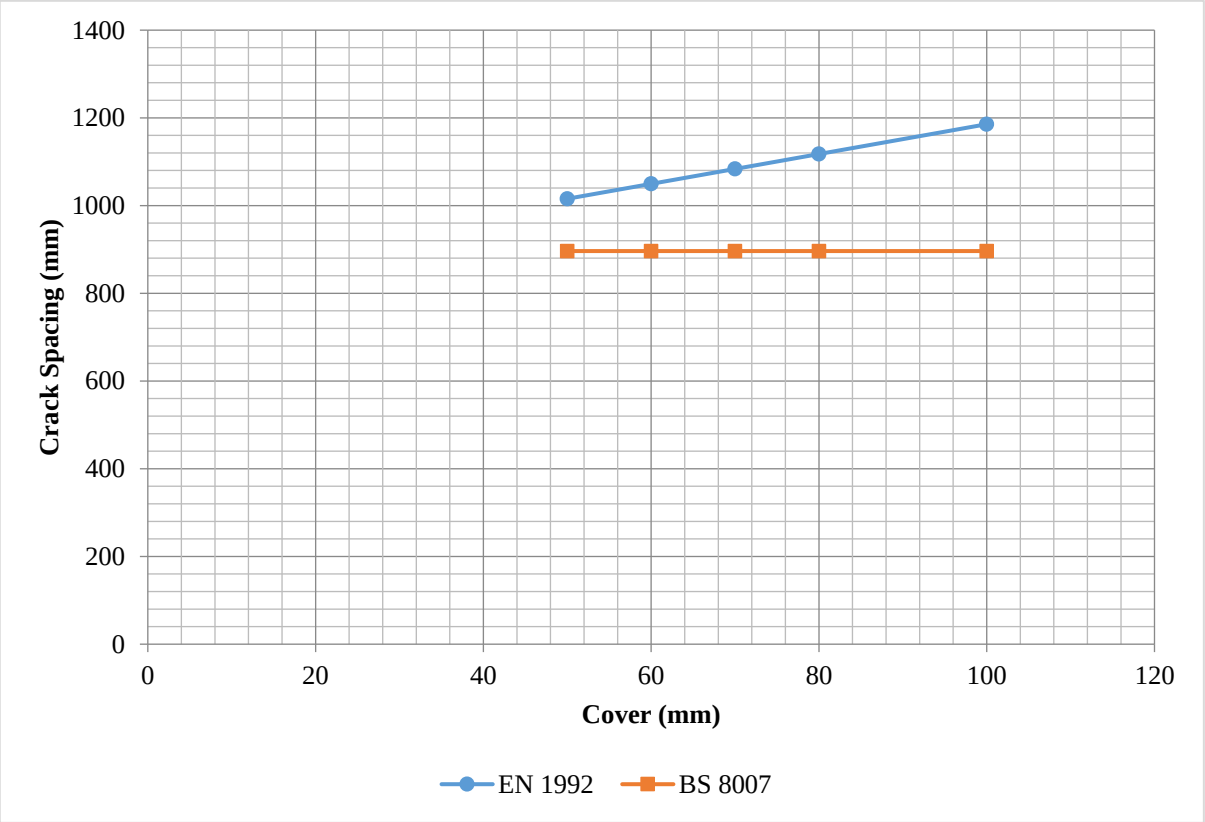

Figure 4.1: Influence of Cover on Crack Spacing for Both EN 1992 and BS 8007

4.4.2 Influence of the $\varphi/\rho_{p,\,eff}$ Ratio on Cracking

To determine the influence of the $\varphi/\rho_{p,\,eff}$ ratio, the bar diameter was varied in order to vary the $\varphi/\rho_{p,\,eff}$ ratio. The cover was kept constant at 40 mm and the bar spacing was set at 250 mm centre to centre. The section thickness in this study was fixed at 250 mm. The results of this analysis are presented in Table 4.2. Considering the contribution the $\varphi/\rho_{p,\,eff}$ ratio makes to the estimated crack spacing (i.e. regarding term 'Y' = $0.425k_1k_2\phi/\rho_{p,\,eff}$) – it can be clearly seen that this ratio is once again a sizeable contributor to the overall value of the crack spacing. Concrete cover, once again, has no impact on term 'Y' since the limiting effective depth was h/2 for the selection of concrete covers, bar diameters and section thickness considered in this analysis.

Table 4.2: The Influence of the $\varphi/p_{\rho,\,eff}$ Ratio on Crack Spacing as per EN 1992

			$h_{e,eff}$ (mm)					
cover (mm)	**bar dia. (mm)**	**A_s/face (mm^2)**	**h/2**	**2.5(c + φ/2)**	**$\rho_{p,eff}$**	**$\varphi/\rho_{p,eff}$**	**$S_{r,max}$ (mm)**	**Term 'Y' %**
40	16	804	125	120	0.0067	2387	948	86
40	20	1257	125	125	0.0101	1989	812	83
40	25	1963	125	131	0.0157	1592	677	80
40	32	3217	125	140	0.0257	1243	559	77
40	40	5027	125	150	0.0402	995	474	71

Notes:

- 250 mm center to center spacing for reinforcement
- Term $Y = 0.425k_1k_2\varphi/\rho_{p,\,eff}$

The graphical representation of the effect of the $\varphi/\rho_{p,\,eff}$ ratio on the crack spacing is displayed in Figure 4.2. It is clear from Figure 4.2 that increases in the $\varphi/\rho_{p,\,eff}$ brought about an increase in the predicted crack spacing, as would be expected.

The influence of the $\varphi/\rho_{p,\,eff}$ (or φ/ρ) ratio on crack spacing for both the EN 1992 design code and BS 8007 was compared. The Figure 4.2 shows this comparison between the two codes, here the section thickness was kept constant at 250 mm and the cover to reinforcement remained 40 mm throughout the analysis. It is evident from Figure 4.2 that the crack spacing values obtained through the EN 1992 are greater than those obtained by way of BS 8007. This may be attributed to the inclusion of the cover term in the EN 1992 crack spacing estimation. For instance, considering a reinforcing bar diameter to effective reinforcement ratio of 1592 mm, EN 1992 predicted a crack spacing value of 677 mm whilst the BS 8007 crack spacing model estimated a value of 573 mm (about decrease in value of factor 1.18) – $\varphi/\rho_{p,\,eff}$ was equal to φ/ρ in this instance since the limiting effective depth was h/2 under both EN 1992 and BS 8007 for reinforcing bar diameter 25 mm. Concrete cover plays an even greater role on the EN 1992 calculated crack spacing at lower reinforcing bar diameters (namely, the 16 and 20 mm wide bars considered in this analysis), thus the difference between the calculated crack spacing of EN 1992 and BS 8007 increases at lower reinforcing bar diameters.

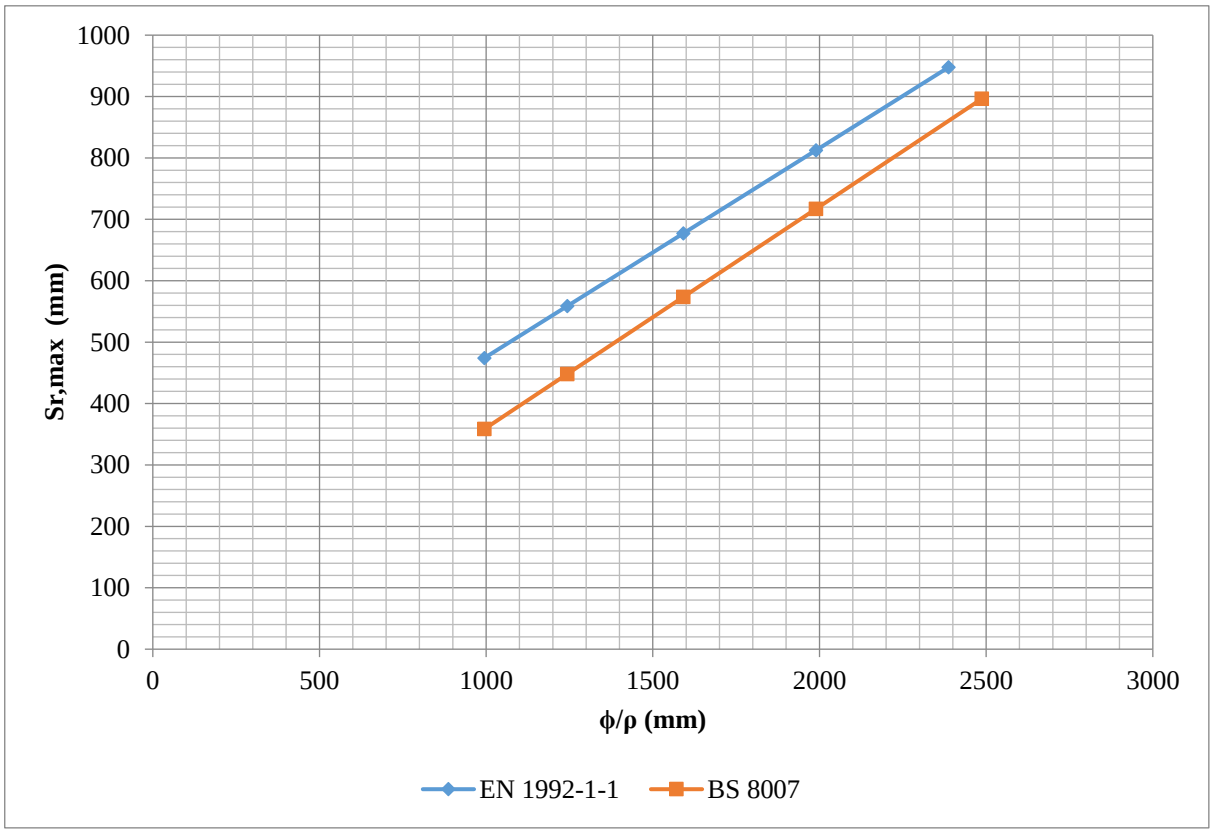

Figure 4.2: The influence of $\varphi/\rho_{p,\,eff}$ (or φ/ρ) Ratio on Crack Spacing for BS 8007 and EN 1992-1-1 (40 mm Cover and 250 mm Section Thickness).

It is clear from the analysis conducted that the influence of the bar diameter to effective steel content ratio is quite great than that of concrete cover under both codes, making up a large portion of the final crack spacing predicted. This would ultimately affect the crack widths estimated under both codes and in turn the amount of reinforcement required to maintain the stipulated rack width limit. Based on the analysis conducted above, it appears as though EN 1992 is the more conservative of the two codes, requiring more reinforcement to maintain the crack width limit.

4.5 Depth of effective area

Another way in which the British code differs from the Eurocode is the way in which the effective tension area is defined. This difference in definition affects the overall value of the crack spacing and thus the crack width. Therefore, a comparison of the effective tension areas between the codes was undertaken. Table 4.3 gives a summary of the findings on the effect of concrete cover and section thickness on the effective depth of the tension zone. The discussion corresponding to the results is referred to in the subsequent section.

Table 4.3: Influence of section thickness and cover on effective depth of tension zone (φ = 16 mm)

		EN 1992		BS 8007
Cover (mm)	**h (mm)**	**$h_{c,eff}$ (mm)**		**$h_{c,eff}$ (mm)**
		h/2	**2.5(c + φ/2)**	**h/2**
40	250	125	120	125
	300	150	120	150
	350	175	120	175
	400	200	120	200
	450	225	120	225
	500	250	120	250
50	250	125	145	125
	300	150	145	150
	350	175	145	175
	400	200	145	200
	450	225	145	225
	500	250	145	250
60	250	125	170	125
	300	150	170	150
	350	175	170	175
	400	200	170	200
	450	225	170	225
	500	250	170	250
Note: Limiting effective depth highlighted.				

4.5.1 Influence of Section Thickness and Concrete Cover on Effective Tension Depth

To examine how the choice of section thickness and concrete cover influences the value of the effective tension depth, the concrete cover (40, 50 and 60 mm) and reinforcing bar (16 mm) were kept constant whilst the section thicknesses were varied. This was done under the guidelines of both EN 1992 and BS 8007 and subsequently compared. EN 1992 proposes that the depth of the effective depth for members in tension is the lesser of h/2 and 2.5(c + φ/2) (denoted by the highlighted cells in Table 4.4). In the BS 8007, for section thicknesses of walls and suspended slabs less than 500 mm thick, the effective tension area is taken as being half the section thickness (h/2). Where the section thickness is greater than 500 mm the effective tension height is said to be 250 mm thick.

Reading from Table 4.3 above, it was apparent here that for EN 1992 the limiting effective tension depth was where $h_{c,eff} = 2.5(c + \varphi/2)$. The effective depth value was 120 mm for all section thicknesses where the bar diameter was set at 16 mm and concrete cover was 40 mm. The effective tension depth found using BS 8007 showed values consistently greater than those determined by EN 1992.

Where the concrete cover was 50 mm, the depth of effective tension depth in accordance to BS 8007 was expectedly unaffected by a change in concrete cover or the choice of bar diameter since these variables were not included in the formula for effective depth in BS 8007. For EN 1992, the effective tension depth was limited by $h_{c,eff} = 2.5(c + \varphi/2)$ only after a section thickness of 300 mm. Section thicknesses determined using BS 8007 were found to either be equal to or greater than those obtained by EN 1992, as in the previous cases. As the cover was further increased to 60 mm it can be seen that for EN 1992 the effective tension was also mostly limited to $h_{c,eff} = 2.5(c+ \varphi/2)$.

Conclusively, it may be determined that the effective tension depths determined using EN 1992 were generally smaller than those determined using BS 8007. The limiting effective depth was $2.5(c + \varphi/2)$ for most combinations of section thickness and concrete cover values considered. Thus, the bar diameter to effective steel ratio ($\varphi/\rho_{p,\,eff}$) as determined by EN 1992 would generally be smaller than those obtained using BS 8007 given that the bar diameter and steel content was the same in both cases. Although, even where EN 1992 may estimate a smaller effective steel content ratio ($\varphi/\rho_{p,\,eff}$), the exclusion of the concrete cover term in the BS 8007 variation of the crack spacing model would mean that EN 1992 still predicts greater crack spacing values.

4.5.2 Influence on Reinforcement Bar Diameter on Effective Tension Area

The influence of the reinforcement bar diameter may be found by varying the bar diameter whilst maintaining the same section thickness (250 mm) and cover value (40, 50 and 60 mm). It was determined that bar diameters 20 mm and greater generally gave equal effective tension depths of h/2 for both codes EN 1992 and BS 8007 (Table 4.4). This may be attributed more so to the increasing concrete cover value rather than the choice of reinforcing bar diameter (since where $h_{c,eff} = 2.5(c + \varphi/2)$ the cover value has a larger helping of the overall value of the effective tension depth) .

Table 4.4 Influence of bar diameter on effective depth (h = 250 mm)

		EN 1992		BS 8007
Cover (mm)	**Bar diameter (mm)**	**$h_{c,eff}$ (mm)**		**$h_{c,eff}$ (mm)**
		h/2	**2.5(c + ϕ/2)**	**h/2**
40	16	125	120	125
	20	125	125	125
	25	125	131	125
50	16	125	145	125
	20	125	150	125
	25	125	156	125
60	16	125	170	125
	20	125	175	125
	25	125	181	125

4.6 Comparison of BS 8007 and EN 1992 Edge Restraint Estimation on Crack Width

4.6.1 Influence of Section Thickness on the EN 1992 Edge Restraint Crack Model

To assess the influence of section thickness on the edge restraint crack model, the section thickness was varied whilst the, amongst other variables, the cover was kept constant at 40 mm and the reinforcing bar diameter remained 16 mm throughout. Thus, the effective depth was limited to 2.5(c + φ/2) for all considered section thicknesses.

Increases in the section thickness results in a decrease in the crack width calculated. The restrained strain as calculated from EN 1992-3 gave a constant restrained strain value for all section thicknesses considered. It was uncovered, in this analysis, that there was little difference in the amount of area required to achieve a 0.2 mm crack width for each section thickness considered. More specifically, a range of reinforcing from 1.4 to 0.7 %A_s was required to meet the crack width limit 0.2 mm for 250 to 500 mm thick sections respectively (a ± 15% average relative decrease in reinforcement with each 50 mm increase in section thickness as observed in Figure 4.3).

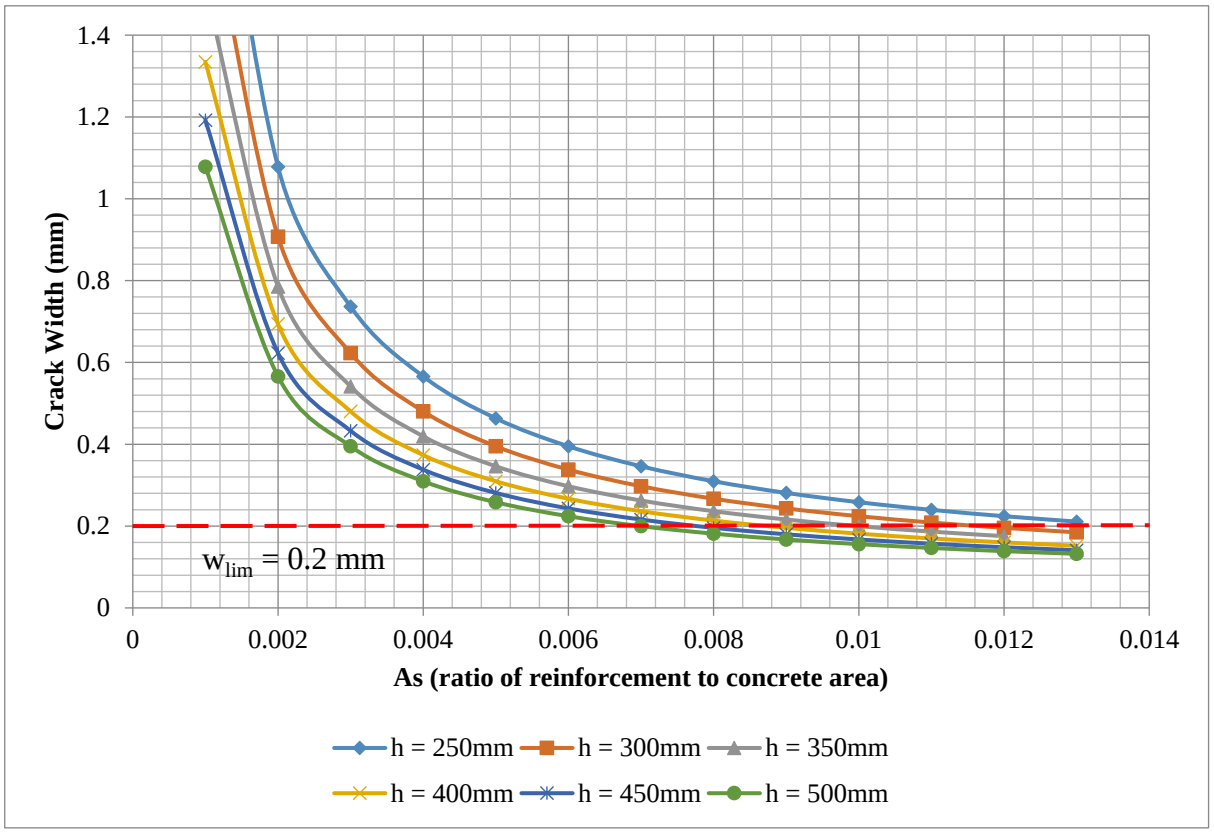

Figure 4.3: Influence of Section Thickness on Crack Width for Edge Restrained Crack Model (EN 1992)

The only real difference that is presumed to have come from changing the section thickness was the amount of tension steel area required to maintain a particular ratio of steel to gross concrete cross-sectional area for each section thickness considered. This effects the effective steel ratio ($\rho_{p,eff}$) and thus the crack spacing (and the eventual crack width) calculated.

The limiting crack width of 0.2 mm was also one that satisfied the BS 8007 crack limit – as was previously established. For BS 8007, the amount of area required to achieve a crack width of 0.2 mm is about 0.8% for all section thicknesses (as was illustrated in Figure 4.4). Thus section thickness had no impact on the crack width for the BS 8007 edge restraint case. Here, we find that EN 1992 was quite conservative when compared to BS 8007 requiring ±63, 50, 25, 13, and 0 % more reinforcement for crack width limit satisfaction for 250, 300, 350, 400 and 450 mm thick section respectively. Whilst for a 500 mm thick section, BS 8007 required 14% more reinforcement than EN 1992 for crack width limit compliance.

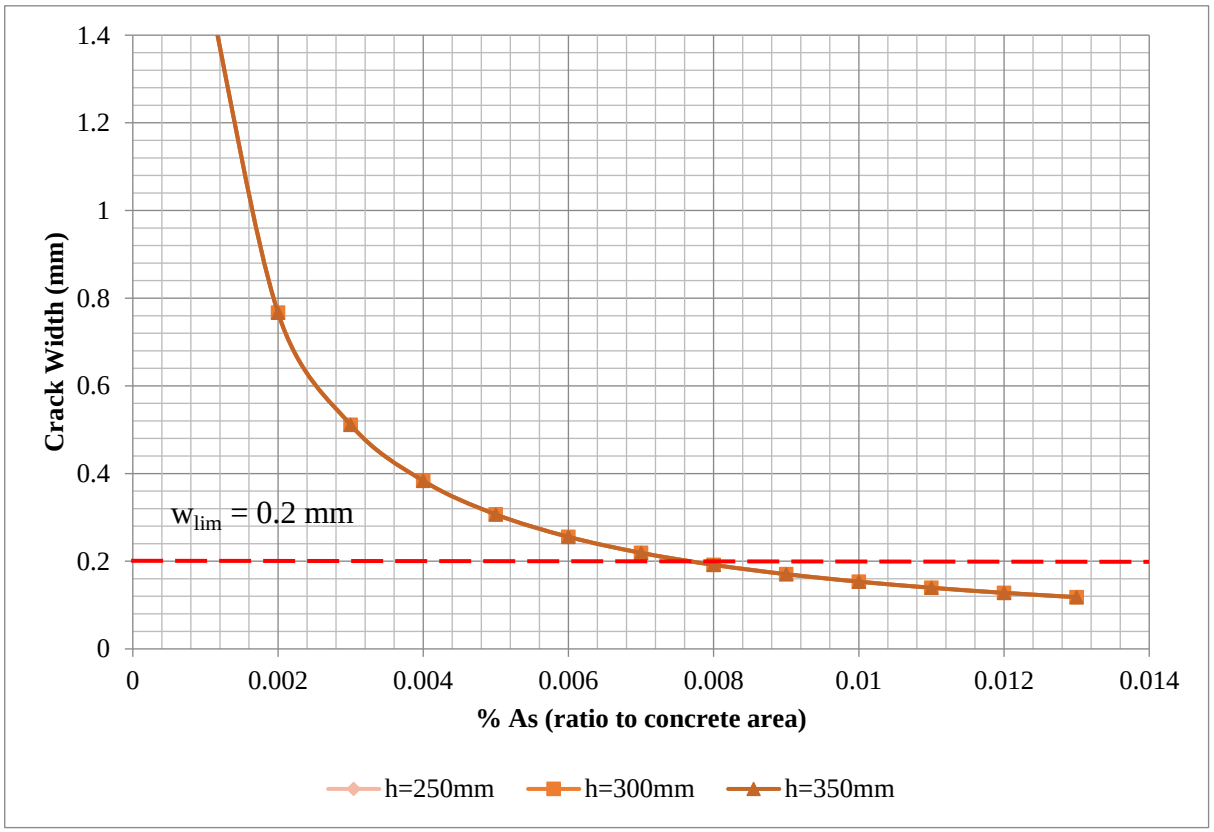

Figure 4.4: Influence of Reinforcement Area on Crack Width for Edge Restrained Crack Model (BS 8007)

4.6.2 Influence of Restraint Factor on EN 1992 Edge Restraint Crack Model

The section thickness was kept constant at 250 mm thick whilst the amount of reinforcement used was varied (φ =16 mm throughout). This exercise is done for a varied array of restraint factors ranging from R = 0.1 up to R = 0.5.

As may be expected, an increase in the restraint factor would result in there being an increase in the estimated crack width. The results of this analysis are presented in Figure 4.5. A larger restraint factor would bring about an increase in the restrained strain and thus a bigger crack width value being calculated and an increase in reinforcement required for a particular crack width to be met. A reinforcement of 0.22% A_s for a restraint factor of R = 0.1, 0.46% A_s at R = 0.2, 0.74% A_s for R = 0.3, 1% A_s at R = 0.4 and 1.30% A_s for R = 0.5 was what was required to meet the 0.2 mm crack width using EN 1992 (a 59% average relative increase in reinforcement required with every 0.1 increment in restraint factor).

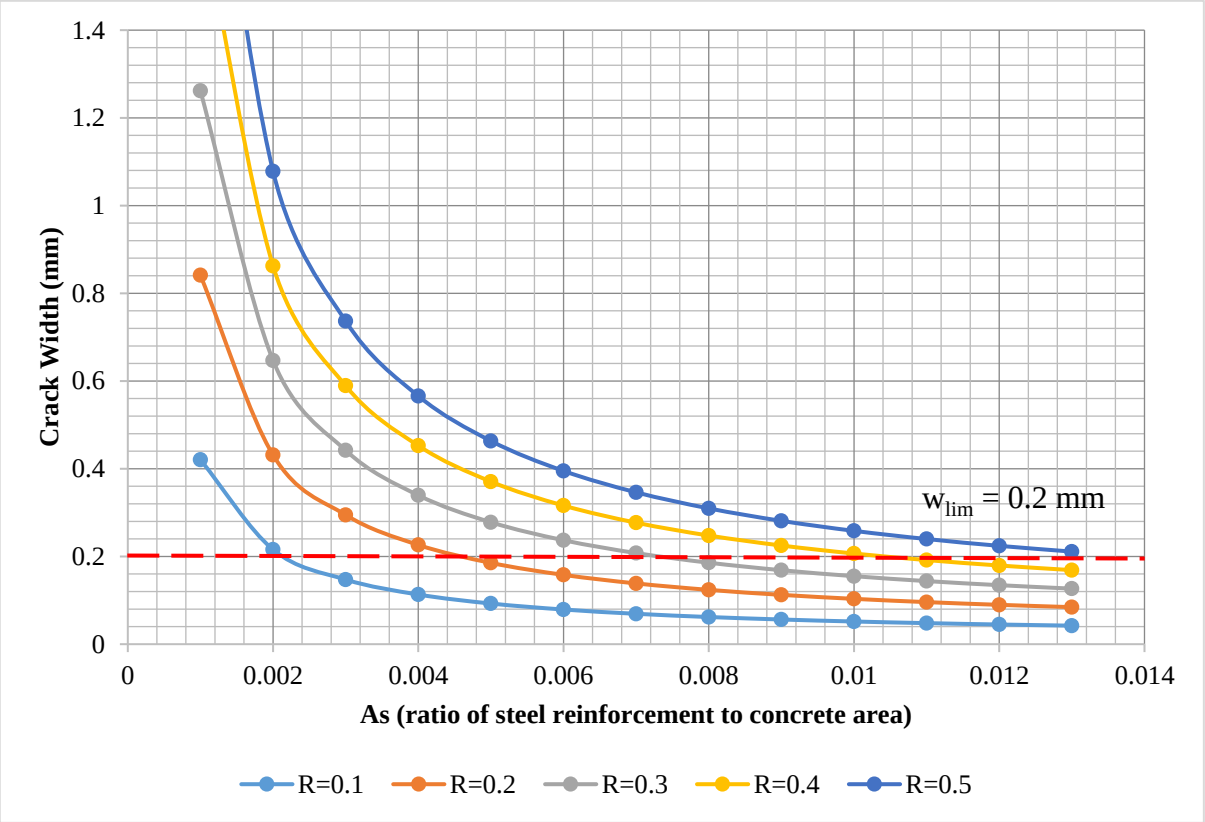

Figure 4.5: Influence of Restraint on the Edge Restrained Crack Model (EN 1992)

4.6.3 Influence of Restraint Factor on BS 8007 Edge Restraint Crack Model

A steel reinforcement amount of about 0.16% at a restraint factor of 0.1 to 0.80% at R = 0.5 would result in the crack width limit being met as shown in Figure 4.6. Comparing this result to those found in the EN 1992 case, A range of from 38% more reinforcement was required to meet the 0.2 mm crack limit at R = 0.1 under EN 1992 to about 63% more reinforcement was necessary for the crack limit compliance where R = 0.5 (a significant jump at full restraint).

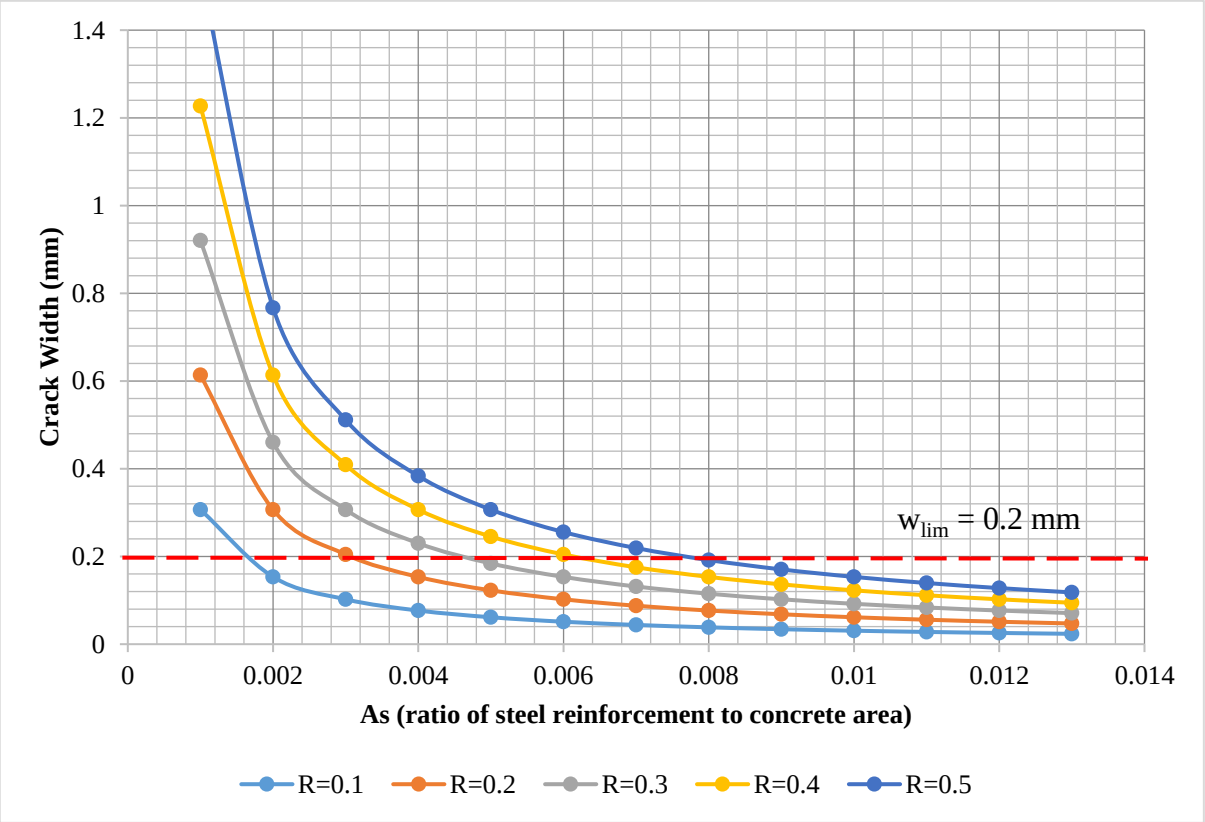

Figure 4.6: Influence of Restraint on the Edge Restrained Crack Model (BS 8007)

It was anticipated that both EN 1992 and BS 8007 would yield very similar results. This expectation comes particularly considering the fact that the formulae for the edge restraint crack width model under EN 1992 and BS 8007 are quite similar in composition. However, it was found that the EN 1992 crack model still gave more conservative results. This might be due to the inclusion of autogenous shrinkage in the estimation of the free unrestrained strain in the EN 1992 crack model, which is not included in the BS 8007 crack model.

4.7 Comparison of BS 8007 and EN 1992 End Restraint Estimation of Crack Width

Another point of interest, in comparing the major differences between the EN 1992 code of practice with BS 8007, is the change in the restrained strain estimation for a concrete member subject to end restraint. It may be observed that no one parameter is shared between either of the restrained strain code formulas for end restraint. A comparison between the two different formulae was conducted. For this comparison, the section thicknesses were varied with a constant 40 mm concrete cover and a 75 mm centre to centre reinforcement spacing (A_s = 2680 mm ^{2}/ section face).

It was determined that the restrained strain from end restraint calculated using EN 1992 estimated much greater crack widths as compared to those crack widths determined using BS 8007 (as may be deduced from Figure 4.7). For instance, in the case where reinforcement spacing was 75 mm centre to centre, cover is 40 mm and 16 mm reinforcing bar diameter, a crack width estimated under EN 1992 for 250 mm concrete section will amount to 0.15 mm. Whilst under the same conditions, BS 8007 will determine that the crack width produced by end restraint will equal 0.07 mm (about half of the value of the crack width determined under EN 1992). Thus, the EN 1992 estimation of end restraint was found to be more conservative than that of BS 8007.

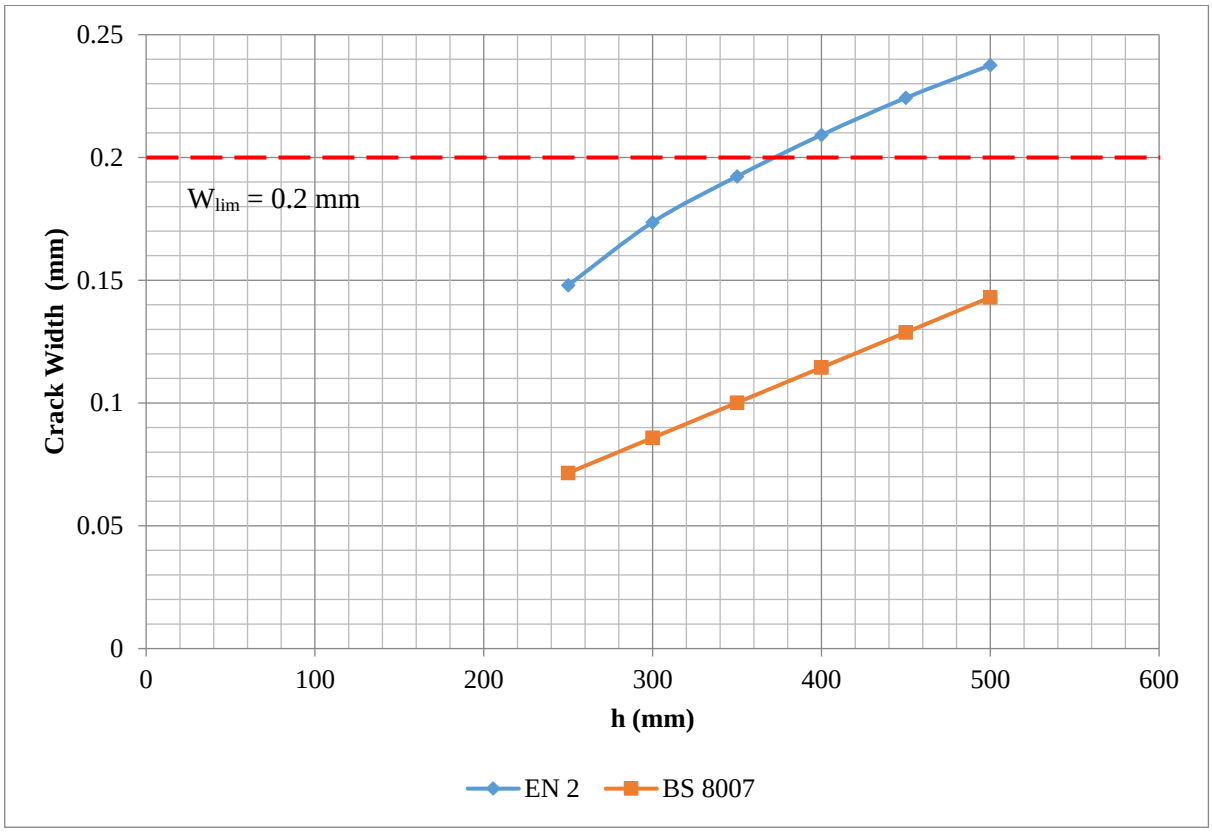

Figure 4.7: Comparing EN 1992 and BS 8007 End Restraint Equation (40 mm cover, 75 mm reinforcement spacing)

4.7.1 Influence of Section Thickness on the EN 1992 End Restraint Crack Model

The influence of section thickness on the end restraint crack width calculations for EN 1992 against BS 8007 were extended for section thicknesses ranging from 250 mm to 500 mm.

Increasing the section thickness decreased the calculated crack widths of members subjected to end restraint. Increases in section thickness resulted in an increase in reinforcement required achieve the crack width limit of 0.2 mm. Clearly, those reinforcement ratios for which section thicknesses 250 mm to 450 mm meet the 0.2 mm crack limit were beyond the range of

reinforcement ratio considered in this analysis (Figure 4.8). A quick calculation of the reinforcing ratio at which the crack width limit 0.2 mm may be met returned values in the range of 1.8 to 1.3% A_s for section thicknesses 250 to 450 mm respectively (a ± 9% average relative decrease in reinforcement per 50 mm increase in section thickness– smaller than the edge restraint case). For section thickness 500 mm, it may be read from Figure 4.8 that 1.2% A_s was required to meet the 0.2 mm crack width limit.

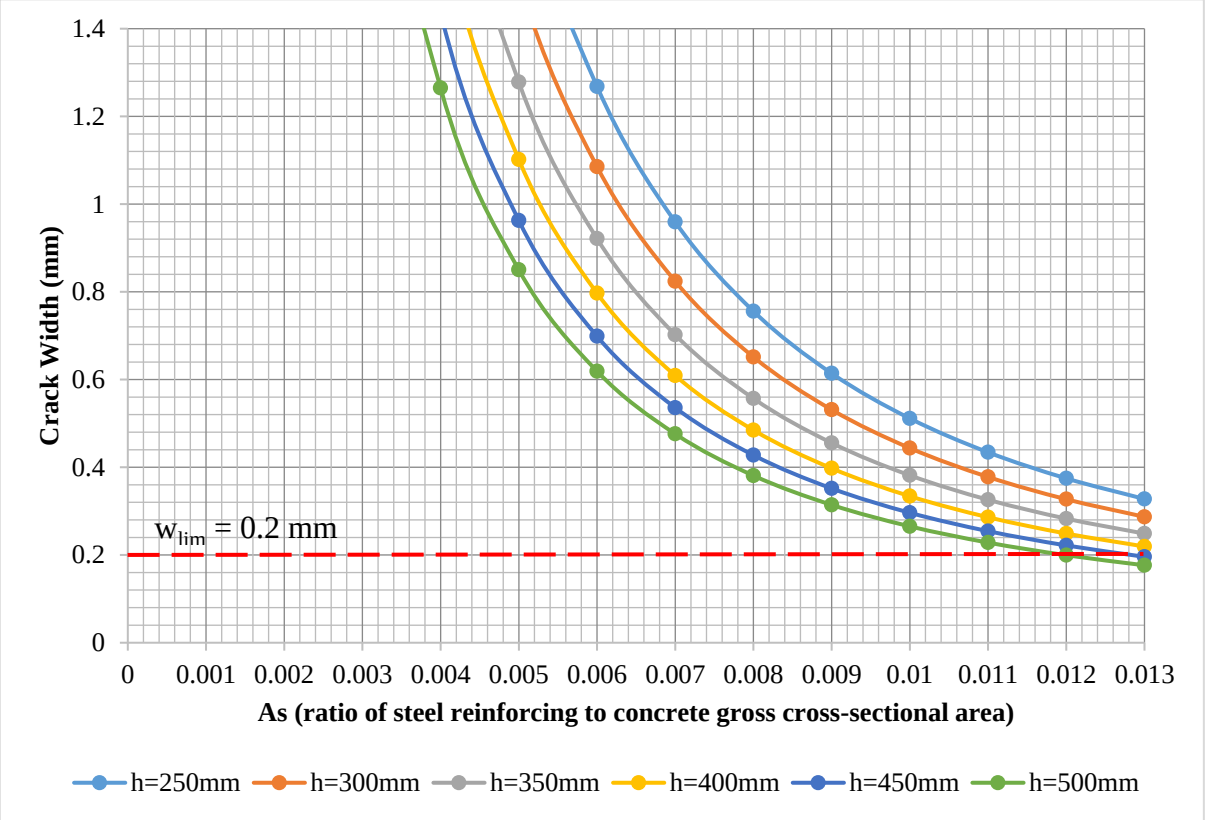

Figure 4.8: Influence of Section Thickness on Crack Width for End Restraint (EN 1992)

The decreasing value of the k coefficient as the section thickness increases decreases the amount of strain calculated for thicker sections (k varies from to 0.65 for $h \geq 800$ mm up to 1 for $h \leq 300$ mm). Increases in section thicknesses means that both the $\rho_{p,eff}$ ($A_s/A_{c,eff}$) and the ρ (A_s/A_c) would increase since the amount of steel included in these ratios was increased for the same steel to gross concrete ratio– this was especially true for the effective steel content ratio, $\rho_{p,eff}$. The increase in these ratios results in a decrease in the amount of restrained strain and crack spacing calculated since the reciprocal of these ratios are included in the estimation of both. However, the increase in the amount of steel reinforcing required for any given steel to concrete ratio as section thickness was increased had the seemingly stronger impact of increasing the overall crack width.

4.7.2 Influence of Section Thickness on the BS 8007 End Restraint Crack Model

The end restraint estimation in BS 8007 follows the same approach as for edge restraint. The relationship of reinforcement to crack width for various section thicknesses will be as mentioned for edge restraint (in the previous section) where a reinforcement ratio of 0.8% A_s was necessary for the 0.2 mm crack width to be met. This would mean that EN 1992 requires from 50% (at 500 mm) to beyond 63% (for section thickness 400 mm down to 250 mm) more reinforcement than BS 8007 to meet the 0.2 mm crack width limit. It is also evident from this result that the EN 1992 end restraint crack model requires more reinforcement to meet the crack width limit than the EN 1992 edge restraint crack model when compared against the BS 8007 crack model– indicating that it was the more conservative of the two EN 1992 models.

4.8 Parameter Sensitivities in Crack Model: Summary and Concluding Remarks

Along with comparing the British Code and Eurocode crack model, the parametric study was conducted to assess the sensitivities of the various parameters of the crack model. The model's sensitivity to various parameters may ultimately affect the failure probability calculated in the reliability analysis of the crack model. Thus, a brief outline of these sensitivities is presented below:

- **Concrete cover:**

Concrete cover proved to have a relatively small effect on the predicted crack spacing, especially where compared to the $\varphi/\rho_{p,\,eff}$ ratio term in the crack spacing model. Although its influence on the reliability of the crack model must still be considered since it was determined from experimental data that concrete cover was a parameter not to be ignored in the assessment of crack spacing (Caldentey *et al*., 2013). Thus, variations in the concrete cover value were used to examine what influence this parameter has on the reliability of the crack model. A reference concrete cover value of 40 mm was selected for the reliability analysis based on the survey of water retaining structures (McLeod, 2013).

- **$\varphi/\rho_{p,\,eff}$ ratio:**

The investigation into the $\varphi/\rho_{p,\,eff}$ ratio's influence on the crack spacing revealed that this ratio contributes considerably to the estimated crack spacing. This, in turn, would result in $\varphi/\rho_{p,\,eff}$ contributing considerably to the ultimate crack model.

- **Effective tension area:**

The effective tension area had been found to be predominately limited to $2.5(c + \varphi/2)$ for similar covers and bar diamters. In the cases where the bar diameter or the concrete cover values are increased, h/2 becomes the limiting effective tension area. For a combination of 40 mm cover and bar diameter of 16 mm or 20 mm, the effective tension area will always give $2.5(c + \varphi/2)$ for any section thickness. For a 250 mm thick concrete section, 40 mm concrete cover and 20 mm reinforcing bar diameter the effective depth for $h_{c,eff} = 2.5(c + \varphi/2)$ and h/2 both return a value of 125 mm. Thus this combination section thickness, cover and bar diameter will be considered in the reliability analysis; giving opportunity for the direct comparison of reliability models containing either effective depth variations. In this way, the effect of the effective tension areas may be assessed. The effective tension area has an obvious effect on the $\varphi/\rho_{p,eff}$ ratio which had already been found to contribute considerably to the crack model.

- **Crack width limit:**

The crack width limit was found to have a considerable influence on the restrained strain crack model for both EN 1992 and BS 8007 design codes. This influence applied both to the edge and end restraint conditions. Thus, as found in previous research, the adoption of the more onerous crack limits of EN 1992 would subsequently have a significantly negative financial implication in design. A decrease in the crack limit results in an increase in the demand for reinforcing (and thus an increase in the cost of construction).

- **Section thickness:**

The section thickness has been found to have some influence on the crack model for both the end and edge restraint. A variation of the section thickness will be used in the reliability model to gauge what influence it bears on the crack model's overall reliability level. Section thickness was found to bear more of an influence on the end restraint crack model than the edge restraint crack model. A reference value of 250 mm section thickness will be used in reliability analysis.

- **Bar diameter:**

Increasing bar diameter, as before mentioned, resulted in h/2 being the limiting effective tension area. Little variability in the influence on the crack model was experienced where the bar

diameters were varied. This was particularly true for bar diameters beyond 20 mm where the same effective tension area is produced each time (h/2).

- **Reinforcement area:**

There was a noticeable correlation between the EN 1992 crack model and the amount of reinforcement used. Clearly, the decline in the crack widths estimated by the crack model came with an increase in the amount of tension reinforcement used. It had been determined in past investigations on the reliability of reinforced concrete members that the failure probability is sensitive to, among other basic variables, the reinforcement ratio in the member (Holický, Retief and Wium, 2010). Therefore, it is suggested that the sensitivity of the reliability of the crack model be tested against a variation of reinforcement ratios for various basic variables. For the selected reference case of 250 mm section thickness, 40 mm cover and 20 mm rebar diameter, a reinforcement ratio of 1748 mm^2 and 2202 mm^2 per section face for edge and end restraint respectively for the 0.2 mm crack limit to be met.

- **Restraint degree:**

The restraint degree is not a parameter used in the estimation of end restraint in EN 1992. The edge restraint crack model has been proven to be noticeably influenced by the restraint under edge restraint conditions. Historically, according to BS 8110-2, the restraint degrees (restraint factors) have been found to be greater than a value of 0.7. EN 1992 includes creep into its restraint degree, giving a value of full restraint of up to 0.5. A fully restrained member will be considered in the reliability analysis. However, much like in the parametric study, the influence of the restraint factor on the reliability of the edge restraint crack model will be investigated by varying the restraint factor from 0.1 to 0.5. Practically, this considers an array of configurations, and thus restraint conditions under which the restrained member is nearly free to move and then increasingly restricted up to full restraint.

Following after the parametric study, it was determined that the end restraint model was the most conservative of the two external restraint conditions assessed using EN 1992 (as BS 8007 modelled edge and end restraint in the same way). In other words, more reinforcement is required for a member subjected end restraint to meet the crack limit as compared to the edge restraint condition. Also, larger crack widths were determined using the end restraint model. Comparing BS 8007 and relevant parts of BS 8110-2 to corresponding codes EN 1992-3 and EN 1992-1-1, Eurocode was found to be more conservative than the British codes. From the parametric study conducted above, a reasonable selection of design variables for which the reliability analysis could be conducted may be established. It was paramount that the effect of influential parameters be tested in the reliability analysis of the EN 1992 crack model. Hence, the variables found to be

particularly influential to the EN 1992 crack model and thus potentially influential to the reliability of the crack model include the following: concrete cover, the $\varphi/\rho_{p,\,eff}$ ratio, the effective tension area, section thickness, the reinforcement area as well as the restraint degree.

Chapter 5: FORM Analysis of EN 1992 Crack Model: Methodology, Results and Discussion

5.1 Introduction:

The absence of an equivalent design code for liquid retaining structures in South Africa formed the primary basis for the reliability analysis conducted herein. In the parametric study of chapter 4, it was found that the crack width limit held a considerable influence on the EN 1992 edge restraint crack model. This influence was experienced less so on the end restraint crack model, but still noteworthy. The more stringent crack width limits of EN 1992 brought with it increased financial demand proportional to the increased requirement for steel reinforcement for the compliance of the permissible crack width limits. The restraint factor was also determined to be a particularly influential parameter in the edge restraint crack model in which it appears. Thus, investigations into the impact had by the above-mentioned variables on the reliability of the crack model were undertaken in this chapter.

In an attempt to further understand the reliability performance of the EN 1992 crack model in the South African context, the influence of variables such as the concrete cover, the bar diameter to effective steel ratio and the section thickness (which were already been assessed deterministically in the parametric study) will be assessed probabilistically (taking into account their stochastic nature). This should indicate the ways in which the EN 1992 model may be adjusted to bring about compliance with South African reliability standards. Moreover, identifications of the circumstances under which the target reliability index is met under South African conditions may be found through the reliability analysis.

Investigations into past research on the matter revealed that, considering the load induced case of the EN 1992 crack model, the serviceability limit state is the more dominant limit state for liquid retaining structures (McLeod, 2013). Bearing this in mind it had also been argued that a higher reliability class and target index be considered for use when designing liquid retaining structures (Barnardo-Viljoen, Mensah *et al*., 2014). These arguments strengthen the need for a reliability analysis of this serviceability limit state, particularly as applied to the South African environment. Additionally, model uncertainty had also been identified in the literature to be a particularly influential parameter in the reliability of reinforced concrete structures. Hence, its impact on the reliability of the cracking serviceability limit state was also investigated.

The First Order Reliability Methodology had been employed to assess a representative liquid retaining structure which had come as a by-product of the parametric study which gave a sense of realistic sets of variables to be used in the reliability analysis of the EN 1992 crack model. The representative structure to be used in the analysis is further described in the subsequent text.

5.2 Methodology of Reliability Analysis:

5.2.1 Reliability Analysis Formation

The calculated crack width is described in EN 1992 as being a simple compatibility equation in which the crack width comes as the product of both the crack spacing (S_{rm}) and the restrained strain (ε_r).

$$w = S_{rm}\varepsilon_r \tag{5.1}$$

The maximum crack spacing equation found in EN 1992-1-1 is used to calculate the characteristic crack width. This is the crack width that has a 5% probability of being exceeded and does not represent the average crack width, being a maximum value.

$$S_{r,max} = 3.4c+0.425k_1k_2\varphi/\rho_{p,eff} \tag{5.2}$$

In the development of the crack spacing formulae, it was found through experimentation that the maximum crack spacing may be estimated to be about 1.7 times the mean crack spacing (Beeby and Narayanan, 2005). The mean crack spacing formula will be adopted in the reliability analysis of the EN 1992 crack model undertaken in this investigation and is given by the following formula:

$$S_{rm} = 2c+0.25k_1k_2\varphi/\rho_{p,eff} \tag{5.3}$$

The mean restrained strain (ε_r) for edge and end restraint are as those given in EN 1992-3 in which the restrained strain for edge restraint is given by,

$$\varepsilon_r = (\varepsilon_{sm} - \varepsilon_{cm}) = R_{ax}\,\varepsilon_{free} \tag{5.4}$$

Where ε_{sm} is the mean strain in the reinforcement and ε_{cm} represents the mean strain in the concrete between cracks. R_{ax} marks the restraint factor (restraint degree) which is indicative of the degree of freedom of movement which is experienced by the concrete member. And $\varepsilon_{free} = \varepsilon_{cd}+\varepsilon_{ca}+\alpha_{T,c}(T_1+T_2)$, where ε_{cd} is the drying shrinkage strain, ε_{ca} is the autogenous shrinkage strain; $\alpha_{T,c}$ is the coefficient of thermal expansion of concrete, T_1 denotes the fall in temperature from hydration peak to mean ambient temperature in the concrete. T_2 is the seasonal fall in temperature.

The mean strain resulting from end restraint is estimated in a different way to edge restraint and is given by the formula:

$$\varepsilon_r = (\varepsilon_{sm} - \varepsilon_{cm}) = \frac{0.5\alpha_e k_c k f_{ct,eff}\left(1+1/\alpha_e\rho\right)}{E_s} \tag{5.5}$$

The modular ratio is represented by the symbol α_e, the factor k_c is the coefficient accounting for the stress distribution within a section and k accounts for the non-uniform self-equilibrating stresses. The parameter ρ describes the reinforcement to gross concrete cross-sectional area ratio, whilst E_s denotes the steel modulus of elasticity.

For the reliability analysis of the EN 1992 crack model the limit state function was first defined, where w_{lim} is the limiting crack width treated as a deterministic value in this analysis. Failure of the performance function will occur where the calculated crack width either just meets or exceeds the limiting crack width. The calculated crack width, calculated using equations 5.3 and 5.4 or 5.5 (for the appropriate restraint condition), was multiplied by the model uncertainty (θ). The model uncertainty was treated as a random variable in this analysis with its mean value taken to be 1.

$$g = w_{lim} - \theta w \tag{5.6}$$

Other random variables of the limit state function include the section thickness (h), the concrete cover (c) and the tensile strength of the concrete ($f_{ct,\,eff}$).

5.2.2 Representative Liquid Retaining Structure

Two restraint conditions were considered: edge and end restraint. Under both restraint conditions, the section thickness was 250 mm with a C30/37 specified strength for OPC concrete ($T_1 = 15^{\circ}C$, for 340kg/m^3 binder content), cast in the summer (giving a seasonal change in temperature of $T_2 = 23^{\circ}C$). Cover to reinforcement was 40 mm and steel formwork was selected for the analysis. The shrinkage strain was determined to be 220με for the South African coastal regions with 80% relative humidity. The steel reinforcement selected was 20 mm diameter high yield bars. Using EN 1992, the autogenous shrinkage strain was determined to be 33με (at 28 days) and the coefficient of thermal expansion of quartzite concrete had been found to amount to 14με. The crack width limit was set at 0.2 mm for the reliability analysis. The choice of section modulus and thus the modular ratio obtained through calculations was found to bear little significance to the overall reliabilities calculated (about a 2% average increase in reliability indices was calculated between the 3, 7 and 28-day elastic moduli). For these analyses, the section modulus for concrete at 3 days was selected since that is the critical time in which cracking most likely occurs.

5.2.3 Probabilistic Theoretical Models of Basic Variables

The basic variables entered into the limit state function are stochastic in nature. The various statistical distributions to which each variable belonged and moreover what statistical parameter best represented they have been collected. Basic variables found to have very little to no real

variability were regarded as being deterministic. Those variables that were found to have a random nature include the concrete cover (c), the concrete section thickness (h), the concrete tensile strength ($f_{ct,eff}$) and the model uncertainty (θ). The basic variables were entered into the limit state function in meters (m) and kilonewtons (kN). A summary of the basic variables featured in the limit state function for the FORM analysis and their respective statistical properties, as entered in Excel, are summarised in Figure 5.1:

Basic Variables		Symbols	Dimimensions	Distrbtribution	Char. Value	Mean	CoV	Std. Dev.
						μx in kN and m		σx in kN and m
	Cross section thickness	h	mm	Normal	250	0.25	0.01	0.0025
Geometry	Cross section width	b	mm	Deterministic	1000	1	0	0
	Concrete cover	c	mm	Gamma	40	0.04	0.15	0.006
	Reinforcement diameter	φ	mm	Deterministic	20	0.02	0	0
	Concrete compressive strength (cube)	f_{cu}	MPa	Deterministic	37	37000	0	0
	Concrete compressive strength (cylinder)	f_{ck}	MPa	Deterministic	30	30000	0	0
	Concrete tensile strength	$f_{ct,eff}$	MPa	Lognormal	2	2900	0.19	551
	Concrete elastic modulus	$E_{c,eff}$	GPa	Deterministic	28	28000000	0	0
	Modular ratio	α_e	none	Deterministic	7.14	7.14	0	0
	Steel modulus	E_s	GPa	Deterministic	200	200000000	0	0
Material	Autogenous Shrinkage Strain	ε_{ca}	με	Deterministic	33	3.30E-05	0	0
	Drying shrinkage strain	ε_{cd}	με	Deterministic	220	2.20E-04	0	0
	Area of Steel	As	mm^2	Deterministic	2513	0.002513	0	0
	Coefficient (reinforcement)	k_1	none	Deterministic	0.8	0.8	0	0
	Coefficient (tension)	k_2	none	Deterministic	1	1	0	0
	Coefficient (for self-equilibrating stresses)	k	none	Deterministic	1	1	0	0
	Coefficient for stress distribution (pure tension)	kc	none	Deterministic	1	1	0	0
Coefficients	Coefficient of Thermal Expansion	α_c	με/˚C	Deterministic	14	1.40E-05	0	0
	Temperature	T_1	˚C	Deterministic	23	23	0	0
	Temperature	T_2	˚C	Deterministic	15	15	0	0
	Restraint Degree	R	none	Deterministic	0.5	0.5	0	0
	Limiting Crack Width	w_{lim}	mm	Deterministic	0.2	0.0002	0	0
	Model Uncertainty	θ	none	Lognormal	1	1	0.3	0.3

Figure 5.1: Summary of Statistical Parameters

The FORM calculation was conducted following the logarithm (after A. H-S. Ang and W. H. Tang (1984)):

1) Define the performance function ($g(x) = w_{lim} - \theta w$).
2) Convert non-normal means and standard deviations of variates to normal equivalent.
3) The initial failure points are usually taken to be the mean values of the variates.
4) Determine the derivative of the performance function, g(x), with respect to each random variables using MATLAB. The partial derivatives ($\frac{\partial g}{\partial X'_i}$) are then evaluated at the failure points (which were initially assumed to be the means of the random variables).
5) The direction cosines/sensitivity factors (α_i*) may be subsequently obtained by dividing each derivative by the root of the sum of the square of each derivative (i.e. each derivative is normalised)

$$\alpha_i^* = \frac{\left(\frac{\partial g}{\partial X'_i}\right)_*}{\sqrt{\Sigma_i \left(\frac{\partial g}{\partial X'_i}\right)_*^2}}$$

6) The failure point at the end of the iteration may then be determined through the equation (represented initially as functions of the unknown 'β' value):

$$x_i^* = \mu_{Xi}^N - \alpha_{xi} * \sigma_{Xi}^N * \beta$$

The normal equivalent of the mean and standard deviation of the random variables are used to determine the failure points of the performance function.

7) This failure point is then substituted into the failure function, g(x) =0), and solved for β. Excel solver is used to solve for β. Microsoft Excel solver is a function in the Excel programme that finds the optimal value of a target cell by adjusting the values in variable cells which are used to calculate the value in the target cell. The limit state function was entered into the target cell whilst the reliability index was entered into the variable cell. The GRG linear is the solving method selected. This method is meant for problems that have a smooth nonlinear nature.

   The performance function is set into Excel solver as being the target (or objective) cell and excel solver is set to solve for zero (0). The reliability index, β, is then entered in as the variable cell in which that value of β that will make the performance function zero is determined by excel solver. Thus a new set of failure points may be found using the now obtained β value. The numerical values of these failure points- found after substituting β into the failure point equation- are then used as the starting points in the next iteration.
8) Steps 2 through to 7 are repeated until convergence of β is reached. The failure points obtained with the final reliability index, β, will then represent the final failure points of the performance function.

Figure 5.2 illustrates the steps taken in the FORM analysis of the EN 1992 crack model. The first two iterations are shown in the figure. For this particular analysis, four iterations (Figure 5.3) were enough to bring β into convergence. The influence of select parameters on the EN 1992 restrained strain crack model was assessed in the FORM analysis. These were the parameters identified in the parametric study as being particularly influential to the crack model.

1st Iteration

convert non-normals to normal (2)

lognormal:		pdf					ξ = c.o.v
	f	ξ	λ	μ^N	σ^N		λ= lnμ-0.5*(c.o.v)^2
Concrete cover	c	0.15	-3.230125825	0.03955	0.006		μ^N= γ*(1-lnγ*+λ)
Model Uncertainty	θ	0.3	-0.045	0.955	0.3		σ^N= γ*ξ

1st iteration logrithm

					*σ		$x^*=\mu^N-\alpha^*\sigma^N*\beta$		
uncorrelated variables		**assumed** (3)			**partial derivatives** (4)	**direction cosine** (5)	**failure point equation** (6)	**failure point** (7)	
h,c, fctm, θ	Xi	xi	μ^Nxi	σ^Nxi	(δg/δXi)	αxi			σ*α
Cross section thickness	h	0.25	0.25	0.0025	0	0	0.25+0*β	0.25	0
Concrete cover	c	0.04	0.03955	0.006	-1.40813E-05	-0.394001578	0.03955+0.002364009*β	0.045398449	-0.002364009
Model Uncertainty	θ	1	0.955	0.3	-3.28482E-05	-0.919109763	0.955+0.275732929*β	1.637150565	-0.275732929
					Σα^2	1			
							β	2.473953936	

substitute

failure function: g(x)= w_{lim} - θw_k = 0.0002-th*wk 0.0002-(0.955+0.275732929*β)*(2*(0.03955+0.002364009*β)+0.25*0.8*1*phi/(As/(2.5*(0.03955+0.002364009*β+0.01)*b)))*(R*(alpha*(T1+T2)+ eca +ecd))

solve for β using excel solver

β	g(x)
2.168419926	-6.87046E-11

2nd Iteration

convert non-normals to normal

lognormal:		pdf					ξ = c.o.v
	f	ξ	λ	μ^N	σ^N		λ= lnμ-0.5*(c.o.v)^2
Concrete cover	c	0.15	-3.230125825	0.039140341	0.006809767		μ^N= γ*(1-lnγ*+λ)
Model Uncertainty	θ	0.3	-0.045	0.756433516	0.49114517		σ^N= γ*ξ

2nd iteration logrithm

					*σ		$x^*=\mu^N-\alpha^*\sigma^N*\beta$		
					partial	**direction**	**failure**	**failure**	
uncorrelated variables		**assumed**			**derivatives**	**cosine**	**point equation**	**point**	
h,c, fctm, θ	Xi	xi	μ^Nxi	σ^Nxi	(δg/δXi)	αxi			σ*α
Cross section thickness	h	0.25	0.25	0.0025	0	0	0.25+0*β	0.25	0
Concrete cover	c	0.045398449	0.039140341	0.006809767	-2.61644E-05	-0.399721592	0.039140341+0.002722011*β	0.044616338	-0.002722011
Model Uncertainty	θ	1.637150565	0.756433516	0.49114517	-6E-05	-0.916636596	0.756433516+0.450201636*β	1.662125239	-0.450201636
					Σα^2	1			
							β	2.011746849	

failure function: g(x)= w_{lim} - θw_k = 0.0002-th*wk 0.0002-(0.756433516+0.450201636*β)*(2*(0.039140341+0.002722011*β)+0.25*0.8*1*0.02/(0.002513/(2.5*(0.039140341+0.002722011*β+0.01)*1)))*(0.5*(0.000014*(15+23)+ 0.000033+0.

Figure 5.2: First and Second Iteration of FORM Analysis of EN 1992 Restrained Shrinkage Crack Model (Edge Restraint, $h_{c,eff}$ = 2.5(c + φ/2))

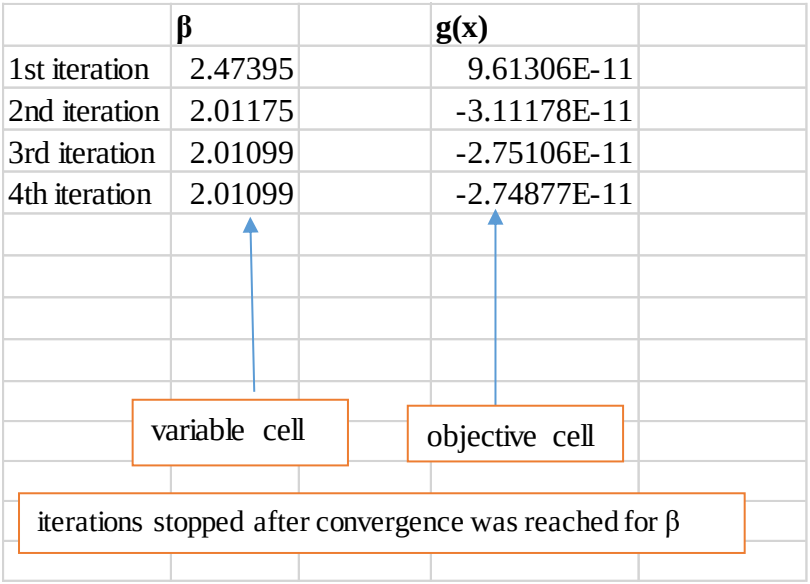

Figure 5.3: Example of Convergence Achieved After Four Iterations (Edge Restraint, $h_{c,eff} = 2.5(c + \varphi/2)$)

A separate spreadsheet was generated for the β values and the corresponding variation of the above-mentioned parameters under which β was attained. The influence of the selected parameters were assessed against a wide array of reinforcement. The steel reinforcement was represented as a percentage amount against the gross cross-sectional area of the concrete member (%A_s). The range selected for each analysis reached up to 3% of steel to concrete. This limit falls just below the feasible limit for reinforcement in a 250 mm thick concrete section (the limit being 3.35% A_s). The feasible minimum bar spacing of 75 mm results in reinforcement to concrete ratios that fall below the SAN 10100-1 maximum limit ($A_s/A_c = 4\%$), thus making the bar spacing the limiting criteria for the amount of reinforcement considered. A summary of the maximum amount of reinforcing that may be implemented for other considered section thicknesses is given in Table 5.1:

Table 5.1: Feasible limit for reinforcement for select section thicknesses (minimum bar spacing 75 mm)

h (mm)	Max. Feasible A_s (%)
250	3.35
300	2.79
350	2.39
400	2.09
450	1.86
500	1.68

It must be reiterated that comparisons of reliability assessments with those of similar past research findings are quite difficult in that unless the same limit state and statistical parameters (mean value and standard deviation of the random variables) are used, direct comparisons would prove to be somewhat inaccurate. Thus alternative measures of results verification may have to be employed. As a measure of assurance that the FORM analysis was correctly executed, hand calculations were conducted alongside those calculations done via Microsoft Excel (acting as a double check of the results obtained).

Reliability models used in the analysis are:

a) Edge restraint with depth of effective tension zone taken to be 2.5(c +φ/2)
b) Edge restraint with depth of effective tension zone taken to be h/2
c) End restraint with depth of effective of tension zone taken to be 2.5(c +φ/2)
d) End restraint with depth effective of tension zone taken to be h/2

The majority of the reliability analysis was conducted with 2.5(c +φ/2) being the depth of effective tension area as it is the limiting depth of effective tension area for most combinations of section thicknesses, concrete covers and bar diameters. However there were certain instance where models containing h/2 was more appropriate, these instances are mentioned where they apply.

5.3 Results and Discussion

5.3.1 Influence of cover and $\varphi/\rho_{p,eff}$

The effects of the concrete cover and bar diameter to effective steel content ratio were assessed to gauge what impact either variable had on the reliability performance of the restrained shrinkage

crack model of EN 1992. The concrete cover affects the formulation of the limit state function by dictating the limiting effective tension depth. Thus the cover value was selected such that the same limit state function was used in the reliability analysis- making direct comparisons of results between concrete covers possible.

5.3.1.1 Edge Restraint

For a 250 mm thick section, the influence of concrete cover and the $\varphi/\rho_{p,\,eff}$ was examined by varying the cover value against a selection of steel reinforcement ratios. Cover values of 50, 60 and 70 mm were used in this analysis, making h/2 the appropriate effective depth of tension area for the analysis. The reliability of the crack model increased with a decrease in concrete cover (as illustrated in Figure 5.4). For example for a steel ratio of say 2%, the reliability indices for 70, 60 and 50 mm are 1.48, 1.68, and 1.90 respectively. A decrease in cover would result in a decrease in the crack spacing attained, thus decreasing the overall crack width obtained. Crack widths beyond the crack width limit are then less likely to occur, hence the increase in reliability with the decrease in concrete cover.

Moreover, irrespective of the cover value selected, the reliability index would increase with an increase in the amount of reinforcement used. Undoubtedly, where more reinforcement is applied to a concrete section the more resistant the member will become against tensile stresses, and so less cracking occurs.

More reinforcement is required to meet the target reliability index as concrete cover increases. The target reliability index ($\beta_t = 1.5$) is met at steel to concrete ratios of about 1.69%, 1.85% and 2.02% for a cover value of 50 mm, 60 mm and 70 mm respectively. This amounts to about an average increase in reinforcement of 10% with every 20% relative increase in covers selected (or otherwise per 10 mm absolute increase in concrete cover value).

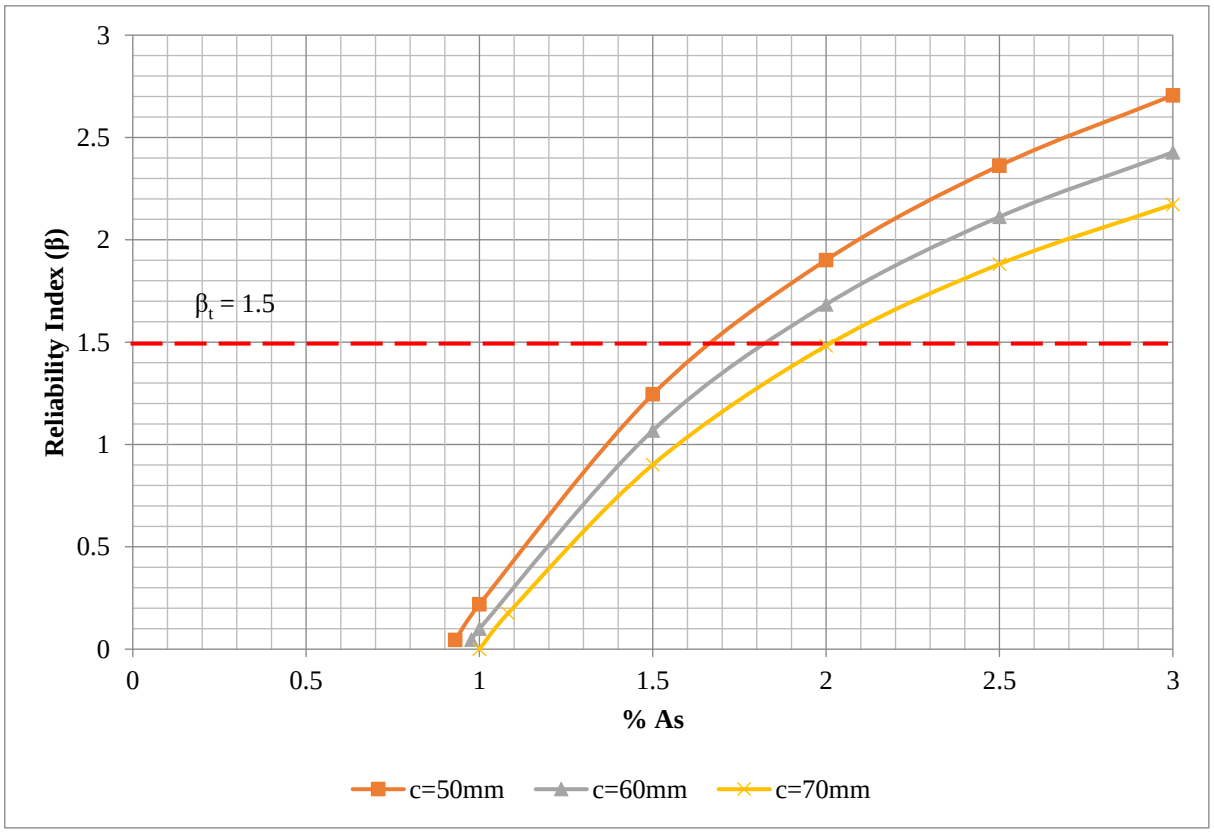

Figure 5.4: Influence of Cover and $\varphi/\rho_{p,\,eff}$ (Edge Restraint)

On comparing the reliability index directly against the $\varphi/\rho_{p,eff}$ ratio (as shown in Figure 5.5) the $\varphi/\rho_{p,eff}$ ratios that ensure that the target reliability index is met for concrete covers 50, 60 and 70 mm are: 1.18, 1.08 and 0.99 m respectively (Figure 5.5). Since an increase in the amount of steel reinforcement used will result in a decrease in the $\varphi/\rho_{p,eff}$ ratio, it may be concluded that the reliability increases with a decrease in the $\varphi/\rho_{p,eff}$ ratio. Where the bar diameter had been found in the deterministic analysis to have little influence on the crack width model, the influence of the $\varphi/\rho_{p,eff}$ ratio may be deduced to have come mostly from the steel reinforcing and partially from the section thickness's stochastic nature within the limiting effective tension depth equation. The gradient of the graph of Figure 5.5 was close to -2 for the cover values considered indicating a strong relationship.

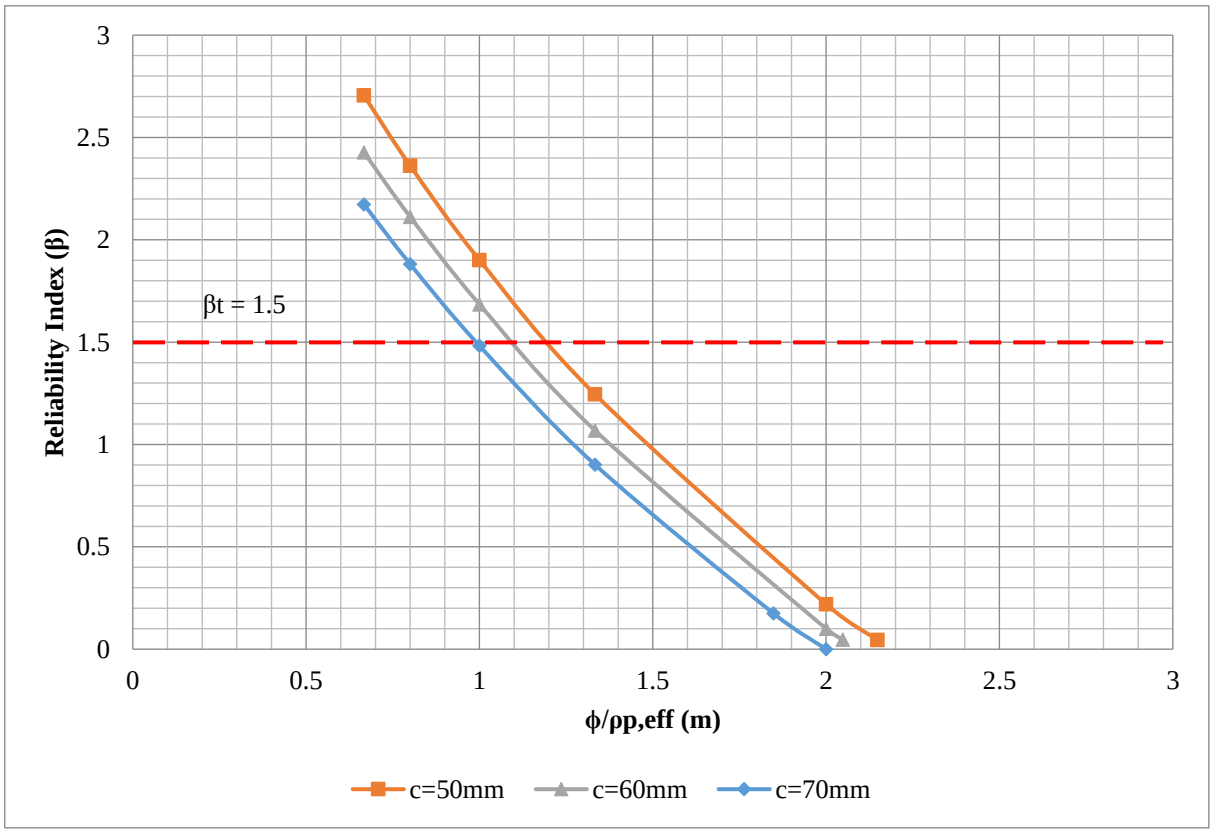

Figure 5.5: Influence of $\varphi/\rho_{p,\,eff}$ Ratio on Reliability Index (Edge Restraint)

5.3.1.2 End Restraint

For end restraint conditions, with the same selection of concrete cover values, as with edge restraint, it can clearly be deduced that a decrease in cover results in an increase in the reliability index calculated (Figure 5.6). For instance, the reliability indices for end restraint at 2% A_s would go from 1.17, 1.34, 1.52 for concrete values 70, 60 and 50 mm respectively (achieving lower reliability indices than edge restraint for the same $\%A_s$ value).

A steel reinforcement to concrete percentage of 1.99%, 2.09% and 2.19% is required for the selected concrete covers 50, 60 and 70 mm respectively to meet the target reliability index (β_t = 1.5). This translates to about a 5% increase in reinforcement required per 20% relative increase in the concrete cover- half the value found for edge restraint. This is indicative of the greater influence had by concrete cover on the edge restraint crack model as compared to that of the end restraint. Comparing this result to that of the edge restraint crack model, it is evident that slightly more reinforcement is required to meet the target reliability index for end restraint. This makes end restraint the more conservative of the two variations of the restrained shrinkage crack model.

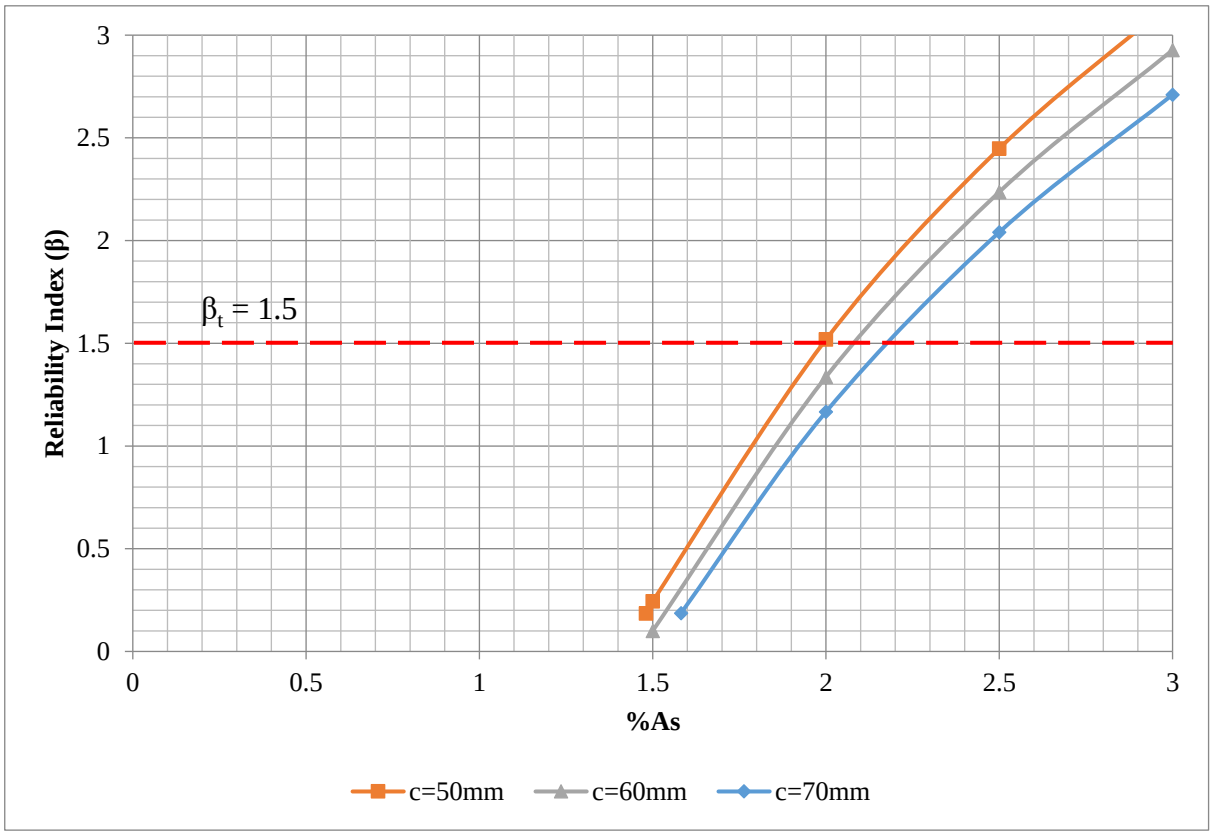

Figure 5.6: Influence of Cover and $\varphi/\rho_{p,\,eff}$ (End Restraint)

Much like for the edge restraint condition, the reliability index decreases as the $\varphi/\rho_{p,\,eff}$ ratio increases. The target reliability index ($\beta_t = 1.5$) is met where the $\varphi/\rho_{p,\,eff}$ ratio is at 1, 0.96 and 0.92 m for covers 50, 60 and 70 mm respectively (Figure 5.7). The gradient of the $\varphi/\rho_{p,\,eff}$ ratio to reliability indices graphs across the concrete cover values selected was about -4, having a strong impact on the reliability of the end restraint crack model (reading from Figure 5.7). This was a stronger relationship than in the edge restraint case.

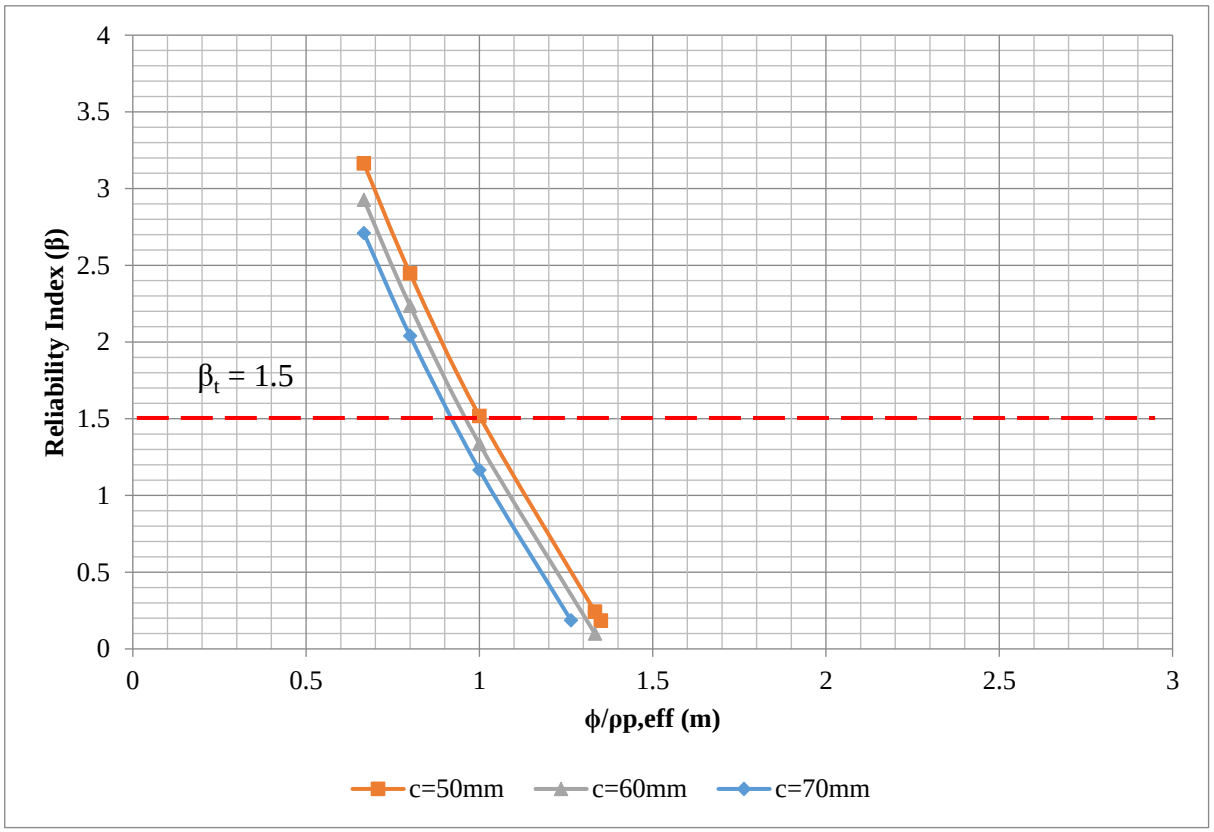

Figure 5.7: Influence of $\varphi/\rho_{p,\,eff}$ Ratio on Reliability Index (End Restraint)

Clearly, the concrete cover selected has some bearing on the reliability of the crack model for both end and edge restraint. For both restraint conditions, increasing the cover decreases the reliability of the crack model. The amount of reinforcing also influences the reliability levels that may be achieved by the crack model and thus the contributions of the $\varphi/\rho_{p,\,eff}$ ratio cannot be ignored. This is evident in the figures representing the change in reliability indices with respect to the $\varphi/\rho_{p,\,eff}$ ratio for both end and edge restraint (Figures 5.5 and 5.7, respectively). So therefore, as the EN 1992 crack model stands, both terms (c and the $\varphi/\rho_{p,\,eff}$ ratio) of the crack spacing have a noteworthy influence on the eventual reliability of the crack model.

5.3.2 Influence of Effective Tension Area

An assessment was done on what influence the depth of the effective tension area had on the reliability of the crack model. For a combination of a 40 mm concrete cover, 250 mm wide concrete section and 20 mm reinforcing bar diameter, the depth of the effective tension area $h_{c,eff}$ may either be taken as h/2 or 2.5(c +φ/2) since both returned the same value ($h_{c,eff}$ = 125 mm in either case). Hence, the crack model for edge restraint containing both variations of the effective depth could be compared directly.

5.3.2.1 Edge Restraint

The edge restraint model with $h_{c,eff} = 2.5(c + \varphi/2)$ resulted in a lower reliability than where $h_{c,eff} = h/2$. The variation is slight, with the greatest absolute difference in reliability being about 0.19 for a reinforcement percentage of 3% (the limit for feasible reinforcement to be used for a section thickness of 250 mm is 3.35% for reinforcement applied on both faces of the section). This difference in reliability indices translates to a difference in failure probability of $p_f = 0.11\%$ (Figure 5.8). However slight the difference between the effective depths might be, the result is contrary to what one would expect. Considering that for most combinations of cover, section thickness and bar diameter, the more limiting effective depth was found to be $2.5(c + \varphi/2)$; this limiting effective depth generally predicts lower crack widths than crack width models containing an effective depth of h/2. It may naturally be expected that the generally more conservative model (where $h_{c,eff} = h/2$) would produce lower reliability indices since the most conservative variation of the crack model predicts wider crack widths that are more likely to exceed the stipulated crack width limit.

Reinforcement to gross concrete ratios of about 1.55% and 1.62% for h/2 and $h_{c,eff} = 2.5(c + \varphi/2)$ respectively mark the ratios at which the target reliability index of 1.5 was met (Figure 5.8). That would mean a difference of about 175 mm^2 (or 85 mm^2/section face per m of wall) in reinforcement is required to meet the target reliability index which is a relatively small margin.

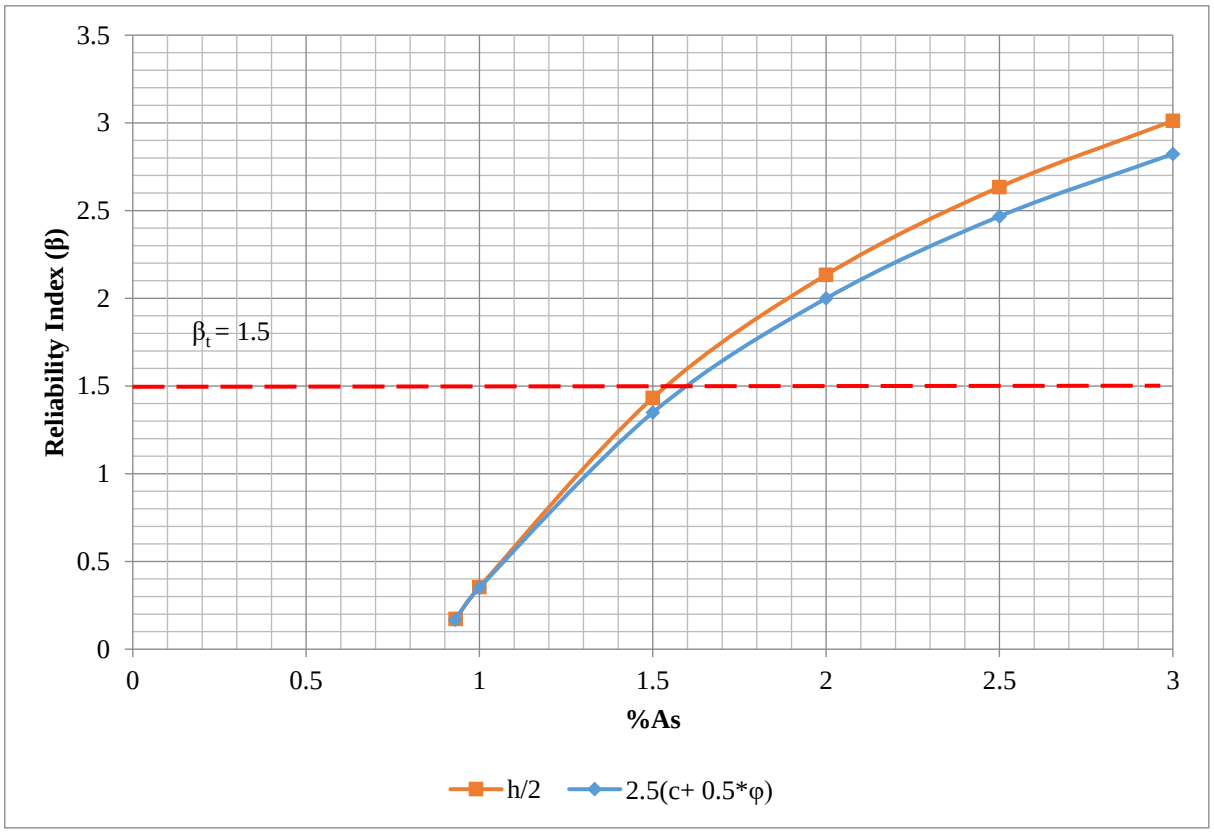

Figure 5.8 Influence of Effective Tension Area (Edge Restraint)

5.3.2.2 End Restraint

For end restraint, the variation in reliability for the different effective depth formulations follows after the edge restraint condition in which $h_{c,eff}$ =2.5(c +φ/2) generates smaller reliability indices than the reliability indices achieved for where $h_{c,eff}$ = h/2. The biggest difference in reliability index observed was 0.16, for 3% reinforcement to concrete. This result is close to the difference found in the case of edge restraint (namely 0.19). This amounts to a difference in failure probability of p_f = 0.024% (as may be seen in Figure 5.9). Again, however slight, this is contrary to what may be expected, considering that for most cases 2.5(c + φ/2) is the limiting effective depth.

The target reliability index is met at 1.92% and 1.94% for $\%A_s$ for the crack models containing an effective depth of h/2 and 2.5(c +φ/2) respectively (Figure 5.9). This corresponds to a reinforcement amount of 4800 mm^2 and 4850 mm^2 (a 50 mm^2 difference in reinforcement). This is a smaller difference than that found in the edge restraint crack model, and is negligible.

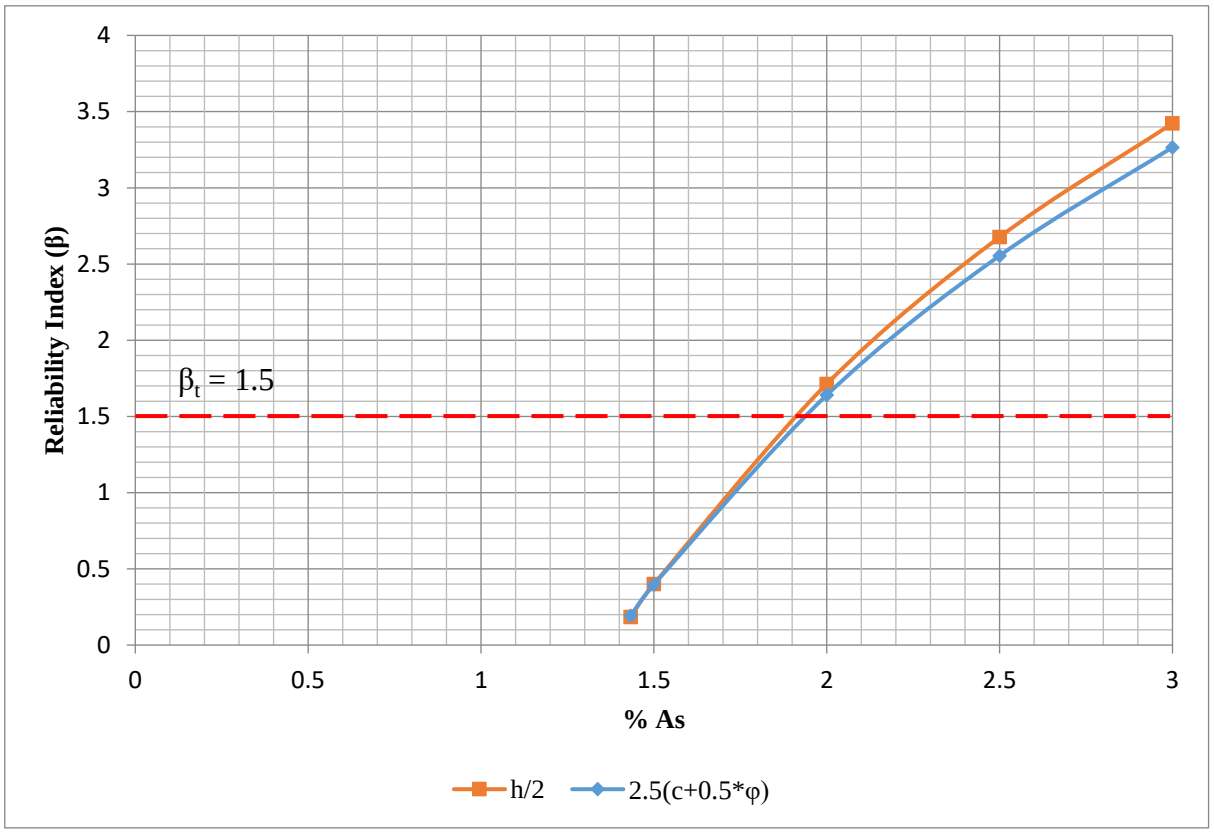

Figure 5.9: Influence of Effective Tension Area (End Restraint)

Clearly, the choice of effective depth of tension area affects the overall reliability of the crack model for both restraint conditions– although this effect was slight for both restraint conditions. During the course of the analysis, where the stochastic nature of the variables had been accounted for, the random variables (cover in particular) increased in magnitude. Meaning that essentially, the concrete cover value at the limit state/ failure point is greater than the initial cover value (40 mm). This increase in value would subsequently lead to an effective depth value that was greater than what would normally be prescribed for the $h_{c,eff} = 2.5(c + \varphi/2)$ variation of the crack model in a deterministic analysis. Thus, a comparably larger than usual effective tension area would be in effect. This would then result in an increase in the likelihood of the limit state being exceeded, and hence a decrease in the reliability indices obtained. A result that is somewhat counterintuitive and could be better explained through a closer examination of the limit state function. This was done by performing a sensitivity analysis of the EN 1992 restrained shrinkage crack model and the results of which are reported in chapter 6.

5.3.3 Influence of Section Thickness

For a cover of 40 mm and reinforcement bar diameter of 20 mm, $2.5(c+ \varphi/2)$ is the limiting effective area for section thicknesses considered in the analysis (250 mm to 500 mm). However, section thickness (h) does not feature in the edge restraint crack model where $h_{c,eff} = 2.5(c+ \varphi/2)$.

Covers beyond 50 mm make h/2 the limiting effective tension depth for a 250 mm thick section, whilst bar diameter contributes little to the effective depth (cover is more influential, as was uncovered in the parametric study). Therefore a small selection of section thicknesses were analysed; namely, 250, 300 and 350 mm for the edge restraint case whilst for end restraint section thicknesses analysed varied from 250 mm to 500mm since section thickness featured in the end restraint case.

5.3.3.1 Edge Restraint

As the section thickness was increased, so did the reliability index (Figure 5.10). The only real difference that section thickness made in the edge restraint case (where $h_{c,eff} = 2.5(c+ \varphi/2)$) was that thicker sections require more reinforcement to meet a particular steel to gross concrete cross-sectional area ratio. For instance for a steel to gross cross-sectional concrete area of say 2% a 250 mm section would require 2500 mm ^{2}/sectional face, while 3000 mm ^{2} and 3500 mm^2/sectional face is required for 300 and 350 mm respectively. The increase in reinforcement area results in an increase in the effective steel content ($\rho_{p,eff}$) and subsequently a decrease in crack spacing and crack widths obtained (since the model contains the reciprocal of the effective steel content ratio). Thus it appears as though the reliability index of the edge restraint crack model increases with an increase in the section thickness.

For the range of section thicknesses analysed, the amount of area required to maintain the target reliability index ($\beta_t = 1.5$) varied slightly, going from 1.62 %A_s (giving a steel reinforcing area of 4050 mm ^{2} for a 250 mm thick section), 1.36 %A_s (4080 mm ^{2} for a 300 mm section thickness and 1.17%A_s (4095 mm ^{2} for a 350 mm thick concrete section) – an average decrease of 18% with each 50 mm increase in section thickness. All in all, the steel content is believed to have had the most impact of the reliability performance of the edge restraint crack model rather than the inherent variabilities of the random variables within the model. Thus the physical model rather than the reliability model influenced the outcome of this particular reliability assessment (where section thickness was varied).

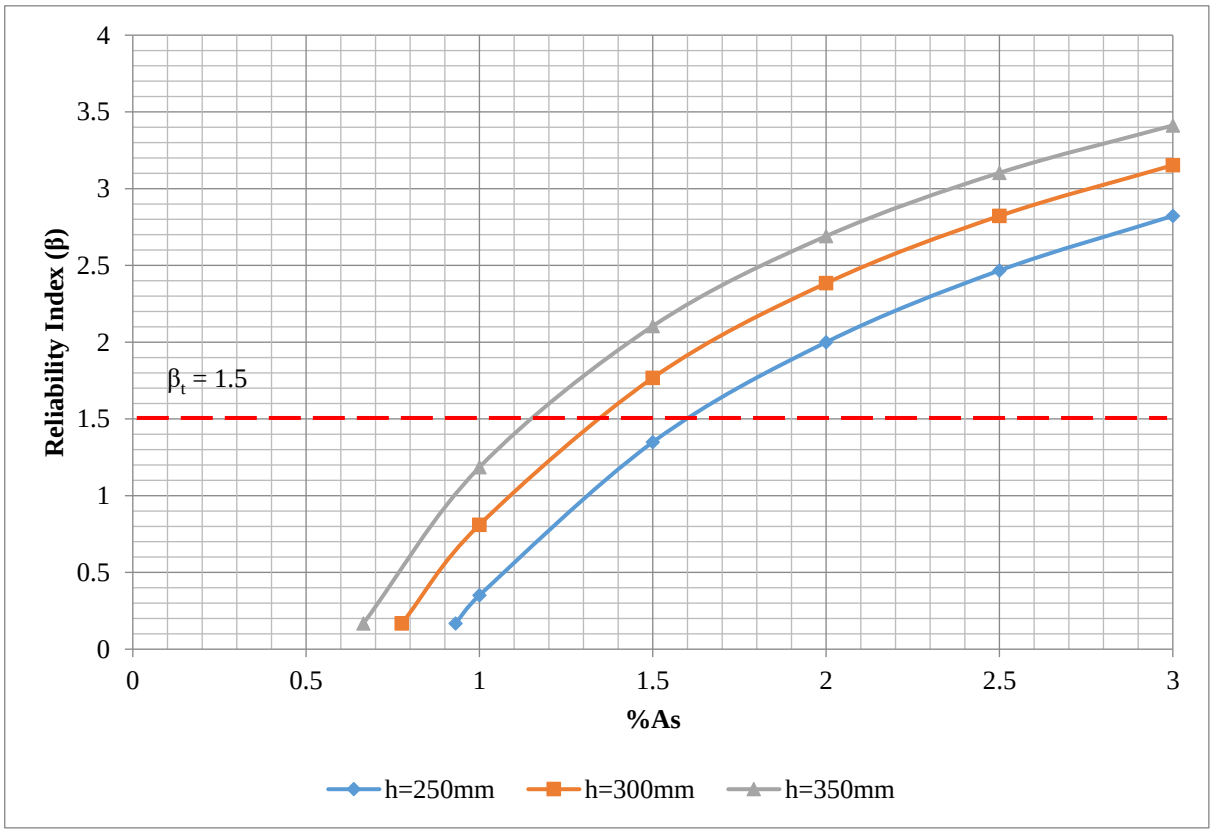

Figure 5.10: Influence of Section Thickness (Edge Restraint)

5.3.3.2 End Restraint

It can be clearly seen that an increase in section thickness results in an increase in the reliability index (Figure 5.11), as was found in the edge restraint case. For reinforcement ratio of say 2%, the reliability index is 1.64, 1.97, 2.3, 2.65, 2.93 and 3.19 for section thicknesses 250, 300, 350, 400, 450 and 500 mm sequentially. Comparing the reliability indices obtained for h = 250, 300 and 350 mm at 2% A_s in the end restraint crack model to those of edge restraint it is observed that the edge restraint crack model produced higher reliability indices (2, 2.38 to 2.69 corresponding to h = 250, 300 and 350mm respectively for the edge restraint case as compared to the 1.64, 1.97 and 2.33 of the end restraint case for h = 250, 300 and 350 mm).

A few factors come into effect in this result. As the section thickness varies, so did the k coefficient- this coefficient accounts for the presence of a non-linear stress distribution (varying between 1 for section thicknesses less than 300 mm and 0.65 for section thicknesses greater than 800 mm, values between these limits being interpolated). Table 5.2 gives those k values used and their corresponding section thickness. Being directly proportional to the restrained strain, the decrease in this coefficient with the increase in section thickness resulted in a decrease in the restrained strain. A decrease in the restrained strain means that a smaller crack width is attained,

resulting in a decrease in the likelihood of the crack width limit being exceeded (increasing the model's reliability).

Table 5.2: Change of k Coefficient with Increasing Section Thickness (by interpolation)

h (mm)	k
250	1
300	1
350	0.965
400	0.93
450	0.895
500	0.86

Also, much like in the case for edge restraint, the increase in amount of reinforcement area required to meet particular ratio of reinforcing steel to gross concrete cross-sectional area may have also influenced the results. Once again, larger section thicknesses require larger amounts of reinforcement to meet a certain steel to concrete ratio. This then decreases the likelihood of crack limit exceedance and increases the reliability performance of the crack model. The amount of reinforcement required for the reliability index to be met ranged from $1.94\%A_s$ (giving a reinforcing steel area of 4859 mm ^{2}) to $1.33\%A_s$ (6655 mm ^{2}) for the range of section thickness from 250 mm to 500 mm considered in this analysis.

To directly compare the results of the end restraint crack model with that of the edge restraint crack model, the amount of reinforcement required to meet the target reliability index for section thicknesses from 250 to 350 mm were examined. At β_t = 1.5, a reinforcement to concrete percentage of 1.94, 1.80 and 1.65% are required for section thicknesses 250, 300 and 350 mm respectively (larger percentages of reinforcement are required here than the 1.62, 1.36 and 1.17% A_s respectively found for edge restraint). An average decrease of about 8% was observed with every 50 mm increase in section thickness, almost half that experienced in the edge restraint case (Figure 5.11). For the remainder section thicknesses of 400, 450 and 500 mm the corresponding percentage of reinforcement required to meet the reliability index are 1.5, 1.41 and $1.33\%A_s$ respectively (Figure 5.11). None of the reinforcement requirements for the section thicknesses analysed exceeded the maximum feasible limit for reinforcement at the target reliability index.

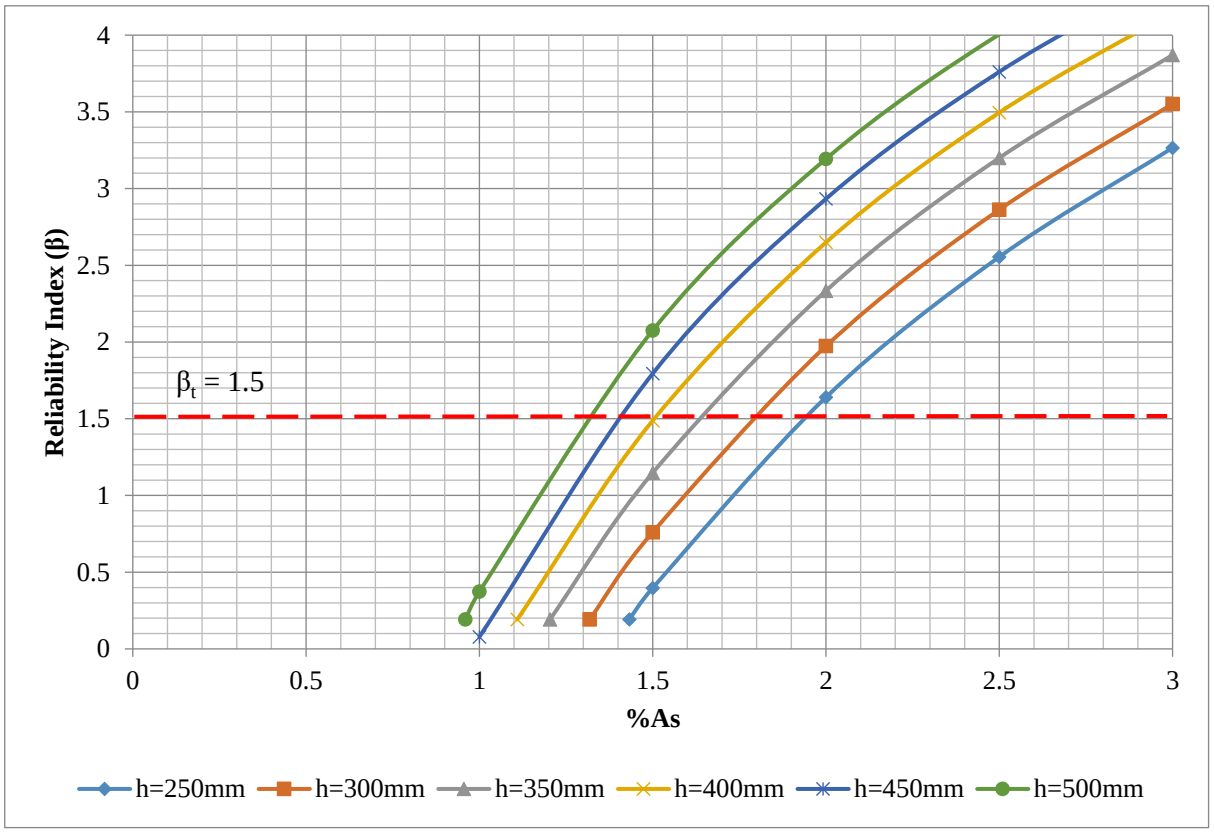

Figure 5.11: Influence of Section Thickness (End Restraint)

Evidently, section thickness does influence the reliability of the crack model, more so in the end restraint crack model than for the edge restraint crack model in that more reinforcing is required to meet the target reliability index. Although, the effect held by section thickness in the edge restraint case has more so to do with the increase in reinforcing required maintaining a particular reinforcement ratio (thus being more a testament to the influence held by the steel reinforcing in the edge restraint crack model) - the variable itself has no role in the edge restraint crack model. Hence, the section thickness actually appearing in the end restraint crack model by default has more of an effect on the end restraint model. A closer examination of the sensitivity factors obtained for a predetermined reliability index should expose to what extent section thickness influences the end restraint crack model.

5.3.4 Influence of Restraint Factor

The influence of the restraint factor was assessed by varying the restraint factor in the edge restraint crack model when performing the FORM analysis. The restraint factors selected (ranging from 0.1 to 0.5) are analysed against an increasing percentage of reinforcement to gross concrete-cross sectional area.

5.3.4.1 Edge Restraint

The restraint factor was found to have a considerable influence on the reliability of the EN 1992 crack model. The smaller the restraint factor applied to the model the greater the reliability (as may be deduced from Figure 5.12). The increase in reliability index for the case of 1% A_s, for instance, goes from 0.35 for restraint factor R = 0.5 to 1.037 (at R = 0.4), 1.92 (at R = 0.3), 3.16 (at R = 0.2) up to 5.28 for restraint factor of R = 0.1. The effects of restraint factor 0.1 are not featured in Figure 5.12 due to the high reliability indices achieved (beyond the considered range). At R = 0.1, the concrete member is virtually free to contract and thus almost unlikely to crack. It's the restriction in movement during the hydration process and shrinkage of the concrete that results in the formation of cracks.

More reinforcement is required to maintain the target reliability as the restraint factor increases. The target reliability index is met at 0.55, 0.88, 1.23, and 1.62 %A_s for restraint factors 0.2, 0.3, 0.4 and 0.5 sequentially (about a 40% increase in reinforcement required with each 36 % relative increase in the restraint factor- equivalent to a 0.1 incremental/absolute increase in the restraint factor). This has obvious financial implications. Thus essentially, the choice of pour configuration and construction sequence significantly affects the reliability of the crack model– resulting in sizeable increases in the reinforcement required to meet the required reliability of the liquid retaining structure.

The clear influence of the restraint factor supports the need for increased knowledge of this parameter. In this way, its influence on the crack model may be better quantified-particularly where the restraint factor is treated as a random variable in reliability assessments rather than a deterministic one. Further research on the restraint factor's stochastic nature is then necessary.

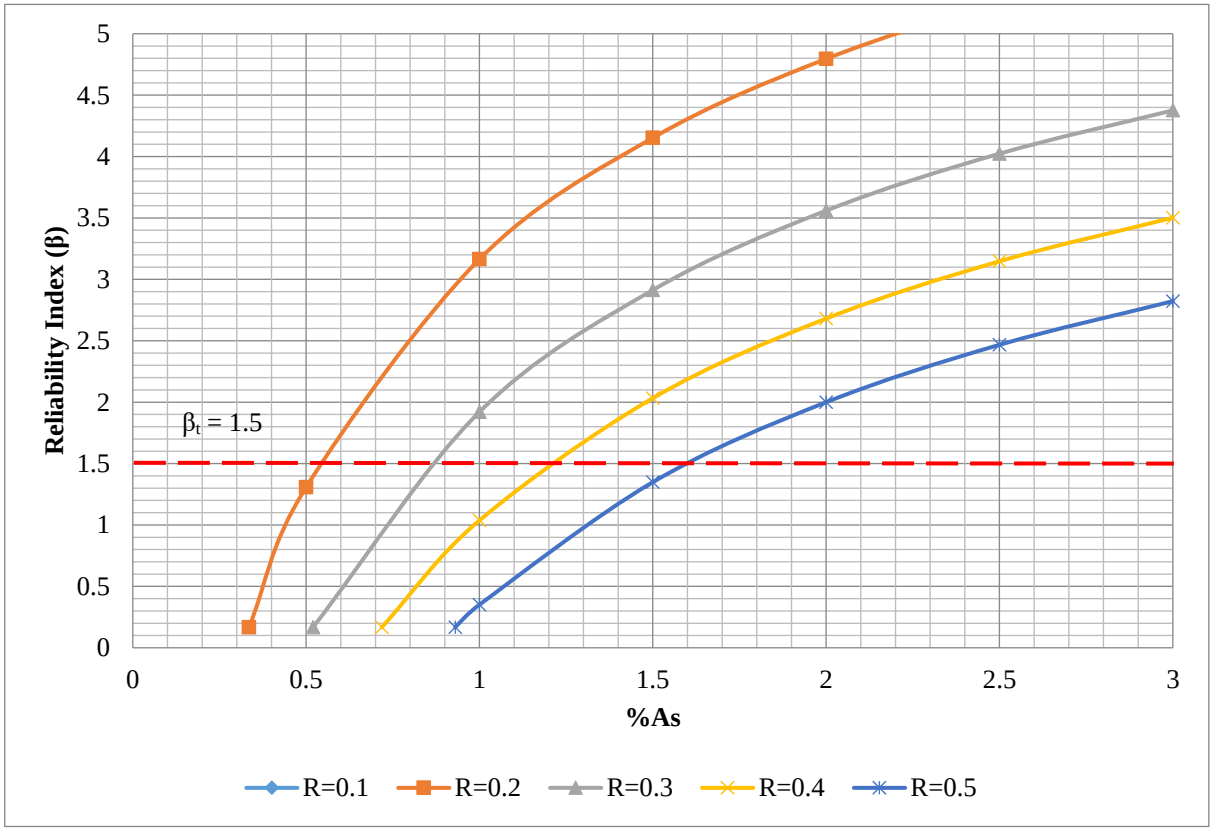

Figure 5.12: Influence of Restraint Factor (Edge Restraint)

5.3.4.2 End Restraint

There is no restraint factor in the end restraint formula and thus no need to assess the influence of the restraint factor in this case.

5.3.5 Influence of Model Uncertainty

The influence of model uncertainty was assessed by changing its coefficient of variance (CoV) for each FORM analysis of the restrained strain crack model. The CoV's assessed ranged from 0.1 to 0.3. The section thickness and other variables of the crack model stood as they did before (h = 250 mm, c = 40 mm, φ = 20 mm with coefficients and strains as mentioned in the table of statistical parameters given in Figure 5.1).

5.3.5.1 Edge Restraint

A decrease in CoV value for the model uncertainty in edge restraint resulted in an increase in the reliability index of the crack model. At 2%A_s the reliability index attained varied from β = 2.0, 2.27, 2.63, 3.11 and 3.70 for CoV = 0.3, 0.25, 0.2, 0.15, 0.1 in turn. This marks a 17% average increase in reliability with every 0.05 incremental increase in model uncertainty variation.

Hence, where the variation between predicted results and empirical results are minimised, good construction practice is followed and other such quality control measures are employed to reduce uncertainties, the results obtained from the existing model would be more reliable. A smaller CoV for model uncertainty would result in a smaller crack width being estimated by the reliability model for cracking and thus produce a crack width that is less likely to surpass the crack width limit, hence the increase in the reliability index calculated. The target reliability index of 1.5 is reached at the following percentages of steel to gross concrete cross-sectional area for the CoV's presented in the Figure 5.13: 1.27%, 1.33%, 1.41%, 1.49% and 1.62% for the corresponding coefficient of variances 0.1, 0.15, 0.2, 0.25 and 0.3 respectively. The increases in the reinforcement required as model uncertainty increases are slight (an average rise of factor 1.06 between increasing model uncertainties).

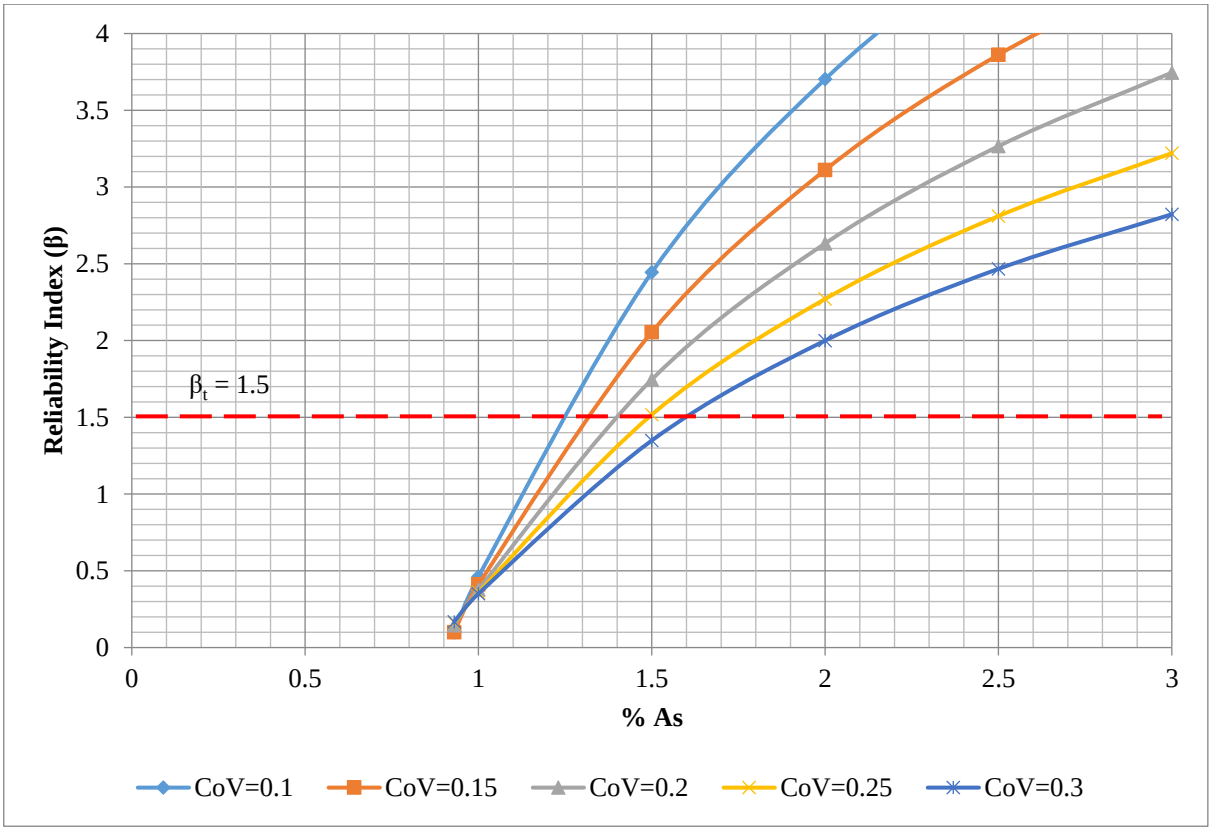

Figure 5.13: Influence of Model Uncertainty (Edge Restraint)

5.3.5.2 End Restraint

Much like in the case of edge restraint, a decrease in model uncertainty resulted in an increase in the reliability of the crack model (Figure 5.14). More precisely, the increase in reliability at say 2%A_s was 1.64, 1.78, 1.95, 2.13 and 2.31 for corresponding model uncertainties 0.3, 0.25, 0.2, 0.15 and 0.1 respectively. This gives an average increase in reliability of 9% for every 0.05 increment of model uncertainty variation, a smaller margin of change as compared to edge

restraint for the same percentage of reinforcement to concrete of 2% A_s (an average increase of 17%). This indicates that variability in the model uncertainty has a larger effect on the edge restraint crack model than it does on the end restraint crack model.

Again, as for the edge restraint case, the increase in the amount of reinforcement required results from an increase in the CoV of the model uncertainty. Percentages at which the target reliability index for liquid retaining structures was met for model uncertainty CoV's of 0.1, 0.15, 0.2, 0.25, and 0.3 are: 1.78%, 1.81%, 1.85%, 1.90% and 1.94% respectively (an average increase in percentage area of factor 1.02, a smaller increase than for edge restraint condition which had an increase factor of 1.06). It may thus be deduced that model uncertainty variations have a greater influence on edge restraint crack model as compared to the end restraint case. It can also be observed here that more reinforcement is required to reach the target reliability index for corresponding CoV's of model uncertainty of the end restraint as compared to the edge restraint crack model- indicating, once again that the end restraint model is the most conservative model of the two.

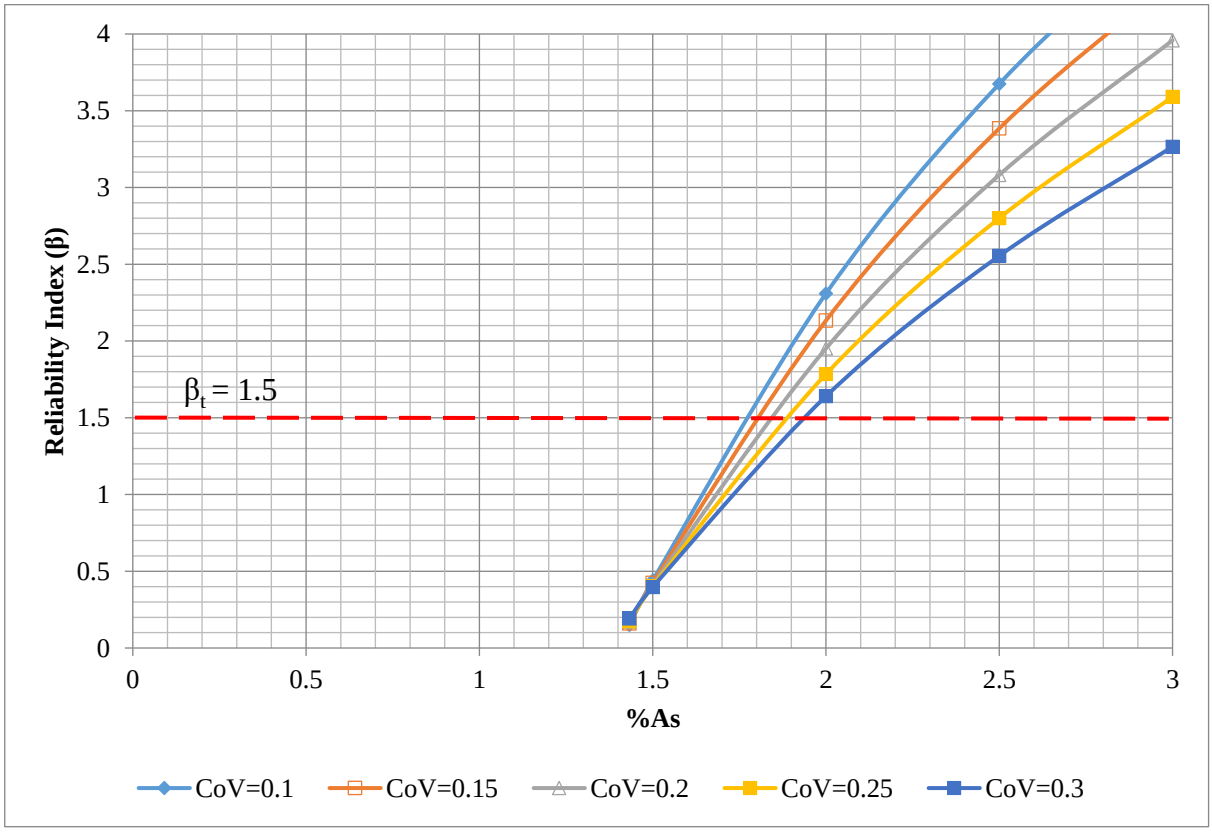

Figure 5.14: Influence of Model Uncertainty (End Restraint)

Past research into the reliability of reinforced concrete structures have proven that model uncertainty has a significant influence on the reliabilities of reinforced concrete structures

(Holický, Retief, Wium, 2010).This is contrary to what was found in this analysis of the EN 1992 restrained strain crack model. However, a better estimate of what influence model uncertainty has on the crack model may be obtained from a sensitivity analysis.

5.4 Summary

An investigation into the influence key identified parameters of the EN 1992 crack model had on the overall reliability of the model was presented in this chapter. The following main findings of the FORM analysis of the EN 1992 crack model for edge and end restraint are summarised below:

- Increasing the concrete cover and the $\varphi/\rho_{p,eff}$ ratio decreased the model's reliability.
- The effective depth of tension area bears some influence on the reliability of both the edge and end restraint crack model, with $h_{c,eff} = h/2$ proving to achieve higher reliability indices than $h_{c,eff} = 2.5(c + \varphi/2)$. However, the difference in reliability between the variations of effective depth is slim. This applies to both the edge and end restraint crack model.
- Section thickness is not a parameter in the edge restraint crack model. An increase in reliability resulting from an increase in section thickness was attributed to the increase in the amount of reinforcement required to meet particular steel to gross concrete ratio for thicker sections. Increased reinforcement used meant an increase in the reliability of the model.
- Similarly, for end restraint, an increase in section thickness resulted in an increase in reliability of the crack model– less so in the edge restraint case.
- The restraint factor had a significant effect on crack model reliability. Increases in restraint factor decreased the reliability of edge restraint crack model. Thus further research into this variable's stochastic nature is necessary so that more can be known about its impact on the reliability of the crack model.
- Increases in model uncertainty CoV resulted in a decrease in reliability for both the edge and end restraint crack model.
- The end restraint model proved to be the more conservative of the two models.

A sensitivity analysis of the reliability crack model for edge and end restraint was then performed to give a clearer perspective of the relative influence held by each random variable. In this way, greater insight would be gained into the influence held by each random variable on the overall reliability of the crack model. The relative influence, or otherwise sensitivity, of each random variable may be measured through an extended reliability analysis. Those sensitivity factors

associated with the target reliability index ($\beta_t = 1.5$) are found by way of a reverse FORM analysis (as reported in chapter 6).

Chapter 6: Sensitivity Analysis of EN 1992 Crack Model: Methodology, Results and Discussion

By determining the relative influence held by each random variable for the target reliability index for the irreversible limit state, the opportunity of determining which variables most affect the reliability of the crack model may be realised. The sensitivity factors give the relative influence of random variables for a given reliability index (β_t) using the reverse of the FORM analysis. Additionally, theoretical partial safety factors, which indicated the adjustments necessary for reliability compliance were also obtained from the reverse FORM analysis. This analysis serves the main objective of, not only further understanding the reliability performance of the EN 1992 crack model as applied to liquid retaining structures in South Africa, but also presents the opportunity of finding the ways in which to improve this crack model for use in the local environment. This sensitivity analysis was conducted for the random variables of the cracking serviceability limit state (namely, the effective concrete cover, section thickness, concrete tensile strength and model uncertainty) against variations in the model uncertainty. Model uncertainty had been determined in previous research to have a significant influence on the reliability of reinforced concrete structures (Holicky, Retief and Wium, 2010). And since the model uncertainty for cracking is not really known, its influence on the EN 1992, restrained cracking serviceability limit state needs to be assessed. This was previously done for the load-induced cracking case (Mcleod, 2013) and so the same will be explored for the restrained shrinkage case.

The influence held by the choice of target reliability index was investigated in this chapter. Considering that the exceedance of the crack limit may result in the loss of structural integrity in the case of liquid retaining structures with a potentially large consequence of loss, an investigation into the influence of the reliability index on the basic variables of the crack model was conducted. The need for this investigation also comes after understanding the increased importance of the serviceability limit state as compared to the ultimate limit state in the design of liquid retaining structures. Previous investigations on the matter that the cracking serviceability limit state was the more demanding limit state, requiring more reinforcing to satisfy its design criteria.

Insights gained through this analysis may be used towards the calibration of the cracking serviceability limit state for a larger scope of liquid retaining structure configurations and expected uses for local conditions.

6.1 Methodology of the Reverse FORM Analysis:

6.1.1 Reliability Analysis Formation

The reverse FORM analysis follows much of the same methodology as for the conventional FORM analysis of chapter 5. The major difference in this instance is that the reliability index is selected from the onset and the steel reinforcement (the unknown parameter) required to meet this target reliability index is then calculated. The statistical parameters of the basic variables are as for the conventional FORM calculation presented in chapter 5. The limit state function remains as for the FORM analysis in the previous section and the reverse FORM algorithm used is as follows:

1) The limit state function is first defined (as defined in equation 5.6)
2) Convert the mean and standard deviation of non-normal variates to their normal equivalent.
3) Assume initial failure points- normally taken as the mean values of the random variables in question.
4) Determine the partial derivatives of the performance function with respect to each random variable using MATLAB. Evaluate these derivatives at the failure points. Then substitute the previously determined value for the area of steel required to satisfy the performance function ($g(x) = w_{lim} - \theta w$) when evaluating the derivatives.
5) Determine the direction cosines (sensitivity factors) by dividing each partial derivative by the root of the sum of the squared partial derivatives (in other words, normalise the partial derivatives).
6) The failure points may then be determined by substituting the target reliability index in the failure point equation (the normal equivalent of the mean and the standard deviation are used in this equation).
7) The new found failure points are then substituted into the performance function and the amount of area required for the performance function to equal zero is calculated using excel solver. Here the area of steel required is set as the variable cell, whilst the performance function is the objective cell set to meet an objective value of zero in excel solver. The area of steel determined is then substituted into the partial derivatives of the next iteration where the partial derivatives are also evaluated at the failure points determined after the current iteration.
8) Steps 2 through to 7 are repeated until convergence of the required area of steel is reached.

Figure 6.1 illustrates the use of the reverse FORM algorithm for the EN 1992 restrained shrinkage crack model,

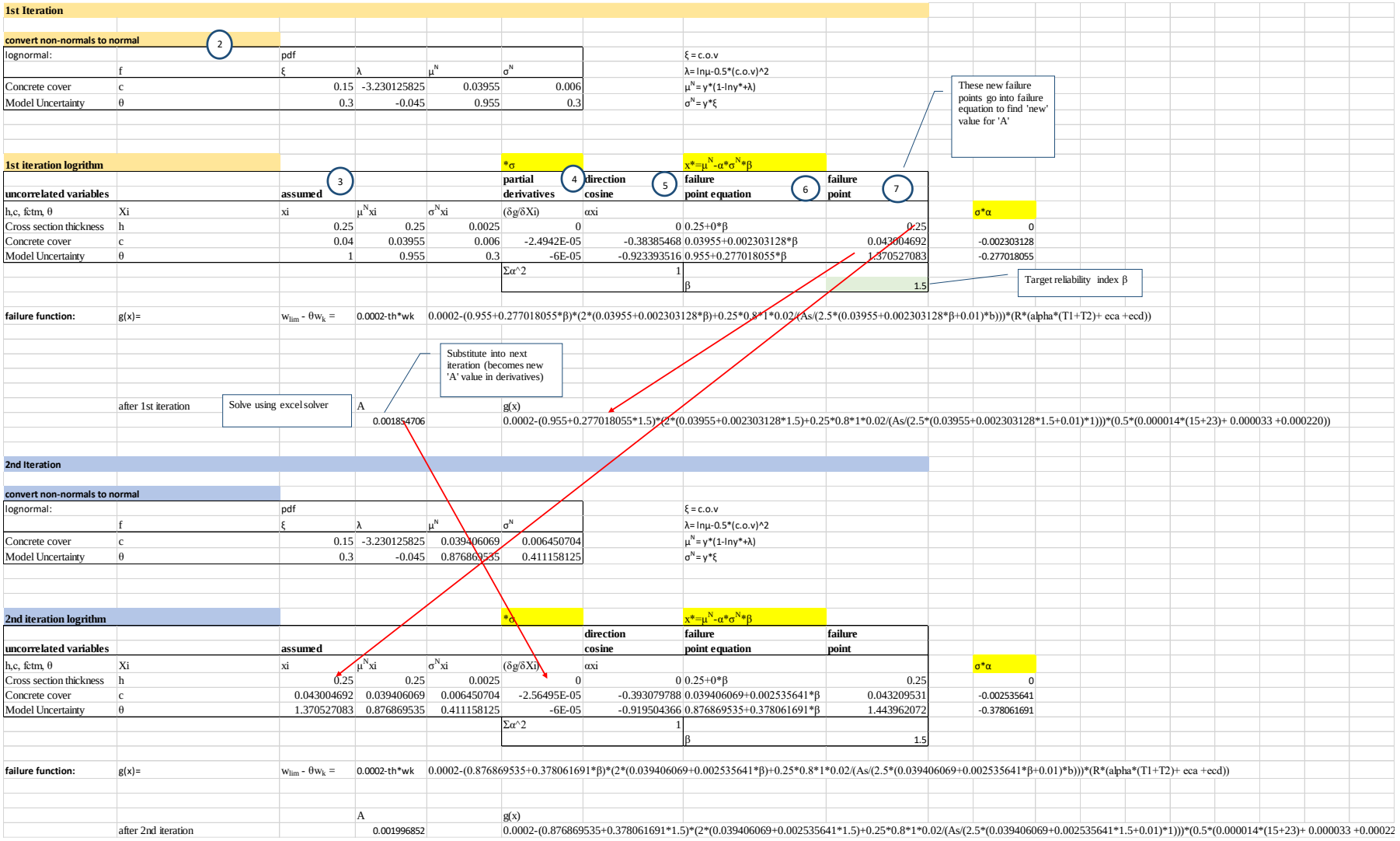

Figure 6.1: First and Second Iteration of the Reverse FORM Analysis of EN 1992 Crack Model

A total of four iterations were required for the convergence of β (as shown in Figure 6.2). Again, a separate spreadsheet is generated for select data obtained after each analysis. Data of particular interest include the direction cosines (sensitivity factors) of each random variable achieved at the end of each calculation. The sensitivity factors are indicative of the influence that each random variable has on the crack model relative to the other random variables. The closer the sensitivity factors are to the number one (+1 or -1) the more influential the variable. Being a normalised factor, the sum of the square of the sensitivity factor of each random variable should add up to one ($\Sigma\ (\alpha_i^*)^2 = 1$). The sensitivity factors of each random variable were plotted against the coefficient of variance (CoV) of the model uncertainty.

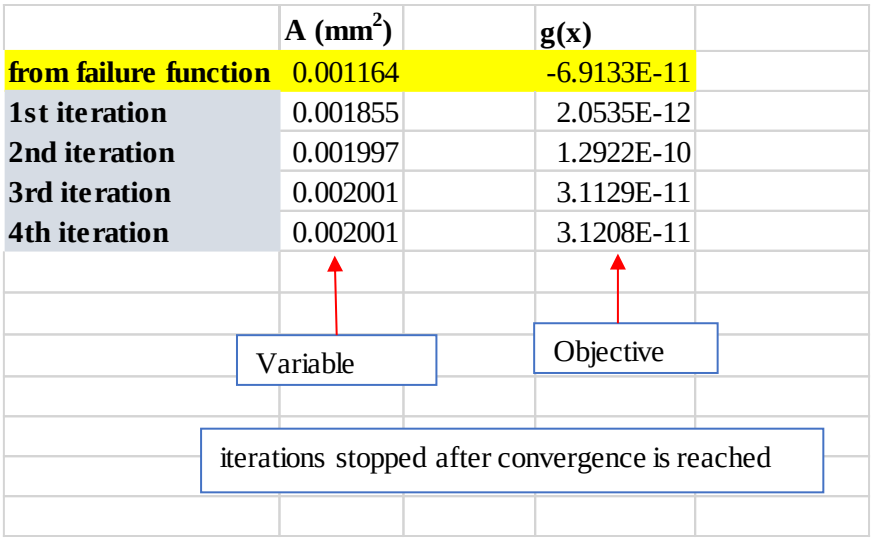

Figure 6.2: Example of Convergence Achieved After Four Iterations (Edge Restraint, $h_{c,eff} = 2.5(c + \phi/2)$)

The theoretical partial safety factors (psf's) for each random variable were calculated with the eventual failure point and mean of the random variable.

$$\overline{\gamma}_i = \frac{x_i^*}{\mu_X} = 1 - \alpha_i^* \beta w_{Xi} \qquad (6.1)$$

The theoretical partial safety factors are indicative of the amounts of adjustment that are required to be made to the input random variables in order for the limit state function to be satisfied and for the given target reliability index to be met. Both the sensitivity factor and the theoretical partial factors were assessed for the crack width limits corresponding to the tightness classes and functions to which liquid retaining structures are designed. The intent of this being that the partial factors and sensitivity factors obtained are meant to represent and work across all expected performance applications.

The restraint crack models assessed were as for the standard FORM analysis, consisting of:

a) Edge restraint with depth of effective tension zone taken to be 2.5(c +φ/2)
b) Edge restraint with depth of effective tension zone taken to be h/2
c) End restraint with depth of effective tension zone taken to be 2.5(c +φ/2)
d) End restraint with depth of effective tension zone taken to be h/2

6.2 Results and Discussion

6.2.1 Sensitivity Factors at Varying Model Uncertainty

The sensitivity factors (direction cosines) reveal the degree to which random variables are influential to the model in question relative to each other. The sensitivity factors were determined for the random variables concrete cover (α_c), section thickness (α_h), concrete tensile strength ($\alpha_{fct,eff}$) and model uncertainty (α_θ). The size, or otherwise strength, of the sensitivity factors are regarded in terms of their absolute magnitude. The sensitivity factors ranged from -1 to 1 and the closer the value was to $|\pm 1|$, the larger its influence. The sensitivity factors were compared against changes in the coefficient of variance of the model uncertainty varying from 0.1 to 0.3. The reliability index was set at 1.5. The crack models containing both variations of the effective depth of the tension zone ($h_{c,\,eff}$ = 2.5(c +φ/2) and h/2) were compared directly, since the combination of concrete cover at 40 mm, a 250 mm section thickness and 20 mm bar diameter meant both effective depth formulations were equally limiting.

6.2.1.1 Edge Restraint ($h_{c,\,eff}$ = 2.5(c +φ/2))

Table 6.1 presents a comparison of the sensitivity factors obtained for the respective random variables where the effective depth was 2.5(c + ϕ/2). Across all crack width limits assessed, model uncertainty proved to be the most influential variable of the edge restraint crack model with its sensitivity factors going up to about -0.92 for all crack limits considered at model uncertainty CoV = 0.3. Concrete cover follows after model uncertainty with its influence on the crack model being about half that of model uncertainty at a model uncertainty CoV of 0.3 for all crack width limits considered in the analysis. Section thickness clearly had no influence on the crack model since this random variable did not feature in the model in question, since the effective depth formulation was 2.5(c +φ/2).

Table 6.1: Sensitivity Factors of Random Variables for Edge Restraint Crack Model (β_t = 1.5, $h_{c,\,eff} = 2.5(c + \varphi/2)$)

w_{lim} (mm)	Model uncertainty CoV	%As required	α_c (concrete cover)	α_θ (model uncertainty)
0.3	0.1	0.756	-0.786	-0.618
	0.15	0.797	-0.646	-0.764
	0.2	0.848	-0.535	-0.845
	0.25	0.902	-0.451	-0.892
	0.3	0.963	-0.388	-0.922
0.2	0.1	1.229	-0.791	-0.612
	0.15	1.302	-0.651	-0.759
	0.2	1.390	-0.541	-0.841
	0.25	1.491	-0.458	-0.889
	0.3	1.600	-0.394	-0.919
0.1	0.1	3.294	-0.802	-0.597
	0.15	3.553	-0.668	-0.745
	0.2	3.884	-0.559	-0.829
	0.25	4.280	-0.476	-0.880
	0.3	4.743	-0.412	-0.911

Figure 6.3 illustrates how the concrete cover decreased in influence as the model uncertainty variability and the crack width limit are increased. The influence of the model uncertainty in the edge restraint crack model increased as the crack width limit and the variability of model uncertainty increased (as indicated in Figure 6.4).

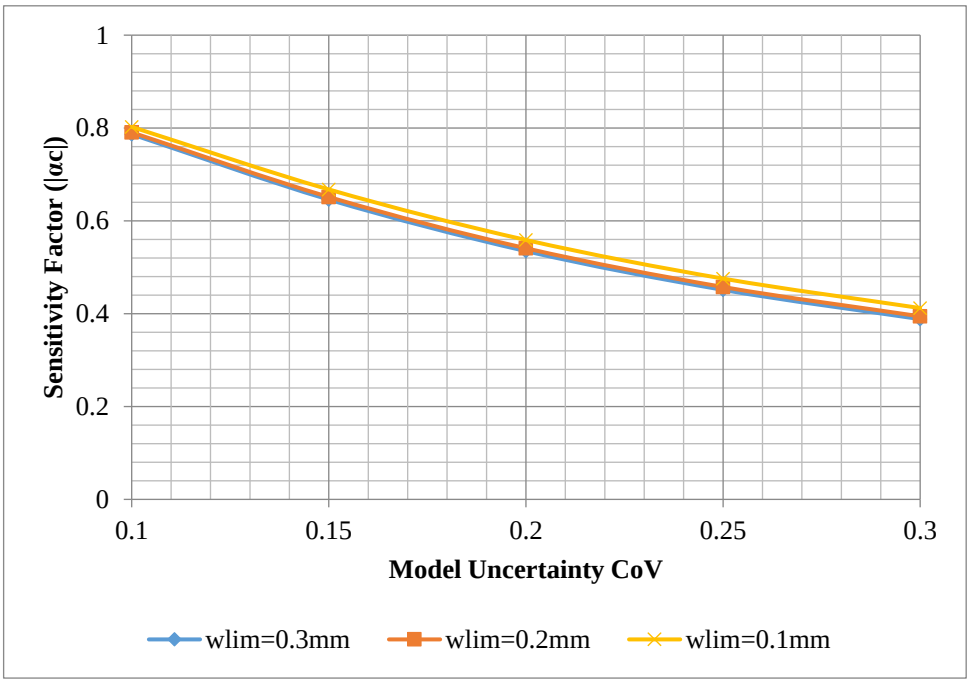

Figure 6.3: Edge Restraint Sensitivity of Concrete Cover (c) for Varying Model Uncertainty Coefficient of Variance ($h_{c, eff} = 2.5(c + \varphi/2)$)

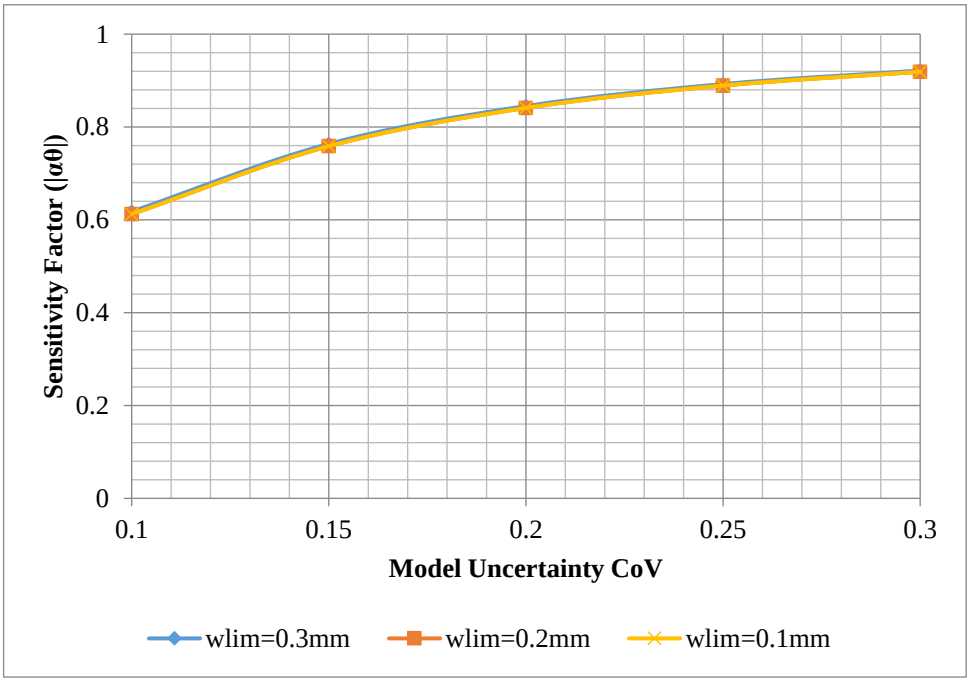

Figure 6.4: Edge Restraint Sensitivity of Model Uncertainty (θ) for Varying Model Uncertainty Coefficient of Variance ($h_{c, eff} = 2.5(c + \varphi/2)$)

6.2.1.2 Edge Restraint ($h_{c, eff} = h/2$)

Table 6.2 demonstrated the relative influence of the random variables in the edge restraint crack model where $h_{c, eff} = h/2$. Model uncertainty, once again, proved to be the most influential

parameter with concrete cover and section thickness following after respectively. Model uncertainty were generally found to be above about -0.86, whilst the sensitivity factors of section thickness were found to be negligible, mostly being greater than about -0.02. Section thickness's negligible influence relates to its indirect influence on the restrained strain resulting from edge restraint- thicker sections would mean that a greater differential in temperature within the concrete may occur.

Table 6.2: Sensitivity Factors of Random Variables for Edge Restraint Crack Model (β_t = 1.5, $h_{c,\,eff}$ = h/2)

w_{lim} (mm)	Model uncertainty CoV	$\%A_s$ Required	α_h (section thickness)	α_c (concrete cover)	α_θ (model uncertainty)
0.3	0.1	0.690	-0.086	-0.183	-0.980
	0.15	0.745	-0.057	-0.130	-0.990
	0.2	0.804	-0.043	-0.104	-0.994
	0.25	0.866	-0.034	-0.089	-0.996
	0.3	0.930	-0.028	-0.079	-0.997
0.2	0.1	1.114	-0.078	-0.273	-0.959
	0.15	1.210	-0.052	-0.196	-0.979
	0.2	1.314	-0.039	-0.157	-0.987
	0.25	1.424	-0.031	-0.134	-0.991
	0.3	1.541	-0.025	-0.118	-0.993
0.1	0.1	2.935	-0.052	-0.508	-0.860
	0.15	3.251	-0.036	-0.381	-0.924
	0.2	3.617	-0.027	-0.309	-0.951
	0.25	4.035	-0.021	-0.265	-0.964
	0.3	4.511	-0.017	-0.236	-0.972

Figures 6.5 and 6.6 both represent graphically how the sensitivity factors of section thickness and concrete cover decreased with an increase in model uncertainty CoV. A trend that was contrary to that of the model uncertainty sensitivity factor which increased with an increase in the model uncertainty CoV (as shown in Figure 6.7). For concrete cover, as the crack width limit was increased, its influence decreased. In the case for section thickness, an increase in the crack width limit meant an increase in its relative influence, although the overall influence of section thickness was found to be negligible. Increasing the crack width limit increased the influence of model uncertainty on the edge restraint crack model (as found in Figure 6.7).

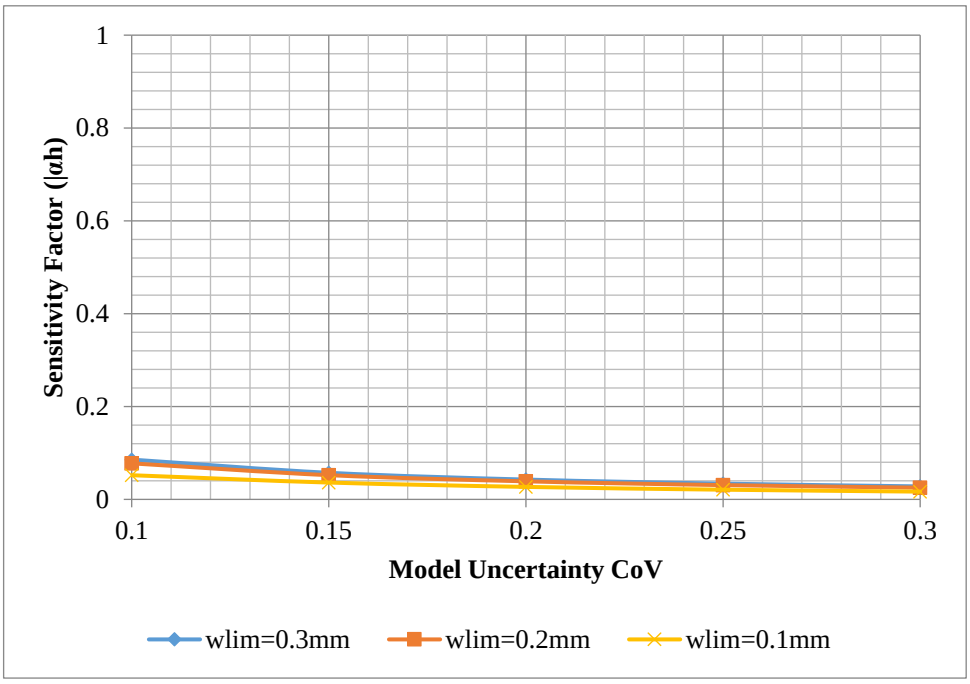

Figure 6.5: Edge Restraint Sensitivity of Section Thickness (h) for Varying Model Uncertainty Coefficient of Variance ($h_{c,\,eff}$ = h/2)

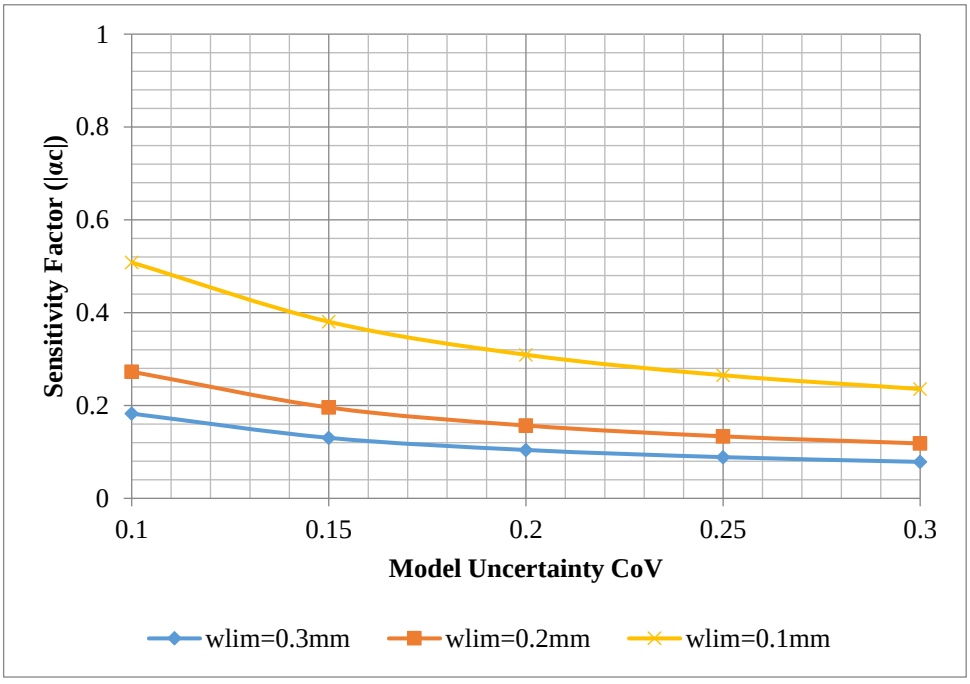

Figure 6.6: Edge Restraint Sensitivity of Concrete Cover (c) for Varying Model Uncertainty Coefficient of Variance ($h_{c,\,eff}$ = h/2)

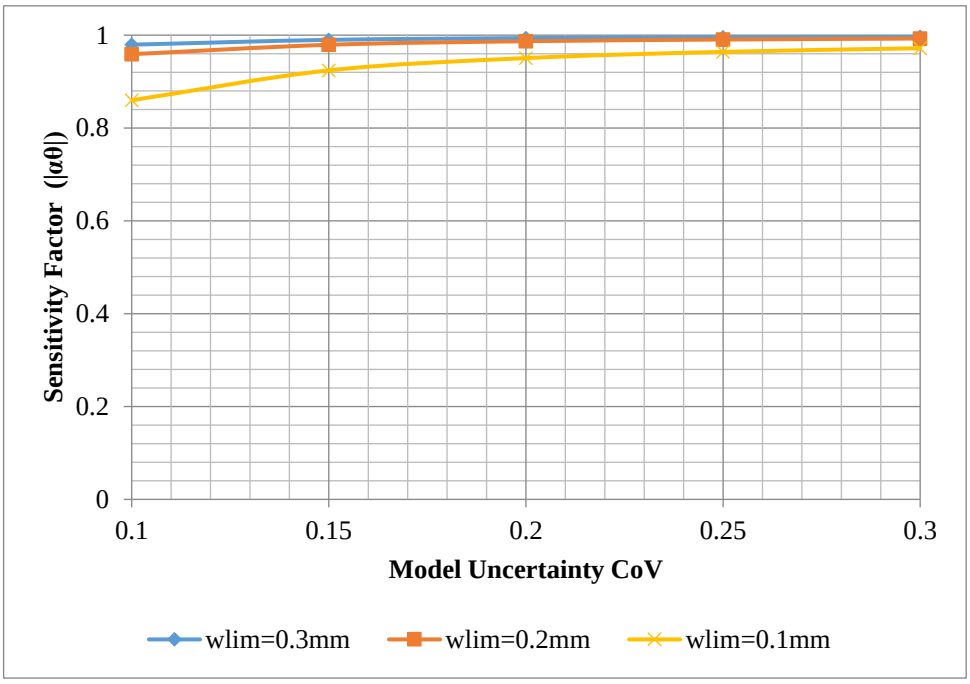

Figure 6.7: Edge Restraint Sensitivity of Model Uncertainty (θ) for Varying Model Uncertainty Coefficient of Variance ($h_{c,\,eff}$ = h/2)

Comparing the effective depth of tension ($h_{c,eff}$ =2.5(c +φ/2) and h/2) it may be observed that the edge restraint model containing $h_{c,eff}$ =h/2 has random variables that held a greater influence on the crack model in comparison to the same random variables acting in the crack model containing $h_{c,eff}$ =2.5(c +φ/2). Considering a model uncertainty CoV of 0.3, where the effective depth was h/2 the relative influence had by model uncertainty at 0.3 mm and 0.2 mm was greater by factor 1.08 than where the effective depth was $h_{c,eff}$ = 2.5(c +φ/2);for crack width limit 0.1 mm this factor decreased slightly to 1.07. At a model uncertainty CoV of 0.3, where the relative influence of concrete cover was at its lowest for either edge restraint models, the concrete cover was about 5 times more influential at a crack width limit of 0.3 mm for the crack model where the effective depth of tension zone was 2.5(c +φ/2). This factor decreases to about 3 at 0.2 mm and 1.75 for w_{lim} = 0.1 mm. Section thickness was only a variable in the edge restraint model where the effective depth was h/2, even the small relative influence held by section thickness in this model was obviously greater than the no influence had by section thickness where $h_{c,eff}$ = 2.5(c + φ/2).

It is suspected, then, that the relative influence held by the concrete cover where $h_{c,eff}$ = 2.5(c +φ/2) resulted in the edge restraint crack model generating smaller reliability indices in the FORM analysis, especially when considering that the relative influence of model uncertainty was comparable for either variations of the edge restraint crack model. Considering the impact of the concrete cover's relative influence in either variation of edge restraint crack model, this variable serves to increase the crack spacing and the eventual crack widths calculated (since the model is

directly proportional to concrete cover). The reliability model of the edge restraint crack model containing $h_{c,eff} = 2.5(c + \varphi/2)$ would then generate crack widths considerably greater than those of the reliability crack model where $h_{c,eff} = h/2$. This would mean that the edge restraint crack model would produce reliability indices that were lower than where $h_{c,eff} = h/2$ since the crack width limit would more likely be exceeded (as observed where the influence of the effective depth for edge restraint was assessed in chapter 5). Although, the dominance in reliability performance where h/2 is limiting was notably slight.

An analysis of the sensitivity factors of the edge restraint revealed that model uncertainty was, in fact, the most influential random variable and adjustments made with respect to this variable by way of partial factors should make the most impact on the crack model for edge restraint.

6.2.1.3 End Restraint ($h_{c,eff} = 2.5(c + \varphi/2)$)

Unlike in the case for edge restraint, the end restraint crack model containing the effective depth of $2.5(c + \varphi/2)$ has section thickness included in the model. However, the influence of section thickness was found to be negligible with the highest obtained value being -0.036 (w_{lim} = 0.3 mm and CoV = 1). Model uncertainty still remains the most influential random variable. Model uncertainty sensitivity factors values were up to about -0.79 across all crack width limits considered in the analysis at a model uncertainty CoV of 0.3. The effective concrete tensile strength was the second most influential random variable followed by concrete cover and then finally section thickness. The above mentioned observed trends were evident for model uncertainty CoV's of 0.2 and greater. At lower CoV's for model uncertainty the effective concrete tensile strength was the most influential random variable with section thickness being the least influential. These results are tabulated in Table 6.3.

Table 6.3: Sensitivity Factors of Random Variables for End Restraint Crack Model (β_t = 1.5, $h_{c,\,eff}$ = 2.5(c +φ/2))

w_{lim} (mm)	Model uncertainty CoV	%As required	α_h (section thickness)	α_c (concrete cover)	$\alpha_{fct,eff}$ (effective concrete tensile strength)	α_θ (model uncertainty)
0.3	0.1	1.380	-0.036	-0.513	-0.759	-0.399
	0.15	1.404	-0.033	-0.468	-0.693	-0.547
	0.2	1.435	-0.030	-0.421	-0.624	-0.657
	0.25	1.471	-0.027	-0.378	-0.560	-0.737
	0.3	1.510	-0.024	-0.339	-0.503	-0.794
0.2	0.1	1.762	-0.035	-0.517	-0.757	-0.398
	0.15	1.794	-0.032	-0.472	-0.692	-0.546
	0.2	1.835	-0.029	-0.425	-0.623	-0.656
	0.25	1.883	-0.026	-0.381	-0.559	-0.736
	0.3	1.935	-0.023	-0.343	-0.503	-0.793
0.1	0.1	2.751	-0.033	-0.524	-0.753	-0.396
	0.15	2.807	-0.030	-0.479	-0.688	-0.543
	0.2	2.877	-0.027	-0.432	-0.621	-0.653
	0.25	2.959	-0.024	-0.388	-0.557	-0.733
	0.3	3.049	-0.022	-0.349	-0.501	-0.791

As crack width limit decreased so did the (negligible) influence of section thickness (as shown in Figure 6.8), effective concrete tensile strength (referring to Figure 6.10) and model uncertainty (Figure 6.11). The influence of concrete cover tended to increase with a decrease in the crack width limit (Figure 6.9). As the coefficient of variance of model uncertainty increased, the relative influence of section thickness, concrete cover and the effective concrete tensile strength would decrease (as illustrated in Figures 6.8, 6.9 and 6.10 respectively), whilst model uncertainty increased in influence (as observed in Figure 6.11).

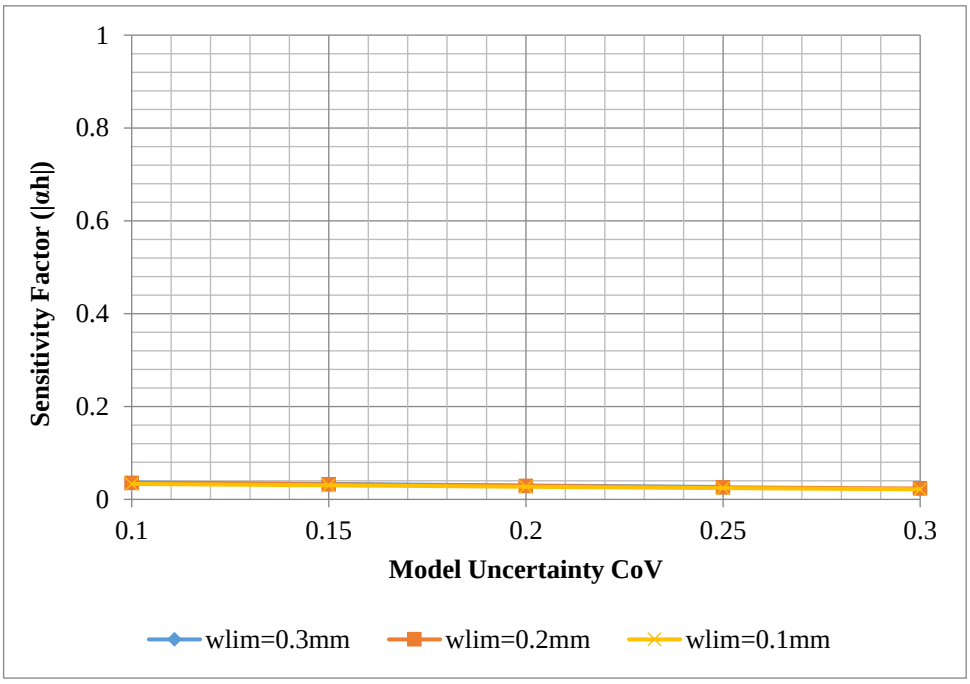

Figure 6.8: End Restraint Sensitivity of Section Thickness (h) for Varying Model Uncertainty Coefficient of Variance ($h_{c,\,eff} = 2.5(c + \varphi/2)$)

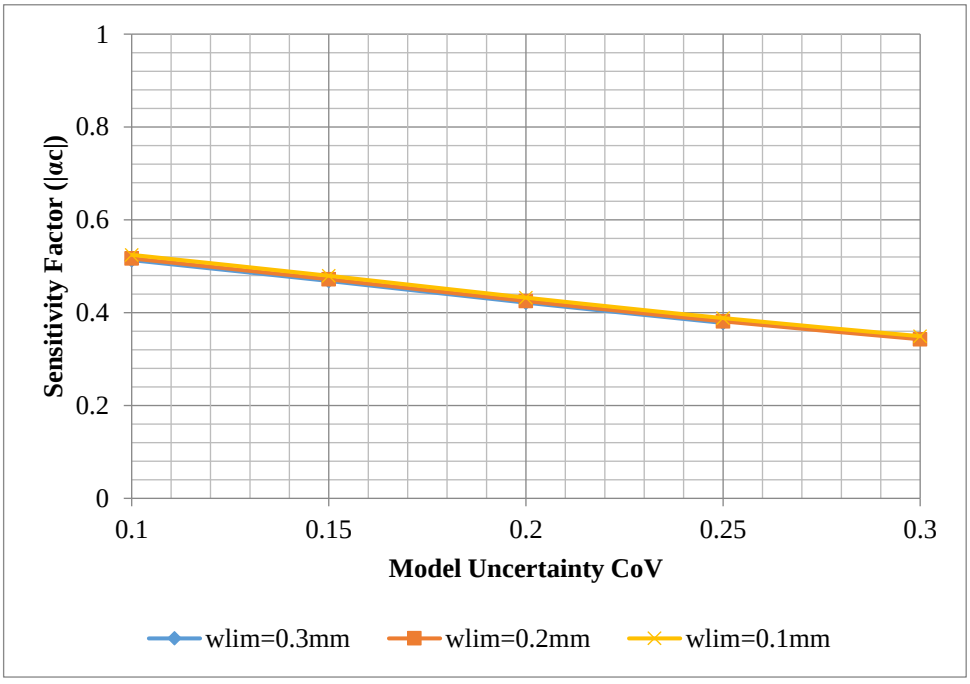

Figure 6.9: End Restraint Sensitivity of Concrete Cover (c) with Varying Model Uncertainty Coefficient of Variance ($h_{c,\,eff} = 2.5(c + \varphi/2)$)

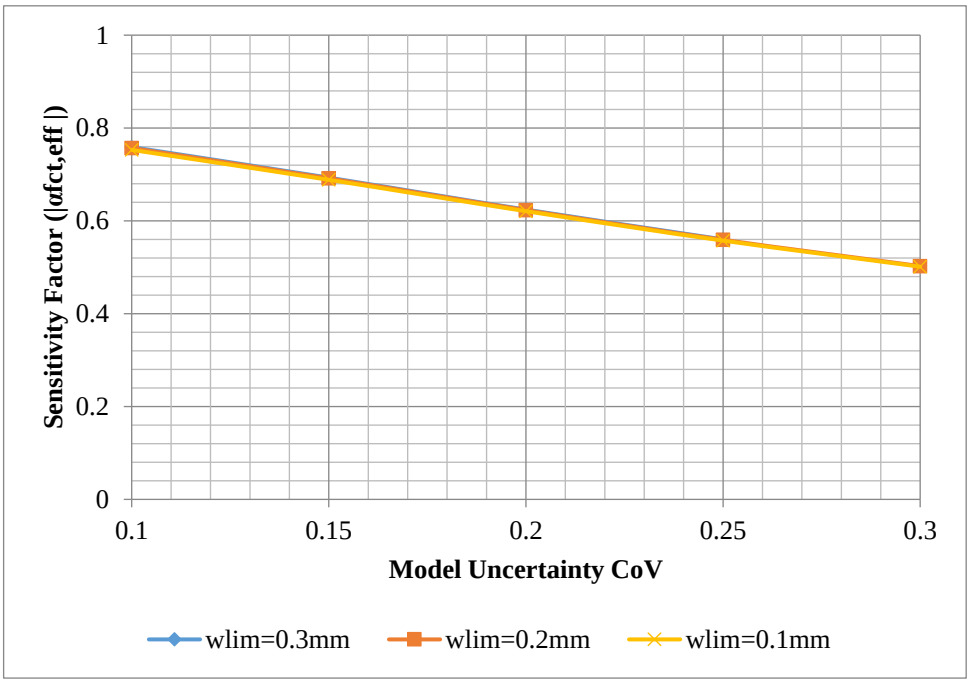

Figure 6.10: End Restraint Sensitivity of the Effective Concrete Tensile Strength ($f_{ct,eff}$) for Varying Model Uncertainty Coefficient of Variance ($h_{c,\,eff} = 2.5(c + \varphi/2)$)

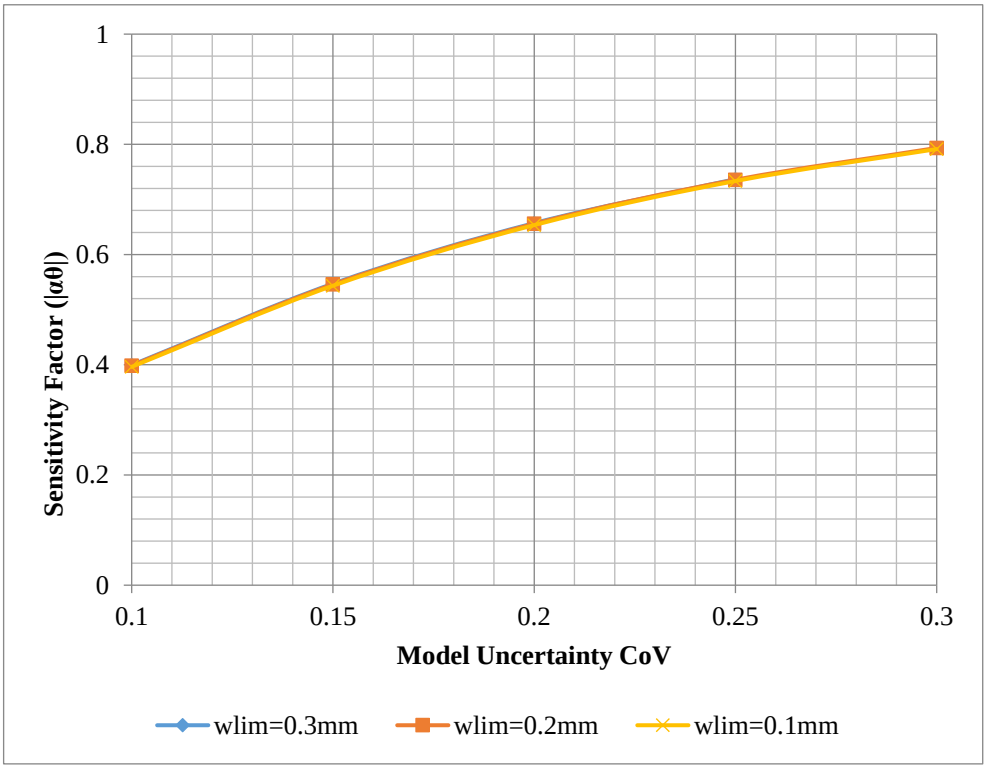

Figure 6.11: End Restraint Sensitivity of Model Uncertainty (θ) for Varying Model Uncertainty Coefficient of Variance ($h_{c,\,eff} = 2.5(c + \varphi/2)$)

6.2.1.4 End Restraint ($h_{c,\,eff} = h/2$)

The most influential random variable was the model uncertainty where the effective depth was h/2. Model uncertainty's sensitivity factors go up to about -0.83 across all crack width limits at model uncertainty CoV of 0.3 (slightly larger in magnitude to those values observed where the effective depth of the crack model was 2.5(c+ φ/2)). The effective concrete tensile strength follows after model uncertainty with sensitivity factors of about -0.53 at the same model uncertainty CoV of 0.3 for the crack width limits considered. Concrete cover follows after the effective concrete tensile strength. Then lastly, section thickness was found to have the least influence on the crack model. These results may be observed in Table 6.4.

Table 6.4: Sensitivity Factors of Random Variables for End Restraint Crack Model (β_t = 1.5, $h_{c,\,eff} = h/2$)

w_{lim}	Model uncertainty CoV	$\%A_s$ Required	α_h (section thickness)	α_c (concrete cover)	$\alpha_{fct,eff}$ (effective concrete tensile strength)	α_θ (model uncertainty)
0.3	0.1	1.347	-0.078	-0.149	-0.872	-0.459
	0.15	1.375	-0.069	-0.134	-0.776	-0.613
	0.2	1.409	-0.061	-0.120	-0.683	-0.718
	0.25	1.447	-0.053	-0.105	-0.601	-0.791
	0.3	1.489	-0.047	-0.097	-0.532	-0.840
0.2	0.1	1.718	-0.074	-0.179	-0.868	-0.457
	0.15	1.755	-0.066	-0.161	-0.773	-0.610
	0.2	1.800	-0.058	-0.144	-0.680	-0.716
	0.25	1.851	-0.051	-0.129	-0.599	-0.788
	0.3	1.906	-0.045	-0.117	-0.531	-0.838
0.1	0.1	2.679	-0.067	-0.242	-0.856	-0.451
	0.15	2.741	-0.059	-0.219	-0.764	-0.604
	0.2	2.818	-0.052	-0.196	-0.674	-0.710
	0.25	2.906	-0.046	-0.176	-0.595	-0.783
	0.3	3.001	-0.040	-0.159	-0.528	-0.833

The graphical representation of the findings are presented in the Figures 6.12 to 6.15. As the crack width limit was decreased, so did the sensitivity factors of section thickness (as shown in Figure 6.12), concrete tensile strength (referring to Figure 6.14) and model uncertainty (Figure 6.15). Concrete cover increases in relative influence as the crack width limit decreases (Figure 6.13). The sensitivity of section thickness, concrete cover and concrete tensile strength decreased as the model uncertainty CoV was increased. Contrary to this, the sensitivity factor of model uncertainty increased with an increase in model uncertainty variability (as illustrated in Figure 6.15).

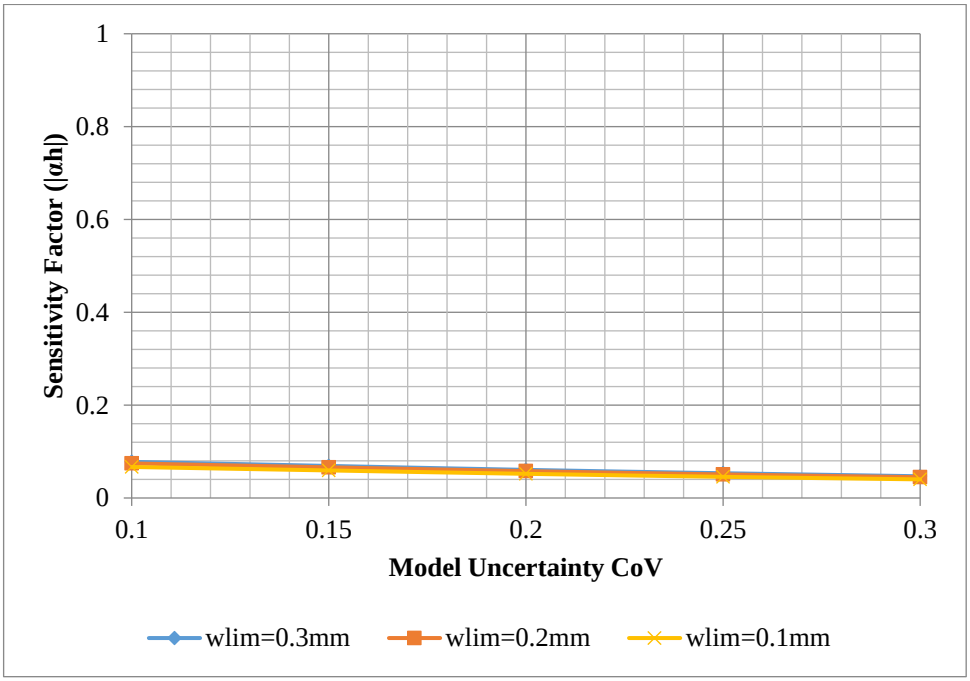

Figure 6.12: End Restraint Sensitivity of Section Thickness (h) for Varying Model Uncertainty Coefficient of Variance ($h_{c,eff}$ = h/2)

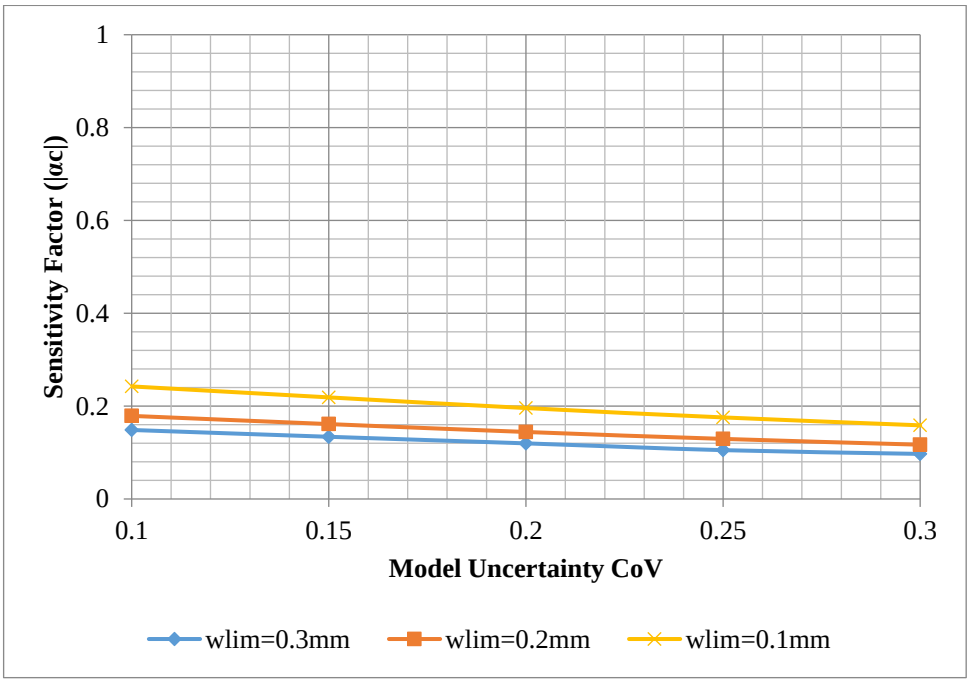

Figure 6.13: End Restraint Sensitivity of Concrete Cover (c) for Varying Model Uncertainty Coefficient of Variance ($h_{c,eff}$ = h/2)

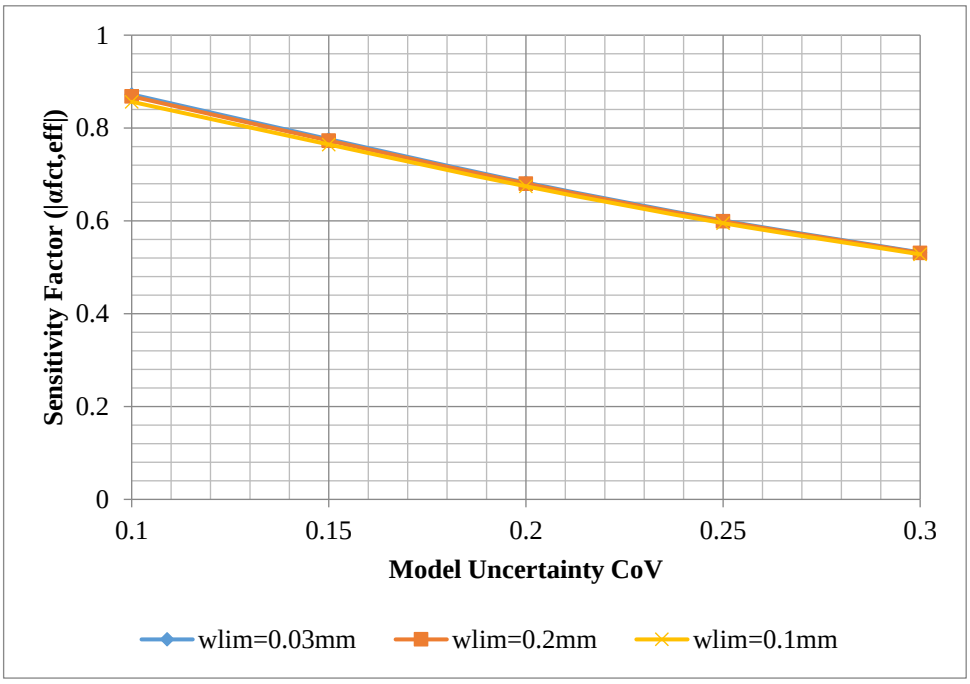

Figure 6.14: End Restraint Sensitivity of the Effective Concrete Tensile Strength ($f_{ct,eff}$) for Varying Model Uncertainty Coefficient of Variance ($h_{c,eff}$ = h/2)

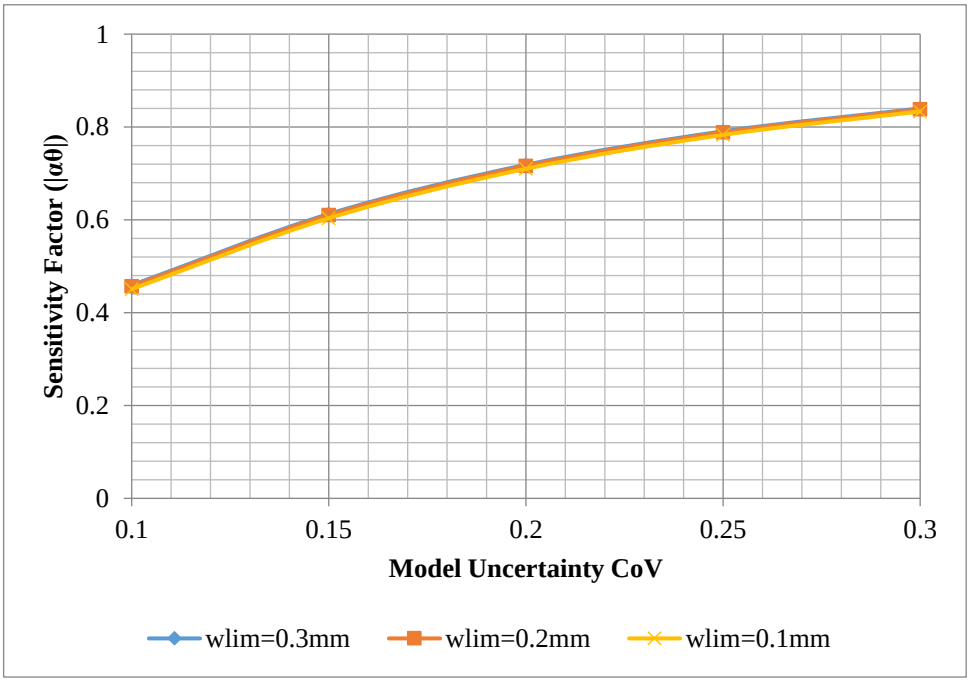

Figure 6.15: End Restraint Sensitivity of Model Uncertainty (θ) for Varying Model Uncertainty Coefficient of Variance ($h_{c,eff}$ = h/2)

At a model uncertainty variation of 0.3 and crack width limits 0.3, 0.2 and 0.1 the concrete cover sensitivity factor for the $h_{c,eff} = 2.5(c + \varphi/2)$ were larger by factors 3.5, 2.9 and 2.3 respectively as compared to the sensitivity factors of the end restraint crack model where the effective depth

was h/2. The sensitivity factors obtained for section thickness where $h_{c,eff}$ = h/2 are greater in magnitude than those obtained where $h_{c,eff}$ = 2.5(c +φ/2), but still negligible. The sensitivity factors of concrete tensile strength are quite comparable between the two variations of the end restraint crack model, with the $h_{c,eff}$ = h/2 containing end restraint crack model slightly larger in magnitude (larger by factor 1.06) at w_{lim} = 0.2 mm and model uncertainty CoV 0.3.

The biggest difference between the two variations of the end restraint crack model was in the influence of the concrete cover variable. The larger magnitude of the concrete cover sensitivity factor in the model containing $h_{c,eff}$ = 2.5(c +φ/2) will mean that larger crack widths are calculated with this reliability model. Thus the reliability indices produced under this model will be lower as compared to the end restraint crack model where the effective depth of tension was h/2.

6.2.2 Theoretical Partial Safety Factors

The theoretical partial safety factors (psf's) of section thickness (γ_h), concrete cover to reinforcement (γ_c), effective concrete tensile strength ($\gamma_{fct,eff}$) and model uncertainty (γ_θ) were calculated. These partial factors were calculated with respect to changes in the variability of the model uncertainty. Variations in degree of restraint applied to edge restraint members were also considered by calculating the theoretical partial factors under a selection of restraint factors.

6.2.2.1 Edge Restraint ($h_{c,\,eff}$ = 2.5(c +φ/2))

Table 6.5 gives the compilation of the theoretical psf's of the random variables calculated for the edge restraint crack model with the target reliability index set at 1.5 and effective depth of tension 2.5(c + φ/2). Section thickness did not feature in the edge restraint crack model where $h_{c,eff}$ =2.5(c +φ/2). Model uncertainty required the largest theoretical psf's with values from ± 1.1. This dominance occurs only from a model uncertainty CoV of 0.2. Theoretical psf's for concrete cover were less than those of model uncertainty with values from ± 1.08.

Table 6.5: Theoretical Partial Factors of Random Variables for Edge Restraint Crack Model (β_t = 1.5, $h_{c,\,eff}$ = 2.5(c +φ/2))

w_{lim} (mm)	Model uncertainty CoV	%As required	γ_c (concrete cover)	γ_θ (model uncertainty)
0.3	0.1	0.756	1.18	1.09
	0.15	0.797	1.14	1.17
	0.2	0.847	1.12	1.26
	0.25	0.902	1.09	1.35
	0.3	0.963	1.08	1.45
0.2	0.1	1.229	1.18	1.09
	0.15	1.302	1.15	1.17
	0.2	1.390	1.12	1.26
	0.25	1.491	1.10	1.35
	0.3	1.600	1.08	1.45
0.1	0.1	3.294	1.18	1.09
	0.15	3.553	1.15	1.17
	0.2	3.884	1.12	1.26
	0.25	4.280	1.10	1.35
	0.3	4.743	1.09	1.44

For concrete cover the theoretical psf's were relatively constant irrespective of the model uncertainty CoV and the crack width limit, Figure 6.16 illustrates this (ranging from approximately 1.1, up to a maximum value of 1.2). A larger range of variations in the theoretical psf's of model uncertainty were found as the model uncertainty CoV increased (approximately from 1.1 to 1.4, as shown in Figure 6.17). An increase in the crack width limit resulted in a decrease in the influence of the concrete cover (as indicated in Figure 6.16) with an increase in influence being found for model uncertainty (referring to Figure 6.17).

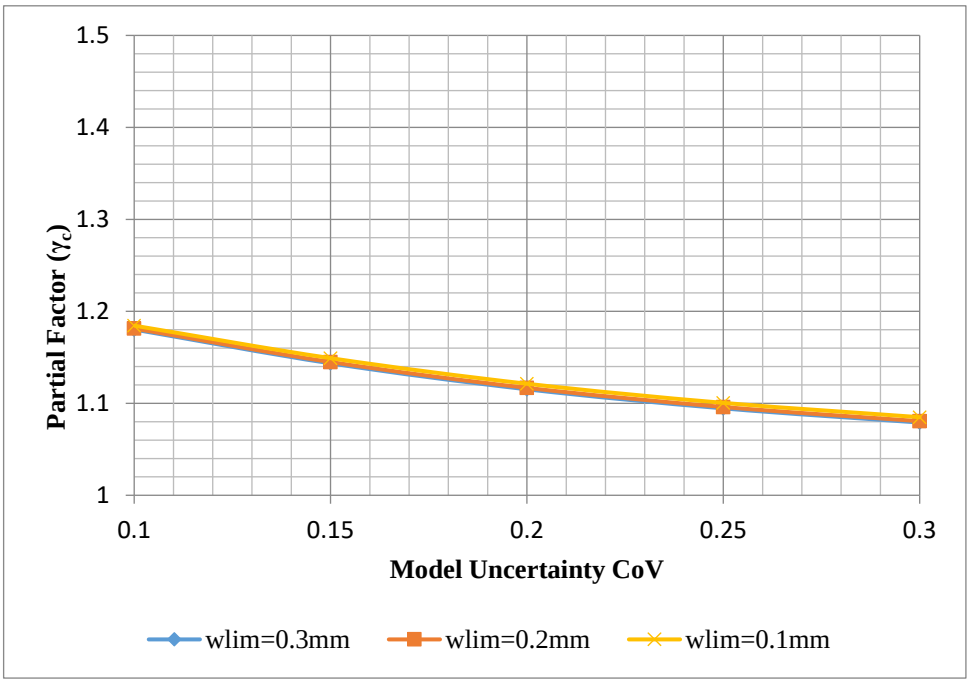

Figure 6.16: Edge Restraint Theoretical Partial Safety Factors of Concrete Cover (c) for Varying Model Uncertainty Coefficient of Variance ($h_{c,\,eff}$ =2.5(c +φ/2))

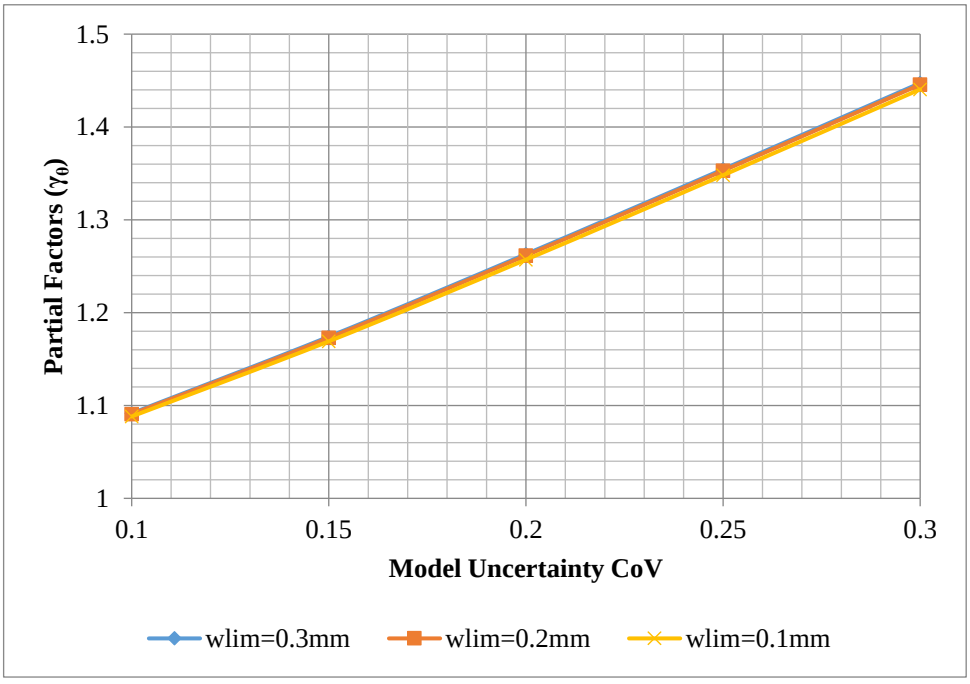

Figure 6.17: Edge Restraint Theoretical Partial Safety Factors of Model Uncertainty (θ) for Varying Model Uncertainty Coefficient of Variance ($h_{c,\,eff}$ =2.5(c +φ/2))

6.2.2.2 Edge Restraint ($h_{c,\,eff}$ = h/2)

Even with where the effective depth of tension area was h/2, no real adjustment was required for section thickness to meet the desired reliability index. This was evident across all assessed crack

width limits and model uncertainty CoV's considered in the analysis. Model uncertainty required the most adjustments to meet the target reliability index, with theoretical psf's from about 1.1 (model uncertainty CoV = 0.1) to 1.5 (model uncertainty CoV = 0.3) for the crack width limits considered. The concrete cover follows after model uncertainty with psf's from 1.01 (w_{lim} = 0.3 mm, model uncertainty CoV = 0.3). This was indicative of the slight influence the concrete cover had on the edge restraint crack model where h/2 was the effective depth of tension area. Presented in Table 6.6 are the theoretical psf's obtained for the edge restraint crack model where $h_{c,eff}$ = h/2.

Table 6.6: Theoretical Partial Factors of Random Variables for Edge Restraint Crack Model (β_t = 1.5, $h_{c,\,eff}$ =h/2)

w_{lim} (mm)	Model uncertainty CoV	%As Required	γ_h (section thickness)	γ_c (concrete cover)	γ_θ (model uncertainty)
0.3	0.1	0.690	1.00	1.03	1.15
	0.15	0.745	1.00	1.02	1.24
	0.2	0.804	1.00	1.01	1.32
	0.25	0.866	1.00	1.01	1.41
	0.3	0.930	1.00	1.01	1.50
0.2	0.1	1.114	1.00	1.05	1.15
	0.15	1.210	1.00	1.03	1.23
	0.2	1.316	1.00	1.02	1.32
	0.25	1.424	1.00	1.02	1.41
	0.3	1.541	1.00	1.02	1.49
0.1	0.1	2.935	1.00	1.11	1.13
	0.15	3.251	1.00	1.08	1.22
	0.2	3.617	1.00	1.06	1.30
	0.25	4.0354	1.00	1.05	1.39
	0.3	4.511	1.00	1.04	1.48

Figure 6.18 illustrates how the theoretical psf's required for section thickness were generally unaffected by the increase in crack width limit. For concrete cover, increases in the crack width resulted in a decrease in the theoretical psf required to attain the target reliability index (observing from Figure 6.19). Model uncertainty psf's increased with an increase in crack width limit (referring to Figure 6.20). Increases in the model uncertainty CoV resulted in decreases in the theoretical psf attained for concrete cover and an increase in those theoretical psf's values obtained for model uncertainty (reading from Figure 6.19 and 6.20 respectively). In the case of section thickness, little variation was experienced across the range model uncertainty CoV's considered in this analysis (as illustrated in Figure 6.18).

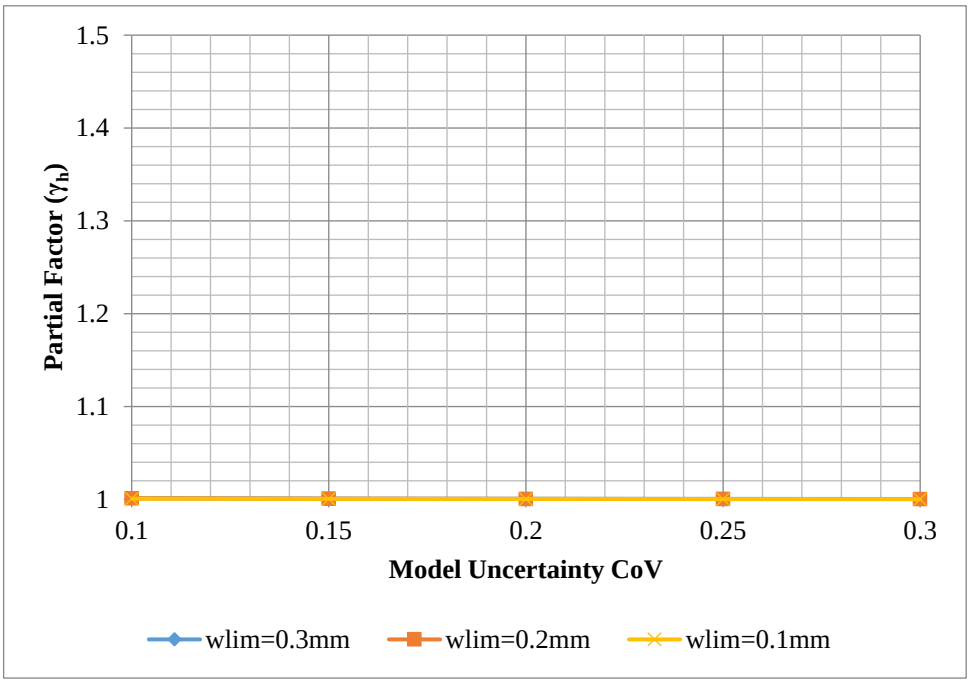

Figure 6.18: Edge Restraint Theoretical Partial Safety Factors of Section Thickness (h) for Varying Model Uncertainty Coefficient of Variance ($h_{c,\,eff}$ = h/2)

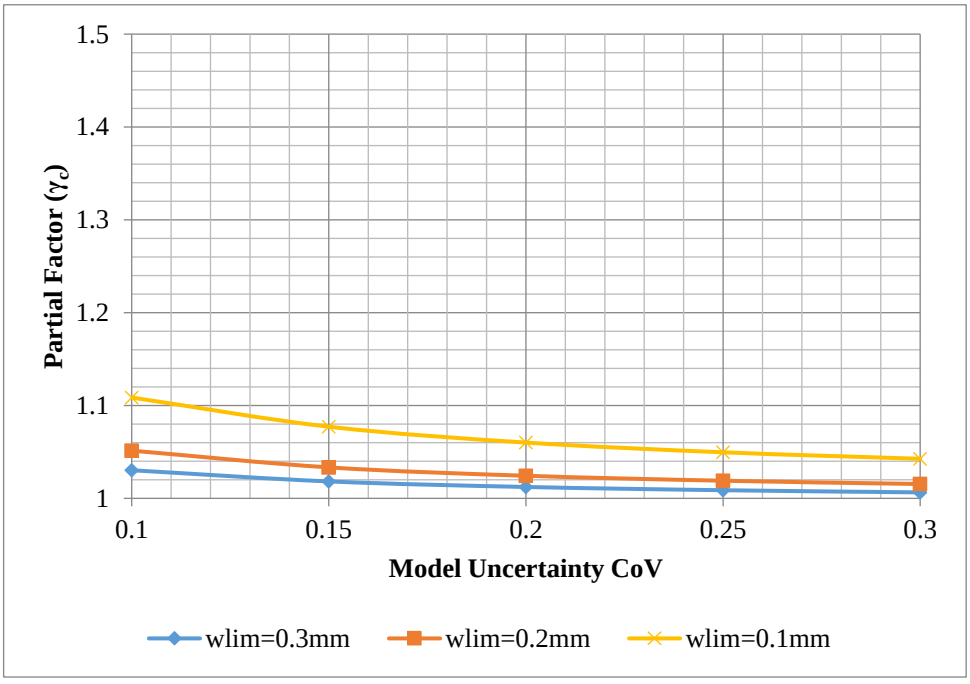

Figure 6.19: Edge Restraint Theoretical Partial Safety Factors of Concrete Cover (c) for Varying Model Uncertainty Coefficient of Variance ($h_{c,\,eff}$ = h/2)

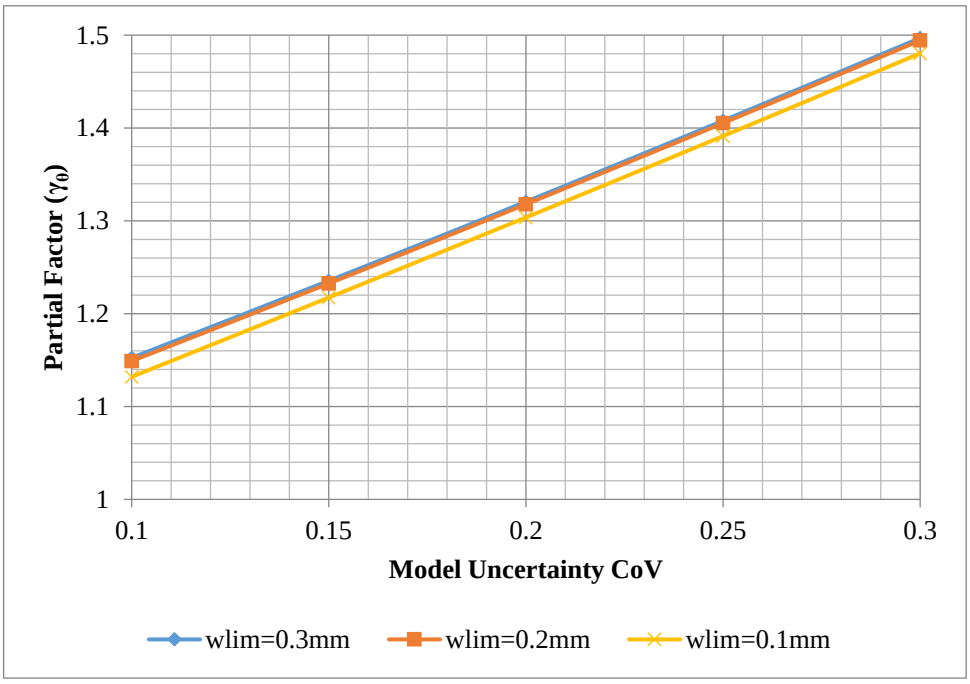

Figure 6.20: Edge Restraint Theoretical Partial Safety Factors of Model Uncertainty (θ) for Varying Model Uncertainty Coefficient of Variance ($h_{c,\,eff}$ = h/2)

The adjustments required for concrete cover to meet the target reliability were greater by a factor of 1.07 where the effective depth of tension zone was 2.5(c +φ/2) –for w_{lim} = 0.2 mm and model uncertainty CoV of 0.3 (a small increase in the psf required between the effective depth $h_{c,eff}$ = h/2 to where $h_{c,eff}$ is 2.5(c +φ/2). The theoretical psf's calculated for model uncertainty where the effective depth is h/2 were 1.03 times greater than where the effective depth of the tension was 2.5(c +φ/2). This slight increase was found where the crack width limit was 0.2 mm and the variability of model uncertainty was set at 0.3.

6.2.2.3 End Restraint ($h_{c,\,eff}$ = 2.5(c +φ/2))

It may be observed from Table 6.7 that the section thickness had obtained negligible theoretical psf's. Being the most influential random variable, model uncertainty had partial factors from about 1.1 to 1.4for the range of crack width limits considered (for corresponding model uncertainty CoV's 0.1 and 0.3). This was followed by concrete cover with theoretical psf's from 1.07 to 1.1 (at model uncertainty CoV of 0.3). The effective concrete tensile strength is a material property and thus a resistance variable, the theoretical partial safety factor for concrete tensile strength would be implemented in design codes as $1/\gamma_{fct,eff}$ to obtain the design value for this variable . For the effective concrete tensile strength theoretical psf's were generally from 1.1 at model uncertainty CoV of 0.3 to about 1.2 for model uncertainty CoV of 0.1 – implemented as 0.91 to 0.83 respectively (referring to Table 6.7).

Table 6.7: Theoretical Partial Factors of Random Variables for β_t = 1.5 ($h_{c,\,eff}$=2.5(c +φ/2))

w_{lim} (mm)	Model uncertainty CoV	%As required	γ_h (section thickness)	γ_c (concrete cover)	$\gamma_{fct,eff}$ (effective concrete tensile strength)	$1/\gamma_{fct,eff}$	γ_θ (model uncertainty)
0.3	0.1	1.380	1.00	1.11	1.22	0.82	1.06
	0.15	1.404	1.00	1.10	1.20	0.84	1.12
	0.2	1.435	1.00	1.09	1.17	0.85	1.19
	0.25	1.471	1.00	1.08	1.15	0.87	1.28
	0.3	1.510	1.00	1.07	1.13	0.88	1.37
0.2	0.1	1.762	1.00	1.11	1.22	0.82	1.06
	0.15	1.794	1.00	1.01	1.20	0.84	1.12
	0.2	1.835	1.00	1.09	1.17	0.85	1.19
	0.25	1.883	1.00	1.08	1.15	0.87	1.28
	0.3	1.935	1.00	1.07	1.13	0.88	1.37
0.1	0.1	2.751	1.00	1.11	1.22	0.82	1.06
	0.15	2.807	1.00	1.10	1.20	0.84	1.12
	0.2	2.877	1.00	1.09	1.17	0.85	1.19
	0.25	2.959	1.00	1.08	1.15	0.87	1.28
	0.3	3.049	1.00	1.07	1.13	0.88	1.37

The theoretical partial safety factors obtained for the random variables remained mostly steady across all crack width limits considered as may be deduced from the Figures 6.21 to 6.24, particularly for section thickness (as shown in Figure 6.21). Nonetheless, as the crack width limit decreased the theoretical psf's of the effective concrete tensile strength and model uncertainty decreased (referring to Figures 6.23 and 6.24 respectively). The theoretical partial safety factors of concrete cover increased with a decrease in crack width limit (reading from Figure 6.22). Increases in the variability of the model uncertainty decreased the theoretical partial safety factors required for section thickness (negligible decrease), concrete cover (decrease was also found to be marginal, but not as small as for section thickness) and for the effective concrete tensile strength for reliability compliance (as may be observed in Figures 6.21, 6.22 and 6.23 respectively). Model uncertainty's theoretical partial safety factors increased considerably with an increase in model uncertainty variability (Figure 6.24).

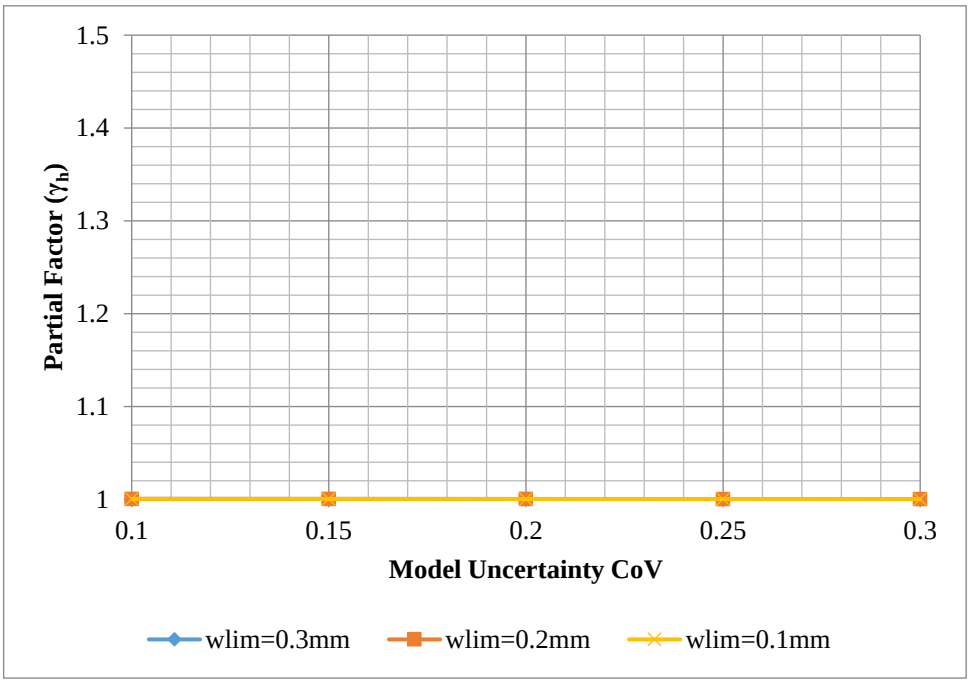

Figure 6.21: End Restraint Theoretical Partial Safety Factors of Section Thickness (h) for Varying Model Uncertainty Coefficient of Variance ($h_{c,\,eff} = 2.5(c + \varphi/2)$)

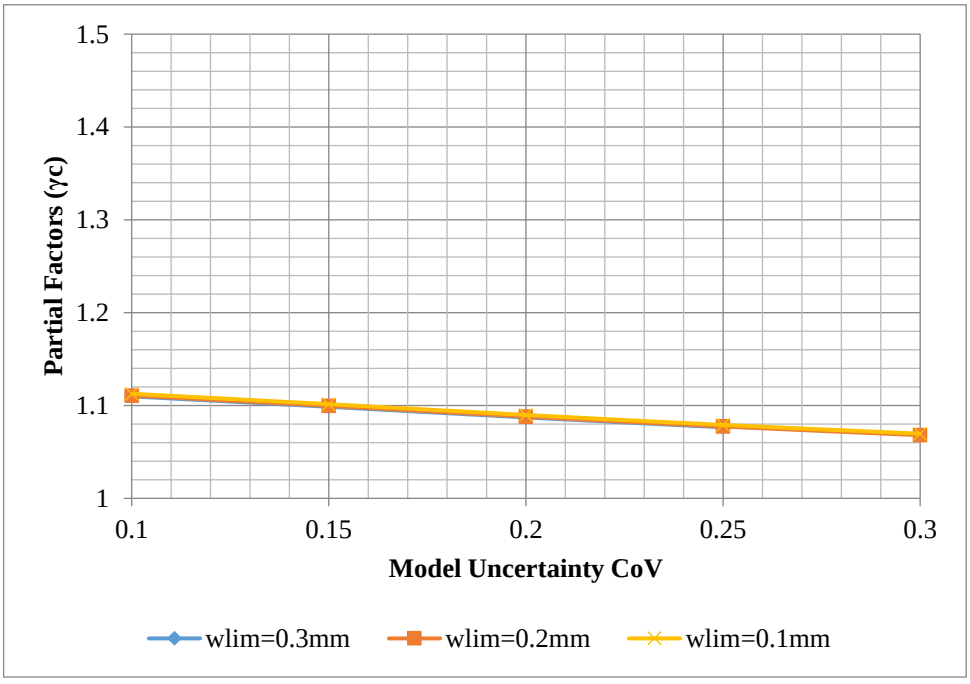

Figure 6.22: End Restraint Partial Safety Factors of Concrete Cover (c) for Varying Model Uncertainty Coefficient of Variance ($h_{c,\,eff} = 2.5(c + \varphi/2)$)

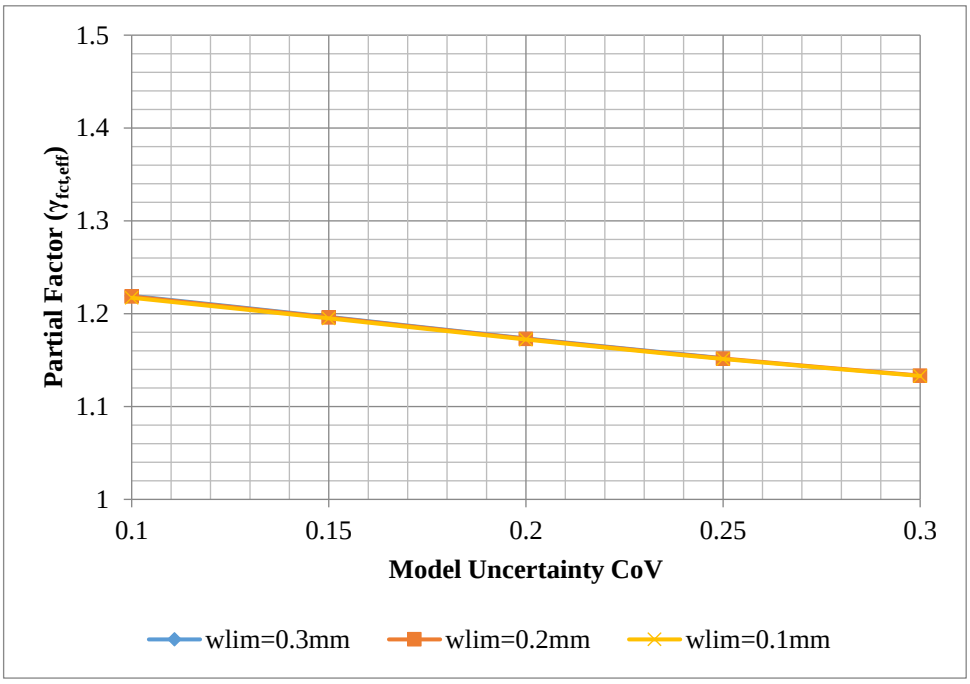

Figure 6.23: End Restraint Theoretical Partial Safety Factors of the Effective Concrete Tensile Strength ($f_{ct,eff}$) for Varying Model Uncertainty Coefficient of Variance ($h_{c,\,eff}$ = 2.5(c +φ/2))

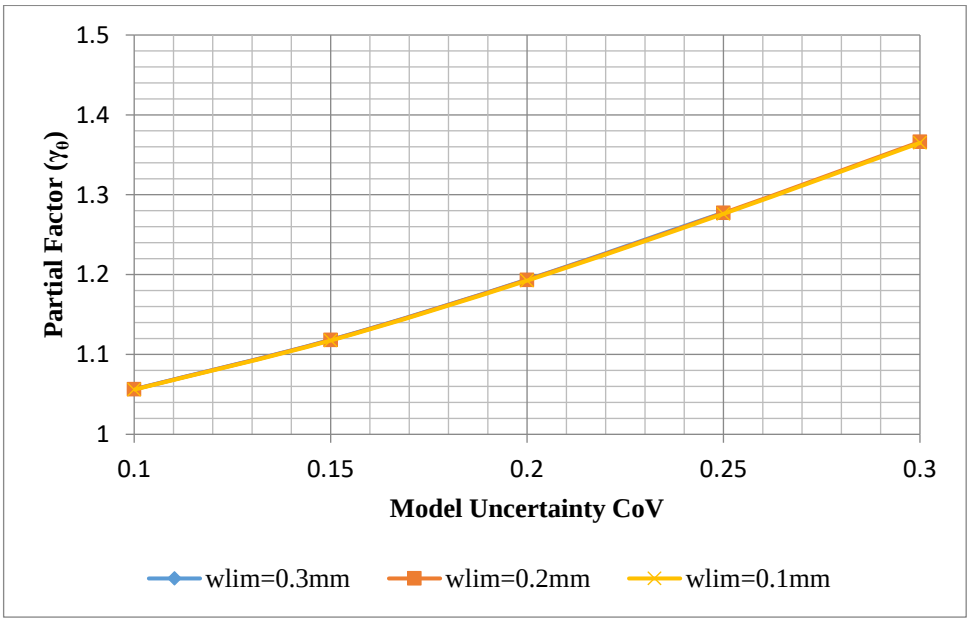

Figure 6.24: End Restraint Theoretical Partial Safety Factors of Model Uncertainty (θ) for Varying Model Uncertainty Coefficient of Variance ($h_{c,\,eff}$ = 2.5(c +φ/2))

6.2.2.4 End Restraint ($h_{c,\,eff}$ = h/2)

Model uncertainty, once again, required the largest theoretical partial safety factor with values from approximately 1.1 to 1.4 (at model uncertainty CoV's of 0.1 and 0.3 respectively) for the

crack width limits considered in this analysis. The theoretical psf's for the effective concrete tensile strength follows after model uncertainty with theoretical psf's from about 1.1. As before mentioned, when applying the calculated theoretical partial safety factor for the effective concrete tensile in a design code the factor $1/\gamma_{fct,eff}$ will be used rather than $\gamma_{fct,eff.}$ since it is a material property (and thus a resistance variable). The theoretical psf's obtained for concrete cover was generally around 1.02. Section thickness had a small influence on the end restraint crack model (where $h_{c,eff} = h/2$) and hence obtained theoretical partial safety factors of about 1 for all crack widths limits and model uncertainty CoV's considered. These results may be observed in Table 6.8.

Table 6.8: Theoretical Partial Factors of Random Variables for β_t = 1.5 ($h_{c,\,eff}$ = h/2)

w_{lim} (mm)	Model Uncertainty CoV	$\%A_s$ Required	γ_h (section thickness)	γ_c (concrete cover)	$\gamma_{fct,eff}$ (effective concrete tensile strength)	$1/\gamma_{fct,eff}$	γ_θ (model uncertainty
0.3	0.1	1.347	1.00	1.02	1.26	0.79	1.07
	0.15	1.375	1.00	1.02	1.23	0.82	1.14
	0.2	1.409	1.00	1.02	1.19	0.84	1.22
	0.25	1.447	1.00	1.01	1.17	0.86	1.30
	0.3	1.489	1.00	1.01	1.14	0.88	1.40
0.2	0.1	1.718	1.00	1.03	1.26	0.80	1.07
	0.15	1.755	1.00	1.03	1.22	0.82	1.13
	0.2	1.800	1.00	1.02	1.19	0.84	1.22
	0.25	1.851	1.00	1.02	1.17	0.86	1.30
	0.3	1.906	1.00	1.02	1.14	0.88	1.39
0.1	0.1	2.679	1.00	1.04	1.25	0.80	1.07
	0.15	2.741	1.00	1.04	1.22	0.82	1.13
	0.2	2.818	1.00	1.03	1.19	0.84	1.21
	0.25	2.906	1.00	1.03	1.16	0.86	1.30
	0.3	3.001	1.00	1.03	1.14	0.88	1.39

There were slight variations in the theoretical partial safety factors obtained across the crack width limits considered for all random variables (particularly for section thickness). Increases in the crack width limit meant an increases in the theoretical partial safety factors required for the effective concrete tensile strength and model uncertainty (as shown in Figures 6.27 and 6.28 respectively). The concrete cover had theoretical partial safety factors that decreased in value as

the crack width limit was increased (referring to Figure 6.26). Increases in the variability of the model uncertainty resulted in there being a decrease in values of the theoretical partial safety factors obtained for concrete cover and the effective concrete tensile strength (as shown in Figures 6.26 and 6.27). The theoretical partial factors obtained for model uncertainty increased as the variability in the model uncertainty was increased (as observed in Figure 6.28).

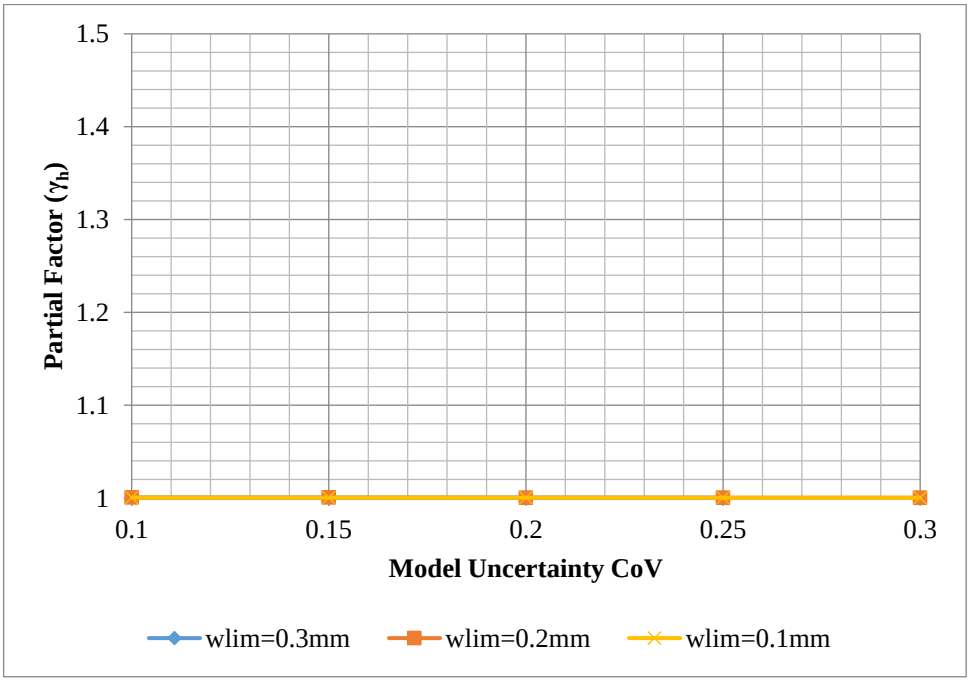

Figure 6.25: End Restraint Theoretical Partial Safety Factors of Section Thickness (h) for Varying Model Uncertainty Coefficient of Variance ($h_{c, eff}$ =h/2)

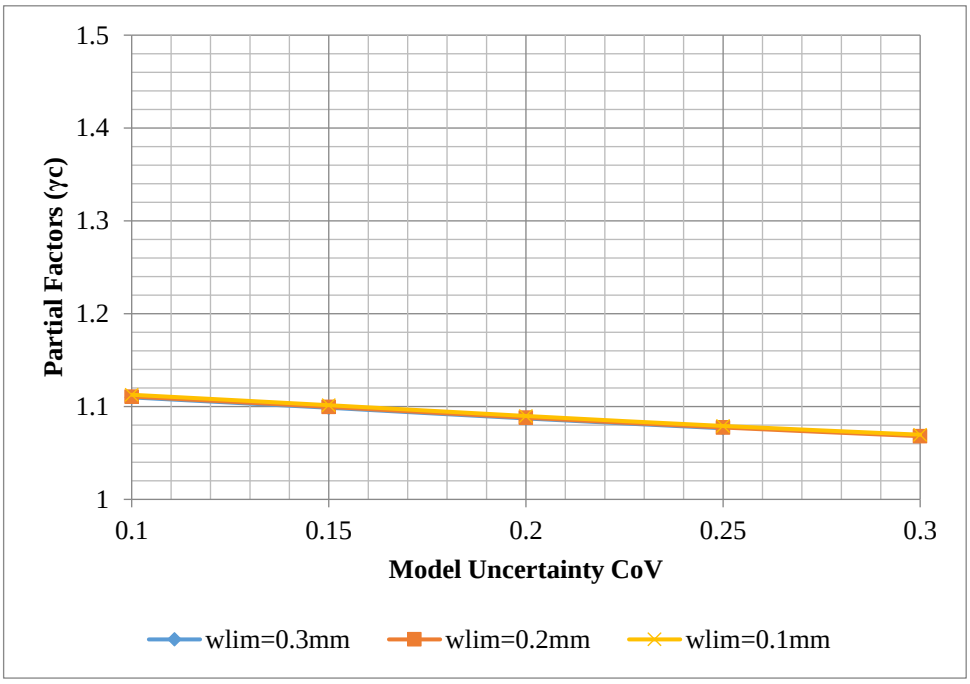

Figure 6.26: End Restraint Theoretical Partial Safety Factors of Concrete Cover (c) for Varying Model Uncertainty Coefficient of Variance ($h_{c,\,eff}$ =h/2)

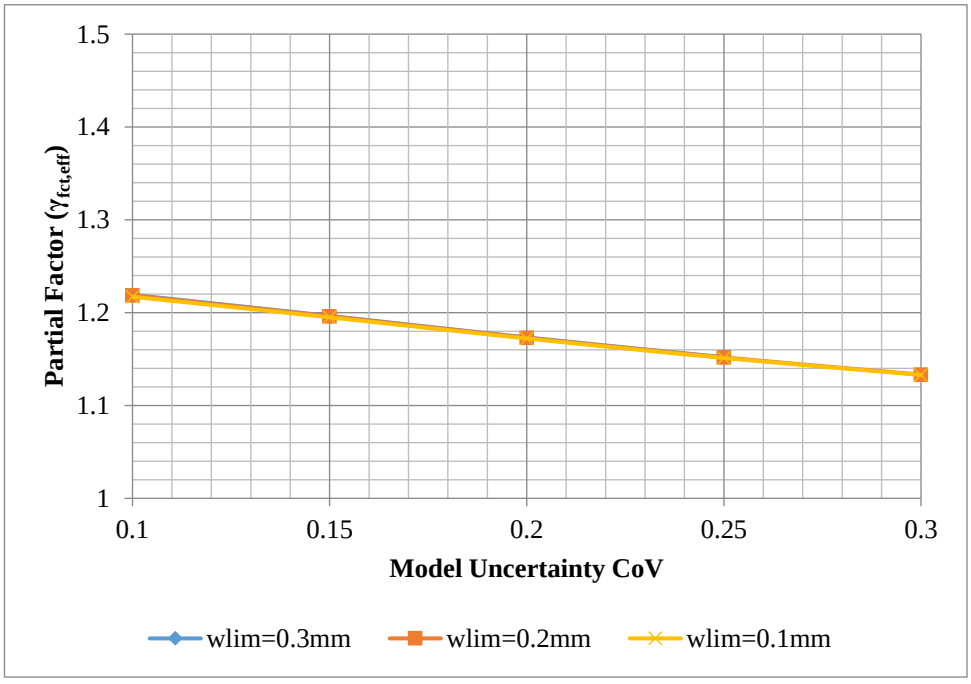

Figure 6.27: End Restraint Theoretical Partial Safety Factors of the Effective Concrete Tensile Strength ($f_{ct,eff}$) for Varying Model Uncertainty Coefficient of Variance ($h_{c,\,eff}$ = h/2)

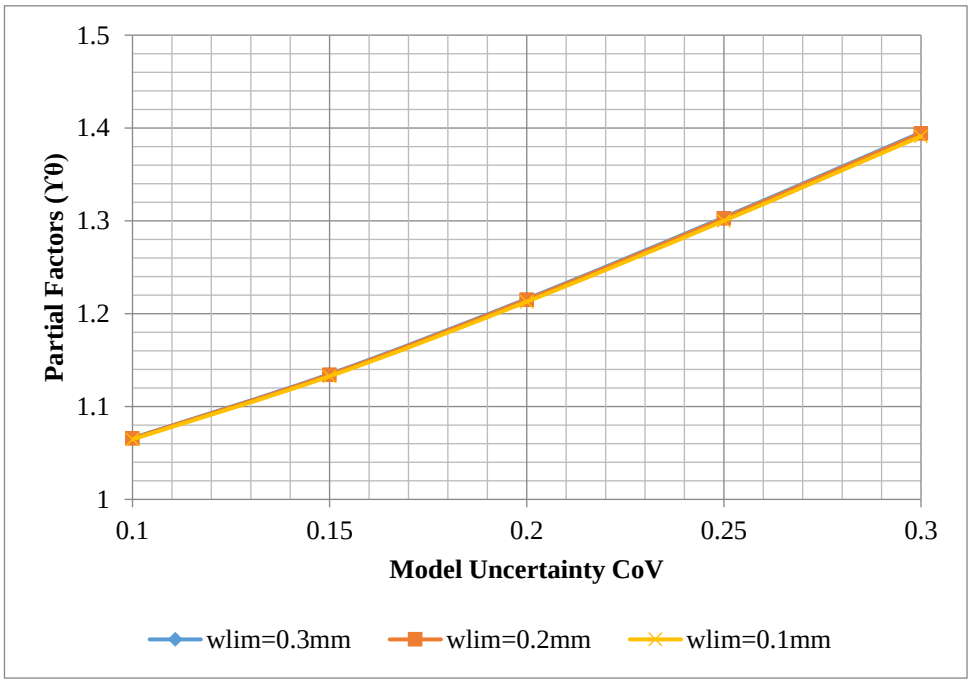

Figure 6.28: End Restraint Theoretical Partial Safety Factors of Model Uncertainty (θ) for Varying Model Uncertainty Coefficient of Variance ($h_{c,\,eff}$ =h/2)

Comparing the theoretical psf's obtained for the end restraint crack model where the effective depth was h/2 to the end restraint crack model where $h_{c,eff} = 2.5(c + \varphi/2)$, it may be found that the theoretical psf's obtained for most variables were greater in value, but only slightly. For a 0.2 mm crack width limit and at a model uncertainty CoV of 0.3, factors of 1.02 and 1.01 were where the model uncertainty and the effective concrete tensile strength's respective theoretical partial safety factors were greater in the case where the effective depth was $h_{c,eff}$ = h/2 as compared to the end restraint crack model where $h_{c,eff} = 2.5(c + \phi/2)$. Considering concrete cover, the theoretical partial safety factors where $h_{c,eff} = 2.5(c + \varphi/2)$ was greater in magnitude by factor 1.06 than where the effective depth were h/2 (a larger difference in magnitude than those experienced by model uncertainty and the effective concrete tensile strength at the same crack limit of 0.2 mm and model uncertainty CoV of 0.3). Additionally, section thickness had theoretical psf's amounting to 1 in either variations of the end restraint crack model. Overall, the theoretical partial safety factors obtained for the respective variables were quite comparable.

6.2.3 Potential Partial Factors for Code Calibration (Edge vs. End Restraint):

The theoretical implication (or otherwise practical application) of the above-mentioned comparison may be that comparable psf's obtained for the respective random variables indicate that the same partial factor may be applied to those variables to obtain the desired reliability irrespective of the restraint model (whether edge or end restraint). This is ideal for developing a design code, where simplification is preferred. However, the theoretical partial factors obtained

for the edge restraint crack model were found to be slightly greater than those obtained for the end restraint model. This implies that if the same partial factors were to be applied to the respective random variables for both the edge and end restraint crack model, these partial factors would be slightly conservative for the end restraint crack model.

The findings of the comparison in theoretical psf's obtained for the edge and end restraint crack model are listed below. In this exercise the edge and end restraint crack model, the theoretical partial safety factors that were obtained for where crack width limit was 0.2 mm and model uncertainty CoV was 0.3 were considered (as for the representative liquid retaining structure case).

- Model uncertainty:
  - Where $h_{c,eff} = 2.5(c + \varphi/2)$, model uncertainty was comparable with (ratio of edge to end partial factor was 1.06)
  - Where $h_{c,eff} = h/2$, model uncertainty was– once again– comparable. The ratio of edge to end was 1.07.
- Effective concrete tensile strength:
  - Only found in the end restraint model, so no comparison could be made between the edge and end restraint crack model in this respect. However, based on the findings of the end restraint for both where $h_{c,eff}$ was $2.5(c + \varphi/2)$ and h/2 ranged from about 1.1 to 1.2, thus a value of 1.2 may then be recommended for the effective concrete tensile strength for use in a design standard.
- Concrete cover:
  - Where $h_{c,eff} = 2.5(c + \varphi/2)$, concrete cover also returned comparable theoretical partial safety factors for edge and end restraint. A ratio of 1.01 was calculated for edge to end restraint theoretical partial safety factors.
  - Where $h_{c,eff} = h/2$, the ratio of edge to end restraint theoretical partial factors was 1.
- Section thickness:
  - Theoretical partial factor obtained were either 1 or very close to 1 across all the restraint models assessed.

6.2.4 Influence of the Choice of Reliability Index (β)

6.2.4.1 Edge Restraint

To determine the impact a change in the target reliability index on the EN 1992 edge restraint crack model with $h_{c,eff} = 2.5(c + \phi/2)$ and where $h_{c,eff} = h/2$ (referring to Table 6.9 and Table 6.10 respectively), the reliability index was changed from 0.5 to 2 whilst maintaining the crack width limit (w_{lim} = 0.2 mm) and model uncertainty CoV (0.3). In the case where the effective depth of the tension zone was given by $h_{c,eff} = 2.5(c + \phi/2)$, the relative influence held by both concrete cover and model uncertainty remained effectively constant through the changes in reliability index. Both the theoretical psf's for concrete cover and model uncertainty increased with an increase in the reliability index. Regarding β = 0.5 as a base, theoretical partial safety factors for concrete cover increased by 6% and 10% with an increase in reliability index to 1.5 and 2 respectively. And for model uncertainty, an increase in theoretical partial factors of 32% and 51% where corresponding reliability indices β = 1.5 and 2 were compared against selected base reliability index 0.5. Clearly, a change in the reliability index has the most effect on the model uncertainty of the EN 1992 edge restraint model. Section thickness, having no part in the edge restraint model where $h_{c,eff} = 2.5(c + \phi/2)$, has no relative influence with a sensitivity factor of 0 and theoretical partial safety factor of 1.

A 50% and 89% respective increase in reinforcement was obtained for reliability index 1.5 and 2 to be met with respect to reliability index 0.5– a substantial increase. A 25% increase in reinforcement was required where the reliability index was increased from 1.5 to 2. Thus a change in reliability index could have a considerable financial effect on the design of liquid retaining structures with elements restrained along their edge.

Table 6.9: Influence of Reliability Index on the Basic Variables of the EN 1992 Edge Restraint Crack Model (w_{lim} = 0.2 mm, model uncertainty CoV = 0.3, $h_{c,eff} = 2.5(c + \phi/2)$)

		Sensitivity Factors			Partial Factors		
β	**%As required**	**α_h**	**α_c**	**α_θ**	**γ_h**	**γ_c**	**γ_θ**
0.5	1.060	0	-0.386	-0.922	1.000	1.018	1.098
1.5	1.600	0	-0.394	-0.919	1.000	1.081	1.446
2	2.000	0	-0.399	-0.917	1.000	1.115	1.657

The same exercise was extended to where the effective depth of tension zone, $h_{c,eff,,}$ was h/2 (results of which were presented in Table 6.10). The sensitivity factors for section thickness and model uncertainty were slightly influenced by the change in reliability index. Concrete cover, on the other hand, increased by 37% and 62% for reliability indices 1.5 and 1.2 when compared against the sensitivity factor when the reliability index was set at 0.5. Section thickness and

concrete cover obtained theoretical psf's that varied only slightly as the reliability index was increased. Model uncertainty's theoretical partial safety factor increased by 35% and 56% for reliability indices 1.5 and 2 respectively when compared against the theoretical partial factor obtained for where the reliability index was set at 0.5. A comparable result to those obtained for when the effective depth of the tension zone was $2.5(c + \phi/2)$.

Reinforcements required to meet a reliability index of 1.5 and 2 as compared to those required for $\beta = 0.5$ are 46% and 79% respectively. A considerable increase in reinforcement, which would have a proportional impact on the cost of design where the reliability index is changed. An amount of 23% more reinforcement was required where the reliability index was changed from 1.5 to 2. These were overall smaller increases as compared to the results for the case where the effective depth of tension was $2.5(c + \phi/2)$.

Table 6.10: Influence of Reliability Index on the Basic Variables of the EN 1992 Edge Restraint Crack Model (w_{lim} = 0.2 mm, model uncertainty CoV = 0.3, $h_{c,eff}$ = h/2)

		Sensitivity Factors			Partial Factors		
β	**%As required**	**α_h**	**α_c**	**α_θ**	**γ_h**	**γ_c**	**γ_θ**
0.5	1.054	-0.027	-0.086	-0.996	1.000	0.995	1.110
1.5	1.541	-0.025	-0.118	-0.993	1.000	1.015	1.495
2	1.889	-0.024	-0.139	-0.990	1.000	1.031	1.732

6.2.4.2 End Restraint

For end restraint, the sensitivity factors for all basic variables remained relatively constant (referring to Table 6.11 where the effect depth of tension was $2.5(c + \varphi/2)$). As the reliability index was increased from 1.5 to 2 the theoretical partial safety factors of concrete cover increases by 5% and 8% correspondingly. For the effective concrete tensile strength this increase was about 10% and 15% for reliability index 1.5 and 2 respectively as compared to the corresponding theoretical partial safety factor for reliability index 0.5. Considering the theoretical partial safety factors of model uncertainty, an increase of 27% and 43% was experienced for reliability indices 1.5 and 2 respectively as compared against the theoretical partial safety factor obtained where β was 0.5. Again, a change in the reliability index had the largest effect on the model uncertainty.

Increases of 26% and 42% in steel reinforcement would be required to meet a reliability index of 1.5 and 2 as compared against $\beta = 0.5$. An increase of the reliability index from 1.5 to 2 resulted in an increase in reinforcement of 13%. These increases were smaller than those required for edge restraint, although there are still significant. Evidently, the target reliability index set for the

EN 1992 cracking serviceability limit state has a considerable impact on the cost of the design of liquid retaining structures.

Table 6.11: Influence of Reliability Index on the Basic Variables of the EN 1992 End Restraint Crack Model (w_{lim} = 0.2 mm, model uncertainty CoV = 0.3, $h_{c,eff}$ = 2.5(c + ϕ/2))

		Sensitivity Factors				Partial Factors				
β	**%As required**	**α_h**	**α_c**	**$\alpha_{fct,eff}$**	**α_θ**	**γh**	**γ_c**	**$\gamma_{fct,eff}$**	**$1/\gamma_{fct,eff}$**	**γ_θ**
0.5	1.540	-0.024	-0.337	-0.504	-0.795	1.000	1.020	1.030	0.971	1.077
1.5	1.935	-0.023	-0.343	-0.503	-0.793	1.000	1.068	1.133	0.882	1.366
2	2.181	-0.023	-0.345	-0.502	-0.793	1.000	1.097	1.189	0.841	1.538

In the case where the effective depth of tension zone was h/2, the sensitivity factors for section thickness, concrete tensile strength and model uncertainty were only slightly affected by the change in reliability index (as evident in Table 6.12). A similar trend may be found for the theoretical partial safety factors where a small variation was experienced as the reliability index was increased. Concrete cover obtains sensitivity factors that increased in value by 19% and 31% for reliability indices 1.5 and 2 correspondingly as compared to the sensitivity factor obtained for a reliability index of 0.5. The same comparison being applied to the theoretical partial safety factors (with β = 0.5 as the base) of concrete cover showed an increase in value of 2% and 3% for β = 1.5 and 2 respectively. However, model uncertainty had increases in value of 29% and 47% for reliability indices 1.5 and 2 respectively, where β = 0.5 was the base of comparison – a comparable finding to where the $h_{c,eff}$ = 2.5(c + φ/2).

The demand in reinforcement increased by 24% and 39% for reliability indices 1.5 and 2 as compared to that which was required for a 0.5 reliability index. An increase in reliability index from 1.5 to 2 results in a 12% steel reinforcement. Once again, a comparable result to where $h_{c,eff}$ = 2.5(c + φ/2).

Table 6.12: Influence of Reliability Index on the Basic Variables of the EN 1992 End Restraint Crack Model (wlim = 0.2 mm, model uncertainty CoV = 0.3, $h_{c,eff}$ = h/2)

		Sensitivity Factors				Partial Factors				
β	**%As required**	**α_h**	**α_c**	**$\alpha_{fct,eff}$**	**α_θ**	**γ_h**	**γ_c**	**$\gamma_{fct,eff}$**	**$1/\gamma_{fct,eff}$**	**γ_θ**
0.5	1.532	-0.047	-0.098	-0.532	-0.840	1.000	0.996	1.033	0.968	1.077
1.5	1.906	-0.045	-0.117	-0.531	-0.838	1.001	1.015	1.143	0.875	1.394
2	2.135	-0.044	-0.128	-0.530	-0.837	1.001	1.027	1.201	0.832	1.580

Overall, a large increase in reinforcement was observed where the reliability index was increased from 0.5 to 2. This was particularly evident for the edge restraint case. Results for where the effective depth of the tension zone was either $2.5(c + \phi/2)$ or h/2 were comparable for both the edge and end restraint case. The above-mentioned observations were much greater than the EN 1992 load-induced cracking case (Retief, 2015) in which the amount of tension steel increased by 10% and 15% for $\beta = 1.5$ and 2 respectively (where $\beta = 0.5$ was set as a default value). Clearly, a change in the choice of reliability index of the EN 1992 restrained shrinkage crack model may be deduced to have a considerable effect on the cost of design. However, these increases in cost may be minor when compared to those required for structural failure where this serviceability limit state is not met. Further research into the cost of failure for the serviceability limit state is required; this should give clearer insight into what the target reliability index should be for liquid retaining structures.

6.3 Comparison of Results for Deterministic and Probabilistic Analysis

Comparisons of the reinforcement required to meet the considered crack width limits for the deterministic analysis and those obtained from the probabilistic analysis (for $\beta_t = 1.5$) were made. The crack width limits was varied (considering only crack width limits 0.3, 0.2 and 0.1 mm) and the section thickness was kept constant at 250 mm. The effective depth of tension zone, $h_{c,eff}$, was $2.5(c + \phi/2)$ for a cover of 40 mm and reinforcing bar diameter of 20 mm (this was also the variation of effective depth that was found to be limiting for most combinations of section thickness, concrete cover and reinforcing bar diameters). It may be observed that analysing the crack model deterministically (ignoring the stochastic nature of the input variables) would result in greater amounts of reinforcement being required for the crack width limit to be met. This was evident for both the 0.2 and 0.3 mm crack width limits considered in this analysis (referring to Table 6.13). The dominance held by the reinforcement requirements of the deterministic analysis in the case of the edge restraint condition was about 15% more than that of the probabilistic case and for end restraint there was a 2% increase in demand of steel reinforcing required than the probabilistic analysis for all the crack width limits considered. Those results obtained for the edge restraint condition are comparable to those obtained by Holický, Retief and Wium (2009) in which 15% more reinforcement was required to meet a 0.2 mm crack width limit using deterministic methods as opposed to a reliability based assessment for the EN 1992 tension load case.

Evidently, applying a probabilistic method of analysis provides a more economically viable design. This was apparent more so in the edge restraint case rather than the end restraint, where

the dominance held by the deterministic analysis was slight. This result suggests that, however more conservative the end restraint crack model may be to that of the edge restraint crack model, those reinforcement amounts calculated for crack limit satisfaction through the end restraint crack model produced results that were close to those required to meet reliability requirements.

Table 6.13: Comparison of Deterministic and Probabilistic Analysis for w_{lim} = 0.3, 0.2 and 0.1 mm ($h_{c,eff} = 2.5(c + \phi/2)$, h = 250 mm, Model Uncertainty CoV = 0.3 and β_t = 1.5)

Edge Restraint			
crack width limit (mm)	**Area Required/Face (mm^2)**		
	Deterministic	**Probabilistic**	**D/P**
0.3	1353	1215	1.11
0.2	2275	2020	1.13
0.1	7156	5928	1.21
End Restraint			
crack width limit (mm)	**Area Required/Face (mm^2)**		
	Deterministic	**Probabilistic**	**D/P**
0.3	1930	1890	1.02
0.2	2474	2430	1.02
0.1	3906	3811	1.02

This finding provides an interesting argument for the need of a more unified approach for restrained strain estimation as proposed by Bamforth (2010). Bamforth (2010) developed in his research a unified alternative means of estimating crack widths in which the restrained strain separated crack formation into two stages. Those parts of the overall restrained strain coming from the first stage of crack formation were based on the formula for the end restrained strain under EN 1992-3: 2006. Further, Bamforth (2010) found in his investigation of the EN 1992 crack model that many of the assumptions made in the development of the edge restraint crack model were not sufficiently robust. It seems that perhaps the development of a crack model that better reflects the occurrence of cracks in practice, as Bamforth (2010) attempted to do, may in fact lead to a model that is more compliant to South African reliability requirements for liquid retaining structures. Further research into a model of crack formation that is more reflective of observations made in practice and its reliability in the South African context is needed. This may be further corroborated by an investigation into the model uncertainty of the EN 1992 restrained shrinkage crack model (particularly for the edge restraint case).

6.4 Conclusion

The relative influence held by each random variable on the reliability of the restrained strain crack models was considered. The relative influence was measured through a reverse FORM calculation

of the crack models. Also, the theoretical partial safety factors of each random variable considered in the analysis were calculated. This extended reliability analysis of the EN 1992 restrained strain crack model provided with it greater insight into the ways in which EN 1992 may be adjusted for compliance to South African reliability requirements. The following observations were made from this sensitivity analysis:

Sensitivity factors indicate which basic variable is most influential on the reliability of the model thus indicating to which random variable applying a partial factor to would have the most effect on reliability of the model.

- Model uncertainty was found to be the most influential random variable for both the edge and end restraint crack model. Model uncertainty was also found to be comparable for the different effective depths considered ($h_{c,eff} = 2.5(c + \varphi/2)$ and $h/2$). Hence, applying a partial factor to this variable could make the most impact on achieving the desired reliability.
- The major difference was found with the relative influence of the concrete cover where the effective depth of tension area ($h_{c,eff}$) was different. Where the effective depth was $2.5(c + \varphi/2)$, the concrete cover's relative influence was notably greater. This was true for both edge and end restraint. It was then concluded that concrete cover was the variable that influenced the difference in reliability generated by the effective depth of tension area for both end and edge restraint.

The partial factor is essentially a factor which scales the nominal value of an input variable to the value of the variable at the failure point of the performance function. A larger partial factor indicates that there is a larger variation from nominal to failure point.

- Model uncertainty was found to require the largest theoretical partial safety factor across all models considered.
- The edge and end restraint crack models were found to require comparable theoretical partial factors for the random variables of the restrained strain crack model. This indicates that the same partial factor may potentially be applied to the same random variable used in either the edge or end restraint crack model.
- All models obtained theoretical partial factors for section thickness that were $\gamma_h = 1$ or close to 1 (both variations of edge and end restraint crack model)
- The choice of reliability index has a significant effect on the design of liquid retaining structure. This was particularly true for the edge restraint case.

The knowledge gained from the sensitivity analysis may then be used towards the full calibration of the EN 1992 restrained shrinkage crack model. Unquestionably, a full calibration involves

more than what was carried out for this research. Particularly since this research looks at a specific configuration of a liquid retaining structure (LRS), with the parameters varied around this particular set up – not considering at a large scope of liquid retaining structures and performance applications. However, taking the above findings into consideration, the observations made from this analysis may be used as a pilot towards a complete calibration for the EN 1992 restrained strain crack model.

Chapter 7: Final Conclusions

7.1 Introduction

The EN 1992-3:2006 and EN 1992-1-1:2004 design code have come to replace the corresponding codes withdrawn of BS 8007:1987 and BS 8110-2:1985 (which South African engineers had conventionally adopted). Currently, with South Africa having not yet developed and implemented its own equivalent code, South African designers are investigating the adoption of the EN 1992 design code. An investigation into the reliability performance of the EN 1992 crack model as applied in the South African context was undertaken in this thesis. Understanding the reliability performance of the EN 1992 crack model as compared to those reliability requirements stipulated in the South African codes provides an opportunity for improvements of the design code for use in the South African environment. Research into current South African practice, with a review of the relevant British and Eurocode was undertaken. This was followed by calculations conducted to quantify the implications of a change in code on the design of LRS under South African conditions. Background knowledge of the reliability theory was also obtained with a compilation of relevant parts presented herein– these tasks consequently fed into the reliability analysis conducted in this dissertation. Important findings made through the above mentioned undertakings are summarised in the subsequent text.

7.2 Literature Review

A review of current practices for liquid retaining structure design returned information on the typical configurations and design selections that could be used in both the deterministic and reliability based analyses of this research. Past research on liquid retaining structure design have highlighted the dominance held by the cracking serviceability limit state as compared to the ultimate limit state (Mcleod, 2013; Holický, Reteif and Wium, 2009). This substantiated the need to conduct an investigation on the serviceability limit state, especially where a foreign code was being applied in the South African environment.

7.3 Parametric study

A parametric study was conducted with the intent to both compare the BS 8007 and relevant parts of BS 8110-2 crack models with that of EN 1992 and establish a reasonable representative liquid retaining structure upon which the reliability assessment would be assessed. Additionally, variables to which the EN 1992 crack model were found to be most sensitive were revealed as a

by-product of the parametric study- the influence of these variables on the crack model were then assessed in a reliability-based assessment of the crack model. Those key identified variables were found to include the following: concrete cover (c), the reinforcing bar diameter to effective steel content ratio ($\varphi/\rho_{p,eff}$), the effective tension area ($A_{c,eff}$), section thickness (h), the reinforcement area (A_s) as well as the restraint degree (R).

7.4 FORM analysis of EN 1992

The influence of concrete cover, the reinforcing bar diameter to effective steel content ratio, section thickness, restraint factor and model uncertainty were measured against increases in the steel reinforcement to gross concrete cross-sectional area ratio (which had been found in previous research to be a particularly influential variable for reinforced concrete structures). The reliability of the crack model would decrease where concrete cover, the $\varphi/\rho_{p,eff}$ ratio, restraint factor and model uncertainty were increased. This was found to be true for both edge and end restraint conditions. Section thickness was found to have the opposite effect on the reliability of the crack model. The difference in reliability amounting from the effective depth ($h_{c,eff}$) of tension zone was found to be slight for both the edge and end restraint crack models. The end restraint crack model was uncovered to be the more conservative of the two restrained shrinkage crack models– requiring more reinforcement to achieve the target reliability index. The restraint factor was found to have a significant influence on the reliability performance of the edge restraint crack model. Increases in restraint factor was also found to decrease the reliability of edge restraint crack model. Data on the restraint factor was found to be limited, thus further research is recommended for this parameter.

7.5 Sensitivity Analysis

The relative influence, or otherwise sensitivity factor, of each random variable may be measured through a sensitivity analysis of the reliability models. Model uncertainty was found to bear the most influence on both the edge and end restraint crack models, thus applying a partial factor to this variable would bring about the most effective adjustments (of the all random variables accounted for in this analysis of the EN 1992 crack model) for compliance of South African reliability performance requirements. Understandably, model uncertainty's theoretical partial factors were found to be the largest amongst all the random variables considered. Moreover, both the edge and end restraint crack models (containing both $h_{c,eff} = h/2$ and $2.5(c + \varphi/2)$) returned theoretical partial factors for section thickness (h) that were either 1 or close to 1.

The difference in reliability between crack models with effective depths of tension zone $h_{c,eff}$ = h/2 and 2.5(c + φ/2) was primarily attributed to the effects of concrete cover.

A comparison of the edge and end restraint crack models found that theoretical partial factors required for both restraint conditions were quite comparable. This indicates that the same partial factor may be used irrespective of the restraint condition being considered- ideal for the simple application of a fully calibrated design standard.

An assessment of the implications of a change in the target reliability index was also carried out. Target reliability indices 0.5, 1.5 and 2 were considered. It was found that significant increases in reinforcement were required for increases in the stipulated target reliability index. This was particularly evident for the edge restraint case.

7.6 Deterministic Versus Probabilistic Approach

A comparison between the reinforcing areas required for crack width limit satisfaction obtained by means of deterministic and reliability based analysis was conducted. It was determined in this exercise that reliability-based calculations returned more economically viable designs. The demand of the deterministic calculation was experienced more so in the edge restraint case. The amount of reinforcement required, found deterministically, for specified crack limit compliance for the end restraint crack model were close to those required to meet the target reliability index. This uncovering provides an interesting argument for a more unified approach to crack width estimation for cracks due to restrained deformation, particularly for application in the South African context. Perhaps an adoption of a crack model that lends itself more so towards the EN 1992 end restraint crack model would result in a crack model that is more conducive to local reliability requirements. This also highlights the need to further investigate the model uncertainty.

7.7 Recommendations

- As mentioned earlier, further research is required on the statistical parameters and characteristics of the restraint factor. Namely, more information is required on the mean, standard deviation and probability distribution that best describe the restraint factor.
- In view of the considerable influence held by model uncertainty on the crack models of both edge and end restraint, more information is required on the model uncertainty of the cracking model for reinforced concrete structures.

- It may be that those crack width limits stipulated by EN 1992 may be stricter than necessary for South African design requirements. Further research is required on crack width limits which are better suited to South African conditions and for South African design practices, especially given their influence on the reliability of the crack model.
- Investigations into a crack model that is more reflective of the formation of cracks in practice may be necessary.

By way of this investigation into the reliability of the EN 1992 crack model, South African engineers are presented with the opportunity of selecting those combinations of variables for which reliability was found to be satisfied. Alternatively, the identification of those variables found to bear the most influence on the reliability of the EN 1992 crack model provide an indication of where adjustments may be most effectively made for compliance to South African safety requirements. Taking the above findings into consideration, a full calibration may thus be attempted for a larger range of liquid retaining structure configurations and design conditions (i.e. considering a larger scope of LRS)– subsequently improving the use of the EN 1992 crack model for restrained deformation in South Africa.

References

1) Addis, B. & Owens, G., eds., 2001. *Fulton's concrete technology.* 8th ed. Midrand: Cement and Concrete Institute.

2) American Concrete Institute, 2002. *ACI 207.2R-95:2002: effect of restraint, volume change, and reinforcement of cracking of mass concrete (reported by ACI committee 207).* American Concrete Institute (ACI).

3) Ang, A. H-S. & Tang, W.H., 1984. *Probability concepts in engineering planning and design: decision, risk and reliability.Volume 2- decision risk and reliability*. John Wiley & Sons.

4) Antona, B. & Johansson, R., 2011. *Crack control of concrete structures.* MSc thesis, Chalmers University Of Technology.

5) Bamforth, P. B., 2007. *Early-age thermal crack control in concrete.* London: CIRIA.

6) Bamforth, P. B., Shave, J. & Denton S., 2011. *Bridge Design to Eurocodes*. [e-book] Thomas Telford Limited. Available through: Iinstitute of Civil Engineers (ICE) Virtual Library. Available at: http://www.icevirtuallibrary.com/doi/abs/10.1680/BDTE.41509.0019

7) Bamforth, Dr. P., Denton, Dr. S. & Shave, Dr. J., 2010. *The development of a revised unified approach for the design of reinforcement to control cracking in concrete resulting from restrained contraction.* Institute of Civil Engineers.

8) Barnardo-Viljoen C., Mensah K.K., Retief, J.V., Wium, J.A., Van Zijl GPAG., 2014. *Background to the Draft SA National Standard for the Design of Water Retaining Structures.* Concrete/Beton

9) Beeby, A.W. & Narayanan, R.S., 2005. *Designer's guide to eurocode 2: design of concrete structures.* London: Author and Thomas Telford Limited.

10) Bertagnoli, G., Gino, D., Mancini, G., 2016. Effect of endogenous deformations in composite bridges. In: Marcinowski, J., ed. *Proceedings of the XIII International Conference on Metal Structures (CMS2016).* Zielona Góra, Poland, 15-17 June 2016. London: Taylor & Francis Group, pp. 287-298.

11) Bhatt, P., MacGinley, T. & Choo S., 2006. *Reinforced concrete design theory and examples.* 3th ed. Abingdon: Taylor and Francis.

12) British Standards Institute, 1984. BS 5400-4:1984. *Steel, concrete and composite bridges-part 4: code of practice for design of concrete bridges.*. London: British Standards Institute (BSI).

13) British Standards Institute, 1985. BS 8110-2:1985. *Structural use of concrete- part 2: code of practice for special circumstances.* London: British Standards Institute (BSI).

14) British Standards Institute, 1987. BS 8007:1987. *Design of concrete structures for retaining aqueous liquids.*London: British Standards Institute (BSI).

15) Caldentey, A.P., Peiretti, H. C., Iribarren, J.P. & Soto, A.J., 2013. Cracking of RC members revisited: influence of cover, $\varphi / \rho_{s,ef}$ and stirrup spacing– an experimental and theoretical study. *Structural Concrete.* 14(1), pp. 69-78.

16) Caldentey, A. P., 2005. *Cracking of reinforced concrete. is φ/ρ_{eff} a relevant parameter? investigating a. beeby's statement.* [pdf] Polytechnic University of Madrid (UPM). Availabe at:

http://hormigon.mecanica.upm.es/files/PDF/TG41/TG4.1-TestingBeebyStatement.pdf

17) Centre of Construction Technology Research, 2000. *Crack Control of Beams. Part 1: AS 3600 Design.* [pdf] One Steel Reinforcing and the University of Western Sydney. Available at:

http://www.reinforcing.com.au/~/media/OneSteel%20Reinforcing/Case%20Study%20PDFs/Technical%20Resources%20PDFs/Crack_Control_of_Beams_Design_Booklet.pdf

18) Climate Change Knowledge Portal, 2009. *Average monthly Temperature and Rainfall for South Africa from 1900-2012.* [online] Available at: http://sdwebx.worldbank.org/climateportal/index.cfm?page=country_historical_climate&ThisRegion=Africa&ThisCCode=ZAF

19) Croce, P., Diamantidis, D., & Vrouwenvelder, T., 2012. Structural reanalysis. In: Diamantidis D. & Milan, H. eds. *Innovative methods for the assessment of existing structures.* Prague: Czech Technical University, pp. 45-50.

20) Edvardsen, C., 1999. Water permeability and autogenous healing of cracks in concrete. *ACI Materials Journal*, 96(4). pp. 448-454.

21) Eligehausen, R., Malle, R. & Rehm, G., 1976. *Rissverhalten von Stahlbetonkörpern bei Zugbeanspruchung*. s.n.

22) European Committee For Standardization, 2004. EN 1992-1-1:2004. *Eurocode 2: design of concrete structures - part 1-1 : general rules and rules for buildings.* CEN.

23) European Committee For Standardization, 2006. EN 1992-3:2006. *Eurocode 2 - design of concrete structures - part 3: liquid retaining and containment structures.* CEN.

24) European Concrete Platform ASBL, 2008. *Eurocode 2 commentary.* [online] Brussels: European Concrete Platform ASBL. Available at: http://www.europeanconcrete.eu/images/stories/publications/Commentary_to_Eurocode.pdf

25) Gilbert, R. I., 2016. Control of Cracking Caused by Early-Age Deformation in Edge Restrained Concrete Walls. In: Zingoni, A., ed. *Proceedings of the 6th International Conference on Structural Engineering Mechanics and Computation (SEMC 2016).* Cape Town, South Africa, 5-7 September 2016. London: Taylor 7 Francis Group, pp. 539-540.

26) Green, A. E. & Bourne A.J., 1972. *Reliability Technology.*Wiley.

27) Greensmith, C.G., 2005. *The effects of cement extenders and water binder ratio on the heat evolution characteristics of concrete.* MSc thesis, University of the Witwatersrand.

28) Harrison, T. A., 1981. *Early-age thermal crack control in concrete.* London: CIRIA.

29) Hartl, G., 1977. *Die Arbeitslinie eingebetteter Stähle bei Erst- und Kurzzeitbelastung*. Universität Innsbruck.

30) Highways England, 1987. Designers Manual for Roads and Bridges (DMRB)) Volume 1, Section 3 Part 14- BA 24/87. *Early thermal cracking of concrete.* Highways England. Available at: http://www.standardsforhighways.co.uk/ha/standards/dmrb/vol1/section3.htm

31) Highways England, 1987. Designers Manual for Roads and Bridges (DMRB) Volume 1 section 3 Part 14- HA BD 28/87. *Early thermal cracking of concrete.* Highways England. Available at: http://www.standardsforhighways.co.uk/ha/standards/dmrb/vol1/section3.htm

32) Holicky, M., 2007. Probabilistic optimisation of concrete cover designed for durability. In: International Congress, *Concrete: construction's sustainable option*. Dundee, September 2007. International Congress.

33) Holicky, M., 2009. *Reliability analysis for structural design.* Stellenbosch: Sun Media Stellenbosch.

34) Holicky, M., Retief, J., Wium, J., 2009. Probabilistic Design for Cracking of Concrete Structures. In: Vrijling, H., van Gelder, P. & Proske, D., eds. *Proceedings of the 7th international probabilistic workshop.* Delft, the Netherlands, 2009. Dresden, Germany: Proske, D. pp. 87-98.

35) Holický, M., Retief J. & Wium J., 2010. Partial factors for selected reinforced concrete members: background to a revision of SANS 10100-1. *Journal of The South African Iinstitution Of Civil Engineering*, 56(1), pp. 36-44.

36) Holický, M. & Marková, J., 2012. Probablistic assessment. In: Diamantidis D. & Milan, H. eds. *Innovative methods for the assessment of existing structures.* Prague: Czech Technical University, pp. 51-75.

37) Joint Committee on Structural Safety (JCSS), 2000. *Probabilistic model code part 3: material properties.* [pdf] JCSS. Available at: http://www.jcss.byg.dtu.dk/Publications/Probabilistic_Model_Code

38) Joint Committee on Structural Safety (JCSS), 2001. *Probabilistic model code part 1: basis of design.* [pdf] JCSS. Available at: http://www.jcss.byg.dtu.dk/Publications/Probabilistic_Model_Code

39) Jones, Dr. T., 2008. Eurocode 2- Design of concrete structures - part 3: liquid retaining and containment structures. *Dissemination of information workshop.* Brussels, 18-20 February.

40) Kamali, A.Z., Svedholm C. & Johansson, M., 2013. *Effects of restrained thermal strains in transversal direction of concrete slab frame bridges.* Stockholm: Kamali A.Z., Svedholm C., Pacoste C.

41) Kaethner, S., 2011. Have EC2 Cracking Rules Advanced the Mystical Art of Crack Width Prediction?. *The Structural Engineer*, 89(19), pp. 14-22.

42) Kheder, G.F., 1997. A New Look at the Control of Volume Change Cracking of Base Restrained Concrete Walls. *ACI Structural Journal*. 94(3), pp. 262-271.

43) Mans, R. 2012. *Will autogenous healing Seal a Concrete Crack with a Surface Width of 0.2mm?* BSc, University of Kwa-Zulu Natal.

44) McLeod, C., Wium, J. & Retief, J.V., 2012. Reliability model for cracking in South African reinforced concrete water retaining structures. In: Moormann, C., Huber, M., Proske, D., eds. *Proceedings of the 10th International Probabilistic Workshop.* Stuttgart, 15-16 November 2012. Institute of Geotechnical Engineering, University of Stuttgart, Germany, pp. 141-156.

45) McLeod, C., 2013. *Investigation into cracking in reinforced concrete water-retaining structures.* MSc thesis. Stellenbosch University.

46) McLeod, C.H., Retief, J.V., Wium, J.A., 2013. Reliability of EN 1992 crack model applied to South African water retaining structures. In: Zingoni, A., ed. *Proceedings of the 5th International Conference on Structural Engineering Mechanics and Computation (SEMC 2013)*. Cape Town, South Africa, 2-4 September 2013. London: Taylor & Francis Group, pp. 553-555.

47) McLeod, C., Viljoen, C., Retief, J., 2016. Quantification of Model Uncertainty of EN 1992 Crack Width Prediction Model. In: Zingoni, A., ed. *Proceedings of the 6th International Conference on Structural Engineering Mechanics and Computation (SEMC 2016).* Cape Town, South Africa, 5-7 September 2016. London: Taylor & Francis Group, pp. 475-476.

48) Mosley, B., Bungey, J. & Hulse, R., 2012. *Reinforced concrete design to eurocode 2.* Seventh Edition. Hampshire: Macmillan Publishers Limited.

49) Nesset, J. & Skoglund, S., 2007. *Reinforced concrete subjected to restraint forces.* MSc thesis, Chalmers University of Technology.

50) Nowak, A. S. & Collins, K.R., 2000. *Reliability of structures.* Mcgraw Hill Companies, Inc.

51) Owens, G., ed., 2013. *Fundamentals of Concrete.* Third Edition. Midrand, South Africa: The Concrete Institute.

52) Quan, Q. & Gengwei, Z., 2002. Calibration of reliability index of rc beams for serviceability limit state of maximum crack width. *Reliability engineering and system safety*. 75(3), pp. 359-366.

53) Rehm, G. & Rüsch, H., 1963. *Versuche mit Betonformstählen*. Deutscher Ausschuss für Stahlbeton Heft.

54) Retief, J. V., 2015. *Contributions to the Implementation of the Principles of Reliability to the Standardized Basis of Structural Design*. PhD thesis, Stellenbosch University.

55) Saassouh, B. & Lounis, Z., 2012. Probabilistic modeling of chloride-induced corrosionin concrete structures using First and Second Order reliability methods. *Cement and Concrete Composites,* Volume 34, pp. 1082-1093.

56) Sajedi, S., Razavizadeh, A., Minaii, Z., Ghassemzadeh, F., Shekarchi, M., 2011. A rational method for calculation of restrained shrinkage stresses in repaired concrete members. In: Grantham, M., Mechtcherine, V., Schneck, U., eds. *4th international conference on concrete repair*. Dresden, Germany, 26-28 September 2011. London: Taylor & Francis Group.

57) South African Bureau of Standards, 2000. SANS 10100-1:2000. *The structural use of concrete: part 1: design.* Pretoria: SABS.

58) South African Bureau of Standards, 2011. SANS 10160-1:2011. *Basis of structural design and actions for buildings and industrial structures, part 1: basis of structural design.* Pretoria: SABS.

59) South African Bureau of Standards, SANS 2394:2004. *General procedures for loading in buildings and industrial structures.* SABS.

60) SouthAfrica.info, 2015. *South Africa's weather and climate*. [online] Brand South Africa. Available at: http://www.southafrica.info/travel/advice/climate.htm#.VcMnkfyUfGJ#ixzz3i1d8Rty3

61) Wium, J., 2008. Concrete code. *Structural eurocode summit.* Pretoria, South Africa, 8 Holicky, Retief and Wium (2009) February.

62) Wium, J., Retief J. V. & Viljoen C. B., 2014. Lessons from development of design standards in South Africa. In: International Association for Bridge and Structural Engineering (IABSE), *37th Madrid IABSE Symposium 2014*. Madrid, Spain, 3-5 September, 2014. Madrid, Spain: International Association for Bridge and Structural Engineering, pp. 3198-3205.

63) Wu, W., Lo, S-C R. & Wang, X.H., 2011. An objective approach to reliability-based risk assessment and mitigation for coastal infrastructure development. *Labour and Management in Development Journal,* [e-journal] Volume 2, pp. 0-16. Available through: National Library of Australia website http://www.nla.gov.au/openpublish/index.php/lmd/article/view/2223/2653

64) Yi, S., Hyun, T., & Kim, J., 2011. The effects of hydraulic pressure and crack width on water permeability of penetration crack- induced concrete. *Construction and building materials.* Volume 25, pp. 2576-2583.

65) Zahalan, R., 2010. *Reliability-Based Analysis of Crack Control in Reinforced Concrete Beams.* MSc thesis, The State University of New Jersey.

66) Zhao, Y-G. & Ono, T., 1999. A general procedure for first/second-order reliability method (FORM/SORM). *Structural Safety.* 21(2), pp. 95-112.

67) Zingoni, A., 2008. The case for the eurocodes for South Africa. *Structural eurocode summit.* Pretoria, South Africa, 8 February.

Appendix

Appendix A: Deterministic Parametric Study

Edge Restraint **EN 1992**	
Input (Constants)	
bar diameter, Φ	16
ρ_{ef}=ρ_{crit}=$f_{ctm(t)}/f_{yk}$ = 1.73/450= 0.384%	0.00384
Φ/ρ_{eff} =	4166.67
k_1	0.8
k_2	1
cover (mm)	40
R	0.5
T_1 (°C)	15
T_2(°C)	23
α_T (με/°C)	14
ε_{ca} (με)	33
ε_{cd} (με)	220
ε (με)	392.5
ε (με)	0.00039
A = $h_{e,ef}$ x 1000	
$h_{e,ef}$ is lesser of h/2 or 2.5(c + Φ/2)	
reinforcement spacing (mm)	75
b (mm)	250
h (mm)	1000
BS 8007	
$f_{ctm\ (t)}$ Mpa	1.73
f_b (deformed bars, type 2) Mpa	2.4
φ, mm	16

Figure A.1: Edge Restraint Crack Model Inputs for Deterministic Analysis

End Restraint	
Eurocode 2 restraint strain	
$(\varepsilon_{sm} - \varepsilon_{cm})$ =	
concrete grade (Mpa)	C30/37
section height (mm)	1000
kc	1
k	1
k	0.65
$f_{ctm(28)}$ (Mpa)	2.9
E_s (Gpa)	200
$E_{cm(t)}$	28
α_e	7.14286
bar diameter, Φ	16
bar spacing (mm)	75
A_s (mm^2) / face	804.248
A_{ct} (mm^2)/ face	200000
$\rho = A_s / A_{ct}$	0.00402
$1+1/\alpha_e \rho$	35.8151
Crack Spacing	
$S_{r,\,max} = 3.4c + 0.425k_1k_2\Phi/\rho_{eff}$	
c, cover	40
k_1 (for high strength bonds)	0.8
k_2 (for pure tension)	1
Φ	16
A_s	804.248
$A_{c,eff}$	
ρeff	
Φ/ρeff	
BS 8007 restraint strain	
$\varepsilon = R\,\alpha\,(T_1 + T_2)$	
R	0.5
thermal expansion, α	14
T_1, (°C)	15
T_2 , (°C)	23
Crack Spacing	
Smax = (fct)/fb x Φ/2ρ	
f_{ctm} (Mpa)	1.73
f_b (Mpa), deformed bars- type 2	2.4
Φ (mm)	16

Figure A.2: End Restraint Crack Model Inputs for Deterministic Analysis

BS 8007

cover (mm)	Φ, bar dia.	A_s / face	h/2	A (area/ face, mm^2)	ρ	φ/ρ (mm)	φ/2ρ (mm)	$S_{r,max}$ (mm)
40	16	804.24772	125	125000	0.006433982	2486.796	1243.39799	896.2827199
50	16	804.24772	125	125000	0.006433982	2486.796	1243.39799	896.2827199
60	16	804.24772	125	125000	0.006433982	2486.796	1243.39799	896.2827199
70	16	804.24772	125	125000	0.006433982	2486.796	1243.39799	896.2827199
80	16	804.24772	125	125000	0.006433982	2486.796	1243.39799	896.2827199
100	16	804.24772	125	125000	0.006433982	2486.796	1243.39799	896.2827199

EN 1992

			$h_{e,ef}$					
cover (mm)	Φ, bar dia.	A_s / face	h/2	2.5(c + Φ/2)	$A_{c,eff}$ (area/ face, mm^2)	ρeff	Φ/ρeff (mm)	$S_{r,max}$ (mm)
40	16	804.24772	125	120	120000	0.0067021	2387.32415	947.6902098
50	16	804.24772	125	145	125000	0.006434	2486.79599	1015.510635
60	16	804.24772	125	170	125000	0.006434	2486.79599	1049.510635
70	16	804.24772	125	195	125000	0.006434	2486.79599	1083.510635
80	16	804.24772	125	220	125000	0.006434	2486.79599	1117.510635
100	16	804.24772	125	270	125000	0.006434	2486.79599	1185.510635

Figure A.3: BS 8007 and EN 1992 Data for Varying Concrete Cover Value

BS 8007

cover (mm)	Φ, bar dia.	A_s / face	h/2	$A_{c,eff}$ (area/ face, mm^2)	ρ	φ/ρ (mm)	φ/2ρ (mm)	$S_{r,max}$ (mm)	ε	w_{max}
40	16	804.2477	125	125000	0.006433982	2486.795986	1243.397993	896.2827199	0.000266	0.238411203
40	20	1256.637	125	125000	0.010053096	1989.436789	994.7183943	717.0261759	0.000266	0.190728963
40	25	1963.495	125	125000	0.015707963	1591.549431	795.7747155	573.6209407	0.000266	0.15258317
40	32	3216.991	125	125000	0.025735927	1243.397993	621.6989965	448.1413599	0.000266	0.119205602
40	40	5026.548	125	125000	0.040212386	994.7183943	497.3591972	358.513088	0.000266	0.095364481

EN 1992

			he,ef							
cover (mm)	Φ, bar dia.	As	h/2	2.5(c + Φ/2)	Ac,eff (area/ face, mm^2)	ρp, eff	Φ/ρp,eff	Sr,max (mm)	wmax	ρp, eff (%)
40	16	804.2477	125	120	120000	0.006702064	2387.324146	947.6902098	0.371968407	85.64931888
40	20	1256.637	125	125	125000	0.010053096	1989.436789	812.4085081	0.318870339	83.25965341
40	25	1963.495	125	131.25	125000	0.015707963	1591.549431	677.1268065	0.265772272	79.91513573
40	32	3216.991	125	140	125000	0.025735927	1243.397993	558.7553176	0.219311462	75.6601869
40	40	5026.548	125	150	125000	0.040212386	994.7183943	474.2042541	0.18612517	71.32037538

Figure A.4: BS 8007 and EN 1992 Data for Varying $\varphi/\rho_{p,eff}$ ratio

Edge Restraint
EN 1992

			$h_{c,eff}$								
h	A_{ct} / face	ρ	h/2	2.5(c + ϕ/2)	$A_{c,eff}$ (area/ face, mm^2)	A_s	$\rho_{p,eff}$	$\varphi/\rho_{p,eff}$ (mm)	$S_{r,max}$ EN 2	ε (EN 2)	W_{max} EN 2
250	125000	0.001	125	120	120000	125	0.00104167	15360	5358.4	0.0003925	2.103172
250	125000	0.002	125	120	120000	250	0.00208333	7680	2747.2	0.0003925	1.078276
250	125000	0.003	125	120	120000	375	0.003125	5120	1876.8	0.0003925	0.736644
250	125000	0.004	125	120	120000	500	0.00416667	3840	1441.6	0.0003925	0.565828
250	125000	0.005	125	120	120000	625	0.00520833	3072	1180.48	0.0003925	0.4633384
250	125000	0.006	125	120	120000	750	0.00625	2560	1006.4	0.0003925	0.395012
250	125000	0.007	125	120	120000	875	0.00729167	2194.285714	882.0571429	0.0003925	0.346207429
250	125000	0.008	125	120	120000	1000	0.00833333	1920	788.8	0.0003925	0.309604
250	125000	0.009	125	120	120000	1125	0.009375	1706.666667	716.2666667	0.0003925	0.281134667
250	125000	0.01	125	120	120000	1250	0.01041667	1536	658.24	0.0003925	0.2583592
250	125000	0.011	125	120	120000	1375	0.01145833	1396.363636	610.7636364	0.0003925	0.239724727
250	125000	0.012	125	120	120000	1500	0.0125	1280	571.2	0.0003925	0.224196
250	125000	0.013	125	120	120000	1625	0.01354167	1181.538462	537.7230769	0.0003925	0.211056308

			$h_{c,eff}$								
h	A_{ct} / face	ρ	h/2	2.5(c + ϕ/2)	$A_{c,eff}$ (area/ face, mm^2)	A_s	$\rho_{p,eff}$	$\varphi/\rho_{p,eff}$ (mm)	$S_{r,max}$ EN 2	ε (EN 2)	W_{max} EN 2
300	150000	0.001	150	120	120000	150	0.00125	12800	4488	0.0003925	1.76154
300	150000	0.002	150	120	120000	300	0.0025	6400	2312	0.0003925	0.90746
300	150000	0.003	150	120	120000	450	0.00375	4266.666667	1586.666667	0.0003925	0.622766667
300	150000	0.004	150	120	120000	600	0.005	3200	1224	0.0003925	0.48042
300	150000	0.005	150	120	120000	750	0.00625	2560	1006.4	0.0003925	0.395012
300	150000	0.006	150	120	120000	900	0.0075	2133.333333	861.3333333	0.0003925	0.338073333
300	150000	0.007	150	120	120000	1050	0.00875	1828.571429	757.7142857	0.0003925	0.297402857
300	150000	0.008	150	120	120000	1200	0.01	1600	680	0.0003925	0.2669
300	150000	0.009	150	120	120000	1350	0.01125	1422.222222	619.5555556	0.0003925	0.243175556
300	150000	0.01	150	120	120000	1500	0.0125	1280	571.2	0.0003925	0.224196
300	150000	0.011	150	120	120000	1650	0.01375	1163.636364	531.6363636	0.0003925	0.208667273
300	150000	0.012	150	120	120000	1800	0.015	1066.666667	498.6666667	0.0003925	0.195726667
300	150000	0.013	150	120	120000	1950	0.01625	984.6153846	470.7692308	0.0003925	0.184776923

			$h_{c,eff}$								
h	A_{ct} / face	ρ	h/2	2.5(c + ϕ/2)	$A_{c,eff}$ (area/ face, mm^2)	A_s	$\rho_{p,eff}$	$\varphi/\rho_{p,eff}$ (mm)	$S_{r,max}$ EN 2	ε (EN 2)	W_{max} EN 2
350	175000	0.001	175	120	120000	175	0.00145833	10971.42857	3866.285714	0.0003925	1.517517143
350	175000	0.002	175	120	120000	350	0.00291667	5485.714286	2001.142857	0.0003925	0.785448571
350	175000	0.003	175	120	120000	525	0.004375	3657.142857	1379.428571	0.0003925	0.541425714
350	175000	0.004	175	120	120000	700	0.00583333	2742.857143	1068.571429	0.0003925	0.419414286
350	175000	0.005	175	120	120000	875	0.00729167	2194.285714	882.0571429	0.0003925	0.346207429
350	175000	0.006	175	120	120000	1050	0.00875	1828.571429	757.7142857	0.0003925	0.297402857
350	175000	0.007	175	120	120000	1225	0.01020833	1567.346939	668.8979592	0.0003925	0.262542449
350	175000	0.008	175	120	120000	1400	0.01166667	1371.428571	602.2857143	0.0003925	0.236397143
350	175000	0.009	175	120	120000	1575	0.013125	1219.047619	550.4761905	0.0003925	0.216061905
350	175000	0.01	175	120	120000	1750	0.01458333	1097.142857	509.0285714	0.0003925	0.199793714
350	175000	0.011	175	120	120000	1925	0.01604167	997.4025974	475.1168831	0.0003925	0.186483377
350	175000	0.012	175	120	120000	2100	0.0175	914.2857143	446.8571429	0.0003925	0.175391429
350	175000	0.013	175	120	120000	2275	0.01895833	843.956044	422.9450549	0.0003925	0.166005934

			$h_{c,eff}$								
h	A_{ct} / face	ρ	h/2	2.5(c + ϕ/2)	$A_{c,eff}$ (area/ face, mm^2)	A_s	$\rho_{p,eff}$	$\varphi/\rho_{p,eff}$ (mm)	$S_{r,max}$ EN 2	ε (EN 2)	W_{max} EN 2
400	200000	0.001	200	120	120000	200	0.00166667	9600	3400	0.0003925	1.3345
400	200000	0.002	200	120	120000	400	0.00333333	4800	1768	0.0003925	0.69394
400	200000	0.003	200	120	120000	600	0.005	3200	1224	0.0003925	0.48042
400	200000	0.004	200	120	120000	800	0.00666667	2400	952	0.0003925	0.37366
400	200000	0.005	200	120	120000	1000	0.00833333	1920	788.8	0.0003925	0.309604
400	200000	0.006	200	120	120000	1200	0.01	1600	680	0.0003925	0.2669
400	200000	0.007	200	120	120000	1400	0.01166667	1371.428571	602.2857143	0.0003925	0.236397143
400	200000	0.008	200	120	120000	1600	0.01333333	1200	544	0.0003925	0.21352
400	200000	0.009	200	120	120000	1800	0.015	1066.666667	498.6666667	0.0003925	0.195726667
400	200000	0.01	200	120	120000	2000	0.01666667	960	462.4	0.0003925	0.181492
400	200000	0.011	200	120	120000	2200	0.01833333	872.7272727	432.7272727	0.0003925	0.169845455
400	200000	0.012	200	120	120000	2400	0.02	800	408	0.0003925	0.16014
400	200000	0.013	200	120	120000	2600	0.02166667	738.4615385	387.0769231	0.0003925	0.151927692

			$h_{c,eff}$								
h	A_{ct} / face	ρ	h/2	2.5(c + ϕ/2)	$A_{c,eff}$ (area/ face, mm^2)	A_s	$\rho_{p,eff}$	$\varphi/\rho_{p,eff}$ (mm)	$S_{r,max}$ EN 2	ε (EN 2)	W_{max} EN 2
450	225000	0.001	225	120	120000	225	0.001875	8533.333333	3037.333333	0.0003925	1.192153333
450	225000	0.002	225	120	120000	450	0.00375	4266.666667	1586.666667	0.0003925	0.622766667
450	225000	0.003	225	120	120000	675	0.005625	2844.444444	1103.111111	0.0003925	0.432971111
450	225000	0.004	225	120	120000	900	0.0075	2133.333333	861.3333333	0.0003925	0.338073333
450	225000	0.005	225	120	120000	1125	0.009375	1706.666667	716.2666667	0.0003925	0.281134667
450	225000	0.006	225	120	120000	1350	0.01125	1422.222222	619.5555556	0.0003925	0.243175556
450	225000	0.007	225	120	120000	1575	0.013125	1219.047619	550.4761905	0.0003925	0.216061905
450	225000	0.008	225	120	120000	1800	0.015	1066.666667	498.6666667	0.0003925	0.195726667
450	225000	0.009	225	120	120000	2025	0.016875	948.1481481	458.3703704	0.0003925	0.17991037
450	225000	0.01	225	120	120000	2250	0.01875	853.3333333	426.1333333	0.0003925	0.167257333
450	225000	0.011	225	120	120000	2475	0.020625	775.7575758	399.7575758	0.0003925	0.156904848
450	225000	0.012	225	120	120000	2700	0.0225	711.1111111	377.7777778	0.0003925	0.148277778
450	225000	0.013	225	120	120000	2925	0.024375	656.4102564	359.1794872	0.0003925	0.140977949

			$h_{c,eff}$								
h	A_{ct} / face	ρ	h/2	2.5(c + ϕ/2)	$A_{c,eff}$ (area/ face, mm^2)	A_s	$\rho_{p,eff}$	$\varphi/\rho_{p,eff}$ (mm)	$S_{r,max}$ EN 2	ε (EN 2)	W_{max} EN 2
500	250000	0.001	250	120	120000	250	0.00208333	7680	2747.2	0.0003925	1.078276
500	250000	0.002	250	120	120000	500	0.00416667	3840	1441.6	0.0003925	0.565828
500	250000	0.003	250	120	120000	750	0.00625	2560	1006.4	0.0003925	0.395012
500	250000	0.004	250	120	120000	1000	0.00833333	1920	788.8	0.0003925	0.309604
500	250000	0.005	250	120	120000	1250	0.01041667	1536	658.24	0.0003925	0.2583592
500	250000	0.006	250	120	120000	1500	0.0125	1280	571.2	0.0003925	0.224196
500	250000	0.007	250	120	120000	1750	0.01458333	1097.142857	509.0285714	0.0003925	0.199793714
500	250000	0.008	250	120	120000	2000	0.01666667	960	462.4	0.0003925	0.181492
500	250000	0.009	250	120	120000	2250	0.01875	853.3333333	426.1333333	0.0003925	0.167257333
500	250000	0.01	250	120	120000	2500	0.02083333	768	397.12	0.0003925	0.1558696
500	250000	0.011	250	120	120000	2750	0.02291667	698.1818182	373.3818182	0.0003925	0.146552364
500	250000	0.012	250	120	120000	3000	0.025	640	353.6	0.0003925	0.138788
500	250000	0.013	250	120	120000	3250	0.02708333	590.7692308	336.8615385	0.0003925	0.132218154

Figure A.5: EN 1992 Data for Edge Restraint with Varying Section Thickness

End Restraint
EN 1992

				$h_{c,eff}$								
h	A_{ct} / face	ρ	$1+1/\alpha_e$ ρ	h/2	2.5(c + φ/2	$A_{c,eff}$ (area/ face, mm	A_s	$\rho_{p,eff}$	φ/$\rho_{p,eff}$ (mm	$S_{r,max}$ EN 2	ε (EN 2)	W_{max} EN 2
250	125000	0.001	141	125	120	120000	125	0.0010417	15360	5358.4	0.0073018	39.125889
250	125000	0.002	71	125	120	120000	250	0.0020833	7680	2747.2	0.0036768	10.100866
250	125000	0.003	47.6666667	125	120	120000	375	0.003125	5120	1876.8	0.0024685	4.6327914
250	125000	0.004	36	125	120	120000	500	0.0041667	3840	1441.6	0.0018643	2.6875543
250	125000	0.005	29	125	120	120000	625	0.0052083	3072	1180.48	0.0015018	1.772828
250	125000	0.006	24.3333333	125	120	120000	750	0.00625	2560	1006.4	0.0012601	1.2681838
250	125000	0.007	21	125	120	120000	875	0.0072917	2194.2857	882.05714	0.0010875	0.9592371
250	125000	0.008	18.5	125	120	120000	1000	0.0083333	1920	788.8	0.000958	0.7556986
250	125000	0.009	16.5555556	125	120	120000	1125	0.009375	1706.6667	716.26667	0.0008573	0.614085
250	125000	0.01	15	125	120	120000	1250	0.0104167	1536	658.24	0.0007768	0.5113114
250	125000	0.011	13.7272727	125	120	120000	1375	0.0114583	1396.3636	610.76364	0.0007109	0.4341776
250	125000	0.012	12.6666667	125	120	120000	1500	0.0125	1280	571.2	0.000656	0.37468
250	125000	0.013	11.7692308	125	120	120000	1625	0.0135417	1181.5385	537.72308	0.0006095	0.3277304

				$h_{c,eff}$								
h	A_{ct} / face	ρ	$1+1/\alpha_e$ ρ	h/2	2.5(c +φ/2	$A_{c,eff}$ (area/ face, mm	A_s	$\rho_{p,eff}$	φ/$\rho_{p,eff}$ (mm	$S_{r,max}$ EN 2	ε (EN 2)	W_{max} EN 2
300	150000	0.001	141	150	120	120000	150	0.00125	12800	4488	0.0073018	32.770414
300	150000	0.002	71	150	120	120000	300	0.0025	6400	2312	0.0036768	8.5007286
300	150000	0.003	47.6666667	150	120	120000	450	0.00375	4266.6667	1586.6667	0.0024685	3.9166111
300	150000	0.004	36	150	120	120000	600	0.005	3200	1224	0.0018643	2.2818857
300	150000	0.005	29	150	120	120000	750	0.00625	2560	1006.4	0.0015018	1.5113971
300	150000	0.006	24.3333333	150	120	120000	900	0.0075	2133.3333	861.33333	0.0012601	1.0853825
300	150000	0.007	21	150	120	120000	1050	0.00875	1828.5714	757.71429	0.0010875	0.8240143
300	150000	0.008	18.5	150	120	120000	1200	0.01	1600	680	0.000958	0.6514643
300	150000	0.009	16.5555556	150	120	120000	1350	0.01125	1422.2222	619.55556	0.0008573	0.5311705
300	150000	0.01	15	150	120	120000	1500	0.0125	1280	571.2	0.0007768	0.4437
300	150000	0.011	13.7272727	150	120	120000	1650	0.01375	1163.6364	531.63636	0.0007109	0.3779279
300	150000	0.012	12.6666667	150	120	120000	1800	0.015	1066.6667	498.66667	0.000656	0.3271016
300	150000	0.013	11.7692308	150	120	120000	1950	0.01625	984.61538	470.76923	0.0006095	0.2869235

				$h_{c,eff}$								
h	A_{ct} / face	ρ	$1+1/\alpha_e$ ρ	h/2	2.5(c +φ/2	$A_{c,eff}$ (area/ face, mm	A_s	$\rho_{p,eff}$	φ/$\rho_{p,eff}$ (mm	$S_{r,max}$ EN 2	ε (EN 2)	W_{max} EN 2
350	175000	0.001	141	175	120	120000	175	0.0014583	10971.429	3866.2857	0.0070462	27.242712
350	175000	0.002	71	175	120	120000	350	0.0029167	5485.7143	2001.1429	0.0035481	7.1002514
350	175000	0.003	47.6666667	175	120	120000	525	0.004375	3657.1429	1379.4286	0.0023821	3.2858769
350	175000	0.004	36	175	120	120000	700	0.0058333	2742.8571	1068.5714	0.001799	1.9223982
350	175000	0.005	29	175	120	120000	875	0.0072917	2194.2857	882.05714	0.0014492	1.2782977
350	175000	0.006	24.3333333	175	120	120000	1050	0.00875	1828.5714	757.71429	0.001216	0.9213918
350	175000	0.007	21	175	120	120000	1225	0.0102083	1567.3469	668.89796	0.0010494	0.7019666
350	175000	0.008	18.5	175	120	120000	1400	0.0116667	1371.4286	602.28571	0.0009245	0.5568158
350	175000	0.009	16.5555556	175	120	120000	1575	0.013125	1219.0476	550.47619	0.0008273	0.4554278
350	175000	0.01	15	175	120	120000	1750	0.0145833	1097.1429	509.02857	0.0007496	0.3815669
350	175000	0.011	13.7272727	175	120	120000	1925	0.0160417	997.4026	475.11688	0.000686	0.3259283
350	175000	0.012	12.6666667	175	120	120000	2100	0.0175	914.28571	446.85714	0.000633	0.2828579
350	175000	0.013	11.7692308	175	120	120000	2275	0.0189583	843.95604	422.94505	0.0005881	0.2487536

				$h_{c,eff}$								
h	A_{ct} / face	ρ	$1+1/\alpha_e$ ρ	h/2	2.5(c +φ/2	$A_{c,eff}$ (area/ face, mm	A_s	$\rho_{p,eff}$	φ/$\rho_{p,eff}$ (mm	$S_{r,max}$ EN 2	ε (EN 2)	W_{max} EN 2
400	200000	0.001	141	200	120	120000	200	0.0016667	9600	3400	0.0067907	23.088246
400	200000	0.002	71	200	120	120000	400	0.0033333	4800	1768	0.0034194	6.0455181
400	200000	0.003	47.6666667	200	120	120000	600	0.005	3200	1224	0.0022957	2.8098887
400	200000	0.004	36	200	120	120000	800	0.0066667	2400	952	0.0017338	1.650564
400	200000	0.005	29	200	120	120000	1000	0.0083333	1920	788.8	0.0013967	1.101686
400	200000	0.006	24.3333333	200	120	120000	1200	0.01	1600	680	0.0011719	0.7968993
400	200000	0.007	21	200	120	120000	1400	0.0116667	1371.4286	602.28571	0.0010114	0.6091367
400	200000	0.008	18.5	200	120	120000	1600	0.0133333	1200	544	0.000891	0.4846894
400	200000	0.009	16.5555556	200	120	120000	1800	0.015	1066.6667	498.66667	0.0007973	0.3976006
400	200000	0.01	15	200	120	120000	2000	0.0166667	960	462.4	0.0007224	0.3340427
400	200000	0.011	13.7272727	200	120	120000	2200	0.0183333	872.72727	432.72727	0.0006611	0.2860826
400	200000	0.012	12.6666667	200	120	120000	2400	0.02	800	408	0.00061	0.2488946
400	200000	0.013	11.7692308	200	120	120000	2600	0.0216667	738.46154	387.07692	0.0005668	0.2194008

				$h_{c,eff}$								
h	A_{ct} / face	ρ	$1+1/\alpha_e$ ρ	h/2	2.5(c +φ/2	$A_{c,eff}$ (area/ face, mm	A_s	$\rho_{p,eff}$	φ/$\rho_{p,eff}$ (mm	$S_{r,max}$ EN 2	ε (EN 2)	W_{max} EN 2
450	225000	0.001	141	225	120	120000	225	0.001875	8533.3333	3037.3333	0.0065351	19.849272
450	225000	0.002	71	225	120	120000	450	0.00375	4266.6667	1586.6667	0.0032907	5.2212808
450	225000	0.003	47.6666667	225	120	120000	675	0.005625	2844.4444	1103.1111	0.0022093	2.4370646
450	225000	0.004	36	225	120	120000	900	0.0075	2133.3333	861.33333	0.0016685	1.4371654
450	225000	0.005	29	225	120	120000	1125	0.009375	1706.6667	716.26667	0.0013441	0.9627327
450	225000	0.006	24.3333333	225	120	120000	1350	0.01125	1422.2222	619.55556	0.0011278	0.6987388
450	225000	0.007	21	225	120	120000	1575	0.013125	1219.0476	550.47619	0.0009733	0.5357854
450	225000	0.008	18.5	225	120	120000	1800	0.015	1066.6667	498.66667	0.0008574	0.4275777
450	225000	0.009	16.5555556	225	120	120000	2025	0.016875	948.14815	458.37037	0.0007673	0.351717
450	225000	0.01	15	225	120	120000	2250	0.01875	853.33333	426.13333	0.0006952	0.2962578
450	225000	0.011	13.7272727	225	120	120000	2475	0.020625	775.75758	399.75758	0.0006362	0.2543396
450	225000	0.012	12.6666667	225	120	120000	2700	0.0225	711.11111	377.77778	0.0005871	0.2217848
450	225000	0.013	11.7692308	225	120	120000	2925	0.024375	656.41026	359.17949	0.0005455	0.1959262

				$h_{c,eff}$								
h	A_{ct} / face	ρ	$1+1/\alpha_e$ ρ	h/2	2.5(c +φ/2	$A_{c,eff}$ (area/ face, mm	A_s	$\rho_{p,eff}$	φ/$\rho_{p,eff}$ (mm	$S_{r,max}$ EN 2	ε (EN 2)	W_{max} EN 2
500	250000	0.001	141	250	120	120000	250	0.0020833	7680	2747.2	0.0062795	17.251141
500	250000	0.002	71	250	120	120000	500	0.0041667	3840	1441.6	0.003162	4.5583907
500	250000	0.003	47.6666667	250	120	120000	750	0.00625	2560	1006.4	0.0021229	2.1364554
500	250000	0.004	36	250	120	120000	1000	0.0083333	1920	788.8	0.0016033	1.2646718
500	250000	0.005	29	250	120	120000	1250	0.0104167	1536	658.24	0.0012915	0.8501405
500	250000	0.006	24.3333333	250	120	120000	1500	0.0125	1280	571.2	0.0010837	0.6190108
500	250000	0.007	21	250	120	120000	1750	0.0145833	1097.1429	509.02857	0.0009353	0.476069
500	250000	0.008	18.5	250	120	120000	2000	0.0166667	960	462.4	0.0008239	0.3809763
500	250000	0.009	16.5555556	250	120	120000	2250	0.01875	853.33333	426.13333	0.0007373	0.3141939
500	250000	0.01	15	250	120	120000	2500	0.0208333	768	397.12	0.000668	0.2652903
500	250000	0.011	13.7272727	250	120	120000	2750	0.0229167	698.18182	373.38182	0.0006114	0.2282684
500	250000	0.012	12.6666667	250	120	120000	3000	0.025	640	353.6	0.0005641	0.1994725
500	250000	0.013	11.7692308	250	120	120000	3250	0.0270833	590.76923	336.86154	0.0005242	0.1765663

Figure A.6: EN 1992 Data for End Restraint Crack Model with Varying Section Thickness

Edge and End Restraint
BS 8007 (same equation for both)

	walls, suspended slabs							
h	h (BS 8007, mm)	A_c (BS 8007)	A_s	ρ	φ/2ρ	$S_{r,max}$ (BS 8007)	ε (BS 8007)	W_{max} BS 8007
250	125	125000	125	0.001	8000	5766.666667	0.000266	1.533933333
250	125	125000	250	0.002	4000	2883.333333	0.000266	0.766966667
250	125	125000	375	0.003	2666.666667	1922.222222	0.000266	0.511311111
250	125	125000	500	0.004	2000	1441.666667	0.000266	0.383483333
250	125	125000	625	0.005	1600	1153.333333	0.000266	0.306786667
250	125	125000	750	0.006	1333.333333	961.1111111	0.000266	0.255655556
250	125	125000	875	0.007	1142.857143	823.8095238	0.000266	0.219133333
250	125	125000	1000	0.008	1000	720.8333333	0.000266	0.191741667
250	125	125000	1125	0.009	888.8888889	640.7407407	0.000266	0.170437037
250	125	125000	1250	0.01	800	576.6666667	0.000266	0.153393333
250	125	125000	1375	0.011	727.2727273	524.2424242	0.000266	0.139448485
250	125	125000	1500	0.012	666.6666667	480.5555556	0.000266	0.127827778
250	125	125000	1625	0.013	615.3846154	443.5897436	0.000266	0.117994872

	walls, suspended slabs							
h	h (BS 8007, mm)	A_c (BS 8007)	A_s	ρ	φ/2ρ	$S_{r,max}$ (BS 8007)	ε (BS 8007)	W_{max} BS 8007
300	150	150000	150	0.001	8000	5766.666667	0.000266	1.533933333
300	150	150000	300	0.002	4000	2883.333333	0.000266	0.766966667
300	150	150000	450	0.003	2666.666667	1922.222222	0.000266	0.511311111
300	150	150000	600	0.004	2000	1441.666667	0.000266	0.383483333
300	150	150000	750	0.005	1600	1153.333333	0.000266	0.306786667
300	150	150000	900	0.006	1333.333333	961.1111111	0.000266	0.255655556
300	150	150000	1050	0.007	1142.857143	823.8095238	0.000266	0.219133333
300	150	150000	1200	0.008	1000	720.8333333	0.000266	0.191741667
300	150	150000	1350	0.009	888.8888889	640.7407407	0.000266	0.170437037
300	150	150000	1500	0.01	800	576.6666667	0.000266	0.153393333
300	150	150000	1650	0.011	727.2727273	524.2424242	0.000266	0.139448485
300	150	150000	1800	0.012	666.6666667	480.5555556	0.000266	0.127827778
300	150	150000	1950	0.013	615.3846154	443.5897436	0.000266	0.117994872

	walls, suspended slabs							
h	h (BS 8007, mm)	A_c (BS 8007)	A_s	ρ	φ/2ρ	$S_{r,max}$ (BS 8007)	ε (BS 8007)	W_{max} BS 8007
350	175	175000	175	0.001	8000	5766.666667	0.000266	1.533933333
350	175	175000	350	0.002	4000	2883.333333	0.000266	0.766966667
350	175	175000	525	0.003	2666.666667	1922.222222	0.000266	0.511311111
350	175	175000	700	0.004	2000	1441.666667	0.000266	0.383483333
350	175	175000	875	0.005	1600	1153.333333	0.000266	0.306786667
350	175	175000	1050	0.006	1333.333333	961.1111111	0.000266	0.255655556
350	175	175000	1225	0.007	1142.857143	823.8095238	0.000266	0.219133333
350	175	175000	1400	0.008	1000	720.8333333	0.000266	0.191741667
350	175	175000	1575	0.009	888.8888889	640.7407407	0.000266	0.170437037
350	175	175000	1750	0.01	800	576.6666667	0.000266	0.153393333
350	175	175000	1925	0.011	727.2727273	524.2424242	0.000266	0.139448485
350	175	175000	2100	0.012	666.6666667	480.5555556	0.000266	0.127827778
350	175	175000	2275	0.013	615.3846154	443.5897436	0.000266	0.117994872

Figure A.7: BS 8007 Edge and End Restraint Crack Model Data

Edge Restraint
EN 1992

h 250 mm constant

R	A_{ct} / face	ρ	h/2	$h_{c,eff}$ 2.5(c + ϕ/2)	$A_{c,eff}$ (area/ face, mm^2)	A_s	$\rho_{p,eff}$	$\phi/\rho_{p,eff}$ (mm)	$S_{r,max}$ EN 2	ε (EN 2)	W_{max} EN 2
0.1	125000	0.001	125	120	120000	125	0.00104167	15360	5358.4	0.0000785	0.4206344
0.1	125000	0.002	125	120	120000	250	0.00208333	7680	2747.2	0.0000785	0.2156552
0.1	125000	0.003	125	120	120000	375	0.003125	5120	1876.8	0.0000785	0.1473288
0.1	125000	0.004	125	120	120000	500	0.00416667	3840	1441.6	0.0000785	0.1131656
0.1	125000	0.005	125	120	120000	625	0.00520833	3072	1180.48	0.0000785	0.09266768
0.1	125000	0.006	125	120	120000	750	0.00625	2560	1006.4	0.0000785	0.0790024
0.1	125000	0.007	125	120	120000	875	0.00729167	2194.285714	882.0571429	0.0000785	0.069241486
0.1	125000	0.008	125	120	120000	1000	0.00833333	1920	788.8	0.0000785	0.0619208
0.1	125000	0.009	125	120	120000	1125	0.009375	1706.666667	716.2666667	0.0000785	0.056226933
0.1	125000	0.01	125	120	120000	1250	0.01041667	1536	658.24	0.0000785	0.05167184
0.1	125000	0.011	125	120	120000	1375	0.01145833	1396.363636	610.7636364	0.0000785	0.047944945
0.1	125000	0.012	125	120	120000	1500	0.0125	1280	571.2	0.0000785	0.0448392
0.1	125000	0.013	125	120	120000	1625	0.01354167	1181.538462	537.7230769	0.0000785	0.042211262

h 250 mm

R	A_{ct} / face	ρ	h/2	$h_{c,eff}$ 2.5(c + ϕ/2)	$A_{c,eff}$ (area/ face, mm^2)	A_s	$\rho_{p,eff}$	$\phi/\rho_{p,eff}$ (mm)	$S_{r,max}$ EN 2	ε (EN 2)	W_{max} EN 2
0.2	125000	0.001	125	120	120000	125	0.00104167	15360	5358.4	0.000157	0.8412688
0.2	125000	0.002	125	120	120000	250	0.00208333	7680	2747.2	0.000157	0.4313104
0.2	125000	0.003	125	120	120000	375	0.003125	5120	1876.8	0.000157	0.2946576
0.2	125000	0.004	125	120	120000	500	0.00416667	3840	1441.6	0.000157	0.2263312
0.2	125000	0.005	125	120	120000	625	0.00520833	3072	1180.48	0.000157	0.18533536
0.2	125000	0.006	125	120	120000	750	0.00625	2560	1006.4	0.000157	0.1580048
0.2	125000	0.007	125	120	120000	875	0.00729167	2194.285714	882.0571429	0.000157	0.138482971
0.2	125000	0.008	125	120	120000	1000	0.00833333	1920	788.8	0.000157	0.1238416
0.2	125000	0.009	125	120	120000	1125	0.009375	1706.666667	716.2666667	0.000157	0.112453867
0.2	125000	0.01	125	120	120000	1250	0.01041667	1536	658.24	0.000157	0.10334368
0.2	125000	0.011	125	120	120000	1375	0.01145833	1396.363636	610.7636364	0.000157	0.095889891
0.2	125000	0.012	125	120	120000	1500	0.0125	1280	571.2	0.000157	0.0896784
0.2	125000	0.013	125	120	120000	1625	0.01354167	1181.538462	537.7230769	0.000157	0.084422523

h 250 mm

R	A_{ct} / face	ρ	h/2	$h_{c,eff}$ 2.5(c + ϕ/2)	$A_{c,eff}$ (area/ face, mm^2)	A_s	$\rho_{p,eff}$	$\phi/\rho_{p,eff}$ (mm)	$S_{r,max}$ EN 2	ε (EN 2)	W_{max} EN 2
0.3	125000	0.001	125	120	120000	125	0.00104167	15360	5358.4	0.0002355	1.2619032
0.3	125000	0.002	125	120	120000	250	0.00208333	7680	2747.2	0.0002355	0.6469656
0.3	125000	0.003	125	120	120000	375	0.003125	5120	1876.8	0.0002355	0.4419864
0.3	125000	0.004	125	120	120000	500	0.00416667	3840	1441.6	0.0002355	0.3394968
0.3	125000	0.005	125	120	120000	625	0.00520833	3072	1180.48	0.0002355	0.27800304
0.3	125000	0.006	125	120	120000	750	0.00625	2560	1006.4	0.0002355	0.2370072
0.3	125000	0.007	125	120	120000	875	0.00729167	2194.285714	882.0571429	0.0002355	0.207724457
0.3	125000	0.008	125	120	120000	1000	0.00833333	1920	788.8	0.0002355	0.1857624
0.3	125000	0.009	125	120	120000	1125	0.009375	1706.666667	716.2666667	0.0002355	0.1686808
0.3	125000	0.01	125	120	120000	1250	0.01041667	1536	658.24	0.0002355	0.15501552
0.3	125000	0.011	125	120	120000	1375	0.01145833	1396.363636	610.7636364	0.0002355	0.143834836
0.3	125000	0.012	125	120	120000	1500	0.0125	1280	571.2	0.0002355	0.1345176
0.3	125000	0.013	125	120	120000	1625	0.01354167	1181.538462	537.7230769	0.0002355	0.126633785

h 250 mm

R	A_{ct} / face	ρ	h/2	$h_{c,eff}$ 2.5(c + ϕ/2)	$A_{c,eff}$ (area/ face, mm^2)	A_s	$\rho_{p,eff}$	$\phi/\rho_{p,eff}$ (mm)	$S_{r,max}$ EN 2	ε (EN 2)	W_{max} EN 2
0.4	125000	0.001	125	120	120000	125	0.00104167	15360	5358.4	0.000314	1.6825376
0.4	125000	0.002	125	120	120000	250	0.00208333	7680	2747.2	0.000314	0.8626208
0.4	125000	0.003	125	120	120000	375	0.003125	5120	1876.8	0.000314	0.5893152
0.4	125000	0.004	125	120	120000	500	0.00416667	3840	1441.6	0.000314	0.4526624
0.4	125000	0.005	125	120	120000	625	0.00520833	3072	1180.48	0.000314	0.37067072
0.4	125000	0.006	125	120	120000	750	0.00625	2560	1006.4	0.000314	0.3160096
0.4	125000	0.007	125	120	120000	875	0.00729167	2194.285714	882.0571429	0.000314	0.276965943
0.4	125000	0.008	125	120	120000	1000	0.00833333	1920	788.8	0.000314	0.2476832
0.4	125000	0.009	125	120	120000	1125	0.009375	1706.666667	716.2666667	0.000314	0.224907733
0.4	125000	0.01	125	120	120000	1250	0.01041667	1536	658.24	0.000314	0.20668736
0.4	125000	0.011	125	120	120000	1375	0.01145833	1396.363636	610.7636364	0.000314	0.191779782
0.4	125000	0.012	125	120	120000	1500	0.0125	1280	571.2	0.000314	0.1793568
0.4	125000	0.013	125	120	120000	1625	0.01354167	1181.538462	537.7230769	0.000314	0.168845046

R	A_{ct} / face	ρ	h/2	$h_{c,eff}$ 2.5(c + ϕ/2)	$A_{c,eff}$ (area/ face, mm^2)	A_s	$\rho_{p,eff}$	$\phi/\rho_{p,eff}$ (mm)	$S_{r,max}$ EN 2	ε (EN 2)	W_{max} EN 2
0.5	125000	0.001	125	120	120000	125	0.00104167	15360	5358.4	0.0003925	2.103172
0.5	125000	0.002	125	120	120000	250	0.00208333	7680	2747.2	0.0003925	1.078276
0.5	125000	0.003	125	120	120000	375	0.003125	5120	1876.8	0.0003925	0.736644
0.5	125000	0.004	125	120	120000	500	0.00416667	3840	1441.6	0.0003925	0.565828
0.5	125000	0.005	125	120	120000	625	0.00520833	3072	1180.48	0.0003925	0.4633384
0.5	125000	0.006	125	120	120000	750	0.00625	2560	1006.4	0.0003925	0.395012
0.5	125000	0.007	125	120	120000	875	0.00729167	2194.285714	882.0571429	0.0003925	0.346207429
0.5	125000	0.008	125	120	120000	1000	0.00833333	1920	788.8	0.0003925	0.309604
0.5	125000	0.009	125	120	120000	1125	0.009375	1706.666667	716.2666667	0.0003925	0.281134667
0.5	125000	0.01	125	120	120000	1250	0.01041667	1536	658.24	0.0003925	0.2583592
0.5	125000	0.011	125	120	120000	1375	0.01145833	1396.363636	610.7636364	0.0003925	0.239724727
0.5	125000	0.012	125	120	120000	1500	0.0125	1280	571.2	0.0003925	0.224196
0.5	125000	0.013	125	120	120000	1625	0.01354167	1181.538462	537.7230769	0.0003925	0.211056308

Figure A.8: EN 1992 Edge Restraint Data with Varying Restraint Factor

Edge Restraint
cover = 40 mm
BS 8007 h=250mm

Restraint Degree	h/2	A_{ct}/ face (mm^2)	A_s/ face (mm^2)	ρ	ϕ/2ρ	$S_{r,max}$ (mm)	ε	W_{max} (mm)
0.1	125	125000	125	0.001	8000	5766.666667	0.0000532	0.30678667
0.1	125	125000	250	0.002	4000	2883.333333	0.0000532	0.15339333
0.1	125	125000	375	0.003	2666.7	1922.222222	0.0000532	0.10226222
0.1	125	125000	500	0.004	2000	1441.666667	0.0000532	0.07669667
0.1	125	125000	625	0.005	1600	1153.333333	0.0000532	0.06135733
0.1	125	125000	750	0.006	1333.3	961.1111111	0.0000532	0.05113111
0.1	125	125000	875	0.007	1142.9	823.8095238	0.0000532	0.04382667
0.1	125	125000	1000	0.008	1000	720.8333333	0.0000532	0.03834833
0.1	125	125000	1125	0.009	888.89	640.7407407	0.0000532	0.03408741
0.1	125	125000	1250	0.01	800	576.6666667	0.0000532	0.03067867
0.1	125	125000	1375	0.011	727.27	524.2424242	0.0000532	0.0278897
0.1	125	125000	1500	0.012	666.67	480.5555556	0.0000532	0.02556556
0.1	125	125000	1625	0.013	615.38	443.5897436	0.0000532	0.02359897

h=250mm

Restraint Degree	h/2	A_{ct}/ face (mm^2)	A_s/ face (mm^2)	ρ	ϕ/2ρ	$S_{r,max}$ (mm)	ε	W_{max} (mm)
0.2	125	125000	125	0.001	8000	5766.666667	0.0001064	0.61357333
0.2	125	125000	250	0.002	4000	2883.333333	0.0001064	0.30678667
0.2	125	125000	375	0.003	2666.7	1922.222222	0.0001064	0.20452444
0.2	125	125000	500	0.004	2000	1441.666667	0.0001064	0.15339333
0.2	125	125000	625	0.005	1600	1153.333333	0.0001064	0.12271467
0.2	125	125000	750	0.006	1333.3	961.1111111	0.0001064	0.10226222
0.2	125	125000	875	0.007	1142.9	823.8095238	0.0001064	0.08765333
0.2	125	125000	1000	0.008	1000	720.8333333	0.0001064	0.07669667
0.2	125	125000	1125	0.009	888.89	640.7407407	0.0001064	0.06817481
0.2	125	125000	1250	0.01	800	576.6666667	0.0001064	0.06135733
0.2	125	125000	1375	0.011	727.27	524.2424242	0.0001064	0.05577939
0.2	125	125000	1500	0.012	666.67	480.5555556	0.0001064	0.05113111
0.2	125	125000	1625	0.013	615.38	443.5897436	0.0001064	0.04719795

h=250mm

Restraint Degree	h/2	A_{ct}/ face (mm^2)	A_s/ face (mm^2)	ρ	ϕ/2ρ	$S_{r,max}$ (mm)	ε	W_{max} (mm)
0.3	125	125000	125	0.001	8000	5766.666667	0.0001596	0.92036
0.3	125	125000	250	0.002	4000	2883.333333	0.0001596	0.46018
0.3	125	125000	375	0.003	2666.7	1922.222222	0.0001596	0.30678667
0.3	125	125000	500	0.004	2000	1441.666667	0.0001596	0.23009
0.3	125	125000	625	0.005	1600	1153.333333	0.0001596	0.184072
0.3	125	125000	750	0.006	1333.3	961.1111111	0.0001596	0.15339333
0.3	125	125000	875	0.007	1142.9	823.8095238	0.0001596	0.13148
0.3	125	125000	1000	0.008	1000	720.8333333	0.0001596	0.115045
0.3	125	125000	1125	0.009	888.89	640.7407407	0.0001596	0.10226222
0.3	125	125000	1250	0.01	800	576.6666667	0.0001596	0.092036
0.3	125	125000	1375	0.011	727.27	524.2424242	0.0001596	0.08366909
0.3	125	125000	1500	0.012	666.67	480.5555556	0.0001596	0.07669667
0.3	125	125000	1625	0.013	615.38	443.5897436	0.0001596	0.07079692

h=250mm

Restraint Degree	h/2	A_{ct}/ face (mm^2)	A_s/ face (mm^2)	ρ	ϕ/2ρ	$S_{r,max}$ (mm)	ε	W_{max} (mm)
0.4	125	125000	125	0.001	8000	5766.666667	0.0002128	1.22714667
0.4	125	125000	250	0.002	4000	2883.333333	0.0002128	0.61357333
0.4	125	125000	375	0.003	2666.7	1922.222222	0.0002128	0.40904889
0.4	125	125000	500	0.004	2000	1441.666667	0.0002128	0.30678667
0.4	125	125000	625	0.005	1600	1153.333333	0.0002128	0.24542933
0.4	125	125000	750	0.006	1333.3	961.1111111	0.0002128	0.20452444
0.4	125	125000	875	0.007	1142.9	823.8095238	0.0002128	0.17530667
0.4	125	125000	1000	0.008	1000	720.8333333	0.0002128	0.15339333
0.4	125	125000	1125	0.009	888.89	640.7407407	0.0002128	0.13634963
0.4	125	125000	1250	0.01	800	576.6666667	0.0002128	0.12271467
0.4	125	125000	1375	0.011	727.27	524.2424242	0.0002128	0.11155879
0.4	125	125000	1500	0.012	666.67	480.5555556	0.0002128	0.10226222
0.4	125	125000	1625	0.013	615.38	443.5897436	0.0002128	0.0943959

h=250mm

Restraint Degree	h/2	A_{ct}/ face (mm^2)	A_s/ face (mm^2)	ρ	ϕ/2ρ	$S_{r,max}$ (mm)	ε	W_{max} (mm)
0.5	125	125000	125	0.001	8000	5766.666667	0.000266	1.53393333
0.5	125	125000	250	0.002	4000	2883.333333	0.000266	0.76696667
0.5	125	125000	375	0.003	2666.7	1922.222222	0.000266	0.51131111
0.5	125	125000	500	0.004	2000	1441.666667	0.000266	0.38348333
0.5	125	125000	625	0.005	1600	1153.333333	0.000266	0.30678667
0.5	125	125000	750	0.006	1333.3	961.1111111	0.000266	0.25565556
0.5	125	125000	875	0.007	1142.9	823.8095238	0.000266	0.21913333
0.5	125	125000	1000	0.008	1000	720.8333333	0.000266	0.19174167
0.5	125	125000	1125	0.009	888.89	640.7407407	0.000266	0.17043704
0.5	125	125000	1250	0.01	800	576.6666667	0.000266	0.15339333
0.5	125	125000	1375	0.011	727.27	524.2424242	0.000266	0.13944848
0.5	125	125000	1500	0.012	666.67	480.5555556	0.000266	0.12782778
0.5	125	125000	1625	0.013	615.38	443.5897436	0.000266	0.11799487

Figure A.9: BS 8007 Edge Restraint Data with Varying Restraint Factor

Appendix B: Data for FORM Analysis

1) Edge Restraint Crack Model ($h_{c,eff}$ = 2.5(c + φ/2))					
Symbols					
Concrete cover	c				
Bar diameter	phi				
Steel reinforcing	A				
Section thickness	H				
Effective tension depth	hc				
Section width	b				
Coefficient of thermal expansion	alpha				
Early age change in temperature	T1				
Seasonal fall in temperature	T2				
Autogenous shrinkage strain	eca				
Drying shrinkage strain	ecd				
Crack width limit	wl				
Model uncertainty	th				
syms c k1 k2 k3 k4 phi A h hc b R alpha T1 T2 eca ecd wl th					
d=h-c-0.5*phi;					
hc=2.5*(h-d);					
pe=A/(hc*b);					
s=k3*c+(k1*k2*k4*phi)/pe;					
e= R*(alpha*(T1+T2)+eca+ecd);					
g= wl - th*s*e;					
diff(g,h)					
diff(g,c)					
diff(g,th)					
Partial Derivatives					
diff(g,h) =					
0					
diff(g,c) =					
-th*(k3+5/2*k1*k2*k4*phi/A*b)*R*(alpha*(T1+T2)+eca+ecd);					
diff(g,th) =					
-(k3*c+k1*k2*k4*phi/A*(5/2*c+5/4*phi)*b)*R*(alpha*(T1+T2)+eca+ecd)					

Figure B.1: Edge Restraint MATLAB Input for FORM Analysis ($h_{c,eff}$ = 2.5(c + φ/2))

2) End Restraint Crack Model ($h_{c,eff}$ = 2.5(c + φ/2))

```
syms c k1 k2 k3 k4 phi A h hc b alphae kc k f E wl th
d=h-c-0.5*phi;
hc=2.5*(h-d);
pe=A/(hc*b);
p=A/(0.5*h*b);
s=k3*c+k1*k2*k4*phi/pe;
e=(0.5*alphae*kc*k*f*(1+(alphae*p)^-1))/E;
g=wl-th*s*e;
diff(g,h)
diff(g,c)
diff(g,f)
diff(g,th)

Partial Derivatives

diff(g,h)

ans =

-1/4*th*(k3*c+k1*k2*k4*phi/A*(5/2*c+5/4*phi)*b)*kc*k*f/A*b/E;

diff(g,c)

ans =

-1/2*th*(k3+5/2*k1*k2*k4*phi/A*b)*alphae*kc*k*f*(1+1/2/alphae/A*h*b)/E;

diff(g,f)

ans =

-1/2*th*(k3*c+k1*k2*k4*phi/A*(5/2*c+5/4*phi)*b)*alphae*kc*k*(1+1/2/alphae/A*h*b)/E;

diff(g,th)

ans =

-1/2*(k3*c+k1*k2*k4*phi/A*(5/2*c+5/4*phi)*b)*alphae*kc*k*f*(1+1/2/alphae/A*h*b)/E;
```

Figure B.2: End Restraint MATLAB Input for FORM Analysis ($h_{c,eff}$ = 2.5(c + φ/2))

1) Edge Restraint Crack Model ($h_{c,eff}$ = h/2)

```
syms c k1 k2 k3 k4 phi A h hc b R alpha T1 T2 eca ecd wl th
hc=0.5*h;
pe=A/(hc*b);
s=k3*c+(k1*k2*k4*phi)/pe;
e= R*(alpha*(T1+T2)+eca+ecd);
g= wl - th*s*e;
diff(g,h)
diff(g,c)
diff(g,th)

derivatives:

>> diff(g,h)

ans =

-1/2*th*k1*k2*k4*phi/A*b*R*(alpha*(T1+T2)+eca+ecd)

>> diff(g,c)

ans =

-th*k3*R*(alpha*(T1+T2)+eca+ecd)

>> diff(g,th)

ans =

-(k3*c+1/2*k1*k2*k4*phi/A*h*b)*R*(alpha*(T1+T2)+eca+ecd)
```

Figure B.3: Edge Restraint MATLAB Input for FORM Analysis ($h_{c,eff}$ = h/2)

2) End Restraint Crack Model ($h_{c,eff}$ = h/2)

```
syms c k1 k2 k3 k4 phi A h hc b alphae kc k f E wl th
hc=0.5*h;
pe=A/(hc*b);
p=A/(0.5*h*b);
s=k3*c+k1*k2*k4*phi/pe;
e=(0.5*alphae*kc*k*f*(1+(alphae*p)^-1))/E;
g=wl-th*s*e;
diff(g,h)
diff(g,c)
diff(g,f)
diff(g,th)

Partial Derivatives

diff(g,h)

ans =

-1/4*th*k1*k2*k4*phi/A*b*alphae*kc*k*f*(1+1/2/alphae/A*h*b)/E-1/4*th*(k3*c+1/2*k1*k2*k4*phi/A*h*b)*kc*k*f/A*b/E

diff(g,c)

ans =

-1/2*th*k3*alphae*kc*k*f*(1+1/2/alphae/A*h*b)/E

 diff(g,f)

ans =

-1/2*th*(k3*c+1/2*k1*k2*k4*phi/A*h*b)*alphae*kc*k*(1+1/2/alphae/A*h*b)/E

diff(g,th)

ans =

-1/2*(k3*c+1/2*k1*k2*k4*phi/A*h*b)*alphae*kc*k*f*(1+1/2/alphae/A*h*b)/E
```

Figure B.4: End Restraint MATLAB Input for FORM Analysis ($h_{c,eff}$ = h/2)

Edge Restraint					**cov:**	0.3								
Constant Variables														
As unkown variable	ε_{ca} = 33με	R=0.5												
c=40mm	ε_{cd} = 220με													
h=250mm	$\alpha_{T,c}$ = 14με													
250mm thick 2.5*(c+ϕ/2)	cover = 40mm													
model uncertainty (cov)	Area (%)	Area (mm^2)	Area/face	β	h*	c*	θ*	Srm	ε	wcalc	g(x)	probability(s)	probability(f)	
0.3	0.5	1250	625	solver could not find feasible solution therefore gave 0										
0.3	0.93	2328	1164	0.16729791	0.25	0.039935	1.001347	0.508869	0.0003925	0.0002	1.11678E-12	0.566432177	0.433567823	min reinf. required
0.3	1	2500	1250	0.35113627	0.25	0.040363	1.053603	0.48363	0.0003925	0.00019	1.74267E-11	0.637256941	0.362743059	
0.3	1.5	3750	1875	1.34889791	0.25	0.042826	1.386947	0.367393	0.0003925	0.000144	-1.43176E-11	0.911315119	0.088684881	
0.3	2	5000	2500	1.99974707	0.25	0.044579	1.657214	0.307476	0.0003925	0.000121	-2.55916E-11	0.977236209	0.022763791	
0.3	2.5	6250	3125	2.46699742	0.25	0.045921	1.881738	0.270789	0.0003925	0.000106	7.62381E-11	0.993187433	0.006812567	
0.3	3	7500	3750	2.82232372	0.25	0.046993	2.071627	0.245968	0.0003925	9.65E-05	-9.84676E-11	0.997616149	0.002383851	
250mm thick h/2	cover = 40mm													
model uncertainty (cov)	Area (%)	Area (mm^2)	Area/face	β	h*	c*	θ*	Srm	ε	wcalc	g(x)	probability(s)	probability(f)	
0.3	0.5	1250	625	solver could not find feasible solution therefore gave 0										
0.3	0.93119824	2328	1164	0.17189348	0.250012	0.039632	1.006413	0.508838	0.0003925	0.0002	-9.99751E-07	0.568239363	0.431760637	min reinf. required
0.3	1	2500	1250	0.35404227	0.250025	0.039726	1.062696	0.479492	0.0003925	0.000188	-1.51783E-12	0.638346397	0.361653603	
0.3	1.5	3750	1875	1.43253849	0.250091	0.040549	1.464822	0.347861	0.0003925	0.000137	3.93235E-12	0.924005114	0.075994886	
0.3	2	5000	2500	2.13387707	0.250124	0.041429	1.800812	0.282958	0.0003925	0.000111	-4.82536E-12	0.983573578	0.016426422	
0.3	2.5	6250	3125	2.63408494	0.250141	0.042306	2.082344	0.244702	0.0003925	9.6E-05	-3.46189E-11	0.995781781	0.004218219	
0.3	3	7500	3750	3.01110895	0.250149	0.043149	2.319209	0.21971	0.0003925	8.62E-05	-6.58466E-11	0.998698523	0.001301477	

Figure B.5: Selected Data of EN 1992 Edge Restraint Crack Model FORM Analysis ($h_{c,eff}$ = 2.5(c + φ/2) and h/2- Effective Depth Comparison)

End Restraint					**cov:**	0.3									
Constant Variables															
As unkown variable	αe=7														
c=40mm	kc=1	Es = 200GPa													
h=250mm	k=1														
250mm thick	cover = 40mm														
2.5*(c+ϕ/2)															
model uncertainty (cov)	Area (%)	Area (mm^2)	Area/face	β	h*	c*	$f_{ct,eff}$	θ*	Srm	ε	wcalc	g(x)	probability(s)	probability(f)	
0.3	0.5	1250	625	solver could not find feasible solution therefore gave 0											
0.3	1	2500	1250	solver could not find feasible solution therefore gave 0											
0.3	1.43267655	3582	1791	0.19237675	0.250012	0.039938	2901.059	1.000911	0.3587251	0.000557	0.000199818	8.01721E-12	0.576276448	0.423723552	min reinf. req.
0.3	1.5	3750	1875	0.39691205	0.250024	0.040354	2958.374	1.05094	0.3492613	0.000545	0.000190306	-2.65663E-12	0.654283841	0.345716159	
0.3	2	5000	2500	1.64017775	0.250095	0.043039	3330.802	1.412409	0.2982366	0.000475	0.000141602	-9.60073E-11	0.949515893	0.050484107	
0.3	2.5	6250	3125	2.55455526	0.250143	0.045201	3632.844	1.753656	0.2670477	0.000427	0.000114047	1.01278E-10	0.994683822	0.005316178	
0.3	3	7500	3750	3.26556127	0.250178	0.047004	3885.534	2.073729	0.2460188	0.000392	9.64446E-05	8.37744E-12	0.999453763	0.000546237	
250mm thick	cover = 40mm				1.00038	1.075986	1.148553	1.412409							
h/2															
model uncertainty (cov)	Area (%)	Area (mm^2)	Area/face	β	h*	c*	$f_{ct,eff}$	θ*	Srm	ε	wcalc	g(x)	probability(s)	probability(f)	
0.3	0.5	1250	625	solver could not find feasible solution therefore gave 0											
0.3	1	2500	1250	solver could not find feasible solution therefore gave 0											
0.3	1.43267655	3581.691376	1790.8	0.18357641	0.250022	0.039654	2901.481	1.001274	0.3585297	0.000557	0.000199746	5.95144E-12	0.572827116	0.427172884	min reinf. req.
0.3	1.5	3750	1875	0.39979824	0.250047	0.039782	2965.571	1.057325	0.3462808	0.000546	0.000189157	-1.22998E-11	0.655347435	0.344652565	
0.3	2	5000	2500	1.71339766	0.25019	0.040805	3385.107	1.47052	0.2817623	0.000483	0.000136006	-6.49981E-11	0.956680297	0.043319703	
0.3	2.5	6250	3125	2.67703137	0.250281	0.041898	3727.549	1.869857	0.2439752	0.000438	0.00010696	3.13578E-11	0.996286116	0.003713884	
0.3	3	7500	3750	3.42315354	0.25034	0.043009	4013.709	2.248497	0.2195327	0.000405	8.89483E-05	4.651E-11	0.999690504	0.000309496	

Figure B.6: Selected Data of EN 1992 End Restraint Crack Model FORM Analysis ($h_{c,eff}$ = 2.5(c + φ/2) and h/2- Effective Depth Comparison)

End Restraint															
250mm thick 2.5*(c+ϕ/2) Elastic Modulus 3 days															
α_e = 7	Gross Area (%	Gross Area (mm^2)	Area/face (mm^2)	β	h*	c*	$f_{ct,eff}$	θ*	Srm	ε	wcalc	g(x)	probability (s	probability (f)	
7	0.5	1250	625	solver could not find feasible solution therefore gave 0											
7	1	2500	1250	solver could not find feasible solution therefore gave 0											
7	1.43267655	3582	1791	0.192376749	0.25001159	0.039937687	2901.059074	1.000910714	0.35872512	0.000557023	0.000199818	8.01721E-12	0.57627645	0.4237236	min reinf. req.
7	1.5	3750	1875	0.39691205	0.2500238	0.040353818	2958.374419	1.050939977	0.349261334	0.000544881	0.000190306	-2.65663E-12	0.65428384	0.3457162	
7	2	5000	2500	1.640177755	0.25009507	0.04303944	3330.802409	1.412409479	0.298236641	0.000474798	0.000141602	-9.60073E-11	0.94951589	0.0504841	
7	2.5	6250	3125	2.554555258	0.250143359	0.045201488	3632.844251	1.753655694	0.267047738	0.000427068	0.000114047	1.01278E-10	0.99468382	0.0053162	
7	3	7500	3750	3.26556127	0.250177662	0.047004019	3885.534025	2.073728658	0.246018755	0.000392021	9.64446E-05	8.37744E-12	0.99945376	0.0005462	
250mm thick 2.5*(c+ϕ/2) Elastic Modulus 7 days															
α_e = 6	Gross Area (%	Gross Area (mm^2)	Area/face (mm^2)	β	h*	c*	$f_{ct,eff}$	θ*	Srm	ε	wcalc	g(x)	probability (s	probability (f)	
6.5	0.5	1250	625												
6.5	1	2500	1250												
6.5	1.42715822	3567.895547	1783.947773	0.192374776	0.25001167	0.039937627	2901.059267	1.00091088	0.359802884	0.000555354	0.000199818	8.01763E-12	0.57627568	0.4237243	min reinf. req.
6.5	1.5	3750	1875	0.414962421	0.250025052	0.040390744	2963.486151	1.055473004	0.349532123	0.000542121	0.000189489	-2.80245E-11	0.66091529	0.3390847	
6.5	2	5000	2500	1.663464977	0.25009727	0.04309161	3338.201438	1.420244525	0.298549661	0.000471683	0.000140821	-9.98417E-11	0.9518903	0.0481097	
6.5	2.5	6250	3125	2.582764092	0.250146494	0.0452691	3642.595444	1.765414423	0.267399318	0.000423665	0.000113288	1.24461E-10	0.99509938	0.0049006	
6.5	3	7500	3750	3.298407179	0.250181692	0.047087016	3897.655473	2.089894632	0.246406075	0.000388378	9.56986E-05	1.87998E-11	0.99951382	0.0004862	
250mm thick 2.5*(c+ϕ/2) Elastic Modulus 28 days				0.990041888	1.010058274										
				0.989078045	1.011042562										
α_e = 6	Gross Area (%	Gross Area (mm^2)	Area/face (mm^2)	β	h*	c*	$f_{ct,eff}$	θ*	Srm	ε	wcalc	g(x)	probability (s	probability (f)	
6	0.5	1250	625	solver could not find feasible solution therefore gave 0											
6	1	2500	1250	solver could not find feasible solution therefore gave 0											
6	1.42166718	3554.167958	1777.083979	0.192372828	0.25001175	0.039937568	2901.05946	1.000911046	0.360883622	0.000553691	0.000199818	8.01803E-12	0.57627491	0.4237251	min reinf. req.
6	1.5	3750	1875	0.433135362	0.250026328	0.040427963	2968.641306	1.060056374	0.349805061	0.000539355	0.000188669	6.23999E-12	0.66754178	0.3324582	
6	2	5000	2500	1.686957883	0.250099521	0.043144319	3345.682071	1.428192391	0.298865912	0.000468562	0.000140037	-6.50273E-11	0.95419427	0.0458057	
6	2.5	6250	3125	2.61127902	0.250149714	0.045337568	3652.478414	1.77738011	0.267755353	0.000420254	0.000112525	-3.62227E-11	0.99548979	0.0045102	
6	3	7500	3750	3.331666358	0.250185847	0.047171238	3909.966942	2.106391046	0.246799109	0.000384722	9.49491E-05	2.10335E-11	0.99956836	0.0004316	
			E37/E24	0.99998987											
		28 to 7 days	E38/E25	1.043794183											
			E39/E26	1.014122874											
			E40/E27	1.011040469											
			E41/E28	1.010083406											
		ave (7 and 28 day)	AVERAGE(E44:E48)	1.01580616											
			E37/E10	0.999979614											
		28 to 3 days	E38/E11	1.091262817											
			E39/E12	1.028521377											
			E40/E13	1.022204946											
			E41/E14	1.020243101											
		ave (3 and 28 day)	AVERAGE(E51:E55)	1.032442371		1.024124266	average								

Figure B.7: Effect of Variation in Elastic Modulus of Concrete

Appendix C: Sensitivity Analysis of EN 1992

Edge Restraint
$h_{c,eff}$ = 2.5(c+ φ/2)

Constant Variables
As unkown variable εca=33με R = 0.5
c = 40mm εcd=220με
h = 250mm αT,c=14με

Ω = c.o.v.=s.dev./mean
Final failure point
Υ_{xi^*}= 1-αi*βΩ = x*/mean
Final direction cosine

w_l= 0.3mm
β=1.5

											Direction Cosines/ Sensitivity Factors						Partial Factors		
model uncertainty c.o.v.	Area/face (m^2)	Gross Area (m^2	As (%)	h*	c*	θ*	Sr,m	ε	wcalc	g(x)	α_h	$\lvert\alpha_h\rvert$	α_c	$\lvert\alpha_c\rvert$	α_θ	$\lvert\alpha_\theta\rvert$	Υ_h	Υ_c	Υ_θ
0.1	0.000944393	0.001888787	0.7555146	0.25	0.0472085	1.0916103	0.70018675	0.000393	0.00027482	4.20768E-11	0	0	-0.7864191	0.78641912	-0.6176933	0.61769327	1	1.18021226	1.09161035
0.15	0.000996228	0.001992456	0.7969824	0.25	0.045738	1.1741475	0.65096691	0.000393	0.0002555	5.25105E-12	0	0	-0.6457821	0.64578211	-0.7635218	0.76352175	1	1.14345109	1.17414755
0.2	0.00105844	0.00211688	0.8467518	0.25	0.04461	1.2630059	0.60516827	0.000393	0.00023753	4.23328E-11	0	0	-0.5347951	0.53479514	-0.8449818	0.84498175	1	1.11525036	1.26300591
0.25	0.001128038	0.002256077	0.9024306	0.25	0.0437798	1.3544421	0.56431441	0.000393	0.00022149	8.35648E-12	0	0	-0.4512998	0.45129983	-0.8923724	0.89237238	1	1.09449431	1.3544421
0.3	0.001203377	0.002406755	0.962702	0.25	0.0431633	1.4472941	0.52811044	0.000393	0.00020728	3.13308E-11	0	0	-0.3882692	0.38826925	-0.921546	0.92154598	1	1.0790819	1.44729412

w_{lim}= 0.2mm
β=1.5

											Direction Cosines/ Sensitivity Factors						Partial Factors		
model uncertainty c.o.v.	Area/face (m^2)	Gross Area (m^2	As (%)	h*	c*	θ*	Sr,m	ε	wcalc	g(x)	α_h	$\lvert\alpha_h\rvert$	α_c	$\lvert\alpha_c\rvert$	α_θ	$\lvert\alpha_\theta\rvert$	Υ_h	Υ_c	Υ_θ
0.1	0.001536328	0.003072656	1.2290622	0.25	0.0472526	1.090739	0.46716411	0.000393	0.00018336	1.36415E-11	0	0	-0.7905716	0.79057162	-0.6123696	0.61236959	1	1.18131546	1.09073899
0.15	0.001627396	0.003254792	1.3019167	0.25	0.045796	1.172881	0.43444658	0.000393	0.00017052	5.45515E-12	0	0	-0.6514113	0.65141125	-0.7587248	0.75872484	1	1.14490026	1.17288097
0.2	0.001737945	0.00347589	1.390356	0.25	0.0446717	1.2615217	0.40392024	0.000393	0.00015854	5.44181E-12	0	0	-0.5409384	0.54093844	-0.8410622	0.84106219	1	1.11679294	1.26152166
0.25	0.001863172	0.003726345	1.4905379	0.25	0.0438409	1.3528365	0.3766561	0.000393	0.00014784	3.11378E-12	0	0	-0.4575005	0.45750048	-0.8892094	0.88920937	1	1.09602239	1.35283652
0.3	0.002000583	0.004001165	1.600466	0.25	0.0432228	1.4456177	0.35248189	0.000393	0.00013835	3.11973E-11	0	0	-0.3943258	0.39432577	-0.9189707	0.91897072	1	1.08056923	1.4456177

w_{lim}= 0.1mm
β=1.5

											Direction Cosines/ Sensitivity Factors						Partial Factors		
model uncertainty c.o.v.	Area/face (m^2)	Gross Area (m^2	As (%)	h*	c*	θ*	Sr,m	ε	wcalc	g(x)	α_h	$\lvert\alpha_h\rvert$	α_c	$\lvert\alpha_c\rvert$	α_θ	$\lvert\alpha_\theta\rvert$	Υ_h	Υ_c	Υ_θ
0.1	0.004116912	0.008233823	3.2935293	0.25	0.0473779	1.0881995	0.23412715	0.000393	9.1895E-05	9.93702E-12	0	0	-0.802367	0.80236704	-0.5968309	0.5968309	1	1.18444823	1.08819949
0.15	0.004441849	0.008883697	3.5534789	0.25	0.0459635	1.1691383	0.21791827	0.000393	8.5533E-05	1.89297E-10	0	0	-0.667602	0.66760202	-0.7445183	0.74451833	1	1.14908635	1.16913829
0.2	0.004855315	0.00971063	3.8842518	0.25	0.044851	1.2570841	0.20267302	0.000393	7.9549E-05	1.7998E-11	0	0	-0.5587797	0.55877969	-0.8293161	0.82931614	1	1.12127483	1.25708407
0.25	0.0053503	0.0107006	4.2802399	0.25	0.0440193	1.3480012	0.18900357	0.000393	7.4184E-05	1.78965E-11	0	0	-0.4756025	0.47560248	-0.8796603	0.87966032	1	1.1004823	1.34800116
0.3	0.005928176	0.011856352	4.7425408	0.25	0.043396	1.4405273	0.17686372	0.000393	6.9419E-05	2.13316E-11	0	0	-0.4121156	0.41211563	-0.9111316	0.91113155	1	1.08490113	1.44052732

Figure C.1: EN 1992 Edge Restraint Crack Model Sensitivity Factors and Theoretical Partial Safety Factors ($h_{c,eff}$ = 2.5(c + φ/2)).

Edge Restraint																				
hc,eff = h/2																				
As varies	εca=33με	R=0.5																		
c=40mm	εcd=220με																			
h=250mm	αT,c=14με																	Υ_{xi*}= 1-αi*βΩ = x*/mean		
w_{lim}= 0.3mm																				
β=1.5												Direction Cosines/ Sensitivity Factors						Partial Factors		
model uncertainty c.	Area/face (m	Gross Area (	As (%)	h*	c*	θ*	Sr,m	ε	wcalc	g(x)	α_h	$\lvert\alpha_h\rvert$	α_c	$\lvert\alpha_c\rvert$	α_θ	$\lvert\alpha_\theta\rvert$	Υ_h	Υ_c	Υ_θ
0.1	0.000862	0.001724	0.68961	0.2503212	0.041211	1.152482	0.6632	0.00039	0.00026	5.61674E-10	-0.08566	0.085662	-0.18259	0.182588	-0.979451	0.979451	1.001285	1.030282	1.152482
0.15	0.0009316	0.0018631	0.74525	0.2502147	0.04073	1.235479	0.61865	0.00039	0.00024	1.29216E-09	-0.05725	0.05725	-0.13033	0.130329	-0.989817	0.989817	1.000859	1.018238	1.235479
0.2	0.0010051	0.0020102	0.80406	0.2501601	0.040491	1.320604	0.57877	0.00039	0.00023	1.75781E-11	-0.0427	0.042703	-0.10427	0.104273	-0.993632	0.993632	1.000641	1.012286	1.320604
0.25	0.0010823	0.0021646	0.86584	0.2501271	0.040351	1.407835	0.54291	0.00039	0.00021	2.38073E-11	-0.03388	0.033883	-0.08878	0.088783	-0.995475	0.995475	1.000508	1.008764	1.407835
0.3	0.0011631	0.0023262	0.93046	0.2501049	0.040258	1.496954	0.51059	0.00039	0.0002	3.97022E-11	-0.02797	0.027967	-0.07857	0.078571	-0.996516	0.996516	1.00042	1.006449	1.496954
w_{lim}= 0.2mm																				
β=1.5												Direction Cosines/ Sensitivity Factors						Partial Factors		
model uncertainty c.	Area/face (m	Gross Area (	As (%)	h*	c*	θ*	Sr,m	ε	wcalc	g(x)	α_h	$\lvert\alpha_h\rvert$	α_c	$\lvert\alpha_c\rvert$	α_θ	$\lvert\alpha_\theta\rvert$	Υ_h	Υ_c	Υ_θ
0.1	0.0013929	0.0027858	1.1143	0.2502911	0.042056	1.14894	0.4435	0.00039	0.00017	2.7208E-11	-0.07762	0.077616	-0.2728	0.272802	-0.958934	0.958934	1.001164	1.051408	1.14894
0.15	0.0015129	0.0030258	1.21033	0.2501957	0.041334	1.232545	0.41342	0.00039	0.00016	6.72761E-11	-0.05219	0.052188	-0.19581	0.195814	-0.979251	0.979251	1.000783	1.033352	1.232545
0.2	0.001642	0.003284	1.31359	0.2501457	0.040974	1.317922	0.38663	0.00039	0.00015	5.06629E-11	-0.03886	0.038862	-0.15687	0.156872	-0.986854	0.986854	1.000583	1.024338	1.317922
0.25	0.0017796	0.0035592	1.42369	0.2501151	0.04076	1.405242	0.36261	0.00039	0.00014	6.76818E-11	-0.0307	0.030701	-0.13361	0.133614	-0.990558	0.990558	1.000461	1.018991	1.405242
0.3	0.0019257	0.0038514	1.54054	0.2500945	0.040619	1.494361	0.34098	0.00039	0.00013	2.03629E-11	-0.0252	0.025196	-0.11825	0.118249	-0.992664	0.992664	1.000378	1.015475	1.494361
w_{lim}= 0.1mm																				
β=1.5												Direction Cosines/ Sensitivity Factors						Partial Factors		
model uncertainty c.	Area/face (m	Gross Area (	As (%)	h*	c*	θ*	Sr,m	ε	wcalc	g(x)	α_h	$\lvert\alpha_h\rvert$	α_c	$\lvert\alpha_c\rvert$	α_θ	$\lvert\alpha_\theta\rvert$	Υ_h	Υ_c	Υ_θ
0.1	0.0036689	0.0073377	2.93509	0.2501952	0.044343	1.131966	0.22507	0.00039	8.8E-05	4.84367E-11	-0.05206	0.052055	-0.50813	0.508127	-0.859708	0.859708	1.000781	1.108578	1.131966
0.15	0.0040635	0.0081269	3.25077	0.2501358	0.043088	1.217339	0.20929	0.00039	8.2E-05	6.79237E-12	-0.03622	0.036219	-0.38049	0.380489	-0.924076	0.924076	1.000543	1.077195	1.217339
0.2	0.0045216	0.0090431	3.61725	0.2501008	0.042404	1.303651	0.19543	0.00039	7.7E-05	1.64703E-11	-0.02689	0.026893	-0.30937	0.309369	-0.950562	0.950562	1.000403	1.060095	1.303651
0.25	0.0050443	0.0100886	4.03544	0.2500783	0.041985	1.391297	0.18312	0.00039	7.2E-05	9.60355E-12	-0.02087	0.020871	-0.26521	0.265211	-0.963964	0.963964	1.000313	1.049614	1.391297
0.3	0.0056386	0.0112773	4.5109	0.2500626	0.041705	1.480355	0.17211	0.00039	6.8E-05	1.8395E-12	-0.01669	0.016689	-0.23547	0.235471	-0.971738	0.971738	1.00025	1.042614	1.480355

Figure C.2: EN 1992 Edge Restraint Crack Model Sensitivity Factors and Theoretical Partial Safety Factors ($h_{c,eff}$ = h/2)

End Restraint
$h_{c,eff}$ = 2.5(c+ ϕ/2)

Constant Variables
As unkown variable αe=7
c=40mm kc=1 Es = 200GPa
h=250mm k=1

w_{lim}= 0.3mm
β=1.5

												Direction Cosines/ Sensitivity Factors								Partial Factors				
model uncertainty c	Area/face (	Gross Area (	As (%)	h*	c*	fct,eff*	θ*	Srm	ε	wcalc	g(x)	α_h	$\lvert\alpha_h\rvert$	α_c	$\lvert\alpha_c\rvert$	$\alpha_{fct,eff}$	$\lvert\alpha_{fct,eff*}\rvert$	α_θ	$\lvert\alpha_\theta\rvert$	Υ_h	Υ_c	$\Upsilon_{fct,eff}$	$1/\Upsilon_{fct,eff}$	Υ_θ
0.1	0.001725	0.00345016	1.380064	0.25014	0.044393	3535.77	1.056444	0.404095	0.000703	0.000284	2.94E-10	-0.03640258	0.0364026	-0.5131462	0.513146	-0.758843	0.75884295	-0.399391	0.399391	1.001	1.11	1.219	0.82	1.056
0.15	0.001755	0.0035109	1.40436	0.25012	0.043947	3470.063	1.118349	0.395207	0.000679	0.000268	3.89E-10	-0.0331952	0.0331952	-0.4682618	0.468262	-0.693025	0.6930248	-0.5471248	0.5471248	1	1.099	1.197	0.836	1.118
0.2	0.001794	0.00358802	1.435208	0.25011	0.043487	3402.701	1.193785	0.385117	0.000653	0.000251	3.55E-10	-0.02984328	0.0298433	-0.4214923	0.421492	-0.624242	0.62424172	-0.6570965	0.6570965	1	1.087	1.173	0.852	1.194
0.25	0.001839	0.00367707	1.470828	0.2501	0.043063	3340.946	1.27769	0.374741	0.000627	0.000235	3.92E-10	-0.02671155	0.0267115	-0.3779204	0.37792	-0.559976	0.55997593	-0.7368104	0.7368104	1	1.077	1.152	0.868	1.278
0.3	0.001887	0.00377454	1.509817	0.25009	0.042692	3287.242	1.366807	0.36458	0.000602	0.000219	2.7E-10	-0.02394094	0.0239409	-0.3394699	0.33947	-0.503116	0.50311599	-0.7943937	0.7943937	1	1.067	1.134	0.882	1.367

w_{lim}= 0.2mm
β=1.5

												Direction Cosines/ Sensitivity Factors								Partial Factors				
model uncertainty c	Area/face (	Gross Area (	As (%)	h*	c*	fct,eff*	θ*	Srm	ε	wcalc	g(x)	α_h	$\lvert\alpha_h\rvert$	α_c	$\lvert\alpha_c\rvert$	$\alpha_{fct,eff}$	$\lvert\alpha_{fct,eff*}\rvert$	α_θ	$\lvert\alpha_\theta\rvert$	Υ_h	Υ_c	$\Upsilon_{fct,eff}$	$1/\Upsilon_{fct,eff}$	Υ_θ
0.1	0.002202	0.00440483	1.761931	0.25013	0.04443	3533.836	1.056284	0.335998	0.000564	0.000189	3.39E-10	-0.03544735	0.0354474	-0.5168192	0.516819	-0.756924	0.75692402	-0.3983811	0.3983811	1.001	1.111	1.219	0.821	1.056
0.15	0.002243	0.00448537	1.794146	0.25012	0.043983	3468.591	1.118053	0.328673	0.000544	0.000179	3.48E-10	-0.03232165	0.0323217	-0.4718829	0.471883	-0.691536	0.69153553	-0.5459491	0.5459491	1	1.1	1.196	0.836	1.118
0.2	0.002294	0.00458782	1.835128	0.25011	0.043521	3401.623	1.193366	0.320363	0.000523	0.000168	3.86E-10	-0.02905168	0.0290517	-0.4250025	0.425003	-0.623129	0.62312944	-0.6559257	0.6559257	1	1.088	1.173	0.853	1.193
0.25	0.002353	0.00470637	1.88255	0.2501	0.043095	3340.163	1.277172	0.311823	0.000502	0.000157	8.44E-11	-0.02599364	0.0259936	-0.381278	0.381278	-0.559154	0.55915437	-0.7357294	0.7357294	1	1.077	1.152	0.868	1.277
0.3	0.002418	0.00483645	1.934582	0.25009	0.042723	3286.67	1.366215	0.303467	0.000482	0.000146	2.95E-10	-0.02328613	0.0232861	-0.342656	0.342656	-0.502506	0.5025061	-0.7934307	0.7934307	1	1.068	1.133	0.882	1.366

w_{lim}= 0.1mm
β=1.5

												Direction Cosines/ Sensitivity Factors								Partial Factors				
model uncertainty c	Area/face (	Gross Area (	As (%)	h*	c*	fct,eff*	θ*	Srm	ε	wcalc	g(x)	α_h	$\lvert\alpha_h\rvert$	α_c	$\lvert\alpha_c\rvert$	$\alpha_{fct,eff}$	$\lvert\alpha_{fct,eff*}\rvert$	α_θ	$\lvert\alpha_\theta\rvert$	Υ_h	Υ_c	$\Upsilon_{fct,eff}$	$1/\Upsilon_{fct,eff}$	Υ_θ
0.1	0.003439	0.00687872	2.751488	0.25012	0.044507	3529.727	1.055944	0.247494	0.000383	9.47E-05	6.6E-10	-0.03321025	0.0332103	-0.5245255	0.524525	-0.752841	0.75284134	-0.3962323	0.3962323	1	1.113	1.217	0.822	1.056
0.15	0.003508	0.00701636	2.806543	0.25011	0.044058	3465.456	1.117423	0.242209	0.000369	8.95E-05	3.17E-10	-0.03026924	0.0302692	-0.479488	0.479488	-0.688363	0.68836278	-0.5434443	0.5434443	1	1.101	1.195	0.837	1.117
0.2	0.003596	0.00719229	2.876917	0.2501	0.043594	3399.324	1.192472	0.236219	0.000355	8.39E-05	6.57E-10	-0.02718559	0.0271856	-0.4323804	0.43238	-0.620757	0.62075705	-0.6534285	0.6534285	1	1.09	1.172	0.853	1.192
0.25	0.003698	0.00739694	2.958776	0.25009	0.043164	3338.494	1.276068	0.230074	0.000341	7.84E-05	3.01E-10	-0.02429598	0.024296	-0.3883382	0.388338	-0.557401	0.55740064	-0.7334219	0.7334219	1	1.079	1.151	0.869	1.276
0.3	0.003811	0.00762281	3.049122	0.25008	0.042787	3285.451	1.364951	0.224072	0.000327	7.33E-05	3.87E-10	-0.0217333	0.0217333	-0.3493554	0.349355	-0.501204	0.50120373	-0.7913743	0.7913743	1	1.07	1.133	0.883	1.365

Figure C.3: EN 1992 End Restraint Crack Model Sensitivity Factors and Theoretical Partial Safety Factors ($h_{c,eff}$ = 2.5(c + φ/2)).

End Restraint

As unkown vari: αe=7
c=40mm kc=1 Es = 200GPa
h=250mm k=1
hc,eff=0.5h
w_{lim}= 0.3mm
β=1.5

												Direction Cosines/ Sensitivity Factors								Partial Factors				
model uncertain	Area/face (	Gross Area (	As (%)	h*	c*	fct,eff*	θ*	Srm	ε	wcalc	g(x)	α_h	$\lvert\alpha_h\rvert$	α_c	$\lvert\alpha_c\rvert$	$\alpha_{fct,eff}$	$\lvert\alpha_{fct,eff}\rvert$	α_θ	$\lvert\alpha_\theta\rvert$	Υ_h	Υ_c	$\Upsilon_{fct,eff}$	$1/\Upsilon_{fct,eff}$	Υ_θ
0.1	0.001684	0.0033678	1.34713	0.2503	0.0409	3652.05	1.06596	0.37907	0.00074	0.00028	3E-11	-0.07788	0.077878	-0.14861	0.14861	-0.8724	0.872374	-0.459144	0.459144	1.0011682	1.022435	1.259326	0.794076	1.065956
0.15	0.001718	0.0034366	1.37464	0.2503	0.04076	3553.02	1.13494	0.37281	0.00071	0.00026	3E-10	-0.06909	0.069092	-0.133954	0.13395	-0.7759	0.775916	-0.612566	0.612566	1.0010364	1.019069	1.225178	0.816208	1.134937
0.2	0.001761	0.0035218	1.40873	0.2502	0.04063	3459.68	1.21596	0.36547	0.00068	0.00025	3E-10	-0.06058	0.060579	-0.119815	0.11981	-0.6825	0.682514	-0.718436	0.718436	1.0009087	1.015832	1.192994	0.838227	1.215956
0.25	0.001809	0.0036182	1.44729	0.2502	0.0405	3380.1	1.30373	0.3576	0.00064	0.00023	2E-11	-0.05335	0.053354	-0.10522	0.10522	-0.6009	0.600858	-0.790602	0.790602	1.0008003	1.012502	1.165552	0.857963	1.303725
0.3	0.001861	0.0037221	1.48885	0.2502	0.04043	3314.35	1.39508	0.3497	0.00061	0.00022	5E-11	-0.04685	0.046847	-0.097092	0.09709	-0.5319	0.531934	-0.839896	0.839896	1.0007027	1.010652	1.14288	0.874983	1.395082

w_{lim}= 0.2mm
β=1.5

												Direction Cosines/ Sensitivity Factors								Partial Factors				
model uncertain	Area/face (	Gross Area (	As (%)	h*	c*	fct,eff*	θ*	Srm	ε	wcalc	g(x)	α_h	$\lvert\alpha_h\rvert$	α_c	$\lvert\alpha_c\rvert$	$\alpha_{fct,eff}$	$\lvert\alpha_{fct,eff*}\rvert$	α_θ	$\lvert\alpha_\theta\rvert$	Υ_h	Υ_c	$\Upsilon_{fct,eff}$	$1/\Upsilon_{fct,eff}$	Υ_θ
0.1	0.002148	0.004296	1.7184	0.2503	0.04118	3647.63	1.0656	0.31539	0.0006	0.00019	3E-10	-0.07447	0.074467	-0.178965	0.17897	-0.8681	0.868134	-0.456913	0.456913	1.001117	1.029442	1.257805	0.795036	1.065599
0.15	0.002193	0.0043869	1.75475	0.2502	0.04101	3549.92	1.13432	0.31021	0.00057	0.00018	3E-10	-0.06609	0.066086	-0.161345	0.16135	-0.7729	0.772861	-0.610153	0.610153	1.0009913	1.025369	1.224111	0.816919	1.134321
0.2	0.00225	0.0044998	1.79992	0.2502	0.04086	3457.57	1.21513	0.30414	0.00054	0.00016	2E-10	-0.05794	0.057943	-0.144316	0.14432	-0.6804	0.68037	-0.716179	0.716179	1.0008692	1.021448	1.192266	0.838739	1.215133
0.25	0.002314	0.0046279	1.85115	0.2502	0.04072	3378.51	1.30266	0.29769	0.00052	0.00015	1E-10	-0.05079	0.050792	-0.12942	0.12942	-0.5992	0.599207	-0.78843	0.78843	1.0007619	1.01803	1.165003	0.858367	1.302664
0.3	0.002383	0.0047662	1.90649	0.2502	0.04061	3313.32	1.394	0.29116	0.00049	0.00014	2E-10	-0.04477	0.044768	-0.116895	0.11689	-0.5308	0.530844	-0.838174	0.838174	1.0006715	1.015165	1.142525	0.875255	1.394002

w_{lim}= 0.1mm
β=1.5

												Direction Cosines/ Sensitivity Factors								Partial Factors				
model uncertain	Area/face (	Gross Area (	As (%)	h*	c*	fct,eff*	θ*	Srm	ε	wcalc	g(x)	α_h	$\lvert\alpha_h\rvert$	α_c	$\lvert\alpha_c\rvert$	$\alpha_{fct,eff}$	$\lvert\alpha_{fct,eff*}\rvert$	α_θ	$\lvert\alpha_\theta\rvert$	Υ_h	Υ_c	$\Upsilon_{fct,eff}$	$1/\Upsilon_{fct,eff}$	Υ_θ
0.1	0.003349	0.0066985	2.6794	0.2503	0.04177	3635.54	1.06462	0.23298	0.0004	9.4E-05	2E-10	-0.06681	0.066811	-0.242457	0.24246	-0.8565	0.856476	-0.450777	0.450777	1.0010022	1.044254	1.253633	0.797682	1.064618
0.15	0.003426	0.0068523	2.74094	0.2502	0.04155	3541.41	1.13263	0.22916	0.00039	8.8E-05	8E-11	-0.05935	0.059353	-0.218839	0.21884	-0.7644	0.76444	-0.603505	0.603505	1.0008903	1.038719	1.221177	0.818882	1.132626
0.2	0.003522	0.0070447	2.81789	0.2502	0.04133	3451.75	1.21287	0.22473	0.00037	8.2E-05	4E-10	-0.05205	0.052052	-0.195873	0.19587	-0.6745	0.674456	-0.709953	0.709953	1.0007808	1.033366	1.190258	0.840154	1.212866
0.25	0.003632	0.0072644	2.90577	0.2502	0.04115	3374.49	1.29998	0.22005	0.00035	7.7E-05	5E-10	-0.0456	0.045601	-0.175686	0.17569	-0.595	0.595033	-0.782938	0.782938	1.000684	1.028683	1.163618	0.859388	1.299984
0.3	0.003752	0.0075034	3.00135	0.2502	0.04099	3310.49	1.39103	0.21533	0.00033	7.2E-05	7E-10	-0.04014	0.04014	-0.158648	0.15865	-0.5278	0.527839	-0.83343	0.83343	1.0006021	1.024747	1.141547	0.876004	1.391029

Figure C.4: EN 1992 End Restraint Crack Model Sensitivity Factors and Theoretical Partial Safety Factors ($h_{c,eff}$ = h/2)

Edge Restraint

$h_{c,eff} = 2.5(c+ \phi/2)$

Constant Variables

As unkown variable | εca=33με | R = 0.5

c=40mm | εcd=220με

h=250mm | αT,c=14με

Wlim = 0.2 mm

Ω = c.o.v.=s.dev./mean

Final failure point

$\Upsilon_{xi*} = 1-\alpha i*\beta\Omega = x*/mean$

Final direction cosine

β	Area/face (m^2)	Gross Area (m^2)	As (%)	h*	c*	θ*	Srm	ε	wcalc	g(x)	α_h	$\lvert\alpha_h\rvert$	α_c	$\lvert\alpha_c\rvert$	α_θ	$\lvert\alpha_\theta\rvert$	Υ_h	Υ_c	Υ_θ
0.5	0.001325177	0.002650353	1.060141	0.25	0.04072	1.09786	0.46413	0.0004	0.0001822	3.42E-11	0	0	-0.386219	0.386219	-0.922407	0.922407	1	1.0178775	1.09786
1.5	0.002000583	0.004001165	1.600466	0.25	0.04322	1.44562	0.35248	0.0004	0.0001383	3.12E-11	0	0	-0.394326	0.394326	-0.918971	0.918971	1	1.0805692	1.44562
2	0.002500293	0.005000586	2.000234	0.25	0.04458	1.65733	0.30746	0.0004	0.0001207	6.955E-11	0	0	-0.398861	0.398861	-0.917011	0.917011	1	1.1145027	1.65733

End Restraint

$h_{c,eff} = 2.5(c+ \phi/2)$

Constant Variables

As unkown variable | αc=7

c=40mm | kc=1 | Es = 200GPa

h=250mm | k=1

Wlim = 0.2 mm

												Direction Cosines/ Sensitivity Factors								Partial Factors				
β	Area/face (m^2)	Gross Area (m^2)	As (%)	h*	c*	fct,eff*	θ*	Srm	ε	wcalc	g(x)	α_h	$\lvert\alpha_h\rvert$	α_c	$\lvert\alpha_c\rvert$	$\alpha_{fct,eff}$	$\lvert\alpha_{fct,eff*}\rvert$	α_θ	$\lvert\alpha_\theta\rvert$	Υ_h	Υ_c	$\Upsilon_{fct,eff}$	$1/\Upsilon_{fct,eff}$	Υ_θ
0.5	0.001919165	0.003838329	1.535332	0.25	0.04057	2987.67	1.07708	0.3446	0.0005388	0.0001857	9.9E-11	-0.023926	0.0239264	-0.337406	0.3374063	-0.503513	0.503513	-0.795021	0.79502	1	1.014	1.03	0.971	1.077
1.5	0.002418227	0.004836454	1.934582	0.25	0.04272	3286.67	1.36621	0.3035	0.0004824	0.0001464	2.95E-10	-0.023286	0.0232861	-0.342656	0.342656	-0.502506	0.502506	-0.793431	0.79343	1	1.068	1.133	0.882	1.366
2	0.00272579	0.00545158	2.180632	0.25	0.04387	3446.69	1.53812	0.2854	0.0004556	0.00013	1.81E-10	-0.022912	0.0229122	-0.345354	0.3453541	-0.501982	0.501982	-0.792603	0.7926	1	1.097	1.189	0.841	1.538

Figure C.5: EN 1992 Edge and End Restraint Crack Model Sensitivity Factors and Theoretical Partial Safety Factors with Varying β Values ($h_{c,eff}$ = 2.5(c + φ/2)

Edge Restraint																									
hc,eff = 0.5h																									
Constant Variables																									
As unkown variab	εca=33με	R = 0.5																							
c=40mm	εcd=220με																								
h=250mm	αT,c=14με																								
Wlim = 0.2 mm																									
β	Area/face (m	Gross Area (r	As (%)	h*	c*	θ*	Srm	ε	wcalc	g(x)	α_h	$\lvert\alpha_h\rvert$	α_c	$\lvert\alpha_c\rvert$	α_θ	$\lvert\alpha_\theta\rvert$									
0.5	0.00131795	0.00263591	1.054363	0.250034	0.03981	1.110025	0.459047	0.000393	0.00018	2.4322E-11	-0.027434739	0.02743474	-0.086365	0.0863653	-0.995886	0.9958857									
1.5	0.00192568	0.00385136	1.540545	0.250094	0.040619	1.494361	0.340985	0.000393	0.000134	2.0363E-11	-0.025196033	0.02519603	-0.118249	0.1182488	-0.992664	0.9926643									
2	0.00236177	0.00472354	1.889415	0.250119	0.041233	1.731569	0.294273	0.000393	0.000116	1.5176E-10	-0.023741961	0.02374196	-0.138725	0.1387247	-0.990046	0.9900464									
End Restraint																									
Constant Variables																									
As unkown variab	αe=7																								
c=40mm	kc=1	Es = 200GPa																							
h=250mm	k=1																								
Wlim = 0.2 mm												Direction Cosines/ Sensitivity Factors								Partial Factors					
β	Area/face (m	Gross Area (r	As (%)	h*	c*	fct,eff*	θ*	Srm	ε	wcalc	g(x)	α_h	$\lvert\alpha_h\rvert$	α_c	$\lvert\alpha_c\rvert$	$\alpha_{fct,eff}$	$\lvert\alpha_{fct,eff}\rvert$	α_θ	$\lvert\alpha_\theta\rvert$	Υ_h	Υ_c	$\Upsilon_{fct,eff}$	$1/\Upsilon_{fct,eff}$	Υ_θ	
0.5	0.00191557	0.00383113	1.532452	0.250058	0.039845	2995.734	1.077079	0.34077	0.000541	0.00018444	3.81648E-10	-0.0467186	0.0467186	-0.098195	0.0981945	-0.531879	0.53187923	-0.839809	0.8398093	1.0002336	0.99612	1.033012	0.968043	1.077079	
1.5	0.00238312	0.00476623	1.906494	0.250168	0.040607	3313.322	1.394002	0.291163	0.000493	0.00014347	1.82688E-10	-0.0447676	0.0447676	-0.116895	0.1168945	-0.530844	0.53084381	-0.838174	0.8381744	1.0006715	1.01517	1.142525	0.875255	1.394002	
2	0.00266823	0.00533646	2.134582	0.250218	0.041095	3483.805	1.579748	0.269744	0.000469	0.0001266	2.63001E-10	-0.0436424	0.0436424	-0.127532	0.1275321	-0.530169	0.5301691	-0.837109	0.8371091	1.0008729	1.02738	1.201312	0.832423	1.579748	

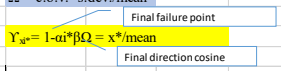

Figure C.6: EN 1992 Edge and End Restraint Crack Model Sensitivity Factors and Theoretical Partial Safety Factors with Varying β Values ($h_{c,eff}$ = h/2)